
**Investigating the neural basis of self-awareness
deficits following traumatic brain injury**

Dr Timothy Ham

Imperial College London

Department of Medicine, Centre for Neuroscience

Computational, Cognitive and Clinical Neuroimaging Laboratory

Degree: PhD

Acknowledgements

I would like to thank the following people for their contributions to my thesis:

David Sharp, who supervised my thesis, gave me the benefit of his expertise, the opportunity to work with TBI patients and expanded my awareness of TBI as a clinical entity that neurologists should engage with;

Rob Leech, who co-supervised the thesis and provided invaluable help with the analysis and design of the studies described;

Richard Wise who co-supervised the thesis and provided clinical and moral support throughout my fellowship;

Valerie Bonnelle, who helped accrue and analyse the data;

Xavier de Boissezon, who designed the paradigms and gathered much of the data for the healthy controls;

Sagar Jilka, Kirsi Kinnunen and Susannah James who performed neuropsychometric assessments on the large group of TBI patients used in the thesis;

Alex Leff, who provided his expertise concerning the DCM analysis;

Emmer Hughes who performed the vast majority of the MRI scanning; and,

Finally, all of the participants who gave of their time to help provide the information used in this thesis.

Statement of publications

The data presented in Chapter 4, 5 and 6 of this thesis have been published in Cerebral Cortex (Ham et al., 2012), the Journal of Neuroscience (Ham et al, 2013), and Brain (Ham et al., in press) respectively.

Ham TE, de Boissezon X, Leff A, Beckmann C, Hughes E, Kinnunen KM, Sharp DJ. Distinct Frontal Networks Are Involved in Adapting to Internally and Externally Signaled Errors. Cerebral Cortex 2012; 23: 703-713.

Ham T, Leff A, de Boissezon X, Joffe A, Sharp DJ. Cognitive Control and the Salience Network: An Investigation of Error Processing and Effective Connectivity. The Journal of Neuroscience 2013; 33:7091-8.

Ham TE, Bonelle V, Hellyer P, Jilka S, Robertson I, Leech R, and Sharp DJ. The neural basis of impaired self-awareness after traumatic brain injury. Brain, 2014,; 137: 586-597.

Copyright declaration

The copyright of this thesis rests with the author and is made available under a Creative Commons Attribution Non-Commercial No Derivatives licence. Researchers are free to copy, distribute or transmit the thesis on the condition that they attribute it, that they do not use it for commercial purposes and that they do not alter, transform or build upon it. For any reuse or redistribution, researchers must make clear to others the license terms of this work.

Statement of originality

Patient recruitment was done in conjunction with David Sharp.

The behavioural paradigms were designed by David Sharp and Xavier de Boissezon, who gathered much of the data for the healthy controls.

Neuropsychometric testing was performed by Sagar Jilka, Kirsi Kinnunen and Susannah James

MRI scanning was done with the help of Emmer Hughes, a radiographer.

All of the other work contained in this thesis is my own and conforms to the rules and guidelines set out for PhD thesis by Imperial College London

Abbreviations

ACC – Anterior cingulate cortex

BOLD – Blood-oxygen-level-dependent

BET – Brain extraction tool

BMA – Bayesian model averaging

BMS – Bayesian model selection

CBF – Cerebral blood flow

CRT – Choice reaction task

CBF – Cerebral blood flow

CBV – Cerebral blood volume

COG – Centre of gravity

CSD – Change-signal delay

CT – Computed tomography

DACC – Dorsal anterior cingulate cortex

DAI – Diffuse axonal injury

DAN – Dorsal attentional network

DCM – Dynamic causal modelling

DMN – Default mode network

DTI – Diffusion tensor imaging

EC – Effective connectivity

ECN – Executive control network

EEG – Electroencephalography

EPI – Echo planar imaging

ERN – Error-related negativity

FA – Fractional anisotropy

FC – Functional connectivity

FDR – False discovery rate

FEAT – FMRI expert analysis tool

FERN – Feedback related negativity

FFX – Fixed effects

FID – Free induction decay

FLAME – FMRIB’s local analysis of fixed effects

FLIRT – FMRIB’s linear image registration tool

FMRI – Functional magnetic resonance imaging

FMRIB – Functional magnetic resonance imaging of the brain

FPCN – Fronto-parietal control network

FSL – FMRIB software library

FWE – Family-wise error

FWHM – Full width half maximum

GLM – General linear model

GRF– Gaussian random field

High-PM – High-performance monitoring patients

HRF – Haemodynamic response function

ICA – Independent component analysis

IFG – Inferior frontal gyrus

IIV – Intra-individual variability

LAI – Left anterior insula cortex

Low-PM – Low-performance monitoring patients

MD – Mean diffusivity

MEG – Magnetoencephalography

MELODIC – Multivariate exploratory linear optimised decomposition into independent components

MEG – Magnetoencephalography

MFG – Middle frontal gyrus

MNI – Montreal Neurological Institute

MPH – Methylphenidate

MRI – Magnetic resonance imaging

NHS – National Health Service

PCA – Principle component analysis

PCC – Posterior cingulate cortex

PDF - Probability density function

PEATE – Perl event-related average time-course extraction

PET – Positron emission tomography

Pre-SMA – Pre-supplementary motor area

PTA – Post-traumatic amnesia

RAI – Right anterior insula cortex

RF – Radiofrequency

RFX –Random effects

ROI – Region of interest

RTA – Road traffic accidents

SCT – Stop-change task

SDCM – Stochastic dynamic causal modelling

SFG – Superior frontal gyrus

SMA – Supplementary motor area

SMG – Supramarginal gyrus

SN – Saliience network

SPM8 – Statistical parametric mapping version 8

SSD –Stop-signal delay

SST – Stop-signal task

SWI – Susceptibility-weighted images

TBI – Traumatic brain injury

TFCE – Threshold free cluster enhancement

TR – Repeat time

TE – Echo time

VAN – Ventral attentional network

VN – Visual Network

XP – Exceedance probability

Chapter 1: Introduction

1.1. Abstract

Self-awareness deficits are a common and disabling consequence of traumatic brain injury (TBI). 'On-line' awareness is one facet of self-awareness that can be studied by examining how people monitor their performance and respond to their errors. Performance monitoring, like many of the cognitive functions disrupted after TBI, is believed to depend on the coordinated activity of neural networks. The fronto-parietal control network (FPCN) is one such network that contains a sub-network called the salience network (SN). The SN consists of the dorsal anterior cingulate (dACC) and bilateral insulae cortex and is thought to monitor salient events (e.g. errors). I used advanced structure and function MRI techniques to investigate these networks and test two overarching hypotheses: first, *performance monitoring is regulated by regions within the FPCN*; and second, *dysfunction of the FPCN leads to impaired self-awareness after TBI*.

My first study demonstrated two distinct frontal networks that respond to different error types. Predictable/internally signalled errors caused SN activation; whereas unpredictable/externally signalled errors caused activation of the ventral attentional network, a network thought to respond to unexpected events. This suggested the presence of parallel performance monitoring systems within the FPCN. My second study established that the 'driving' input into the SN originated in right anterior insula and subsequent behavioural adaptation was regulated by enhanced effective connectivity from the dACC to the left anterior insula. In my third study I identified a large group of TBI patients with impaired performance monitoring. These patients had additional metacognitive evidence of impaired self-awareness and demonstrated reduced functional connectivity between the dACC and the remainder of the FPCN at 'rest', and abnormally large insulae activation in response to errors.

These studies clarified how the brain monitors and responds to salient events; and, provided evidence that self-awareness deficits after TBI are due to FPCN dysfunction, identifying this network as a potential target for future treatments.

Table of contents

Chapter 1: Introduction	10
1.1. Abstract.....	10
1.2. Thesis overview	21
1.2.1. Introduction	21
1.2.2. Methods chapters.....	21
1.2.3. Results chapters	21
1.2.4. Discussion chapter.....	23
1.3. My contribution to the studies.....	23
Chapter 2: Background	24
2.1. Clinical relevance of traumatic brain injury	24
2.1.1. Definition	24
2.1.2. Epidemiology.....	24
2.1.3. Causes and risk factors of TBI	25
2.1.4. Economic impact of TBI	26
2.1.5. Clinical consequences of TBI.....	26
2.2. Pathophysiology of TBI.....	32
2.2.1. Focal injuries	32
2.2.2. Diffuse axonal injury.....	34
2.3. Research imaging techniques in TBI.....	37
2.3.1. Diffusion tensor imaging.....	37
2.3.2. Pathological correlates of DTI	37
2.3.3. Sensitivity of DTI	40
2.3.4. Clinical relevance of DTI	40
2.3.5. Functional magnetic resonance imaging.....	42
2.3.6. Relationship between MRI measures of structural and functional connectivity	43
2.3.7. EEG and MEG assessment of TBI.....	43

2.4. Cognitive functions investigated in this thesis.....	44
2.4.1. Self-awareness	45
2.4.2. Performance monitoring and cognitive control.....	46
2.4.3. Attention	52
2.5. Cognitive impairment after TBI.....	54
2.5.1. The impact of TBI on self-awareness.....	56
2.5.2. The impact of TBI on performance monitoring and cognitive control.....	58
2.5.3. The impact of TBI on attention	59
2.6. The neural basis of the cognitive functions investigated in this thesis ..	60
2.6.1. The neural basis of self-awareness	60
2.6.2. The neural basis of cognitive control and performance monitoring.....	65
2.6.3. The neural basis of attention.....	68
2.7. Neural networks	69
2.7.1. Why study brain networks?	70
2.7.2. Defining neural networks.....	71
2.7.3. The Default Mode Network	73
2.7.4. The Fronto-Parietal Control Network	73
2.7.5. The Salience Network.....	74
2.7.6. The Triple network model.....	75
2.8. Network disruption after TBI.....	76
2.8.1. Fronto-Parietal Control Network dysfunction after TBI.....	77
2.8.2. Default Mode Network dysfunction after TBI.....	78
2.8.3. Dysfunction in other networks	80
2.8.4. Potential benefits of studying brain networks in TBI	80
2.8.5. Limitations of network based analysis.....	81
2.9. Main hypotheses and objectives	82
Chapter 3: Participants, Materials and Methods	84
3.1. Participants.....	84

3.1.1. TBI patient recruitment.....	84
3.1.2. TBI severity classification.....	85
3.1.3. Control groups.....	85
3.2. Neuropsychological assessment	86
3.3. Experimental paradigms	87
3.3.1. The Simon Task.....	87
3.3.2. The Secondary Simon task.....	90
3.3.3. Performance matching in the Simon task	91
3.3.4. Behavioural assessment of the Simon task	92
3.3.5. Analysing strategic differences in performance on the Simon task.....	94
3.3.6. The stop-signal task and stop-change task.....	94
3.3.7. The stop-signal task.....	95
3.3.8. Performance matching in the SST	97
3.3.9. Behavioural assessment of the SST	98
3.3.10. The stop-change task.....	100
3.3.11. Performance matching in the SCT	103
3.3.12. Behavioural assessment of the SCT.....	104
3.3.4. Magnetic Resonance imaging.....	105
3.4.1. Nuclear Magnetic Resonance	105
3.4.2. How MRI images are generated	110
3.4.3. T1 weighted-images.....	111
3.4.4. T2 weighted-images.....	112
3.4.5. T2* weighted images and Echo-planar imaging.....	113
3.4.6. Susceptibility-weighted images	113
3.5. Functional Magnetic Resonance imaging	114
3.5.1. Principles of fMRI.....	114
3.5.2. Event-related fMRI	116
3.5.3. Data pre-processing.....	116

3.5.4. Statistical analysis of fMRI	120
3.5.5. Thresholding	125
3.5.6. Functional Connectivity	128
3.6. Dynamic Causal Modelling.....	133
3.6.1. Principles of DCM	134
3.6.2. Bayesian family level inference.....	136
3.6.3. Bayesian model averaging.....	136
3.7. Limitations of fMRI in TBI.....	137
3.7.1. Performance matching	137
3.7.2. Focal lesions	138
3.7.3. Altered HRF in TBI.....	139
3.8. Advanced structural assessment of TBI	140
3.8.1. Diffusion tensor imaging.....	140
3.8.2. DTI metrics.....	140
3.8.3. Measuring water diffusivity with MRI.....	143
3.8.4. DTI analysis	143
3.8.5. Probabilistic tractography.....	144
Chapter 4: Distinct frontal networks are involved in monitoring and adapting to internally and externally signalled errors.....	145
4.1. Introduction	145
4.2. Materials and Methods	148
4.2.1. Participants	148
4.2.2. Simon Task procedure	149
4.2.3. Scanning protocol	149
4.2.4. Standard whole-brain fMRI analysis of the Simon task.....	150
4.2.5. Region of interest analysis	151
4.2.6. Time-Series Analysis	151
4.2.7. Secondary Simon task controlling for external feedback	152

4.2.8. Analysis of strategic differences in task performance: comparison of high low timing error groups.....	152
4.3. Behavioural results.....	153
4.3.1. Commission errors associated with high conflict situations	153
4.3.2. Timing errors independent of commission errors and congruency	155
4.3.3. Speed accuracy trade off seen on incongruent but not congruent commission error.....	156
4.3.4. Commission and timing errors both produce adaptive changes in behaviour	156
4.4. Neuroimaging results	159
4.4.1. Commission errors activate the dACC	159
4.4.2. Timing errors activate lateral prefrontal and superior frontal regions, but not the dACC.....	163
4.4.3. Common activation for commission and timing errors seen within pars operculari	164
4.4.4. Delayed activation of the dACC was not present after timing errors.....	165
4.4.5. Controlling for the presence of external feedback on timing errors.....	166
4.4.6. Strategic differences in task performance: comparison of High and Low Timing error groups.....	169
4.5. Discussion	171
4.5.1. Results summary	171
4.5.2. The dACC activation is not necessary to engage cognitive control	172
4.5.3. The dACC may signal a subset of learnable errors	172
4.5.4. Comparison with previous studies of timing errors	174
4.5.5. The role of the dACC in conflict detection.....	175
4.5.6. Timing errors do not activate the Salience network	175
4.5.7. VAN activation after both error types	176
4.5.8. Evidence of a rostro-caudal gradient in the lateral prefrontal cortex.....	176
4.5.9. Motivation and the relative salience of different error types.....	177
4.5.10. Addressing potential experimental confounds	178
4.5.11. Conclusions.....	178

Chapter 5: Cognitive control and the Salience Network: an investigation of error processing and effective connectivity	180
5.1. Introduction	180
5.2. Materials and Methods	182
5.2.1. Participants	182
5.2.2. Simon Task procedure	183
5.2.3. Functional MRI analysis	183
5.2.4. Whole brain fMRI analysis	183
5.2.5. Dynamic Causal Modelling analysis.....	184
5.3. Behavioural results.....	191
5.3.1. Behaviour summary of the Simon task performance	191
5.4. Neuroimaging results	191
5.4.1. Congruent and incongruent errors produce similar activation within the Salience Network	191
5.5. Dynamic causal modelling analyses results	195
5.5.1. DCM Analysis 1: Input into Salience network is through the right insula	195
5.5.2. DCM Analysis 2: What are the intrinsic SN connections and are they modulated by errors?	197
5.5.3. DCM Analysis 3: Are there distinct effects of errors in the congruent and incongruent conditions, and do these relate to behaviour?.....	198
5.6. Discussion	198
5.6.1. Results summary	198
5.6.2. The role of the dACC in error processing.....	199
5.6.3. The role of the RAI in error processing	199
5.6.4. Relationship to previous studies	200
5.6.5. Increased sensitivity of effective connectivity measures over traditional univariate analysis.....	201
5.6.7. Study limitations	202
5.6.8. Conclusions.....	203

Chapter 6: The neural basis of impaired self-awareness after traumatic brain injury	204
6.1. Introduction	205
6.2. Materials and methods	207
6.2.1. Patients: demographic and clinical details	207
6.2.2. Standard clinical imaging	214
6.2.3. Control groups.....	214
6.3. Neuropsychological Assessment	215
6.3.1. Methods overview	216
6.3.2. Behavioural assessment: Stop-change task.....	216
6.3.3. Structural and functional magnetic resonance imaging acquisition	218
6.3.4. Clinical imaging	218
6.3.5. Functional connectivity analysis of 'resting' brain networks	220
6.3.6. Stop-signal task.....	225
6.3.7. fMRI analysis of the SST	226
6.3.8. Structural lesion analysis	226
6.4. Behavioural results.....	227
6.4.1. Using the SCT to define self-awareness.....	227
6.4.2. Post-error slowing on the SCT	231
6.4.3. Impaired error processing is a marker of more general self-awareness problems	234
6.5. Neuroimaging results: Resting state analyses	234
6.5.1. Impaired performance monitoring is associated with abnormal function within the FPCN	234
6.6. Neuroimaging results: SST event-related fMRI analysis	236
6.6.1. SST behavioural results	236
6.7 Structural imaging results.....	241
6.7.1. Lesion location and extent does not relate to performance monitoring deficits	241
7.7. Discussion	243

6.7.1. Results summary	243
6.7.2. Role of the salience network in self-awareness	243
6.7.3. Abnormal activation pattern in the salience network may reflect network inefficiency	244
6.7.4. Benefits and limitations of using the SST instead of SCT in event-related fMRI analysis.....	245
6.7.5. Compensatory activation of the right MFG seen in High-PM patients ...	245
6.7.6. Low-PM patients showed altered self-awareness on metacognitive testing	246
6.7.7. Self-awareness deficits not predicted by lesion load, location or DTI metrics.....	247
6.7.8. Limitations	248
6.7.9. Conclusion	249
Chapter 7: Discussion	250
7.1. Results summary	250
7.2. Relationship of the main findings to existing work	252
7.2.1. Neural networks involved in performance monitoring	252
7.2.2. Right anterior insula provides the input into salience network	253
7.2.3. Effective connectivity measures provide additional information to traditional univariate fMRI analyses	254
7.3. Development of existing models of performance monitoring and awareness.....	255
7.3.1. Modified model of performance monitoring.....	255
7.3.2. Craig's model of self-awareness	259
7.4. Future developments.....	260
7.4.1. Experimentally vary the predictability of timing errors.....	260
7.4.2. Expansion of DCM analysis	261
7.4.3. Examining other facets of self-awareness	263
7.4.4. Brain stem imaging	264
7.5. Potential treatment of self-awareness deficits after TBI	265
7.5.1. Dopamine and the salience network.....	265

7.5.2. Dopamine and cognition	265
7.5.3. Previous trials of dopamine potentiating agents in TBI	266
7.5.4. Methods of targeting patients	267
7.6. Conclusion.....	268
8. References.....	270

1.2. Thesis overview

1.2.1. Introduction

In **Chapter 2** I discuss the clinical impact of TBI, the risk factors associated with it, and the cognitive disabilities that it causes. I then review the existing work on the changes in brain structure and function caused by TBI with particular focus on the impact of TBI on self-awareness, performance monitoring, cognitive control and attention. I introduce the concept of neural networks and how they provide a useful framework to discuss cognitive dysfunction, particularly in the context of diffuse axonal injury.

1.2.2. Methods chapters

In **Chapter 3** I outline the recruitment procedures, behavioral assessments and MRI analytical methods used to investigate the neural basis of performance monitoring, error processing, and self-awareness in healthy controls and TBI patients.

1.2.3. Results chapters

In **Chapter 4** I present the results of an event related fMRI study designed to clarify the neural mechanisms involved in monitoring different types of errors. Previous literature has proposed that the dACC acts as a generic performance monitor responding to all error types. Importantly many of these studies have confounded errors by associating them with reward or punishment. I provide evidence that the dACC is not a generic performance monitor. The dACC and other regions of the SN are activated in association with a subset of errors that can be internally signaled as prediction error (e.g. commission errors). Other unpredictable and externally signaled error types (e.g. externally signaled timing errors) cause activation primarily within a bilateral network that overlaps with regions of the ventral attentional network.

Importantly, this result demonstrates that monitoring of errors can occur via two distinct frontal lobe networks.

In **Chapter 5** I present the results of a dynamic causal modeling study designed to investigate the underlying functional organization of the salience network and its response to commission errors. This is the first time that such a technique has been applied specifically to look at the hierarchical organization within the salience network. I demonstrate that the input to the salience network comes via the right anterior insula and therefore this is most likely the node that ‘detects’ salient events (as opposed to alternative hypotheses, which assigns this function to the dACC). I also demonstrate that the effective connectivity between the dACC and the left anterior insula correlated with the post-error behavioral adaptation. This result suggests that although the dACC may not detect salient events it is intimately involved in the regulating the behavioral response to them.

In **Chapter 6** present the results of a multimodal study of TBI patients and controls with varying levels of self-awareness and performance monitoring ability. I used neuropsychometric, diffusion tensor imaging (DTI), resting-state fMRI and task fMRI measures to assess the neural basis of self-awareness deficits following TBI. I provide evidence that neural activity within the FPCN, particularly the salience network sub-component, is abnormal in patients with impaired self-awareness. The dACC showed reduced functional connectivity to the rest of the FPCN at ‘rest’, and the anterior insulae showed increased activity following errors in the impaired group. The results suggested that impairments of self-awareness after TBI result from breakdown of functional interactions between nodes within the FPCN.

1.2.4. Discussion chapter

In **Chapter 7** I discuss the results as a whole and how they fit into current network based theories of human brain function. I particularly focus on the pivotal role of the right insula and adjacent inferior frontal gyrus in regulating activity across distributed neural networks, and the importance of integrated activity within the salience network in facilitating awareness of on-going behaviorally salient events. I also discuss some of the future directions for my research and the potential clinical benefits of employing network based techniques to the TBI population.

1.3. My contribution to the studies

My research took place as part of a larger project examining the cognitive and psychiatric sequelae of TBI. I have outlined my contributions to each study below:

Study 1: I analysed and interpreted the fMRI and behavioral data on the main Simon task paradigm. I modified the main Simon task paradigm to make the ‘Secondary Simon task’, then acquired, analysed and interpreted the fMRI data on this task.

Study 2: This study used the data acquired for the first Simon task study. I designed and performed the dynamic causal modeling (DCM) analysis described in Chapter 5.

Study 3: As part of a larger group study I helped to acquire the behavioral, neuropsychometric and imaging data on TBI patients and healthy controls. I also analysed and interpreted the behavioral, fMRI and DTI data.

Chapter 2: Background

2.1. Clinical relevance of traumatic brain injury

2.1.1. Definition

TBI has been defined as “*an alteration in brain function or other evidence of brain pathology, caused by an external force*” (Menon, Schwab et al. 2010). In this context, altered brain function includes loss of consciousness, post-traumatic amnesia and other focal neurological deficits (e.g. paraesthesia, apraxia, plegia, paresis) occurring or deteriorating following an external force. This covers a range of clinical scenarios varying from severe penetrating head injury to mild TBI not necessarily associated with loss of consciousness (Malec, Brown et al. 2007). From a scientific perspective, TBI represents a complex cascade of structural and physiological events that occur in the brain as consequence of mechanical stress (Povlishock 1993). For practical purposes concerning image registration and data acquisition my work has focused on closed head injuries, which make up the vast majority of all TBI cases.

2.1.2. Epidemiology

TBI is the leading cause of disability among young individuals in high-income countries (Maas, Stocchetti et al. 2008). In 2007 it was estimated that over 600,000 people in the UK suffered a head injury sufficient for assessment in hospital (NICE 2007), although substantial local variation has been noted across the UK (Tennant 2005, Yates, Williams et al. 2006). The vast majority (70–90%) of TBI cases are labeled ‘mild’ using conventional criteria (Kraus and Nourjah 1988, Kraus, McArthur et al. 1994, Bazarian, McClung et al. 2005, NICE 2007). However, the definition of what constitutes mild TBI is variable (Malec, Brown et al. 2007), and the diagnostic criteria used to define injury severity are discussed below. The immediate mortality

from TBI is low. Only 0.2% of patients that present to an emergency department with TBI will die from the brain injury and only 1-3% of patients admitted to hospital will require neurosurgical intervention (NICE 2007). However, there is increasing recognition of long-term morbidity and mortality in TBI patients (Thornhill, Teasdale et al. 2000, Whitnall, McMillan et al. 2006, McMillan, Teasdale et al. 2011).

2.1.3. Causes and risk factors of TBI

The cause of TBI varies with geographical distribution and injury severity (Yates, Williams et al. 2006). This is emphasised by discrepancies in epidemiological studies that look at the causes of TBI of different severity across different populations. One large epidemiological study concluded that the commonest causes of moderate-to-severe TBI across Europe were road traffic accidents (RTA) (61%), falls (20%), assault (2.6%), and sport injuries (2.3%) (Tagliaferri, Compagnone et al. 2006). Conversely, another study found the commonest causes of mild TBI requiring emergency assessment in the UK were assault (30-50%), falls (22-43%), and RTA (25%) (NICE 2007). The single largest risk factor for TBI in an adult is male gender and this is most marked between the ages of 15-29 years (Yates, Williams et al. 2006). Urban environment, low premorbid intelligence and lower socio-economic class also confer an increased risk of TBI. These factors can largely be explained by participation in high-risk leisure activities and occupations, increased risk of crime and substance abuse (Tennant 2005, Yates, Williams et al. 2006, Nordstrom, Edin et al. 2013). Alcohol is involved in up to 65% of head injuries seen in the emergency department in the UK (NICE 2007).

2.1.4. Economic impact of TBI

The NHS spends over £1 billion a year on the acute management of the 10,000 patients with head injuries requiring admission to hospital (NICE 2007). Figures from 2010 estimated that TBI cost the UK economy €5.7 billion, (Gustavsson, Svensson et al. 2011) a significant increase from the 2004 estimate of €341 million (Andlin-Sobocki, Jonsson et al. 2005). The increase was due to a massive increase in the recorded incidence of TBI rather than a significant increase in the cost of intervention (Gustavsson, Svensson et al. 2011). Outside of the UK, TBI was estimated to cost the American economy over \$60 billion in 1999 due to the direct and indirect costs (Thurman, Alverson et al. 1999). A more recent study suggested that 50 to 70% of this is spent on the management of long-term disability rather than the acute medical care, depending upon the injury severity (Corso, Finkelstein et al. 2006). Unlike most disabling medical conditions, TBI is predominantly a disease of young people and leads potentially to a lifetime of reduced productivity or dependence (Tennant 2005, Yates, Williams et al. 2006).

2.1.5. Clinical consequences of TBI

TBI is a heterogeneous condition with a wide range of consequences ranging from coma or death to disabling cognitive and neuropsychiatric symptoms. The types of long-term disability seen after TBI include physical, cognitive and psychiatric disorders. It has been shown that approximately 50% of all TBI cases, regardless of severity, have some residual disability affecting their lifestyle at 1 year (Thornhill, Teasdale et al. 2000), and the cognitive and psychiatric disturbances that follow TBI are often the most disabling (Ponsford, Draper et al. 2008).

2.1.5.1. TBI severity

There are several clinical scales used to grade TBI severity. These scales are important clinically as they help decide acute management and indicate long-term outcome (Levin, Gary et al. 1990, Levin 1995, Cifu, Keyser-Marcus et al. 1997). TBI severity scales typically use a combination of measures such as the duration of loss of consciousness (LOC); length of post-traumatic amnesia (PTA); and, lowest recorded Glasgow coma scale (GCS) in the first 24 hours to grade severity. Much of the time these details are poorly documented and difficult to assess retrospectively (Malec, Brown et al. 2007, NICE 2007). In the original research described in this thesis the severity of the TBI was assessed according to the Mayo Classification system (Malec, Brown et al. 2007). This system integrates the duration of loss of consciousness; length of PTA; lowest recorded GCS in the first 24 hours; and neuroimaging results (table 2.1). It provides a validated way of assessing TBI severity retrospectively using information from both the patient and their clinical images without relying heavily on contemporaneous medical notes, which are often incomplete. This is particularly relevant to mild TBI where it is estimated that only 50% of those admitted for observation have documented neurological observations (NICE 2007).

Table 2.1: Mayo classification of TBI severity

Injury severity	Diagnostic criteria
<i>Moderate-to-severe (Definite) TBI if one or more of the following criteria apply:</i>	
	<ol style="list-style-type: none"> 1. Death secondary to TBI 2. LOC over 30 minutes 3. Anterograde PTA over 24 hours after injury 4. GCS <13/15 recorded in the first 24 hours after injury (attributable to TBI and no other confounding factors) <p><i>One of more of the following imaging findings:</i></p> <ol style="list-style-type: none"> 1. Intracerebral, subdural or epidural haematoma 2. Cerebral contusion 3. Penetration of the dura 4. Subarachnoid haemorrhage 5. Brainstem injury
<i>Mild (Probable) TBI if none of the above criteria apply but patients have one or more of the following:</i>	
	<ol style="list-style-type: none"> 1. LOC for any time less than 30 minutes 2. Anterograde PTA for any time less than 24 hours 3. Depressed basilar or linear skull fracture with intact dura
<i>Symptomatic (Possible) TBI if none of the above criteria apply but patients have one or more of the following symptoms after their injury:</i>	
	<ol style="list-style-type: none"> 1. Blurred vision 2. Headache 3. Focal neurological symptoms 4. Dazed 5. Dizziness

6. Nausea

7. Confusion

I used the Mayo Classification system as it was designed in part to facilitate post-hoc assessment of TBI severity in research studies and non-acute clinical settings. The system also attempts to reduce the false positive rate in diagnosing mild TBI by requiring positive evidence of a brain injury in this group (Malec, Brown et al. 2007).

2.1.5.2. Moderate-to-severe traumatic brain injury

In this discussion I have grouped moderate and severe TBI patients together as they are in the Mayo classification system. As expected, several studies have demonstrated that patients with moderate-to-severe TBI have the highest mortality and lowest rate of good recovery in the time immediately after injury (Thornhill, Teasdale et al. 2000, McMillan and Teasdale 2007, Martins, Linhares et al. 2009). They are much more likely to have neurosurgical intervention based upon the criteria used to define them (i.e. the presence of intra-cranial haemorrhage and contusion). Acute mortality rates are variable across studies with mortality rates between 19% and 33% in the first few months after severe injuries (Thornhill, Teasdale et al. 2000, McMillan and Teasdale 2007, Martins, Linhares et al. 2009). The mortality rate continues to be elevated for many years after moderate and severe TBI (McMillan and Teasdale 2007, McMillan, Teasdale et al. 2011).

2.1.5.3. Mild traumatic brain injury

In the past, mild TBI had been considered by many physicians to be a relatively benign condition. While the majority of mild TBI cases make a full recovery within six

months (Belanger, Curtiss et al. 2005), there is a growing body of evidence that many patients go on to suffer long-term disabling cognitive and psychological symptoms (Thornhill, Teasdale et al. 2000, Bernstein 2002, Carroll, Cassidy et al. 2004, Vanderploeg, Curtiss et al. 2005, Miles, Grossman et al. 2008, McMillan, Teasdale et al. 2011). A study examining the one-year outcomes of a large cohort of unselected head injuries requiring assessment in an accident and emergency department found some unexpected results in terms of long-term outcomes after TBI. The incidence of moderate-severe disability at 1-2 years was roughly the same in mild, moderate and severe TBI. Disability (either moderate or severe) was reported at 1-2 years in 47%, 45% and 48% of patients with mild, moderate and severe TBI respectively (Thornhill, Teasdale et al. 2000). This work and other similar studies (Bernstein 2002, Vanderploeg, Curtiss et al. 2005, Himanen, Portin et al. 2006, Miles, Grossman et al. 2008) contradict the previous view that mild TBI was either without consequence or that any consequences were psychogenic (Matthews 2009).

1.5.4. Long-term outcome after TBI

Morbidity

One of the most comprehensive longitudinal observational studies in TBI followed a group of unselected TBI patients with varying severity levels at 1-2 year (n=549) (Thornhill, Teasdale et al. 2000), 5-7 years (n=475) (Whitnall, McMillan et al. 2006), and 12-14 years (n=219) (McMillan, Teasdale et al. 2012) after their initial injury. As a group they showed no significant overall improvement in patients' disability scores over the next 14 years (Whitnall, McMillan et al. 2006, McMillan, Teasdale et al. 2011, McMillan, Teasdale et al. 2012). Over the first seven years after TBI approximately one quarter (29%) of patients improved in terms of their extended Glasgow outcome scale scores. However, over the same time period approximately

the same percentage (26%) deteriorated (Whitnall, McMillan et al. 2006). A similar finding was shown between 7 and 14 years with 32% deteriorating and 23% improving in terms of disability rating scales (McMillan, Teasdale et al. 2012). These studies suggest that TBI has a progressive component, rather than being a single injury with a static effect. Other long-term follow-up studies have shown to varying extents that TBI patients deteriorate over time (Himanen, Portin et al. 2006). This deterioration occurs in terms of both psychiatric disorders (Koponen, Taiminen et al. 2002) and cognitive symptoms (Himanen, Portin et al. 2006) up to 30 years after the initial injury. These studies also showed that symptom progression is not dependent upon injury severity. Mild TBI patients show a similar pattern of cognitive decline to severe patients at 30 years (Himanen, Portin et al. 2006).

Mortality

Perhaps more concerning, TBI patients also showed an increase in long-term all-cause mortality that continues to deviate from demographically matched non-head injury patients at 13 years (McMillan, Teasdale et al. 2011). The mortality of a large group of TBI patients (n=757) seen in Glaswegian emergency department followed up at 13 years was significantly greater than socio-economically matched controls (40.3% vs. 19.0%). Mortality was also significantly greater than a second control group of patients admitted to the same emergency department with comparably severe physical injuries but no head injuries (40.3% vs. 28.2%). This increase was not isolated to the severe TBI group, where increased long-term mortality might have been expected. Over the same time scale mild TBI patients had roughly twice the mortality rate of demographically matched orthopaedic injury patients (27.85 vs. 13.72 per 1000 per year). I should emphasise that the increased mortality was not simply related to risk taking behaviour and psychiatric disturbances (e.g. suicide and

use of antipsychotic medication) although a pre-morbid psychiatric history was associated with a higher risk of death. The long-term increase in mortality was mainly due to cardiovascular disease, respiratory disease and cancer. The underlying pathophysiology of this increase is not well understood.

2.2. Pathophysiology of TBI

TBI may result in focal or generalised brain damage. Clinically much emphasis is placed on focal injuries, (e.g. contusions, lacerations and intra-cranial haemorrhages) as they often determine the need for acute intervention. Diffuse generalised damage to the white matter or diffuse axonal injury (DAI) results from acceleration and rotational forces causing shear stress across axons (Meaney, Smith et al. 1995, Meaney and Smith 2011). This results in damage to the white matter connecting different cortical regions affecting their ability to interact with one another. DAI has long been recognised as a bad prognostic marker in severe TBI. It was originally described in a pathological study of TBI patients whose brain injuries caused them to develop severe cognitive problems despite an absence of focal lesions (Strich 1956). However, due in part to our increased ability to detect it *in vivo*, DAI has been recognised as a major cause of disability in TBI of all severities. Diffuse and focal injuries commonly occur together but are conceptually quite distinct and are therefore discussed separately below.

2.2.1. Focal injuries

Contusions (both haemorrhagic and non-haemorrhagic) are caused by local dysregulation of cerebral blood flow as a result of mechanical strain, prostaglandin induced vasoconstriction, and insufficient nitric oxide (Werner and Engelhard 2007). This results in a focal 'ischaemic-like' state and a cascade of cellular events follow.

Inadequate cerebral blood flow leads to anaerobic glycolysis and accumulation of lactic acid (Kochanek 1993). Acidosis causes increased membrane permeability and subsequent oedema formation. This is followed by the release of excitatory neurotransmitters, (e.g. glutamate), an influx of intracellular calcium, that leads to excitotoxicity and catabolic intracellular processes. The end point of this cascade is the programmed cell death of neurons to form a contusion.

2.2.1.1. Clinical imaging of focal injuries

Contusions are usually easy to identify using conventional Computer Tomography (CT) and MRI. The role of clinical imaging in the acute setting is primarily to determine if surgical intervention is required. Scales of injury severity, such as the Marshall scale, use the presence of high or mixed density mass lesions (i.e. contusion or haemorrhage greater than 25 cm³), along with radiological signs of raised intracranial pressure to define six subgroups of TBI severity that relate to the likelihood that neurosurgical intervention will be required (Marshall, Marshall et al. 1992).

CT findings in acute TBI, (e.g. intracranial hematoma), can be used to predict mortality at 1-year (Signorini, Andrews et al. 1999, Wardlaw, Easton et al. 2002). However, these CT findings are poor predictors of functional outcome (Sherer, Stouter et al. 2006). This is not simply a case of CT being relatively insensitive to lesion identification. While traditional MR is significantly more sensitive than CT in detecting damage following TBI, particularly non-haemorrhagic damage (Gentry, Godersky et al. 1988, Mittl, Grossman et al. 1994, Lee, Wintermark et al. 2008, Smits, Hunink et al. 2008), several MRI studies have also found that lesion load and location do not adequately explain functional outcome (Levine, Black et al. 2005, Lee, Wintermark et al. 2008, Niogi, Mukherjee et al. 2008). A possible explanation for

the inability of CT and MRI to predict functional outcome is the presence of DAI, which is easily missed with conventional imaging.

2.2.2. Diffuse axonal injury

An important yet under-diagnosed mechanism for significant brain injury is DAI. TBI may shear the axons, but more commonly damages the axonal neuro-filaments disrupting axoplasmic transport and ultimately causing neuronal disconnection (Povlishock 1993). White matter damage is initially associated with axonal swelling as the fibres accumulate intracellular cytoskeletal proteins (Raghupathi, Graham et al. 2000). Subsequently these fibres may undergo complete axotomy and Wallerian degeneration, with associated death of the neighbouring astrocytes (Povlishock, Becker et al. 1983). This type of white matter damage is referred to as DAI and causes cognitive impairment in the absence of cortical damage (i.e. “pure” DAI (Scheid, Walther et al. 2006)). This phenomenon was first described in print in 1956 (Strich 1956). They used the term ‘diffuse degeneration of the cerebral white matter’, to describe the histological findings in a group of five patients that survived severe closed head injury but were left with a severe ‘dementia’ despite the absence of intracranial haematomas, cerebral contusions or skull fractures.

Until the 1980s DAI was a histologically confirmed diagnosis, and graded into three categories based upon the distribution of focal lesions in addition to microscopic evidence of DAI. Grade 1 involved only microscopic evidence of DAI; Grade 2 required additional macroscopic lesions localized to the corpus callosum; and, Grade 3 required addition of macroscopic lesions in the dorsolateral quadrant of the rostral brain stem (Adams, Graham et al. 1991) As imaging techniques have improved, particularly with the advent of MRI, milder forms of DAI have been identified and recognition of DAI as a disorder with a range of severity has been established.

2.2.2.1. Clinical imaging of diffuse axonal injury

Conventional neuroimaging methods have underestimated the presence of DAI following TBI (Gentry, Godersky et al. 1988, Park, Park et al. 2009). CT is the first line imaging modality used to assess head injury and has a low sensitivity for DAI (less than 20% in some studies) (Gentry, Godersky et al. 1988). Similarly, DAI cannot be specifically detected on standard MRI sequences. However, MR sequences sensitive to iron deposition, such as gradient echo and susceptibility-weighted imaging (SWI), are being increasingly used clinically in the assessment of haemorrhages after TBI. SWI capitalizes on differences in magnetic susceptibility between tissues to provide a novel type of MR contrast (Haacke, Mittal et al. 2009, Mittal, Wu et al. 2009). SWI and gradient echo MR sequences have a particular role in the detection of tiny haemorrhages within the white matter (micro-bleeds) (Scheid, Preul et al. 2003). Micro-bleeds are a surrogate marker of DAI not usually visible on conventional MRI (Scheid, Preul et al. 2003). SWI has recently been shown to be particularly sensitive at detecting micro-bleeds (Chastain, Oyoyo et al. 2009, Beauchamp, Ditchfield et al. 2011)(Figure 2.1). Micro-bleed load alone appears to be a limited predictor of functional outcome (Chastain, Oyoyo et al. 2009), although the distribution of micro-bleeds may be a better indicator of their functional significance (Scheid, Preul et al. 2003, Scheid, Walther et al. 2006). However, assessment with SWI is potentially limited by its insensitivity to non-haemorrhagic DAI (Chastain, Oyoyo et al. 2009).

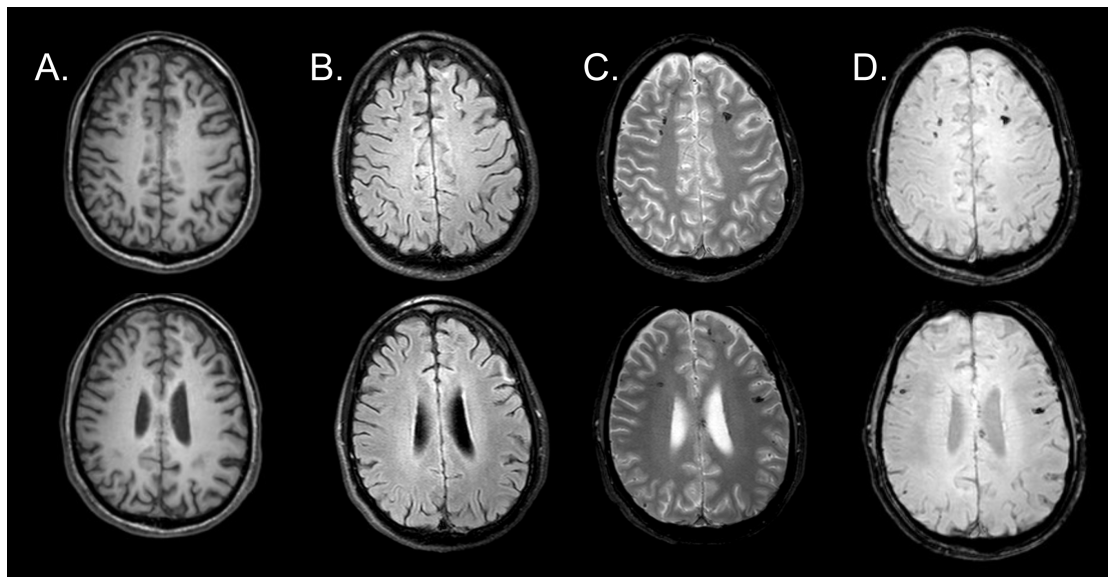


Figure 2.1: Micro-bleeds.

All panels are of the same TBI patient with haemorrhagic micro-bleeds in the frontal lobes demonstrated on different MRI modalities. (A) T1 weighted MRI, (B) T2-FLAIR, (C) T2-FFE, and (D) SWI.

Despite techniques such as SWI increasing its sensitivity, animal studies have shown that histologically proven axonal injury can appear normal even on traditional MRI sequences (i.e. T1, T2 and diffusion weighted images (DWI)) (Mac Donald, Dikranian et al. 2007, Li, Li et al. 2011). DAI has even been demonstrated neuropathologically in a small number mild TBI patients who died from unrelated causes (Blumbergs, Scott et al. 1994, Bigler 2004). The amount of DAI also appears to be an important factor determining long-term cognitive and neuropsychiatric disability following TBI (Adams 1982, Medana and Esiri 2003).

Current CT and traditional MRI can only detect the “tip-of-the-iceberg” in terms of structural abnormalities (Bigler 2001). Histological studies have proven that even the most advanced current clinical imaging modalities can miss histologically proven brain damage in the form of DAI (Blumbergs, Scott et al. 1994, Bigler 2004). Neuroimaging techniques that provide a non-invasive way of studying white matter structure in greater detail could significantly impact the management of TBI. Diffusion tensor imaging is such a technique (DTI) (discussed in detail below) and represents an important developing avenue in TBI research. DTI may be especially relevant to

mild TBI where the presence of normal conventional imaging often results in uncertainty about whether a patient's symptoms have an organic basis.

2.3. Research imaging techniques in TBI

2.3.1. Diffusion tensor imaging

Recently developed MRI sequences such as DTI allow white matter integrity to be quantified (Huisman, Schwamm et al. 2004, Kinnunen, Greenwood et al. 2011, Hellyer, Leech et al. 2012). By providing a non-invasive way of investigating white matter structure at particular anatomical locations DTI provides a more flexible way of investigating white matter damage than the previously described structural MRI sequences. The theory behind DTI is discussed in depth in Chapter 3. In brief, DTI provides several measures of white matter integrity based upon how well water diffuses in different directions. The key measures used in the discussion below are: fractional anisotropy, a measure of the directionality of water diffusion; mean diffusivity, a measure of how easily water diffuses in any direction; axial diffusivity, a measure of how easily water diffuses along the direction water diffuses most easily; and, radial diffusivity, a measure of how easily water diffuses in directions perpendicular to the direction water diffuses most easily. In general, large fractional anisotropy and lower mean diffusivity is thought to be associated with greater white matter axonal integrity. The other measures are more difficult to interpret, especially in the context of acute TBI (discussed below).

2.3.2. Pathological correlates of DTI

DAI represents a complex series of pathological processes that lead to neuronal dysfunction. DTI may be able to distinguish underlying pathologies such as axonal injury and demyelination, as axial diffusivity and radial diffusivity appear to

predominantly reflect axonal and myelin sheath abnormalities, respectively (Beaulieu, Does et al. 1996, Song, Sun et al. 2002, Sun, Liang et al. 2008). However, these relationships are likely to depend in part upon the mechanism of injury (Obenaus, Robbins et al. 2007) and a detailed understanding of the way in which DTI metrics relate to the evolving pattern of injury after TBI is still needed. Animal studies have demonstrated that DTI measures of white matter integrity become abnormal quickly after brain injury and evolve dynamically over time (Mac Donald, Dikranian et al. 2007).

Although studies have largely confirmed that DTI provides a sensitive way of identifying white matter abnormality (Inglese, Makani et al. 2005, Kumar, Gupta et al. 2009, Smits, Houston et al. 2010, Cubon, Putukian et al. 2011, Kinnunen, Greenwood et al. 2011, Messe, Caplain et al. 2011). It is still uncertain which the most sensitive DTI measurement is. This partly reflects the way DTI measures dynamically change after injury, which means that time since injury is an important factor in interpreting DTI results. Studies of mild TBI where most or all patients were scanned over 2 weeks after injury have shown either increased mean diffusivity, or decreased fractional anisotropy or a combination of the two (Inglese, Makani et al. 2005, Kumar, Gupta et al. 2009, Smits, Houston et al. 2010, Cubon, Putukian et al. 2011, Kinnunen, Greenwood et al. 2011, Messe, Caplain et al. 2011). Two studies have noted increased mean diffusivity without a decrease in fractional anisotropy (Cubon, Putukian et al. 2011, Messe, Caplain et al. 2011) and two a decrease in fractional anisotropy without an associated increase in mean diffusivity (Kumar, Gupta et al. 2009, Smits, Houston et al. 2010).

The type of DTI abnormality is different in the more acute phase of mild TBI. This is likely to reflect neuropathological processes occurring early after injury. Studies investigating patients in the first week provide evidence that increased fractional anisotropy and decreased mean diffusivity and/or reduced radial diffusivity are seen

acutely after mild TBI (Bazarian, Zhong et al. 2007, Wilde, McCauley et al. 2008, Chu, Wilde et al. 2010, Mayer, Ling et al. 2010, Wu, Wilde et al. 2010) (although there are exceptions (Arfanakis, Haughton et al. 2002)). These acute changes have been shown to correlate with symptom severity (Bazarian, Zhong et al. 2007, Wilde, McCauley et al. 2008, Chu, Wilde et al. 2010, Mayer, Ling et al. 2010, Wu, Wilde et al. 2010). The numbers of participants in these studies have in general been small, although a slightly larger longitudinal study of 22 adults with mild TBI and no abnormalities on standard clinical neuroimaging recently reported similar DTI results (Mayer, Ling et al. 2010). Patients investigated a mean of 12 days post injury showed increased fractional anisotropy and reduced radial diffusivity in the corpus callosum and a number of tracts in the left hemisphere. These DTI measures assisted with the classification of mild TBI vs. age-matched controls, which neuropsychological tests did not.

Due in part to recent high profile media coverage, there is growing interest in sports related post-concussive symptoms. The results of DTI studies of sport related concussions have been variable. Cubon et al. (Cubon, Putukian et al. 2011) assessed DTI measures in nine patients with sport related post-concussive symptoms for more than one month after injury. These patients showed DTI changes comparable to previous studies of mild TBI, (i.e. elevated mean diffusivity and reduced fractional anisotropy). In contrast, Henry et al, (Henry, Tremblay et al. 2011) reported reduced mean diffusivity and elevated fractional anisotropy in a group of athletes with post-concussive symptoms. Another study, (Zhang, Johnson et al. 2010) failed to find clear abnormalities in 15 asymptomatic concussed athletes 30 days after injury. The reason for these inconsistencies is unclear but may reflect between study differences in mechanisms of injury, injury severity, time since injury, or simply under sampling of a heterogeneous patient group.

2.3.3. Sensitivity of DTI

All published DTI studies of moderate-to-severe TBI have shown some form of DTI abnormalities in the white matter even without other evidence of trauma on traditional MRI sequences (Kinnunen, Greenwood et al. 2010, Hellyer, Leech et al. 2012). Importantly DTI changes have been shown in white matter regions that do not contain micro-bleeds, emphasizing the notion that DAI does not necessarily produce micro-bleeds (Kinnunen, Greenwood et al. 2010, Smits, Houston et al. 2010, Hellyer, Leech et al. 2012). Recent studies have largely confirmed that DTI provides a sensitive way of identifying white matter abnormality even following mild TBI (Inglese, Makani et al. 2005, Kumar, Gupta et al. 2009, Smits, Houston et al. 2010, Cubon, Putukian et al. 2011, Kinnunen, Greenwood et al. 2011, Messe, Caplain et al. 2011). However, not all studies of mild TBI have found evidence for DTI abnormalities (Zhang, Johnson et al. 2010). Although this study examined a group of mild TBI patients that were asymptomatic at the time of scanning. Their null result may reflect the importance of injury severity in determining the magnitude of DTI changes (Kinnunen, Greenwood et al. 2011) and the problems of studying heterogeneous groups of mild TBI patients. Clinically this null result is important as it indicates that DTI changes are specific to patients with a symptomatic pathology.

2.3.4. Clinical relevance of DTI

Most previous work has focused on the more severe end of the TBI spectrum. In this context, DTI abnormalities appear to be clinically relevant as they partly predict clinical outcome (Sidaros, Engberg et al. 2008) and have been shown to correlate with cognitive impairment (Salmond, Menon et al. 2006). Longitudinal studies have shown that the degree of white matter disruption, measured by DTI and micro-bleed load, correlates with patients' recovery (Marquez de la Plata, Ardelean et al. 2007, Sidaros, Engberg et al. 2008), and the acute disruption, measured less than 2 weeks

(Scheid, Preul et al. 2003, Marquez de la Plata, Ardelean et al. 2007) and 5-11 weeks post-TBI (Sidaros, Engberg et al. 2008), predicts outcome at 6 and 12 months respectively.

An important question is whether white matter damage after TBI causes specific clinical problems. A number of recent studies have shown that the pattern of DTI abnormality is correlated with cognitive impairment (Sugiyama, Kondo et al. 2009, Levin, Wilde et al. 2010, Smits, Houston et al. 2010, Kinnunen, Greenwood et al. 2011, Newcombe, Outtrim et al. 2011). White matter integrity has been shown to be correlated with general post-concussive symptoms (Smits, Houston et al. 2010), as well as with more specific cognitive impairments (Sugiyama, Kondo et al. 2009). Neuropsychiatric symptoms such as depression and anxiety are also prominent after TBI (Whitnall, McMillan et al. 2006). Chu et al (Chu, Wilde et al. 2010), provided evidence that DTI measures in the acute phase (< 6 days) after injury correlate with the severity of emotional symptoms in a group of ten mild TBI patients. In addition, grey matter DTI measurements have also been shown to correlate with impairments of impulsivity in patients of mixed severity TBI (Newcombe, Outtrim et al. 2011). These studies are important as they suggest that although the damage produced by TBI may be diffuse, damage to key tracts or brain regions involved in a particular cognitive function may determine the specific pattern of cognitive impairment that an individual experiences after TBI. A clear example of this principle is provided by the demonstration that aspects of memory function after TBI are correlated with the structural integrity of the fornix, a white matter tract connected to the hippocampi and forming part of the Papez circuit, this finding was reported for a group of patients with mixed severity TBI (Kinnunen, Greenwood et al. 2011) and a separate group with mild TBI alone (Sugiyama, Kondo et al. 2009).

2.3.5. Functional magnetic resonance imaging

Assessing the integrity of critical brain networks through structural imaging provides a way of measuring structural damage. However, this assessment does not give a measure of brain function. Functional imaging is commonly used to provide such a measure. There are several modalities of functional imaging but in this thesis I focus on functional (f)MRI because of its flexibility and excellent spatial resolution compared to other modalities.

Functional MRI utilises the different magnetic properties of oxyhaemoglobin and deoxyhaemoglobin to make use of a blood oxygen level dependent (BOLD) contrast, which reflects regional blood flow in the brain (discussed in detail in Chapter 3). The blood flow is then used as a surrogate marker of neuronal activity to map regional variations in brain activity that can be related to specific cognitive functions (see Chapter 3 for a detailed discussion). Several studies have used fMRI to show differences in regional brain activity between TBI patients and healthy controls during task (McAllister, Saykin et al. 1999, Scheibel, Pearson et al. 2003, Soeda, Nakashima et al. 2005, Schmitz, Rowley et al. 2006, Witt, Lovejoy et al. 2010, Bonnelle, Leech et al. 2011, Bonnelle, Ham et al. 2012). Functional MRI can also be used to provide measures of the correlation of brain activity across distinct brain regions (i.e. functional connectivity). The functional relationship between different nodes of a network may be particularly useful in studying network breakdown following TBI as their cognitive impairments are likely mediated, at least in part, by disruption of the white matter tracts connecting the nodes within networks. Studies using both functional connectivity and changes in local brain activity in the context of specific neural networks are discussed in detail below.

2.3.6. Relationship between MRI measures of structural and functional connectivity

In the healthy brain there is a clear relationship between structural connectivity, measured by DTI metrics, and functional connectivity (Greicius, Supekar et al. 2009). Regions that show large white matter connections tend to show high-levels of functional connectivity (van den Heuvel, Mandl et al. 2009). Although this is not essential, and regions can be functionally connected without a white matter connection (Damoiseaux and Greicius 2009). A multimodal MRI study has shown that DTI measures of damage to the splenium of the corpus callosum correlates with reduced functional connectivity within the brain's 'default' mode network, providing convincing evidence that white matter damage can disrupt the functional interactions of nodes in a network (Sharp, Beckmann et al. 2011). Hence, the pattern of white matter damage produced by TBI may predict changes in functional connectivity after TBI. Evidence supporting this hypothesis is beginning to accumulate (Mayer, Mannell et al. 2011, Sharp, Beckmann et al. 2011, Stevens, Lovejoy et al. 2012).

2.3.7. EEG and MEG assessment of TBI

My thesis focuses on MRI techniques; however other modalities have been used to assess brain function following TBI. As I have not used these methods in my original research I shall only mention them briefly. fMRI studies have the advantage of high spatial resolution, but lack temporal resolution. Electroencephalography (EEG) and magnetoencephalography (MEG) provide high temporal resolution, but poor spatial resolution, and have been used extensively to study TBI (Kane, Moss et al. 1998, Huang, Theilmann et al. 2009, Castellanos, Paul et al. 2010, McCrea, Prichep et al. 2010, Naunheim, Treaster et al. 2010, Huang, Nichols et al. 2012, Prichep, McCrea et al. 2012). A numbers of recent EEG studies have focused on their use as a potential aid to diagnosis and prognostication after TBI. In the acute phase,

quantitative EEG measures, such as the EEG power spectrum, have been able to accurately stratify TBI severity (Kane, Moss et al. 1998, Naunheim, Treaster et al. 2010) and to differentiate sport-related concussions from controls (McCrea, Prichep et al. 2010, Prichep, McCrea et al. 2012). In addition, two recent MEG studies detected abnormal slow-wave activity in soldiers exposed to blast and also mild TBI patients, when both group had normal clinical imaging (Huang, Theilmann et al. 2009, Huang, Nichols et al. 2012). The first of these studies found MEG abnormalities to be an even more sensitive measure of injury severity than DTI (Huang, Nichols et al. 2012). Another MEG study has shown excessive slow-wave activity compared to controls after TBI, which tends to normalize with recovery, suggesting a dynamic marker of injury that could potentially facilitate clinical decisions (Castellanos, Paul et al. 2010). A longitudinal EEG study of sports related concussions suggested that quantitative EEG may be a sensitive tool in diagnosing mild TBI, and may be better than clinical measures at assessing how long patients will take to recover (McCrea, Prichep et al. 2010).

2.4. Cognitive functions investigated in this thesis

In this thesis I investigate the neural basis of self-awareness deficits following TBI. Self-awareness is a complex cognitive process and in order to study it I have focused on one of its key components, 'on-line' awareness of on-going events (Prigatano and Schacter 1991, O'Keefe, Dockree et al. 2004). This has been examined previously by using performance monitoring as a surrogate marker (Hart, Giovannetti et al. 1998, O'Keefe, Dockree et al. 2004). Before discussing the impact of TBI on and the proposed neural basis of these functions, I shall review some of the prevailing cognitive theories behind self-awareness, performance monitoring, how they relate to one another and how they can be assessed experimentally.

2.4.1. Self-awareness

There is no universally accepted definition of self-awareness. In general terms it can be thought of as the integration of information about the external environment and matching it to one's perceptions of one's self (Fleming, Strong et al. 1996). This requires the ability to monitor new information and use that information to modify your beliefs. Like a lot of people, patients with self-awareness deficits may have inappropriate prior beliefs about their abilities. However, patients with self-awareness deficits do not adapt those beliefs even when they are tested and found to be incorrect.

In terms of disability, self-awareness can be separated into a three level hierarchy: firstly, recognition of the disability; secondly, recognition of that disability's likely impact on one's life; and, thirdly, making realistic plans and goals for future development (Prigatano, Altman et al. 1990, Fleming, Strong et al. 1996). Every level of this hierarchy requires the ability to accurately accrue external information and weigh it against internal beliefs.

2.4.1.1. Measuring self-awareness

Self-awareness has been quantified in a number of ways (Fleming, Strong et al. 1996, O'Keeffe, Dockree et al. 2007). Questionnaires have been widely used to identify discrepancies between assessments of disability made by the patient and others, providing a 'meta-cognitive' measure of self-awareness (O'Keeffe, Dockree et al. 2007, Vanderploeg, Belanger et al. 2007). Whilst useful, this type of assessment is limited by its subjective nature, and by the influence of transient factors such as mood, and the inconsistency of observer evaluations (Fleming, Strong et al. 1996). An alternative approach is to have subjects perform a task and then rate how good

they were at the task. This provides an objective semi-quantified measure of how accurately subjects rate their performance (Hart, Giovannetti et al. 1998). Building upon this, some groups have suggested that lack of more general self-awareness is associated with lack of local awareness of on-going performance (Prigatano and Schacter 1991, O'Keeffe, Dockree et al. 2004). It has been shown in several studies that TBI patients with impaired awareness on meta-cognitive measures correct fewer errors and show reduced physiological response to errors they do correct (O'Keeffe, Dockree et al. 2004, Larson, Kaufman et al. 2007). This suggests that the patients have broad problems monitoring on-going activity. Studies have further proposed that patients' abilities to respond to their own errors or 'on-line' performance monitoring can be used as a surrogate marker of more general problems with self-awareness (Hart, Giovannetti et al. 1998, O'Keeffe, Dockree et al. 2004). Using performance monitoring as an 'on-line' measure of awareness offers an alternative to questionnaire assessments that is both quantifiable and operator independent.

2.4.2. Performance monitoring and cognitive control

In this thesis I have used 'on-line' performance monitoring as a surrogate marker of self-awareness after TBI, as it provided a quantifiable measure that was particularly amenable to testing with a task-based fMRI paradigm (see Chapter 3). It can be measured by looking at the adaptive behaviour that occurs in response to an unplanned or unwanted event (e.g. an error) (Larson, Kaufman et al. 2007, Ornstein, Levin et al. 2009). In order for such events to be responded to they need to be detected by some form of monitoring system. If an error is detected then it frequently leads to behavioural adaptation, often described in terms of increased 'cognitive control'. I discuss in detail below how performance monitoring, and cognitive control relate to one another and how they can be assessed.

2.4.2.1. Cognitive control

Cognitive control is a term used to describe the process where one “overrides or augments reflexive and habitual reactions in order to orchestrate behavior in accord with our intentions” (Miller 2000). It is an effortful process that requires allocation of attentional resources, response biasing and selection of contextually relevant information to adapt behaviour (Botvinick, Braver et al. 2001, Ridderinkhof, Ullsperger et al. 2004). It forms an essential element in the control of adaptive goal-directed behaviour (Botvinick, Braver et al. 2001). Cognitive control involves monitoring on-going behaviour to check if an outcome is as expected and changing behaviour (adaptation) if it is not (Figure 2.2).

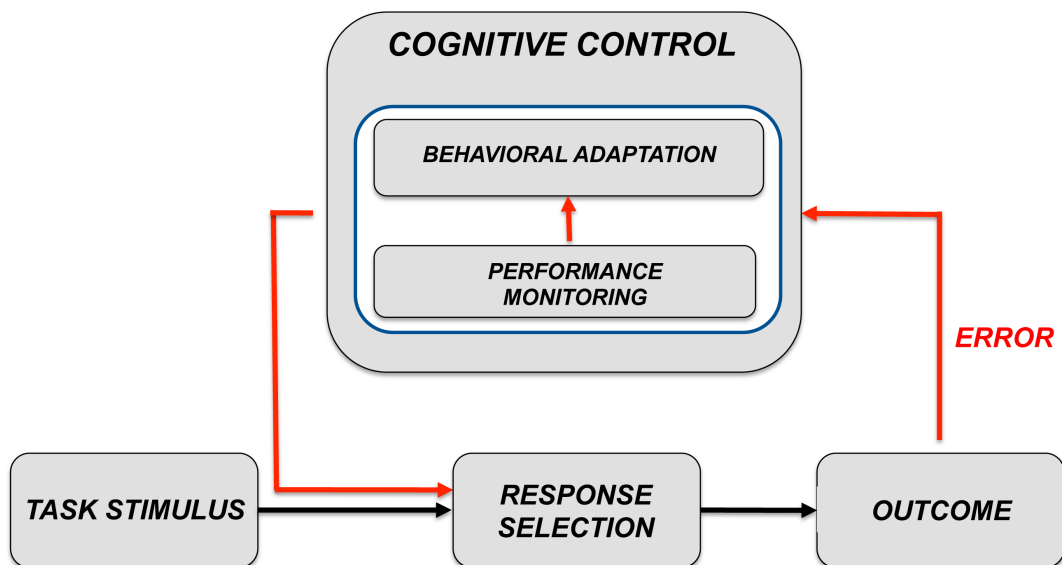
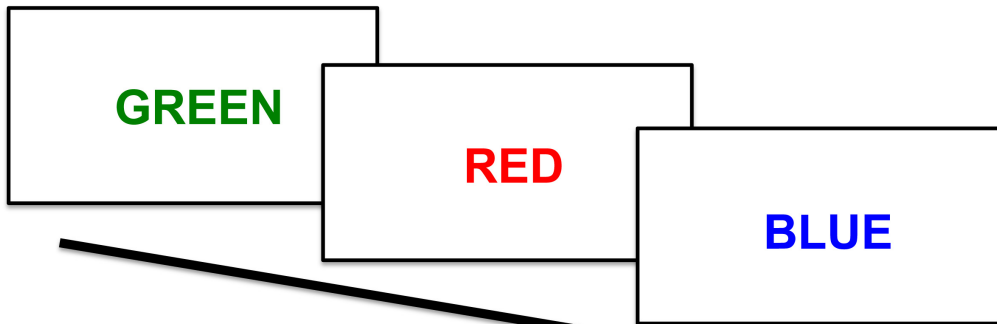


Figure 2.2: Schematic representation of the processes involved in cognitive control

These principles can be illustrated by thinking about the Stroop task (Stroop 1935), which is a classical test of cognitive control. Subjects are presented with written

words and in one condition instructed to respond with the colour of the ink not the word itself (Figure 2.3).

a. Congruent trials



b. Incongruent trials

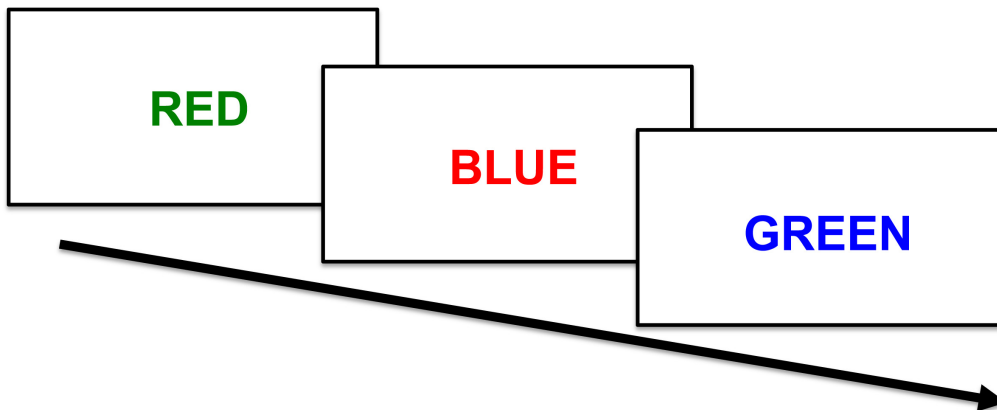


Figure 2.3: The Stroop test

Each panel is an example of possible stimuli subjects would be presented with on: a.) congruent and b.) incongruent trials of the Stroop test.

Because reading is such an over-learned activity the subjects' automatic prepotent response is to read the word. The trials in which the word is the same as the ink colour (i.e. congruent trials) involve little control because the prepotent response is the correct one. Cognitive control is engaged when the two features of the stimuli are incongruent, (e.g. when the word 'blue' appears in red ink). In incongruent trials if subjects do not inhibit the prepotent response they respond incorrectly (a commission error).

Post-error behavioural adaptation can be used to measure cognitive control after an error has been detected. The more complicated the task the more difficult it becomes to interpret the behavioural adaptation. Some of the simplest, and therefore most interpretable, tasks designed to produce errors use 'conflict'. Most theories of cognitive control propose some degree of separation between the monitoring and implementation of adaptation. The 'conflict-monitoring' model theorises that cognitive control is engaged when 'conflict' is detected (Botvinick, Braver et al. 2001). It is assumed that multiple cognitive processes take place parallel to one another. Conflict exists when these parallel processes require different outputs. In the context of the Stroop task, ink colour recognition and word reading are two separate but tandem processes. Congruent trials are low conflict because both processes have the same output. Incongruent trials are high conflict because the processes call for different mutually-exclusive outputs. Situations with high degrees of conflict are more likely to be associated with commission errors (e.g. the Stroop and Simon tasks). Commission errors engage cognitive control and lead to a predictable post-error slowing of response times (Rabbitt 1966, Rabbitt 1966, Rabbitt 1968, Hajcak, McDonald et al. 2003). This behavioural adaptation makes subsequent errors less likely and can be used to detect if cognitive control has been engaged.

2.4.2.2. Engaging cognitive control: error types

An important question is how cognitive control is engaged. Errors by their nature are unwanted outcomes of one's actions. Therefore, errors often signal the need for increased cognitive control to avoid future errors being made. Investigating subjects' response to different types of error provides an eloquent way of examining cognitive control and by extension performance monitoring (as accurate performance monitoring is necessary for cognitive control it to be engaged appropriately). There are many different types of error that can be grouped together into broad categories.

In this thesis I examine the behavioural and neurological response to commission, inhibition and timing errors.

Commission errors

Commission errors occur when subjects' responses are inappropriate for the given stimuli. There are many reasons why subjects perform commission errors. Errors on a task can be produced by rule changes (e.g. the Wisconsin Card Sorting task (Milner 1963)), or providing misrepresentative or incomplete task information, (e.g. the information sampling task used in the Cambridge neuropsychological test automated battery (CANTAB)). As mentioned above, conflict is a useful way of producing commission errors as it can be implemented using very simple choice reaction tasks, (e.g. the Simon tasks, described in Chapter 3). The simplicity of these tasks facilitates the examination of the behavioural adaptation that follows the error. Commission errors are normally associated with a predictable behavioural adaptation in the form of post-error slowing (Rabbitt 1966, Rabbitt 1966, Rabbitt 1968, Hajcak, McDonald et al. 2003) (described above). In this thesis I use measures of post-error slowing to confirm that cognitive control has been engaged following an error.

Inhibition errors

Inhibition errors involve failure to suppress or 'inhibit' one's response to stimuli. They differ from commission errors in that the correct response is no response at all. The stop-signal task (SST) is used to produce inhibition errors (Logan, Cowan et al. 1984, Li, Yan et al. 2007, Li, Huang et al. 2008, Li, Chao et al. 2009, Ornstein, Levin et al. 2009, Verbruggen and Logan 2009, Sharp, Bonnelle et al. 2010). It has previously been used to investigate attention, response inhibition and error processing in

healthy controls and TBI patients (Sharp, Bonnelle et al. 2010, Bonnelle, Leech et al. 2011, Bonnelle, Ham et al. 2012). The SST is a simple choice reaction task where subjects are presented with arrow cues that require them to respond with either a left or right-sided button press depending on the direction of the arrows. The stop-signal appears on a sub-set of trials to instruct subjects that they are not to respond to that trial. If subjects respond when the stop-signal is present that is termed an 'inhibition error' (the SST is discussed in detail in Chapter 3). Inhibition errors share many features with commission errors. Both involve the inappropriate response to a stimuli and both engage cognitive control and a predictable behavioural adaptation in the form of post-error slowing.

Timing errors

Responding correctly is not just making the correct choice but doing so at the appropriate time. Errors can be considered to occur when subjects respond outside of the rules of the task. Therefore, if subjects are instructed to respond within a certain time frame and fail to do so this is considered a 'timing error' (Miltner, Braun et al. 1997, Luu, Flaisch et al. 2000). This type of error has been studied much less than either commission or inhibition errors and differs from these errors in two key respects. Firstly, they are difficult to recognise and often require external feedback (Miltner, Braun et al. 1997, Luu, Flaisch et al. 2000). Secondly, they do not involve an inappropriate response or conflict (Miltner, Braun et al. 1997). Thirdly, timing errors should signal the opposite behavioural adaptation to commission and inhibition errors, (i.e. the post-error behavioural adaptation should be an accelerated response time).

2.4.3. Attention

The cognitive control model outlined in above (Figure 2.2) makes the significant assumption that subjects are attending to the task. It is important to consider cognitive control in the context of broader behaviour where the focus of attention is a key factor. Subjects often do not find the paradigms captivating and as a consequence have to exert cognitive effort to pay attention to the tasks designed. The appropriate allocation of attentional resources to task relevant information and suppression of task irrelevant information is one aspect of attention discussed below (Botvinick, Braver et al. 2001).

2.4.3.1. Existing models of attention

Attention has been defined as the cognitive process of selectively concentrating on one aspect of the environment while ignoring others (James 1890). Several models have tried to separate this broad definition into more useful components. One influential model has been proposed by Posner (Posner and Petersen 1990). In Posner's model attention has three main functions: firstly, orienting to sensory stimuli; secondly, detecting signals for conscious processing; and thirdly, maintaining a state of alertness.

The three functions work synergistically. The first two functions relate to action selection or selective attention. Selective attention involves prioritising the relevant features in incoming information that need to be attended to in order to best achieve one's goals. These processes seem to overlap to a degree with what other models consider to be cognitive control. For example, according to Botvinick's description a key function of cognitive control is the appropriate allocation of cognitive and attentional resources (Botvinick, Braver et al. 2001). There is considerable overlap between the constructs of selective attention and cognitive control and it is slightly artificial, although useful for discussion, to separate them. An 'attentional load model' has been developed, which attempts to merge these descriptive terms and states

that appropriate orientation to sensory stimuli and signal detection is the result of cognitive control selectively weighting different features for attentional processing (Lavie, Hirst et al. 2004, Lavie 2011). For example, successful performance of the Stroop test could be interpreted as cognitive control mechanisms weighting the word colour as the key feature to attend to and de-weighting the lexical information.

The third element in Posner's model (alertness) is a measure how ready a subject is to respond to stimuli. Alertness is distinct from cognitive control and is described as a measure of attention intensity (i.e. how primed the system is to respond to any stimuli). Alertness can be further divided into: tonic alertness, defined as the internal control of arousal in the absence of external cues; and phasic alertness, defined as the externally driven increase in response readiness for a short time period after a sensory cue.

A second prominent theory of attention that has emerged mainly from neuroimaging work has been proposed by (Corbetta and Shulman 2002). This model states that attention can be separated conceptually into endogenous and exogenous attention. Endogenous attention comprises the internally driven, goal-directed 'top-down' process of preparing oneself to respond to stimuli, whereas exogenous attention involves increases in attention driven by 'bottom-up' sensory stimuli (Corbetta and Shulman 2002). This model differs conceptually from Posner's model by focusing on mechanisms of alertness. In this model the selective attention aspects of Posner's model are combined under the umbrella of endogenous attention. Importantly, as this model is derived from neuroimaging work it has a strong anatomical description of the systems involved in these processes. It describes exogenous and endogenous attention as being regulated by the ventral and dorsal attentional networks respectively (the anatomy of these networks is described below).

2.4.3.2. Measuring attention

Subjects' attention to a task can be assessed by measuring their reaction times in response to task stimuli (Posner and Petersen 1990). Variability in subjects' reaction times is considered a reflection of how well individuals sustain their attention over the course of the task (i.e. sustained attention). It has been shown that the use of a warning signal can transiently augment subjects' attention during a task (Sturm, de Simone et al. 1999, Stuss, Alexander et al. 2005, Perin, Godefroy et al. 2010). This phenomenon could be interpreted as an example of taking advantage of the exogenous 'bottom-up' modulation of attention when the endogenous 'top-down' system is not functioning effectively.

2.5. Cognitive impairment after TBI

TBI produces a heterogeneous patient group with a broad range of neurological symptoms. Despite the heterogeneity of the group, the cognitive deficits described in TBI follow a consistent pattern. Several studies have shown predominantly deficits of attention, executive function, memory, and processing speed. One study of 60 chronic TBI patients with of varying severity showed predominantly deficits of attention, executive function and memory. In this study severity of injury, assessed clinically, was related to the severity but not the type of cognitive deficits seen (Draper and Ponsford 2008). A large body of literature exists that examines some of the specific cognitive deficits produced by TBI. These include studies of self-awareness, (Fleming, Strong et al. 1996, Sherer, Hart et al. 2003, Bach and David 2006), performance monitoring and cognitive control (Larson, Fair et al. 2011, Larson, Farrer et al. 2011), working memory (Gronwall and Wrightson 1981, Mcallister, Flashman et al. 2004) and attention (Robertson, Manly et al. 1997, Arciniegas, Held et al. 2002, Draper and Ponsford 2008, Bonnelle, Leech et al. 2011, Bonnelle, Ham et al. 2012). These cognitive deficits experienced after TBI are

important functionally, and can be used to help predict long-term outcome. One of the largest studies examined a cohort of inpatients (n=388) in the acute phase (<1 month) after injury across six different trauma rehabilitation units (Sherer, Sander et al. 2002). They used multivariate analysis taking into account PTA duration, education level and premorbid productivity level, and found that patients who scored in the top 25 percentile on a range of on a range neuropsychometric tests including logical memory, in the acute setting were much more likely to be productive at 1 year post-injury (odds ratio 1.61 corrected for covariant factors such as severity). Other studies have also shown that better scores on a range of neuropsychometric tests are associated with better outcomes in terms of returning to work or education at 1-10 years post-injury (Fraser, Dikmen et al. 1988, Dikmen, Temkin et al. 1994, Boake, Millis et al. 2001, Ponsford, Draper et al. 2008). Acute tests of working memory have been used retrospectively to differentiate TBI patient in work at one year, taking into account injury severity (Cifu, Keyser-Marcus et al. 1997). Similarly, working memory scores 10 years after TBI have been shown to correlate with employment (Wood and Rutterford 2006). Wechsler Adult Intelligence Scale-Revised (WAIS-R) scores taken in the acute phase after TBI have been used to predict employment at 1 year post-injury with an accuracy of 92% (Goran, Fabiano et al. 1997). There is some evidence that this relationship persists long term with better scores on neuropsychometric tests of processing speed and verbal memory being associated with improved outcome on the Glasgow Outcome Scale at 5-7 years (Whitnall, McMillan et al. 2006).

As mentioned above, self-awareness deficits are a particularly disabling cognitive feature of TBI and linked in many cognitive models to performance monitoring and attention. Below I discuss the existing evidence of how TBI affects these functions, before reviewing the literature on their neural basis in the healthy brain.

2.5.1. The impact of TBI on self-awareness

One of the most frequent and disabling cognitive consequences of TBI are the impairments of self-awareness they can experience (Prigatano and Altman 1990, Vanderploeg, Belanger et al. 2007). The accuracy of one's self-perception affects how subjects interact with the world at large (Johnson, Baxter et al. 2002). For this reason, persistently impaired self-awareness and abnormal perception of oneself can be a major clinical problem as it limits the effectiveness of rehabilitation (Sherer, Hart et al. 2005), and is associated with poor functional outcomes (Sherer, Hart et al. 2003, O'Keeffe, Dockree et al. 2007). There is some evidence that awareness of physical disability after TBI is more likely to recover than awareness of emotional or cognitive disabilities (Prigatano, Altman et al. 1990). This suggests that these deficits can improve and may reflect the subtle nature of many of the cognitive deficits relative to the physical ones. No longitudinal studies have addressed the issue of how quickly self-awareness recovers.

Despite the large clinical problem it represents there is relatively little literature on the neural basis of self-awareness problems after TBI. Other neurological diseases associated with self-awareness deficits have been studied in more detail. Deficits of awareness are commonly seen after stroke. Anosognosia, or the inability to detect one's disability, is a cardinal feature of neglect syndromes commonly seen when strokes damage the right frontal and parietal lobes (Husain, Shapiro et al. 1997, Husain and Rorden 2003, He, Snyder et al. 2007, Corbetta and Shulman 2011). In keeping with awareness being an emergent property of long-distance interactions between brain regions (Mesulam 1990, Taylor 1997), fronto-parietal functional connectivity is reduced in patients with spatial neglect after stroke (He, Snyder et al. 2007).

Self-awareness deficits after TBI have been reported as being more common following right hemisphere damage in TBI (Anderson and Tranel 1989, Prigatano, Altman et al. 1990), although, this is not a consistent finding across all studies (Sherer, Hart et al. 2005). A study assessing lesions load and distribution in a large group of chronic severe TBI patients (n=91) found an association between lesion load and impaired self-awareness, but no relationship to hemispheric or frontal lesion distribution (Sherer, Hart et al. 2005). The fact that lesion analysis is a poor predictor of this symptom may reflect the importance of DAI disrupting the white matter connections between regions in the right hemisphere or it may indicate that damage to a large number of different regions may cause self-awareness deficits making anatomical associations difficult to predict from univariate analyses.

One previous fMRI study provided preliminary evidence that self-awareness impairment after TBI may be associated with abnormally activity in the right superior frontal gyrus (SFG) and medial prefrontal cortex including the anterior cingulate cortex (ACC) (Schmitz, Rowley et al. 2006). This study compared brain activations in a group of 20 sub-acute TBI patients with meta-cognitive measures of impaired self-awareness to a group of healthy controls. The task involved assessing self-referential and non-self-referential personality traits (i.e. whether a trait such as 'shyness' described them or was a positive or negative attribute generally). The TBI group showed greater activation on the self-referential task in the ACC, precuneus and right temporal pole. A linear regression analysis showed a linear relationship between lower activation of the right SFG and worse self-awareness. This study concluded that self-awareness deficits might be the result of dysfunction of a neural network involving the right dorsal prefrontal cortex (Schmitz, Rowley et al. 2006). However, the main results were underpowered and did not survive statistical correction.

2.5.2. The impact of TBI on performance monitoring and cognitive control

TBI is often associated with impaired cognitive control. This has been inferred from tasks that involve multi-tasking (McDowell, Whyte et al. 1997), ignoring distractors (Polo, Newton et al. 2002), and the strategic aspects of working memory (Perlstein, Cole et al. 2004). It has also been shown directly by their behaviour on tests of cognitive control, (e.g. the Stroop test (Seignourel, Robins et al. 2005, Perlstein, Larson et al. 2006), AX-CPT task (Larson, Perlstein et al. 2006)). These studies have shown behaviourally that TBI patients have reduced ability to recognise and respond to conflict (Perlstein, Larson et al. 2006) and to maintain a task-set (Seignourel, Robins et al. 2005). Another study of children with chronic TBI showed behaviour consistent with impaired performance monitoring (i.e. reduced post error slowing) (Ornstein, Levin et al. 2009). Importantly, damage to no single region has been found to be the cause of impaired cognitive control after TBI. This may be because cognitive control is a complex process and likely involves the interaction of multiple brain regions, therefore damage to any number of regions and their connections may result in impairment.

Functional MRI studies have suggested that abnormal activation in the medial prefrontal cortical structures play a key role in cognitive control after TBI (Scheibel, Pearson et al. 2003, Scheibel, Newsome et al. 2007). The larger of these studies examined the brain activation in a group of 14 chronic severe TBI patients performing a test of cognitive control. The TBI group was compared to a control group of patient with comparably severe orthopaedic injuries. The study gave TBI patients extra training on the task to equalise performance across groups. Behaviours were matched, by design, but TBI patients showed greater activation within the anterior medial cortical structures, including the ACC, middle frontal gyrus (MFG) and supramarginal gyrus (SMG), compared to the control group despite equal

performance. This study also found a relationship between excess activity in these regions and TBI severity, although not lesion load (Scheibel, Newsome et al. 2007). They concluded that the extra activation related to increased cortical recruitment within these regions in order to adequately complete the task.

An electro-encephalography study on a large group of chronic severe TBI patients used the Stroop test to examine cognitive control. They found reduced physiological response to high conflict situations, in terms of the wave-forms associated with both detecting and responding to conflict (Perlstein, Larson et al. 2006). Other work has demonstrated that TBI can be associated with altered responses to errors both in terms of the physiological response (O'Keefe, Dockree et al. 2004); behavioural adaptation (Larson, Farrer et al. 2011); and reduced error related negativity (ERN), an EEG marker of error detection thought to arise from the dACC (Larson, Kaufman et al. 2007) (see Chapter 4).

2.5.3. The impact of TBI on attention

Problems with attention are a common complaint after TBI, and sustained attention is particularly affected (Robertson, Manly et al. 1997). Poor sustained attention contributes to the variability in task performance seen in the TBI patient group (Bleiberg, Garmoe et al. 1997), and impaired attention is likely to impede recovery of other cognitive abilities (Park and Ingles 2001). It has also been theorised that problems TBI patients have performing tasks previously attributed to executive dysfunction. For example, one study suggested that impaired performance on the Wisconsin Card-sorting test and the Tower of Hanoi task were actually due to impairments of attention rather than executive control (Rueckert and Grafman 1996). Similarly, because attention to task is measured largely by reaction times there is

some controversy over whether the assessments of attentional deficits reported after TBI are confounded by problems with processing speed (Rios, Perianez et al. 2004). Finally, although attention is primarily assessed through reaction times (Posner and Petersen 1990) studies of TBI patients have suggested that moment-to-moment lapses in attention are the cause of errors in situations that cannot be explained by conflict or other error provoking mechanisms (Robertson, Manly et al. 1997). This suggests that attentional deficits may show more behavioural problems than simply slow or variable reaction times.

2.6. The neural basis of the cognitive functions investigated in this thesis

A considerable body of literature has attempted to describe the brain structures and interactions that give rise to self-awareness, performance monitoring and attention. Below I describe some of the most influential theories concerning the neural systems that support each of these cognitive functions.

2.6.1. The neural basis of self-awareness

Philosophers and psychologists have long debated the ideas of 'self', but until recently little work had been performed to investigate its neural basis. Awareness is likely to be the result of integrative cognitive processes across distributed cortical regions rather than the sole responsibility of a particular cortical area (Mesulam 1990, Taylor 1997, Christensen, Ramsøy et al. 2006).

The theories of self-awareness I describe below share several common features. Importantly they both emphasise the importance of monitoring information and using that information to adjust ones beliefs (Northoff and Bermpohl 2004, Craig 2009). The models differ mainly in terms of the anatomical regions ascribed with these

functions. The first model states that the insulae play a pivotal role in the process of awareness (Craig 2009), in part because of its strong functional and anatomical connections to other brain regions involved in adaptive behaviour and monitoring salient events (Corbetta and Shulman 2002, Seeley, Menon et al. 2007, Uddin and Menon 2009, Uddin, Supekar et al. 2010, Kucyi, Moayedi et al. 2012). Craig's model states that there is an anterior-posterior gradient in the insulae with internal representations of 'self' being located in the posterior insulae. The mid insulae has 're-represented' versions of the self that can be modulated by on-going visceral stimuli important for the regulation of homeostasis (e.g. environmental conditions, hunger, heat and cold) (Craig 2009). Further forward, the anterior insulae has more 're-representation' of self that can be modulated by more complex behaviourally salient events and higher cognitive processes (e.g. motivation, social and cognitive considerations) (Craig 2009). This model proposes that by continual integration of all of these representations/re-representations the insulae contains a dynamic versatile representation of one's self, capable of being continually updated based upon on going information.

Evidence for this model comes from largely from neuroimaging literature. Anterior insulae activation, both bilateral and unilateral, has been associated with awareness of sensory stimuli and is commonly seen after errors (Klein, Endrass et al. 2007). Mostly this activation occurs in conjunction with activation in the anterior cingulate cortex (ACC). However, one study has demonstrated that error awareness is associated specifically with activity in the anterior insulae (Klein, Endrass et al. 2007). This study used a simple saccadic eye movement tasks to induce errors. If subjects made an error they were instructed to press a button signifying that they recognised their mistake. In this way the experiment provided an explicit measure of error awareness. Anterior insulae activation (left greater than right) was associated errors that occurred with but not without awareness (Klein, Endrass et al. 2007).

Dorsal (d)ACC activation was seen in errors with and without awareness suggesting that the insulae have a role specific to awareness rather than errors *per se*.

Applying Craig's model to primary sensory processing, several interesting studies have demonstrated objective sensory sensations are encoded in the posterior insulae, whereas subjective perceptions of the same stimuli are encoded in the anterior insulae (Craig, Chen et al. 2000, Hofbauer, Rainville et al. 2001). This was first demonstrated in a positron emission tomography (PET) study, which showed that the objective temperature of a stimulus cooling the right hand was correlated with activation in the contra-lateral posterior and mid insulae. However, the subjects' perceptions of the stimuli (i.e. how hot or cold they felt it was) correlated with activity in the right anterior insula (Craig, Chen et al. 2000). Similarly designed studies have showed a comparable result when examining the pain modulatory effect of hypnosis (Hofbauer, Rainville et al. 2001). Although, this study also found that dACC and primary sensory cortex activation altered with pain perception. Another study found a linear relationship between pain perception and dACC activity when the sensory stimuli remained the same but subjects perceptions were altered using hypnosis (Rainville, Duncan et al. 1997). Functional MRI studies have shown that both the anterior insulae and dACC are activated in both the evaluation and encoding of noxious stimuli (Kong, White et al. 2006) and suggested that the regions work synergistically in a 'pain matrix'.

Not all models of awareness give the insulae such a prominent role. An alternative theory based primarily on the fMRI literature proposes that the neural basis of 'self' has four distinct processes (monitoring, evaluation, integration, and representation of self-referential stimuli), and that these are supported by spatially distinct structures along the midline of the brain (Northoff and Bermpohl 2004).

In Northhoff's model monitoring of self-referential stimuli is governed by cortical midline structures that include the ACC. In keeping with this model, several studies comparing brain activation while attending to self-referential compared to non-self-referential stimuli have shown greater activation of the most anterior regions of the ACC (Frith and Frith 1999, Gusnard, Akbudak et al. 2001, Johnson, Baxter et al. 2002, Ochsner, Beer et al. 2005). Functional MRI studies in healthy (Gusnard, Akbudak et al. 2001, Johnson, Baxter et al. 2002, Ochsner, Beer et al. 2005), and alexothymic patients, who have difficulty recognising emotions in themselves and others, (Moriguchi, Ohnishi et al. 2006) have shown increased activation of the ACC and para-cingulate cortex in registering of self-referential over non-self-referential stimuli.

Evaluation and monitoring are closely linked in Northhoff's model both anatomically and conceptually. The Northhoff model states that the dorso-medial prefrontal cortex extending from the dACC into the adjacent para-cingulate and dorsal aspect of the middle frontal gyrus are implicated with the role of evaluating the self-referential information detected by the monitoring system in the more anterior inferior midline frontal structures. Evidence of this comes from studies where these regions activate preferentially to the evaluation rather than the simple perception of self-relevant stimuli. For example, one fMRI study in healthy volunteers showed greater activation of these regions during tasks that required evaluation of personal preferences (e.g. "I enjoy going to new year's eve parties") compared to episodic or semantic memory decisions (e.g. "where were you for new year's eve") (Zysset, Huber et al. 2002). A similarly designed study showed comparable results in healthy controls (Johnson, Baxter et al. 2002). Another fMRI study, with arguably more balanced tasks, showed greater brain activity in these regions while subjects decided whether positive and negative character traits described themselves or others (Fossati, Hevenor et al. 2003). Interestingly, this task was repeated in patients with major depressive

disorders who showed increased activation of the dorsal MFG on evaluation of qualities relating to themselves (Lemogne, le Bastard et al. 2009). The authors suggested this might relate to a pathological process of self-appraisal in major depression.

The Northoff model also suggests that orbitofrontal/ventro-medial pre-frontal cortex and posterior cingulate cortex (PCC) are the anatomical loci for self-representation and integration respectively (Northoff and Bermpohl 2004). This is in keeping with the proposed roles of the PCC and ventro-medial pre-frontal cortex as part of a distributed neural network referred to as the default mode network (DMN) (Raichle, MacLeod et al. 2001). This network is thought to be involved in self-reflective processes, among other things, and is discussed in detail in below.

Both models of self-awareness outlined above are incomplete but they do provide a useful framework upon which to investigate awareness. Importantly both emphasise the pivotal role monitoring and evaluation of salient stimuli in self-awareness. One of the limitations of Craig's model is that it recognises the tight link between the dACC and anterior insulae but does not adequately resolve their roles. Similarly, the model's author recognises anatomical and functional differences have been observed between the left and right insulae but does not address this. Several studies have shown relative differences between the left and right insula function in terms of activation patterns (Bartels and Zeki 2004, Johnstone, van Reekum et al. 2006, Jabbi, Swart et al. 2007) and functional connectivity (Seeley, Menon et al. 2007), indicating that they do have distinct roles in cognition (Craig 2005). The Northoff model is also limited in the fact that it does not take into account any structures outside of the midline and selectively reports the results of studies only attending to the midline structures. For example, several of the studies reporting

ACC activation also report insula activation for the same contrasts (Gusnard, Akbudak et al. 2001, Johnson, Baxter et al. 2002, Ochsner, Beer et al. 2005). In the Northoff model there is also considerable overlap between the monitoring and evaluation functions, both in terms of the concepts and anatomical areas associated with them.

I have discussed both of these models and their flaws because currently, there is not a globally accepted model that adequately explains the neural basis of awareness. These models are not perfect but do emphasise the importance of the ACC and insulae our current understanding of awareness, even though their exact roles remain unclear.

2.6.2. The neural basis of cognitive control and performance monitoring

The dACC has been placed at the heart of the cognitive control system (Miltner, Braun et al. 1997, Botvinick, Braver et al. 2001, Holroyd, Nieuwenhuis et al. 2004, Ridderinkhof, Ullsperger et al. 2004). The region is often activated by errors (Miltner, Braun et al. 1997, Holroyd, Nieuwenhuis et al. 2004, Ridderinkhof, Ullsperger et al. 2004) and other high conflict situations (Carter, Braver et al. 1998, Botvinick, Braver et al. 2001). It has been proposed that the region responds to prediction errors signals from the mesencephalic dopamine system regardless of the source of the error (Holroyd and Coles 2002, Holroyd, Nieuwenhuis et al. 2004), and has also been proposed as the site of conflict-monitoring (Botvinick, Braver et al. 2001), error avoidance (Magno, Foxe et al. 2006), and self-reflection (Modinos, Ormel et al. 2009, van der Meer, Costafreda et al. 2010).

An influential theory, expanding upon Botvinick's conflict monitoring model, proposes that the application of cognitive control results from an interaction between the dACC and regions in the lateral prefrontal cortex (Kerns, Cohen et al. 2004, Ridderinkhof,

Ullsperger et al. 2004, Badre and D'Esposito 2007, Kouneiher, Charron et al. 2009). In this model the dACC monitors on-going behaviour and signals the need for behavioural adaptation through its interaction with lateral prefrontal regions. The amount of dACC activation has also been related to the magnitude of behavioural adaptation (Gehring, Goss et al. 1993, Kerns, Cohen et al. 2004), although this is not a consistent finding across all studies (Li et al., 2008). There is a large body of evidence that the dACC plays an important role in some aspect of performance monitoring and cognitive control.

However, human lesion studies have shown preservation of certain post-error behaviour despite damage to the dACC (Fellows and Farah 2005, Kennerley, Walton et al. 2006, Modirrousta and Fellows 2008). Damage to the dACC impairs rapid, anticipatory error monitoring, but other measures of error awareness such as post-error slowing remained unaffected (Swick and Turken 2002, di Pellegrino, Ciaramelli et al. 2007, Modirrousta and Fellows 2008). Similarly, animal work on monkeys with dACC lesions have shown preservation of immediate response to errors, but impaired subsequent strategic learning from these errors (Kennerley, Walton et al. 2006). These findings suggest that certain aspects of cognitive control can be engaged without dACC involvement. An important question is whether the dACC is involved in the monitoring of all types of error or conflict information. Activation of the dACC is observed in many situations where cognitive control is exerted, (Ridderinkhof, Ullsperger et al. 2004), regardless of whether the information is internal (as a result of efference copy) or external (as the result of feedback) (Ullsperger and von Cramon 2003, Holroyd, Nieuwenhuis et al. 2004). However, the interpretation of these results is complicated by the fact that the dACC also responds in many other cognitively demanding situations (Miltner, Braun et al. 1997, Botvinick, Braver et al. 2001, Ridderinkhof, Ullsperger et al. 2004, Menon 2011).

An alternative theory proposes that the right anterior insula (RAI) acts as a key neural region involved in the monitoring of sensory information and recruitment of other cortical areas (such as the dACC) to act on that information (Sridharan, Levitin et al. 2008, Menon and Uddin 2010, Bonnelle, Ham et al. 2012). This theory puts the RAI at the heart of performance monitoring and behavioural adaptation, and there is mounting evidence for it. The RAI is connected to a several neural networks that have been implicated in adaptive behaviour. The RAI provides an area of anatomical area of overlap between the Salience (Seeley, Menon et al. 2007) and ventral attentional networks (Corbetta and Shulman 2002) both of which have been suggested play key roles in the detection of new information (the anatomy and function of these networks are discussed in detail below). Tractography evidence has shown that the anterior insulae have direct white matter connections regions frequently activated in cognitively demanding tasks including the temporo-parietal junction (Kucyi, Moayed et al. 2012), and the inferior parietal lobe (Singh-Curry and Husain 2009, Uddin, Supekar et al. 2010). It has been suggested that this connectivity make the RAI well placed to perform the role of monitoring on-going events reorienting attention (Ullsperger, Harsay et al. 2010), evaluating (Eckert, Menon et al. 2009) and switching between cognitive resources in response to salient events (Uddin and Menon 2009, Menon 2011).

Currently there is no consensus as to whether the dACC or the RAI is primarily involved in performance monitoring. Because the two regions are so tightly linked functionally differentiating between their roles using traditional fMRI methods has proven difficult (Friston, Price et al. 1996, Ullsperger, Harsay et al. 2010). However, fMRI studies that have attempted to discriminate their roles have shown that the RAI respond in a much more generic way to errors than the dACC (Magno, Foxe et al. 2006) and Granger causality analysis has provided some support for the view that the RAI causally influences activity in other brain networks (Sridharan, Levitin et al.

2008). These results suggest that the RAI rather than the dACC plays the key role in performance monitoring and the initiation of cognitive control.

2.6.3. The neural basis of attention

There is a substantial literature about the neural basis for attention (Rueckert and Grafman 1996, Bleiberg, Garmoe et al. 1997, Lawrence, Ross et al. 2003, Manly, Owen et al. 2003). Corbetta and Shulmans theory maps well onto anatomical divisions seen in neuroimaging data. They define dorsal (DAN) and ventral (VAN) attention networks (Corbetta and Shulman 2002, Fox, Corbetta et al. 2006, He, Snyder et al. 2007). The DAN is proposed to support 'top-down' attentional control (endogenous attention) and anatomically is bilateral and made of parts of the dorsal posterior superior parietal lobes and areas of the superior frontal sulci, including the frontal eye fields. The VAN is thought to support stimulus driven changes in attention (exogenous attention) and is strongly lateralized to the right temporo-parietal junction and right ventral frontal cortex including the right insula. Its action has been conceptualised as a circuit-breaking function on current neural activity, which allows the adaptive change in behaviour to emerge. This anatomical distribution has been replicated using event-related task fMRI and resting functional connectivity studies in healthy individuals (Fox, Corbetta et al. 2006).

However, the Corbetta and Shulman model is by no means universally accepted and the anatomical distributions of the proposed networks are still the subject of some debate. A recent functional imaging study was performed to establish whether the DAN described was truly an amodal attentional network or whether the prominence of the frontal eye fields primarily reflected the visual nature of many of the tasks used to assess it (Braga, Wilson et al. 2013). This study examined 'top-down' attention in both auditory and visual sustained attention tasks and determined that the only

region to showed common activation in both sensory modalities was the right MFG and adjacent IFG. They concluded that if an amodal DAN type structure did exist that it was centred around these regions rather than a bilateral dorsal distribution suggested by Corbetta (Braga, Wilson et al. 2013). Furthermore, several other studies have shown a bilateral neural response to unexpected behaviourally relevant 'odd-ball' events (Stevens, Skudlarski et al. 2000, Fichtenholtz, Dean et al. 2004). One would have predicted, from the Corbetta model, that these events would have activated a right lateralised VAN. These studies have been performed in both visual and auditory modalities. One study showed bilateral IFG activation when aversive emotional visual stimuli were interspaced into a counting task (Fichtenholtz, Dean et al. 2004). A second directly compared visual and auditory odd-ball tasks and demonstrated bilateral IFG and MFG activation in both conditions (Stevens, Skudlarski et al. 2000, Fichtenholtz, Dean et al. 2004). It may be that the 'right lateralised VAN' can recruit regions from the contralateral hemisphere given the appropriate task demands.

2.7. Neural networks

Individual brain regions do not act in isolation and the cognitive functions disrupted after TBI are likely supported by complex interactions between remote brain regions, making them particularly vulnerable to the effects of DAI (Geschwind 1965, Mesulam 1990, Smith, Meaney et al. 2003). DAI has the potential to disconnect brain regions, and may be an important determinant of clinical outcome after TBI (Sidaros, Engberg et al. 2008). The studies described in this thesis frame cognitive functions in terms of large-scale brain networks and their intra and inter-network interactions. New neural network analysis techniques are providing novel insights into global brain architecture both in health and disease (Menon 2011). Major advances have been made in our understanding of these networks and new MRI techniques have allowed

quantification of the structural and functional connections between network nodes. As much of the pathology is thought to be secondary to white matter damage affecting efficient communication between cortical regions, the development of networks analysis tools is particularly relevant to TBI.

2.7.1. Why study brain networks?

Distinct cortical regions must operate together to support high-level cognition (Mesulam 1981, Bagurdes, Mesulam et al. 2008). Spatially separate neuronal populations (nodes) in distributed networks are connected to one another through white matter tracts, and together they form processing networks. The importance of these white matter tracts in critical brain networks has been investigated in normal aging population as well as several disease states including mild cognitive impairment, Alzheimer's disease and TBI (O'Sullivan, Jones et al. 2001, Charlton, Barrick et al. 2006, Murphy, Gunning-Dixon et al. 2007, Miles, Grossman et al. 2008). In general this work demonstrates that the structural integrity of white matter connections is an important predictor of cognitive function. This has led to the proposal that structural 'disconnection' of networks leads to loss of function and a decline in performance (Geschwind 1965, Geschwind 1965, O'Sullivan, Jones et al. 2001, Catani and ffytche 2005, Charlton, Barrick et al. 2006).

Developing a comprehensive description of these networks and how their interactions produce higher cognitive functions is a major goal for neuroscience (e.g. <http://www.humanconnectomeproject.org/>). Networks can be studied at different spatial levels. At the microscopic level, a detailed description of the synaptic, axonal and dendritic structure of connected neurons is being derived (e.g. (Seung 2009)). At a much larger-scale, long-distance interactions between remote brain regions produce distributed brain networks with distinct functions. These networks are

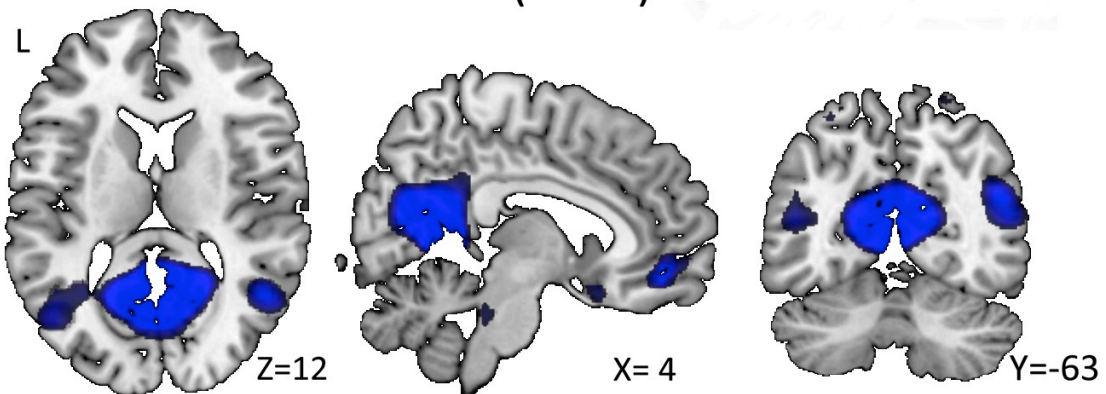
referred to as intrinsic connectivity networks (ICNs) (Beckmann, DeLuca et al. 2005, Smith, Fox et al. 2009). Nodes (brain regions) within ICNs show highly consistent interactions, which can be studied using fMRI to measure correlated brain activity (functional connectivity – described in detail in Chapter 3) (Friston 1994, Damoiseaux, Rombouts et al. 2006). The pattern of these interactions may reflect the underlying structure of white matter connections within the brain (van den Heuvel, Mandl et al. 2009). Abnormalities in ICNs have been observed in many neurological and psychiatric diseases (Greicius 2008, Seeley, Crawford et al. 2009, Zhang and Raichle 2010) and application of these techniques to TBI promises to be particularly fruitful.

2.7.2. Defining neural networks

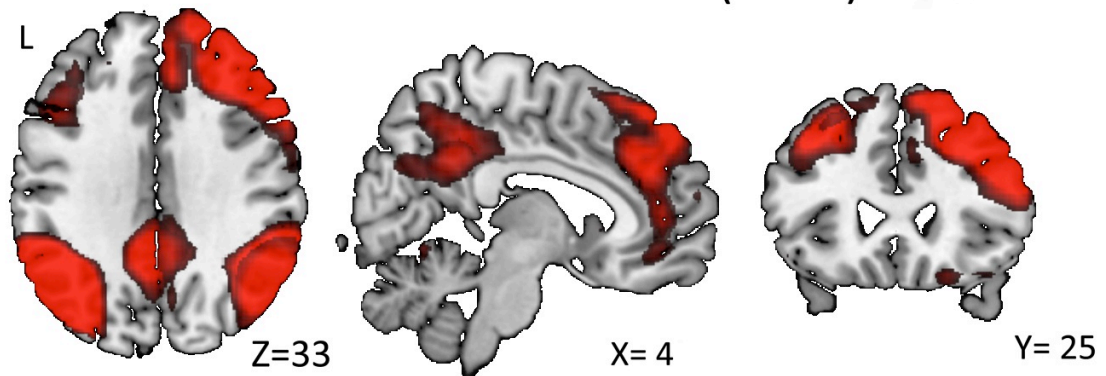
As mentioned above, functional connectivity is a term used to describe the statistical association between remote neurophysiological events (Friston 2002). When the activities of separate brain regions are strongly correlated the regions are considered to make up a network with a functional specialisation. Functional connectivity techniques, such as independent component analysis (ICA) (described in Chapter 3) applied to fMRI data have demonstrated consistent relationships between spatially distributed brain regions. The biological plausibility of the ICNs is helped by the fact that functional connectivity studies have replicated the anatomical distribution of various well-recognised networks previously defined on task-related fMRI studies (e.g. somatosensory (Biswal, Yetkin et al. 1995) and attention networks (Fox, Corbetta et al. 2006)). This was shown dramatically by reproducing the network activation patterns seen across 2000 task-based fMRI studies (over 30,000 subjects) using functional connectivity analysis of fMRI data from 36 subjects in the absence of task ('resting state' data) (Smith, Fox et al. 2009). This study demonstrated convincingly that brain regions work together in networks and that the same networks

are preserved across different studies, during different tasks, and even in the absence of task (Smith, Fox et al. 2009). It is generally accepted that these network represent a fundamental organisation unit of the brain. Below I have outlined the anatomy and proposed functions of the key networks referred to in my thesis (Figure 2.4).

Default mode network (DMN)



Fronto-Parietal Control Network (FPCN)



Saliience network (SN)

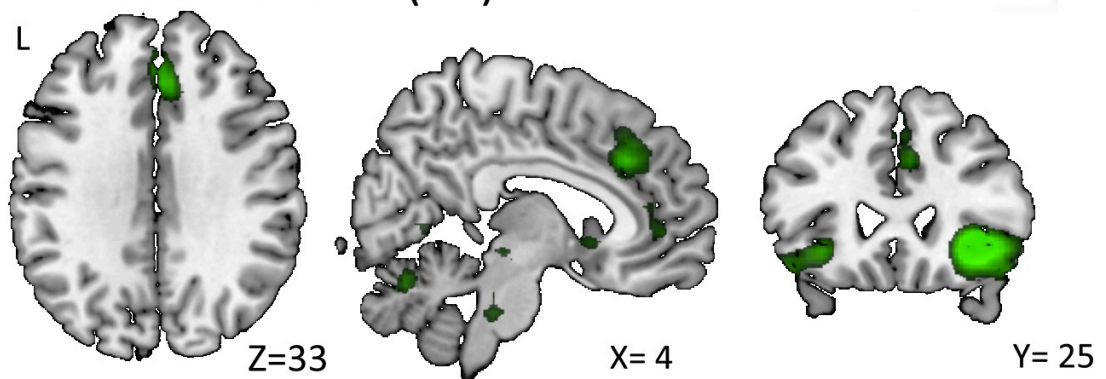


Figure 2.4: Intrinsic connectivity networks

Examples of three commonly described ICNs: the Default mode network (blue); the Fronto-parietal control network (red); and, the Saliience network (green).

2.7.3. The Default Mode Network

The DMN is one of the most consistently produced ICNs (Raichle, MacLeod et al. 2001, Greicius, Supekar et al. 2009, Margulies, Vincent et al. 2009, Leech, Kamourieh et al. 2011). Its main nodes are the posterior cingulate cortex (PCC), the ventromedial prefrontal cortex, lateral inferior parietal lobes and medial temporal structures (Raichle, MacLeod et al. 2001) (Figure 2.4A). The DMN shows highly correlated activity at 'rest' and a rapid deactivation during most tasks where attention is directed externally (Shulman, Fiez et al. 1997, Gusnard, Akbudak et al. 2001, Raichle, MacLeod et al. 2001, Buckner, Andrews-Hanna et al. 2008). The magnitude of DMN deactivation is related to cognitive load (Singh and Fawcett 2008), and a failure to deactivate the network is associated with inefficient cognitive function (Weissman, Roberts et al. 2006, Sonuga-Barke and Castellanos 2007, Bonnelle, Leech et al. 2011, Bonnelle, Ham et al. 2012).

2.7.4. The Fronto-Parietal Control Network

In contrast to the DMN, a set of fronto-parietal brain regions often show increased activity during experimental tasks. A network involved in cognitive control and other aspects of executive function has been termed the fronto-parietal control network (FPCN) (Dosenbach, Fair et al. 2007, Vincent, Kahn et al. 2008, Spreng, Stevens et al. 2010, Spreng 2012). This network is largely symmetrical and includes parts of the frontal pole and lateral prefrontal cortex, the dACC/pre-supplementary motor area (SMA), the anterior insulae, the lateral posterior parietal cortex and part of the posterior cingulate cortex (PCC) (Figure 2.4).

The FPCN is a relatively recent construct in functional imaging so much of the literature does not assign functions to it by name. However, many previous studies have shown activation in the brain regions included in the FPCN during a wide range

of cognitively demanding tasks including: the selection of appropriate behavioural adaptation (Dosenbach, Fair et al. 2007); manipulating information in working memory (Muller and Knight 2006); and more broadly decision making and the initiation of goal directed behaviour (Koechlin, Ody et al. 2003, Koechlin and Summerfield 2007). The FPCN contains within it the dACC and bilateral anterior insulae. These regions are referred to collectively as the Salience network (Seeley, Menon et al. 2007) and have been proposed as a distinct function unit involved in the detection and response to behaviourally salient events.

2.7.5. The Salience Network

The dACC is tightly functionally linked to the right and left anterior insulae (RAI/LAI) (Seeley, Menon et al. 2007, Ullsperger, Harsay et al. 2010). These regions have been grouped together, along with subcortical structures in the thalamus, and termed the Salience network (SN). The first study to coin the phrase 'salience network' and establish the SN and executive control network (ECN) as distinct entities used functional connectivity techniques (Seeley, Menon et al. 2007). They found that functional connectivity within the SN was positively associated with subjects' pre-scanning anxiety score. Whereas a subject's ability to perform a task of executive function (i.e. a trail making task) positively associated with functional connectivity within the executive control network (ECN) (Seeley, Menon et al. 2007). This study used a data driven approach to provide evidence that these commonly co-activated regions could be separated into functionally distinct neural networks. This supported previous theories suggesting that, despite frequent co-activation, the lateral parietal and frontal regions were primarily engaged in task specific activities, whereas the dACC and anterior insulae were responding in a more general way to situations with a degree of 'personal salience' (Critchley, Wiens et al. 2004). It has been suggested that the SN acts as an interface between the limbic and cognitive aspects

of behavioural control (Seeley, Menon et al. 2007). The SN responds to behaviourally salient events (Seeley, Menon et al. 2007), and is thought important for the initiation of cognitive control (Menon and Uddin 2010), the maintenance and implementation of task sets (Dosenbach, Visscher et al. 2006, Nelson, Bernat et al. 2008) and the coordination of behavioural responses to salient events (Medford and Critchley 2010). As outlined previously, errors are behaviourally salient events and one would expect them to cause SN activation. Therefore studying the neural response to errors should offer insight into the underlying functional organisation of the SN (discussed in detail in Chapter 5). Recent work has clarified the brain regions involved in performance monitoring and response to errors (Ullsperger and von Cramon 2004, Sharp, Scott et al. 2006, Modirrousta and Fellows 2008, Ullsperger, Harsay et al. 2010). Structures within the medial prefrontal cortex, particularly the dACC, play key roles and appear to be necessary for rapid on-line error processing (Dehaene, Posner et al. 1994, Ridderinkhof, Ullsperger et al. 2004, Modirrousta and Fellows 2008). Partly for this reason the dACC has been suggested as a generic performance monitor detecting, putting the dACC at the heart of the SN organisation.

2.7.6. The Triple network model

The triple-network model (Menon 2011) describes how healthy and pathological cognitive processes could be viewed in terms of the interaction between the SN, ECN and DMN. The 'triple network model' proposes that the SN monitors and filters relevant important information before assigning appropriate cognitive resources to respond (i.e. coordinates ECN and DMN activation/deactivation (Menon 2011)). This model also assigns particular significance to the anterior insulae in performing this function. This proposal is supported by the anatomical overlap that the anterior insulae shows across neural networks making it optimally placed to perform this function, and also by the results of functional imaging studies suggesting that the RAI

regulates activity in other neural networks (Sridharan, Levitin et al. 2008). Abnormal activation of the insulae has been reported in various neurological and psychiatric diseases. Anterior insulae over activation is seen in anxiety disorders (Paulus and Stein 2006, Stein, Simmons et al. 2007), neurosis (Feinstein, Stein et al. 2006) and chronic pain syndromes (Wiech, Ploner et al. 2008). Whereas, reduced activation and atrophy of the insulae and dACC are seen in schizophrenia (Palaniyappan, Mallikarjun et al. 2011), autism (Di Martino, Ross et al. 2009), and behavioural variant fronto-temporal dementia (White, Joseph et al. 2010). The triple network model suggests that this abnormal activation reflects the SN assigning inappropriate levels of salience to internal and external stimuli. This process leads to impaired allocation of cognitive resources and reduced ability to monitor and assign consequences to ones actions.

There are considerable similarities between the 'triple network' model and another proposed model of network interaction. An influential model proposed by Vincent et al., (Vincent, Kahn et al. 2008) suggests that a comparable organisation to the triple network model only with the FPCN integrating information from the externally directed DAN and the internally directed DMN. This model assigned the FPCN rather than the SN as the network that mediates interactions between the externally and internally directed cognitive processes. However, as stated above, the FPCN contains within it key regions of the SN (i.e. the ACC and insulae) with additional lateral prefrontal structures. Therefore there is considerable overlap between the two models both conceptually and anatomically.

2.8. Network disruption after TBI

There are a number of methods available to assess brain injury and network function after TBI. In a network framework this can be thought of as assessing the nodes

(brain regions that act together in the network) and the edges (the white matter that connects the nodes).

2.8.1. Fronto-Parietal Control Network dysfunction after TBI

TBI patients often show increased brain activity during cognitively demanding tasks in regions that overlap with the FPCN (McAllister, Saykin et al. 1999, Christodoulou, DeLuca et al. 2001, Rasmussen, Xu et al. 2008, Turner and Levine 2008, Kim, Yoo et al. 2009, Kasahara, Menon et al. 2011, Raja Beharelle, Tisserand et al. 2011). For example, a recent study showed increased activity in a number of FPCN regions when patients with moderate-severe TBI performed a simple choice reaction task (Bonnelle, Leech et al. 2011). This finding is not unique to TBI and has been seen in other white matter diseases (e.g. multiple sclerosis (Mainero, Pantano et al. 2006)). The increased activity has been interpreted in several ways, including a compensatory increase in cognitive control (Turner and Levine 2008, Kim, Yoo et al. 2009, Turner, McIntosh et al. 2011, Stevens, Lovejoy et al. 2012), a reorganization of damaged networks (Mainero, Pantano et al. 2006) and disinhibition of cortical activity due to deafferentation (Levine, Cabeza et al. 2002, Raja Beharelle, Tisserand et al. 2011). Increased FPCN activity may be accompanied by normal behavioural performance (Newsome, Steinberg et al. 2008, Turner and Levine 2008), and has also been associated with improved task accuracy (Turner, McIntosh et al. 2011). This last study showed greater lateral prefrontal cortical activity in healthy controls as cognitive load increased in a manner similar to that seen in the TBI patients. The authors therefore suggested that the increased FPCN activity seen in patients is likely to be the result of compensatory increases in cognitive control, rather than network reorganization triggered by brain injury.

Even when patients show behavioural problems after TBI, increased FPCN activity is not always observed. For example, a study that investigated a group of moderate-severe TBI patients and found normal levels of FPCN activity during a response inhibition task, despite abnormal behavioural performance and altered DMN activity (Bonnelle, Ham et al. 2012). Another study of mild TBI showed reduced activity in the right lateral prefrontal cortex during an auditory oddball task (Witt, Lovejoy et al. 2010). It is likely that FPCN activity after TBI is dependent on the precise cognitive demands of the task, and in a subset of patients compensatory increases in cognitive control may not be possible because of the nature of their injuries.

2.8.2. Default Mode Network dysfunction after TBI

The DMN often shows abnormal activity after TBI (Bonnelle, Leech et al. 2011, Hillary, Slocumb et al. 2011, Mayer, Mannell et al. 2011, Sharp, Beckmann et al. 2011, Bonnelle, Ham et al. 2012, Stevens, Lovejoy et al. 2012). DMN activity is often abnormally high when TBI patients perform difficult tasks (Kim, Yoo et al. 2009, Bonnelle, Leech et al. 2011, Bonnelle, Ham et al. 2012). In a similar way to the FPCN, one interpretation is that this represents a compensatory change (Caeyenberghs, Wenderoth et al. 2009, Kim, Yoo et al. 2009). However, the failure to deactivate the DMN is associated with cognitive impairment in many situations (Weissman, Roberts et al. 2006, Sonuga-Barke and Castellanos 2007), and recent work suggests that this is the case after TBI (Bonnelle, Leech et al. 2011, Bonnelle, Ham et al. 2012). Impaired sustained attention after TBI was associated with failure to maintain deactivation of the DMN in one study (Bonnelle, Leech et al. 2011). A second study showed that failures of rapid response inhibition were associated with a lack of deactivation within the DMN, again suggesting that a lack of control over DMN activity is linked to cognitive impairment after TBI (Bonnelle, Ham et al. 2012). Interestingly, this last study showed that patients' ability to deactivate the DMN was

related to the integrity of the white matter connecting the RAI to the dACC. Suggesting that integrity of the SN was necessary for successful deactivation of the DMN.

The DMN also shows abnormal functional connectivity following TBI. Using resting state fMRI several studies have shown enhanced functional connectivity within the DMN (Hillary, Slocomb et al. 2011, Sharp, Beckmann et al. 2011, Stevens, Lovejoy et al. 2012) after TBI. These changes may depend on the timing of assessment and/or the severity of injury, as another study of mild TBI patients without neuropsychological impairments found evidence for decreased DMN functional connectivity (Mayer, Mannell et al. 2011). One study of mainly moderate-severe patients showed that increased DMN functional connectivity was associated with faster information processing speed, in keeping with a compensatory interpretation of this network change (Sharp, Beckmann et al. 2011). This study also demonstrated a relationship between DMN functional connectivity and behaviour during task performance (Bonnelle, Leech et al. 2011). Low levels of DMN functional connectivity predicted impairments in sustained attention. Importantly, DMN functional connectivity at the start the task, when behaviour was normal, predicted the development of attentional problems towards the end of the task.

The potential clinical utility of functional connectivity measurements has been most clearly demonstrated in work on patients with altered levels of consciousness. Functional connectivity within the DMN was shown to differentiate patients with levels of consciousness varying from light anaesthesia, vegetative state, brain death and coma (Greicius, Kiviniemi et al. 2008, Boly, Tshibanda et al. 2009, Cauda, Micon et al. 2009, Vanhaudenhuyse, Noirhomme et al. 2010, Norton, Hutchison et al. 2012). One pilot study distinguished a single vegetative state and brain dead patient solely on the basis of their DMN functional connectivity (Boly, Tshibanda et al. 2009), and this result was then replicated in a larger sample of non-communicating patients

(Vanhaudenhuyse, Noirhomme et al. 2010). Similarly, another study has shown that DMN functional connectivity predicts recovery from coma (Norton, Hutchison et al. 2012).

2.8.3. Dysfunction in other networks

As expected network abnormalities after TBI are not isolated to the neural networks described above and have also been observed in other brain networks (Hillary, Slocomb et al. 2011, Mayer, Mannell et al. 2011, Shumskaya, Andriessen et al. 2012, Stevens, Lovejoy et al. 2012). For example, TBI patients have been shown to exhibit reduced functional connectivity from the motor cortex to the rest of the motor network during simple motor tasks (Kasahara, Menon et al. 2010) and rest (Shumskaya, Andriessen et al. 2012). Here, reductions in functional connectivity were interpreted as a reduction in the motor cortex's influence on other parts of the motor-network, suggesting a breakdown of the network's normal interactions. However, as the focus of my thesis is on the cognitive sequelae of TBI I shall not discuss these studies in detail.

2.8.4. Potential benefits of studying brain networks in TBI

There are a number of potential benefits for studying the effect of TBI on the structural and functional connectivity of ICNs. From a practical scientific standpoint, network based analysis offers a framework for interrogating cognitive processes that span over several brain regions. This is particularly relevant for TBI patients for several reasons. Firstly, the underlying cause for cognitive impairment can be difficult to identify. For example, attentional problems might result from the effects of traumatic axonal injury, from neuropsychiatric problems such as depression or from the side effects of medications. Therefore, defining the structure and function of

networks after injury may facilitate the identification of sub-groups of TBI patients with particular underlying pathologies. Secondly, It is not currently possible to accurately predict clinical outcome after TBI (Lowenstein 2009). This is a major problem; particularly as many patients have persistent problems after injuries that were initially classified as minor. The neuroimaging of white matter injury can improve the prediction of outcome (e.g. (Sidaros, Engberg et al. 2008)), and a more refined analysis of network structure and function holds the promise of greatly improving prognostic accuracy. Finally, identifying specific network dysfunction in individuals may allow the targeted treatment of cognitive deficits and assist in the development of new treatments. This is important because TBI is such a heterogeneous condition. Most previous clinical trials in TBI have failed to take this complexity into account, and accurately defining subgroups of TBI will improve the power of future studies to identify treatment effects.

2.8.5. Limitations of network based analysis

The ICN framework is not perfect. In the same way that the cognitive models of attention and cognitive control overlap and do not necessarily fit neatly together, ICNs are not named uniformly and do not always have distinct cognitive functions assigned to them. For example, the SN (Seeley, Menon et al. 2007) and VAN (Corbetta and Shulman 2002) overlap anatomically in the RAI and have similarities in their putative roles in cognition (i.e. the VAN is a network primarily involved in allocating attention to unexpected events, but the SN also responds to behaviourally salient events that may or may not be unexpected). Furthermore, a consistent taxonomy of ICNs has not yet been established. This can create confusion when comparing across studies (Spreng 2012). For example, the SN could be considered a subcomponent of the FPCN as the FPCN contains within it the key cortical regions from the SN. But the SN but was originally defined in the context of the ECN not the

FPCN (Seeley, Menon et al. 2007). The ECN, although clearly a distinct entity from the SN (Seeley, Menon et al. 2007), also contains regions in the lateral prefrontal cortex that overlap with the FPCN. How these networks should be referred to and how they relate to one another is not clear from the existing literature (Spreng 2012). Variable naming of ICNs partly reflects methodological differences, but there is also a more fundamental issue that network interactions are context dependent, so the spatial organisation of networks defined by their functional interactions change over time. While many intrinsic connectivity networks have been defined (indeed the only limit in how many can be defined using an ICA process is the number of time-points available for analysis), my thesis primarily involves studying the FPCN and its sub-network the SN.

2.9. Main hypotheses and objectives

I have focused my thesis on self-awareness. As elaborated on in the section above, self-awareness is dependent upon accurate performance monitoring and this can be assessed using behavioural measures of cognitive control. I have therefore focused my investigations on the FPCN and SN. These networks are thought to be intimately involved in salience detection and action selection and are likely candidate to mediate self-awareness deficits after TBI.

In this thesis I present the results of fMRI and DTI studies of healthy and TBI patients to test the following hypotheses:

Hypothesis 1: The dorsal anterior cingulate cortex within the fronto-parietal control network acts as a generic performance monitor and responds to many different error types that can be measured by fMRI during performance of the Simon task.

Hypothesis 2: The dorsal anterior cingulate cortex and right anterior insula have distinct roles in the salience network that can be established using dynamic causal modeling fMRI techniques

Hypothesis 3: Dysfunction of the fronto-parietal control network leads to self-awareness deficits following traumatic brain injury. This dysfunction can be observed from the functional connectivity of the network at rest.

Hypothesis 4: Fronto-parietal control network dysfunction following traumatic brain injury can be observed from the activation of the network in response to errors during a cognitively demanding task.

Hypothesis 5: Fronto-parietal control network dysfunction after traumatic brain injury is due to structural disconnection between key nodes of the network, which can be measure using diffusion tensor imaging.

The specific hypotheses for each study are discussed in detail in the associated results sections.

Chapter 3: Participants, Materials and Methods

This chapter contains the methodological details of the three separate studies performed as part of my thesis. I have provided details of the participants, the assessments they undertook, and the MRI methods used to probe the neural basis of performance monitoring, error processing and self-awareness. The first two studies involved fMRI assessment of a large group of healthy volunteers performing the Simon task, a cognitively demanding stimulus/response compatibility task. The third study involved multi-modal assessment of a large group of TBI subjects and healthy controls. I have used three distinct behavioural paradigms (i.e. the Simon task, stop-signal task and stop-change task), which I discuss in detail below. I review the principles behind the MRI techniques I used to investigate the structure and function of neural networks. The end of the chapter concerns some of the potential limitations of fMRI and the appropriate steps I have taken to compensate for them.

3.1. Participants

3.1.1. TBI patient recruitment

Seventy-three patients with a history of TBI were recruited from a neurology clinic where they had been referred for persistent neurological symptoms related to their brain injury. Patients with a range of injury severities were selected to provide variability of cognitive disabilities. Exclusion criteria were as follows: neurosurgery, except for invasive intracranial pressure monitoring (one patient); history of psychiatric or neurological illness prior to their head injury; history of significant previous TBI; current or previous drug or alcohol abuse; or contraindication to MRI. Subjects had no neurological, major medical, or psychiatric disorders prior to TBI. All TBI patients were in the post-acute/chronic phase after their injury (i.e. > 2 months

after injury). Previous studies have shown that DTI metrics and histological evidence of injury change dynamically in the first months after TBI, therefore I selected patients whose' time since injury fell outside of this time frame (Mac Donald, Dikranian et al. 2007) (discussed in Chapter 2).

3.1.2. TBI severity classification

TBI severity was assessed according to the Mayo Classification system (Malec, Brown et al. 2007). This integrates the duration of loss of consciousness; length of post-traumatic amnesia (PTA); lowest recorded Glasgow coma scale (GCS) in the first 24 hours; and neuroimaging results. The Mayo system classifies patients as moderate-severe (definite) TBI, mild (probable) TBI, and symptomatic (possible) TBI. The diagnostic criteria are described in detail in Chapter 2. I used Mayo system because it was designed to facilitate post-hoc assessment of TBI severity in research studies and non-acute clinical settings. The Mayo system also requires patients to have some evidence of a brain injury before they can be classified as mild TBI. Hopefully this reduced the false positive rate of patients classified as mild brain injury who may have had a 'head injury' without injuring their brain (Malec, Brown et al. 2007).

3.1.3. Control groups

Different control groups were used for different aspects of this thesis. The individual groups are described in more detail in the relevant results chapters. Controls had no history of neurological or psychiatric illness. When comparing between control groups and TBI patients groups were well matched for age and sex.

3.2. Neuropsychological assessment

A battery of standardised neuropsychological tests sensitive to cognitive impairments commonly observed following TBI was used. The Wechsler Test of Adult Reading (WTAR) (Wechsler 2001) provided an estimate of pre-morbid intellectual functioning. Current verbal and nonverbal reasoning ability was assessed using Wechsler Abbreviated Scale of Intelligence (WASI) Similarities and Matrix Reasoning subtests (Wechsler 1999). Verbal Fluency Letter Fluency (F-A-S) and Colour-Word Interference (Stroop) tests were administered from the Delis-Kaplan Executive Function System (D-KEFS) to assess word generation fluency, cognitive flexibility, inhibition and set-shifting (Delis, Kaplan et al. 2001). The Trail Making Test (Forms A and B) was used to further assess executive functions (Reitan 1958). The Digit Span (DS) subtest of the Wechsler Memory Scale-Third Edition (WMS-III) was included in the battery to assess working memory (Wechsler 1997). The Logical Memory I and II subtests of the WMS-III were included to obtain a measure of immediate and delayed recall of structured verbal material. The People Test (PT) from the Doors and People Test battery was used as a measure of associative learning and recall (immediate and delayed) (Baddeley, Emslie et al. 1994). The two baseline conditions of the D-KEFS Stroop test (Colour Naming and Word Reading) and the TMT-A are also sensitive to impairments in information processing speed. TBI subjects were also asked to complete a Frontal Systems Behaviour (FrSBe) questionnaire (Grace, Stout et al. 1999). The FrSBe gives a measure of pre-TBI and post-TBI dysexecutive symptoms as assessed by the patient and an observer who knows the patient well. The Hospital Anxiety and Depression Scale (HADS) was used to measure the intensity and frequency of mood symptoms (Zigmond and Snaith 1983), often seen following TBI (Jorge and Robinson 2003).

3.3. Experimental paradigms

I used three different experimental paradigms in this thesis and I shall discuss them in the order they are presented in the results section.

3.3.1. The Simon Task

One of the key aims of my thesis is to investigate the neural basis of performance monitoring to provide an insight in to self-awareness. Performance monitoring can be studied by examining the behavioural response to errors. Failure to adapt ones behaviour in response to errors indicates a failure to monitor ones performance adequately (discussed in detail in Chapter 2). In Chapters 4 and 5 I investigate the neural basis of error processing using two versions of the Simon task to generate a large number of behaviourally distinct error types (i.e. commission and timing errors).

3.3.1.1. Principles of the Simon task

The Simon task is a stimulus/response compatibility task that uses incongruency between the salient and non-salient features of a stimulus to generate response conflict (Simon 1969, Simon and Small 1969). It is similar in this respect to the Stroop test described in Chapter 2. The non-salient stimuli feature in the Simon task is irrelevant spatial information. Although irrelevant to the task the spatial information can either be on the side of appropriate response (congruent conditions) or on the side opposite to the appropriate response (incongruent conditions). The Simon effect refers to the fact that responses are significantly slower during incongruent conditions. The Simon effect becomes reduced, (i.e. the difference between conditions becomes less), when more incongruent conditions are present.

3.3.1.2. Paradigm description

Building on previous electrophysiological work (Christ, Falkenstein et al. 2000), I used a version of the Simon task designed to produce large numbers of both commission and timing errors. Subjects were presented with a coloured cue to the right or left of a fixation cross (Figure 3.1). Cue colour determined the direction of the required response: red signified a right hand response, and blue a left hand response. Spatial location and cue direction were either congruent or incongruent with respect to each other. In the incongruent condition the prepotent response - to respond in the direction of the spatial location of the cue rather than the direction signalled by the colour - must be inhibited. Two thirds of trials were 'congruent' and one third 'incongruent'. Subjects needed to respond within a variable time limit from the cue presentation. All subjects performed six runs of 120 pseudo-randomly ordered trials with inter-stimulus intervals of 2.25 seconds. To increase task difficulty we introduced a pre-cue in the form of empty rectangle that filled in after 200 milliseconds with the colour that indicated response direction. The pre-cue increased the interference effect produced by a spatially incongruent colour cue. All subjects performed 120 trials (80 congruent and 40 incongruent) as training prior to scanning.

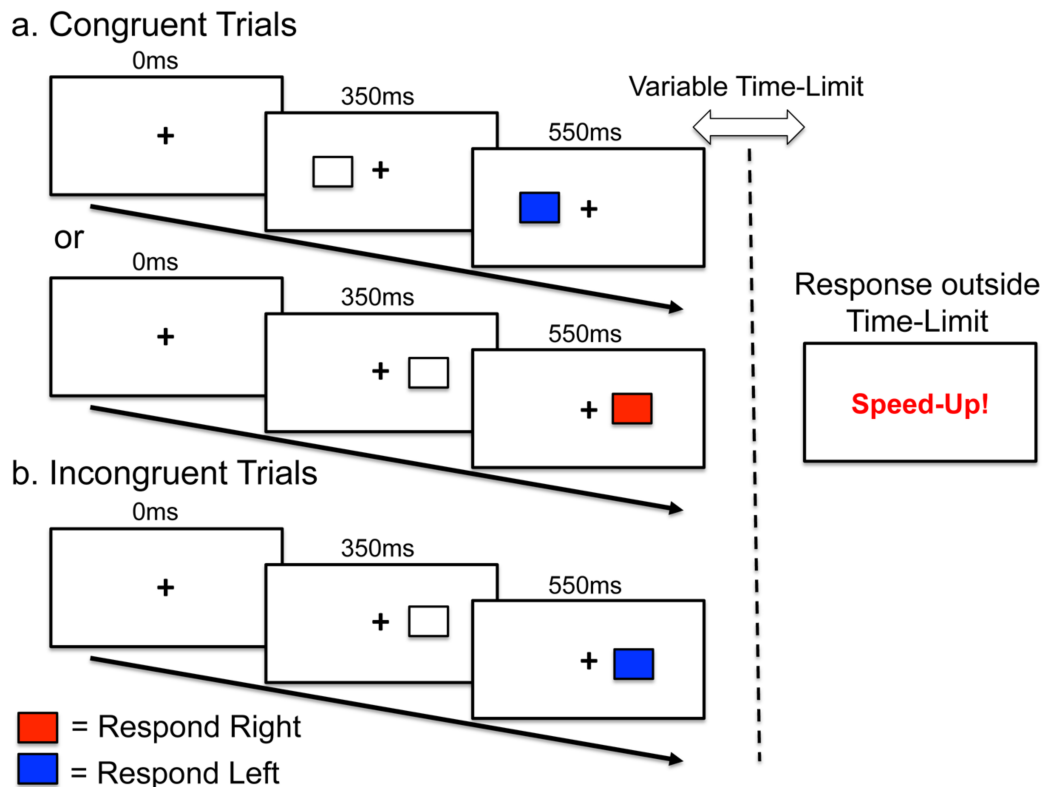


Figure 3.1: Simon task paradigm

Subjects responded with a right or left finger press for red and blue cues respectively. The pre-cue, an empty square, appeared to either the left or right side of the fixation cross for 200 msec before filling in with the cue colour (either red or blue). (a) On congruent trials the spatial location of the cue corresponded to the side of the appropriate response press. (b) On incongruent trials the spatial location conflicted with the side of the response. Trials responded to outside of the variable time limit (timing errors) were re-enforced by audio-visual feedback.

Commission errors

Errors of commission occur when the subject's direction of response is not that signalled by the colour. The relative timing of the pre-cue and colour cues was designed to generate the maximum number of errors of commission (Christ, Falkenstein et al. 2000). In the main part of the experiment explicit feedback about errors or commission was not provided. Hence, any neural response to these errors was internally generated.

Timing errors

Errors of timing occurred when subjects responded outside of the variable time limit, the timing of which is detailed below. Audio-visual feedback was presented in the form of the words 'Speed up' displayed on the screen accompanied by a 400Hz auditory tone, which emphasised the error and made subjects aware of their mistake. The visual and auditory feedback lasted 500 milliseconds. Subjects were told at the start of each run to perform the task as accurately and quickly as possible, and were aware that slowing down would result in error signal about the timing of their responses. This was emphasised during training and also between runs of the paradigm performed in the scanner.

3.3.2. The Secondary Simon task

The 'Secondary Simon task' was designed to address a potential confound in the design of the original study by providing explicit feedback after both types of error (i.e. in the main version of the Simon task errors of timing were signalled by explicit 'error' feedback, but errors of commission were not). To test whether this difference influenced neural activation and behaviour an additional study was performed with a separate group of 14 subjects, the 'Secondary Simon task'. Here both types of error were accompanied by explicit feedback (Figure 3.2). The design of the experiment was the same as that described above except for the presence of audio-visual feedback for errors of commission. This took the form of the word "Wrong!" presented after an error of commission, accompanied by a 400 Hz tone. The timing and duration was the same as for error of timing described above.

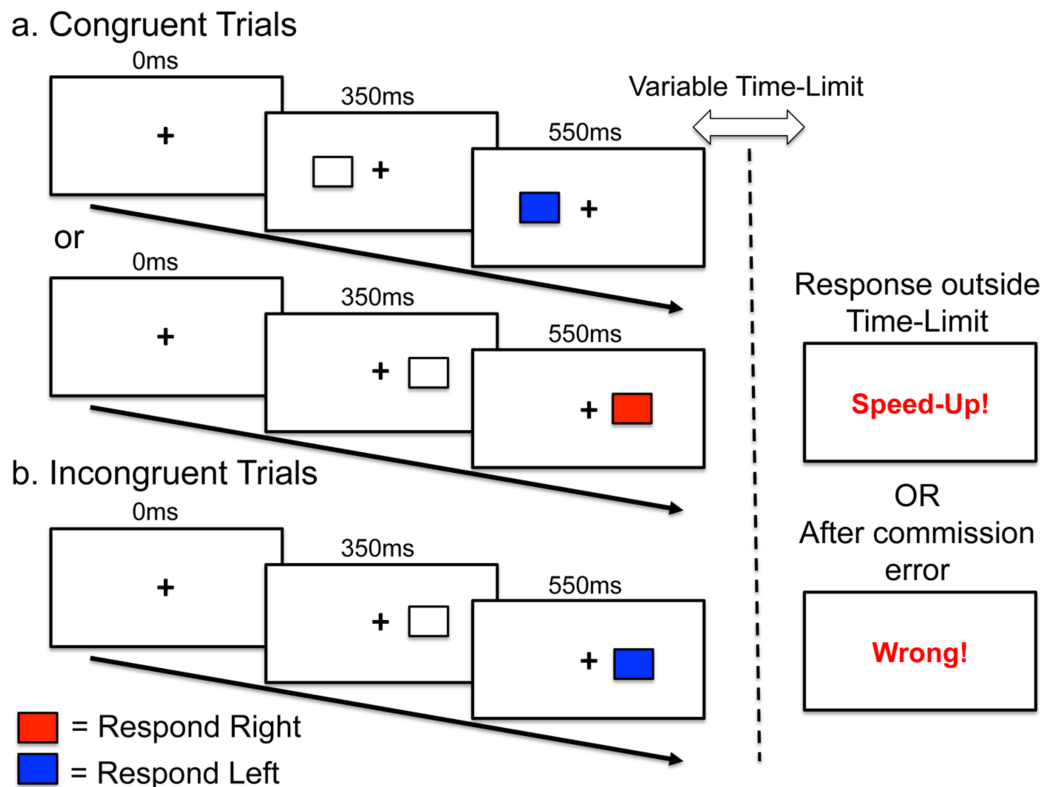


Figure 3.2: Secondary Simon task paradigm

As with the original Simon task, subjects responded with a right or left finger press for red and blue cues respectively. (a) On congruent trials the spatial location of the cue corresponded to the side of the appropriate response press. (b) On incongruent trials the spatial location conflicted with the side of the response. On this version both commission and timing errors were re-enforced by audio-visual feedback.

3.3.3. Performance matching in the Simon task

The tasks employed various methods to ensure that they produced similar numbers of errors across subjects. An adaptive staircase procedure was used to vary the response delay necessary to trigger timing feedback with the goal of producing errors of commission within a target range. At the start of the experiment feedback was triggered if a subject's response was more than 500 milliseconds after the presentation of the colour stimulus. After the first 15 trials the rate of commission errors was calculated after each trial, and the time limit was adjusted if this rate fell outside the target range. For congruent trials a target commission error range of 8-12% was used. The time limit was increased by 50 milliseconds if the error rate was

high, and decreased by the same amount if it was too low. Adaptation was performed separately for incongruent trials, aiming for a range of 17-25% incongruent commission errors. The time limit was adapted within a range of 400 - 1000 milliseconds. For subsequent runs the starting time limit was carried over from the previous run.

3.3.4. Behavioural assessment of the Simon task

In the Simon task five trial types were considered for both congruent and incongruent conditions: correct trials (appropriate response within the time limit), commission errors (incorrect button press but within the time limit), timing errors (correct button press but outside of the time limit), errors of both timing and commission, and confounded trials where timing or commission errors occurred directly after another timing or commission error. To control for slow fluctuations in subject's attention over the length of the run reaction times were compared to a 'baseline' performance on trials for that condition, (i.e. congruent or incongruent) (Bonnelle, Leech et al. 2011). The 'baseline' performance was calculated from the mean of the last ten stable correct trials of a particular type. Stable correct trials were defined as correct and timely trials that had also been preceded by a correct timely trial. This was done to avoid contamination from the effects of errors on preceding trials.

Post-error behavioural adaptation

Performance monitoring during both versions of the Simon task was assessed by studying how subjects engaged cognitive control after each type of error (Ornstein, Levin et al. 2009). Reaction times on the error trial (N), the trial immediately before an error (N-1), and the three trials directly after an error (N+1, N+2, N+3) were compared to the baseline reaction times of trials of that condition (i.e. congruent or

incongruent). Post-error slowing was expected after commission errors. In theory post-error slowing should allow greater time for correct decisions and greater accuracy on subsequent trials (Falkenstein, Hoormann et al. 2000). Timing errors are a different situation as they signal the need to speed-up on subsequent trials (Figure 3.3). If timing errors were not salient events I would not have expected the trials immediately following timing errors to have been associated with accelerated reaction times. If timing errors were followed by quicker reaction times but worse response accuracy (i.e. more commission errors) then it may have indicated that appropriate cognitive control had not been engaged either. For this reason I assessed both the speed and accuracy on the trials immediately preceding and following each error type.

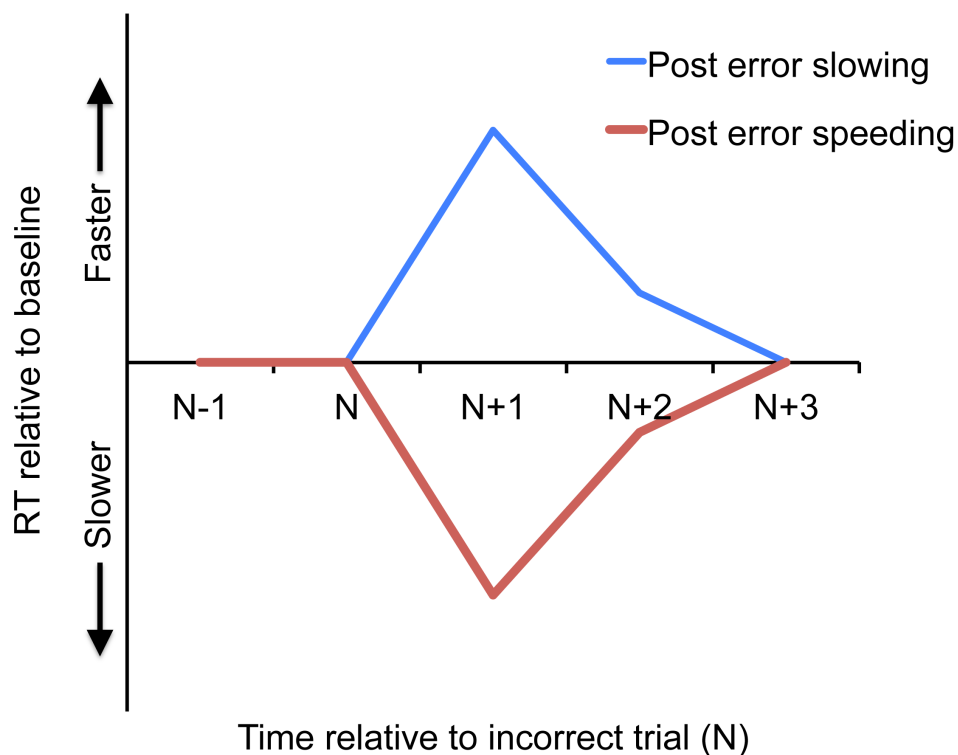


Figure 3.3: Predicted post error behavioural adaptation

In an ideal system without attentional drift correct trials of a particular condition would all have the same reaction times (RT) and not differ from baseline performance. After a commission error (N) I expected post-error slowing on subsequent trials before returning to baseline performance (red line). After a timing error (N) I expected

subjects' reaction times to accelerate in accordance with the explicit instructions ('Speed-up!') provided by the task (blue line).

3.3.5. Analysing strategic differences in performance on the Simon task

Timing and commission errors require different behavioural responses, (i.e. after commission errors subjects should slow-down and after timing errors subjects should speed-up). The conflicting nature of these situations may lead subjects to prioritise one error type over the other (e.g. sacrifice speed for accuracy or vice versa). Subjects may also adjust their speed-accuracy trade-off in a more complex way to achieve an optimum reduction in both error types. Unlike commission errors, the number of timing errors on a particular run was not manipulated to fall within a certain range and is likely to reflect a subject's strategy on that run. I analysed the behavioural data from all subjects and compared runs with high numbers of timing errors to those with low numbers (defined by taking the upper and lower thirds of the distribution). To focus on the effects of variable strategy with respect to timing I only included runs where the commission error rate fell approximately within the ranges the paradigm was designed to produce (i.e. 3%-17% congruent and 12%-30% incongruent errors).

3.3.6. The stop-signal task and stop-change task

In Chapter 6 I used the stop-change and stop-signal tasks (SCT and SST) (Logan, Cowan et al. 1984, Aron, Fletcher et al. 2003, Bekker, Overtom et al. 2005, Li, Yan et al. 2007, Verbruggen and Logan 2008, Verbruggen and Logan 2009, Enriquez-Geppert, Eichele et al. 2012). These are both tests of inhibition that produce inhibition errors. The SCT offers the opportunity to correct one's errors and was therefore used to define subjects' on-line performance monitoring abilities. Due to methodological issues (discussed below) the SCT is not well suited for the type of

fMRI analysis I planned to perform. Therefore, I used the SST, a simpler variation on the SCT, in the event-related fMRI analysis to measure subjects' neural responses to errors.

3.3.7. The stop-signal task

The stop-signal task (SST) is a test of inhibitory control that has been studied extensively in both healthy individuals and TBI patient groups. It requires subjects to suppress responses that are no longer appropriate. The ability to suppress unwanted or inappropriate responses is a key feature of executive control. TBI patients often have disinhibition or perseveration of responses and find such tasks difficult to perform. I used this task primarily as a way of producing inhibition errors (i.e. situations where subjects fail to inhibit their inappropriate responses).

3.3.7.1. Principles of the SST

The SST is a timed choice-reaction task where subjects are presented with a cue that they respond to with either a right or left button press. On an unpredictable subset of trials after a variable delay a stop-signal (e.g. a coloured shape) is presented that signifies that subjects should withhold their response (Figure 3.4). Inhibition errors occur when subjects fail to withhold their responses. During stop-trials the time between presenting the initial cue and the stop-signal is referred to as the stop-signal delay (SSD). The shorter the SSD the easier it is for subjects to inhibit their initial response. Subjects are usually able to successfully inhibit their initial responses if the stop-signal occurs simultaneously with or shortly after the cue. The longer the SSD, and the closer to the moment of response execution that the stop-signal appears, the more difficult it is for subjects to inhibit their response and the more likely inhibition errors. The 'horse race model' is commonly used to explain this

phenomenon (for a review see (Logan, Cowan et al. 1984)). The model states that the 'go' response and 'stop' inhibition can be modelled as two independent and competing neural processes. The 'go' response starts when the cue is presented and once it reaches a threshold the subject will respond. The 'stop' inhibitory process starts when the stop-signal is presented and if it reaches its threshold before the 'go' response then it will successfully inhibit any response. The model makes the assumption that the two neural processes are independent. Although this is unlikely to be entirely true the model provides a useful framework for creating a predictable number of inhibition errors in both the SST and SCT.

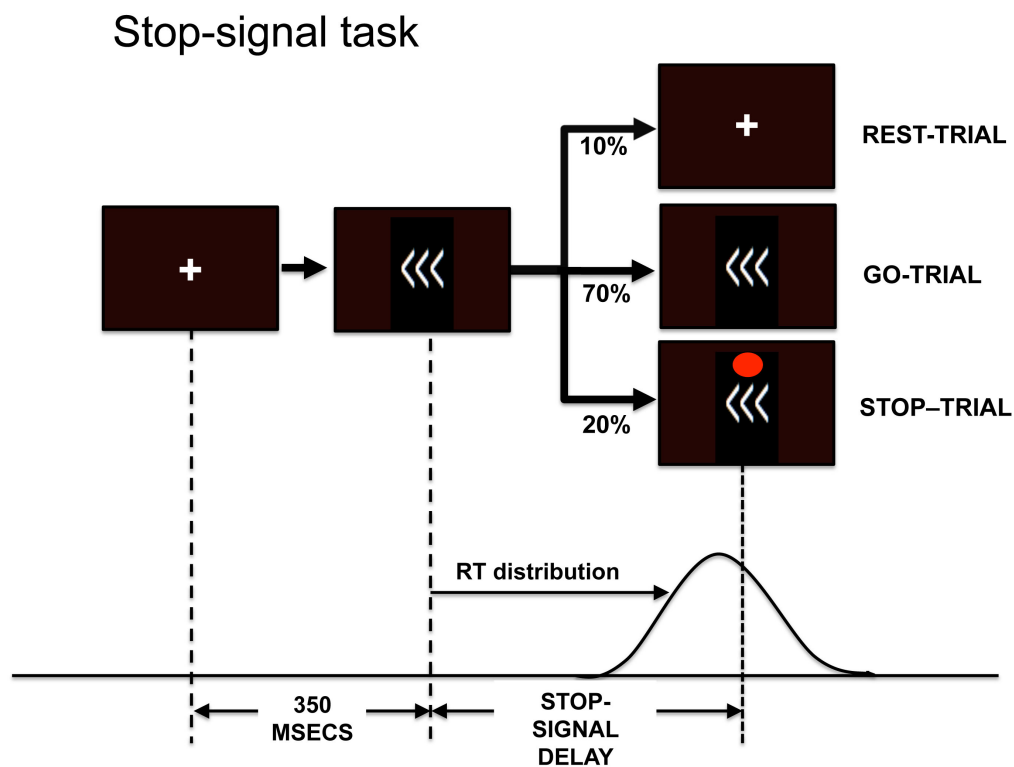


Figure 3.4: Stop Signal Task paradigm

(Moving from left to right), the fixation cross appears on screen for 350 msecs and then the arrow cue appears signalling for subjects to respond with their left or right index finger. On an unpredictable 20% of trials (stop-trials) after a variable period (the stop-signal delay) a red circle appears (the stop-signal) signifying that subjects should withhold their response.

3.3.7.2. Description of the SST paradigm

All subject performed two runs of the SST in the MRI scanner. Each run consisted of 184 pseudo-randomly ordered trials with an inter-stimulus interval of 1.75 seconds. 70% of trials were go-trials, 20% stop-trials and 10% rest-trials. During go-trials a fixation-cross appeared for 350 milliseconds before the arrow cues were presented (either <<< or >>>). The arrows were on screen for a further 1400 milliseconds before the next trial started. On stop-trials the arrows appeared and following a short stop-signal delay (SSD) the stop-signal (a red circle) appeared slightly above them (Figure 3.4). The SSD was adaptive and changed according to a staircase procedure determined by each subject's on-going performance (see below). Speed was emphasized in the task instructions and in explicit adaptive negative feedback during the task. Any subject with less than 30% success on stop-trials was excluded from the analysis (one TBI subject was removed for this reason).

3.3.8. Performance matching in the SST

As with all tasks in this thesis, the SST paradigm was designed to produce similar levels of performance accuracy across different individuals. The primary aim of the SST was to produce a predictable number of inhibition errors. This was achieved by adaptive manipulation of the SSD and the negative feedback associated with slow responses. These manipulations are described below.

The stop-signal delay

The larger the SSD the more difficult it is for a subject to inhibit their initial response. In order to produce a consistent number of errors between subjects an adaptive staircase procedure manipulates the SSD depending upon a subject's performance.

Each subject starts with a SSD of 200 milliseconds. After the first two stop-trials, if a subject is more than 50% accurate on the stop-trials the SSD increases by 50 milliseconds with no upper limit. Similarly, if a subject is less than 50% accurate on the stop-trials the SSD is decreased by 50 milliseconds with a lower limit of 250 milliseconds.

Negative feedback

To produce more errors, and avoid a situation where subjects simply wait for either the arrows to change direction or the appearance of the stop-signal, a negative feedback cue was presented when subjects' responses were particularly slow. The feedback was a visual cue. The phrase "Speed Up!" appeared on screen for 1400 milliseconds immediately after the slow trial. Slow trials were defined as a response that fell outside a variable time limit. The time limit was established for each subject at the start of SST runs based upon the subject's reaction times in the previously performed choice-reaction task (CRT). The initial time limit was set as the 95% percentile of a subject's correct reaction times in the CRT. As subjects performed the SST and SCT, this time limit was adapted to include correct go-trials from the on-going tasks.

3.3.9. Behavioural assessment of the SST

Baseline reaction times were calculated as a rolling average of the last five successful go-trials for a subject during that run (excluding incorrect trials and stop/change-trials). This measure was used to accommodate for attentional drift and trial-to-trial variability across the runs (Bonnelle, Leech et al. 2011).

Post–error behavioural adaptation

In a manner very similar to that described in the Simon task section, the reaction times for trials immediately before and the three trials following errors were calculated. All measures were taken relative to a 'baseline' performance on the last five correct go-trials immediately preceding an error to accommodate for attentional drift throughout the task.

Intra-individual variability and mean reaction times

A subjects' attention to task can be estimated by calculating the mean reaction time on correct go-trials. A more involved measure, which takes into account how subjects' attention to task varied over the course of a run, is the intra-individual variability (IIV) of the reaction times (Stuss, Stethem et al. 1989). Subjects' intra-individual variability (IIV) in reaction time was calculated as the standard deviation divided by the mean of the reaction times for all correctly answered go-trials for that run (Stuss, Stethem et al. 1989).

The stop-signal reaction time

In addition to measures of post-error behavioural adaptation and attention, the SST also provides a direct measure of inhibition in the form of the stop-signal reaction time (SSRT). The SSRT represents the delay between the start of the 'go-response' and the 'stop inhibition' processes. The SSRT is a measure of a subject's ability to inhibit one's self. Because successful response inhibition does not result in an observable response it has to be estimated and there are various ways of calculating it. In tasks where the SSD is manipulated the SSRT can be derived by subtracting the mean SSD required to produce 50% inhibition errors on stop-trials from the mean

reaction time on correct go-trials (Logan, Cowan et al. 1984). The SSRT has been linked to self-reported impulsivity (Logan, Schachar et al. 1997) as well as other measures of inhibition and executive control (Friedman and Miyake 2004). I have not discussed the SSRT in detail here, as I have not used the task primarily as a test of inhibition.

3.3.10. The stop-change task

The SCT provides a measure of subject's ability to monitor their performance. The SCT is another simple task that produces inhibition errors. Importantly, the SCT also instructs subjects to correct any perceived errors. The correction response provides an explicit measure of whether errors were detected. A mismatch between errors committed and those corrected indicates impaired on-line performance monitoring (Bekker, Overtom et al. 2005, Verbruggen and Logan 2008, Verbruggen and Logan 2009). I used the SCT to identify groups of TBI patients with normal and impaired on-line performance monitoring compared to healthy controls. These groups were then used to investigate how impaired on-line performance monitoring related to broader measures of self-awareness, behavioural anomalies, and altered neural network structure and function.

3.3.10.1. Principles of the SCT

The SCT is a timed choice-reaction task where subjects are presented with a cue that they respond to with either a right or left button press. On an unpredictable subset of trials, subjects are signalled to withhold their initial response and respond with the alternate button press by a change-signal (change-trials, see Figure 3.5). Failure to withhold the initial response leads to an inhibition error. Subjects are instructed that if they fail to inhibit their initial response they should correct

themselves by subsequently pressing the correct button. This provides a rapid on-line performance monitoring measure. Patients were split into Low Performance-Monitoring (Low-PM) and High Performance-Monitoring (High-PM) groups on the basis of the number of errors they corrected compared to healthy controls (see results in Chapter 6). During change-trials the time between the initial cue and the signal to change response (the change signal) is referred to as the change-signal delay (CSD). As with the SSD, the shorter the CSD the easier it is for subjects to inhibit their initial response.

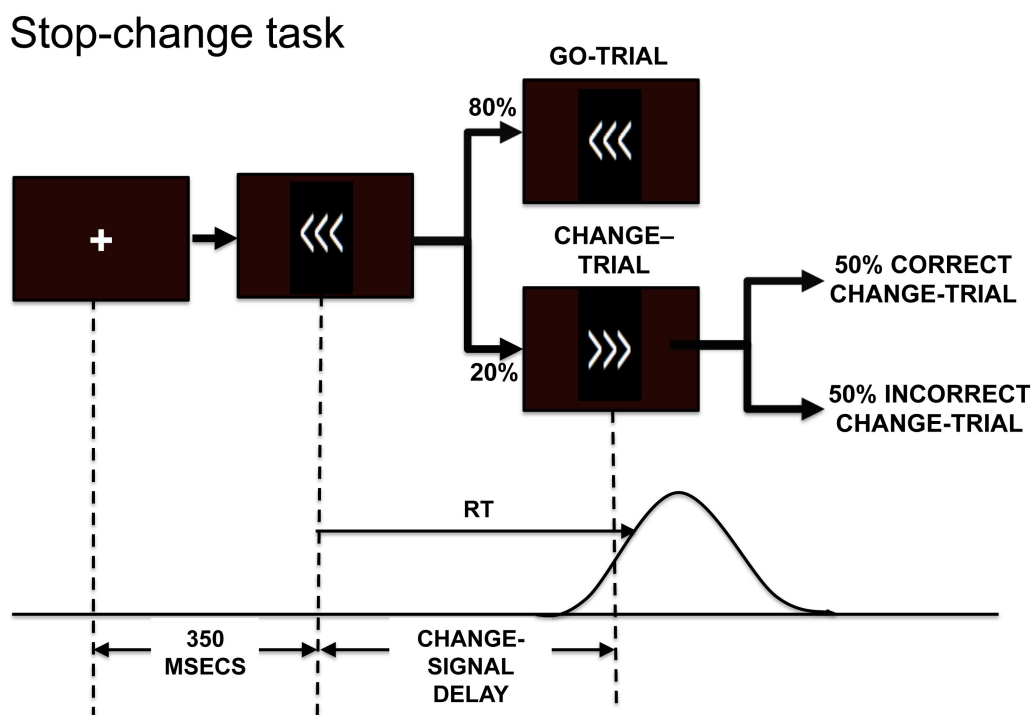


Figure 3.5: Stop-change task paradigm

Moving from left to right, the fixation cross appears on screen for 350 msec and then the arrow cue appears signalling for subjects to respond with their left or right index finger. On an unpredictable 20% of trials (change-trials) after a variable period (the change-signal delay) the arrows change direction. Subjects are asked to respond to the final direction of the arrows. If subjects respond to the initial arrow direction then they are instructed to correct themselves. The RT arrow indicated subjects' reaction times, which should occur in an approximately normal distribution.

3.3.10.2. Description of SCT paradigm

The SCT was designed to produce large numbers of inhibition errors in all subjects (Bekker, Overtoom et al. 2005, Verbruggen and Logan 2008, Verbruggen and Logan 2009). The paradigm had two different trial types: go-trials and change-trials. During go-trials subjects were presented with a series of arrows in the centre of the screen pointing to either the right (>>>) or left (<<<) (Figure 3.5). The direction of the arrows determined the direction of subjects' finger press response, (i.e. arrows pointing to the right were responded to with the right-hand and vice versa). During change-trials the arrows appeared, just as in the go-trials, then after a variable delay (the CSD) the arrows changed direction. Subjects were instructed to respond to the final direction of the arrows. If they responded incorrectly then they were instructed to correct themselves immediately by making the appropriate response. Normally subjects correct all or nearly all of their errors. The failure to correct errors provides an explicit measure of impaired performance monitoring. Explicit feedback about performance accuracy was not provided.

All subjects performed one run of the SCT after a training session. The run consisted of 204 pseudo-randomly ordered trials with an inter-stimulus interval of 1.75 seconds. Seventy percent were go-trials, 20% change-trials and 10% rest-trials. For go-trials a fixation-cross appeared for 350 milliseconds before the arrow cues were presented (either <<< or >>>). The arrows were on screen for a further 1400 milliseconds before the next trial started. On change-trials the arrows appeared and then, following a CSD of at least 200 milliseconds, the arrows changed direction. The CSD was adaptive and changed according to a staircase procedure determined by each subject's performance (described below). During SCT training subjects were explicitly instructed to correct any mistakes made during the task by pressing the

correct key after recognizing their error. Furthermore, to ensure that the failure to perform this aspect of the task was not simply due to misunderstanding the instructions, any subjects that failed to correct any of their errors were excluded from analyses (2 TBI patients). Previous studies have noted that subjects tend to slow down in order to avoid making errors (Falkenstein, Hoormann et al. 2000). As the primary outcome of the SCT was to observe subjects' response to inhibition errors this tendency needed to be tempered. This was achieved by emphasizing the importance of speed in two ways: firstly, all subjects were instructed to respond to cues as quickly and accurately as possible; secondly, a visual "Speed Up!" cue provided negative feedback if subjects responded outside of a variable time limit (see below).

3.3.11. Performance matching in the SCT

As with the Simon task and SST, the SCT produced a predictable number of errors in each subject by adaptive manipulation of the CSD and the negative feedback associated with slow responses.

The Change Signal Delay

The CSD was varied using the same specifications as the adaptive staircase procedure used to alter the SSD (see above).

Negative feedback

As in the SST, to avoid a situation where subjects simply wait for the appearance of the change-signal, a negative feedback cue was presented when subjects'

responses were particularly slow. The feedback was a visual cue. The phrase “Speed Up!” appeared on screen for 1400 milliseconds immediately after the slow trial. The method for calculating when negative feedback should be provided is the same as for the SST (see above).

3.3.12. Behavioural assessment of the SCT

Despite the relative simplicity of the task, the SCT produced many performance measures that relate to basic cognitive functions. For the behavioural analysis of the SCT I considered five separate trial types: i) correct go-trials, ii) incorrect go-trials (very small numbers), iii) correct change-trials, iv) corrected inhibition errors (incorrect change-trials that were corrected), and v) uncorrected inhibition errors (incorrect change-trials that were not corrected). Baseline reaction times were again calculated as a rolling average of the last five successful go-trials for a subject during that run (excluding incorrect trials and stop/change-trials). All post-error slowing behavioural values were calculated as differences from the baseline reaction time. The IIV for the SCT analysis was calculated in the same manner it was for the SST.

Percentage errors corrected

The number of errors produced on change-trials was manipulated using the SCD. This allowed the paradigm to produce inhibition errors on approximately 50% of all change-trials across subjects. The numbers of errors corrected provided a measure of on-line performance monitoring. The percentage errors corrected was calculated by dividing the number of incorrect change-trials that were corrected by the total number of incorrect change-trials. To ensure subjects understood the task, they were instructed at the start of each run and during training that all errors should be

corrected. In addition any subject that did not correct any errors was excluded from the analysis with the assumption that they did not understand the task.

3.3.4. Magnetic Resonance imaging

MRI techniques provide detailed images of tissues using the principle of nuclear magnetic resonance. This principle states that when atomic nuclei with an odd atomic number are placed in a strong uniform magnetic field and stimulated by radiofrequency (RF) pulses, they will re-emit radio waves (Pykett, Newhouse et al. 1982). The characteristics of these radio waves are dependent upon both the organization of the specific atoms being stimulated within the tissue, and the feature of the excitatory RF pulse. In MRI the commonly used atomic nuclei is hydrogen as this is found in abundance in the body. Using these principles MRI scanners are able to create images that differentiate between soft tissues that have very similar radiodensities but very different hydrogen contents, (e.g. grey and white matter of the brain in structural MRI), and magnetic properties, (e.g. oxyhaemoglobin and deoxyhaemoglobin in fMRI).

3.4.1. Nuclear Magnetic Resonance

Atomic nuclei contain protons and neutrons with the exception of hydrogen, which contains a lone proton. These particles carry an angular momentum or 'spin'. When possible, each particle is paired with another particle of the same type. They are arranged in such a manner that the spins of each particle cancel each other out. However, in atoms with odd number of neutrons and/or protons not all particles can be paired. These atoms have atomic nuclei with a net angular momentum and they 'spin' along an axis (Figure 3.6A). As atomic nuclei are electrically charged, the spin creates a magnetic field along this axis. This axis can be referred to as the

'magnetisation vector' of the atom. Atomic nuclei in this sense can be likened to bar magnets with their dipoles lying along the length of their magnetisation vector.

Outside of any external influence the arrangement of the magnetisation vectors within a non-magnetic tissue are random and the net magnetic vector (M) of the tissue is zero (Figure 3.6B). When a strong static magnetic field (B_0) is applied to the nuclei the atomic magnetisation vectors realign themselves, either parallel or antiparallel to the main axis of B_0 . The magnetic vectors of the atoms then precess around this axis, rather like gyroscopes (Figure 3.6C). In three-dimensional space the main axis of the field B_0 is normally referred to as the z-axis, I shall conform to this convention for the remainder of the section. Atoms aligned parallel and antiparallel to B_0 are referred to as 'low-energy' and 'high-energy' atoms respectively. The stronger the B_0 magnetic field applied to a tissue the more parallel/low-energy atoms and the larger the net magnetisation vector (M) in the z-axis (Figure 3.6.C).

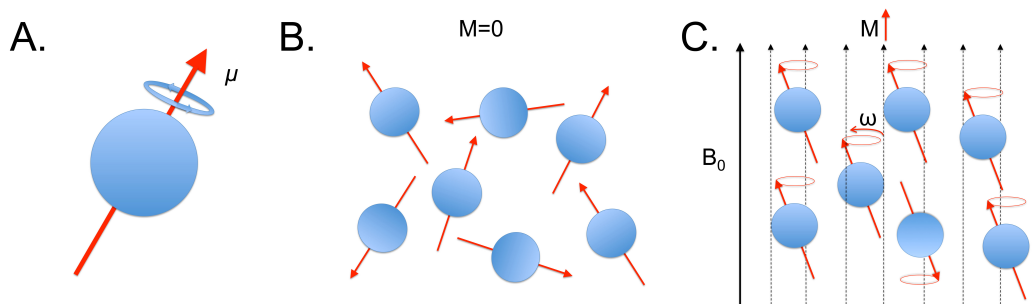


Figure 3.6: Principles of MRI

(A) The hydrogen atomic nuclei 'spin' and create a magnetic vector (μ) along their spin axis. Atoms are represented by the blue circles and the magnetic vector by red arrows. (B) The magnetic vectors in normal (non-magnetic) material are randomly arranged and there is no net magnetic vector (M) for the tissue. (C) In a strong static magnetic field (B_0) magnetic vectors align with the static field to become either parallel ('low energy') or antiparallel ('high-energy') atoms. This creates a net magnetic field in the direction of B_0 . The stronger the static field the more low-energy atoms and the larger M becomes in the direction of B_0 . B_0 is indicated by the dashed black arrows. ' ω ' represents the angular momentum with which the hydrogen nuclei precess around the B_0 axis.

Once aligned the nuclei can be 'flipped' from low-energy to high-energy states by RF pulses acting along the x-y plane perpendicular to the z-axis. In exchanging low-energy for high-energy atoms the net magnetic vector of the tissue moves into the x-y plane (Figure 3.7). The flip angle (θ) is the angle between the z-axis and the net magnetisation vector created by the RF pulse. Increasing the strength or duration of the excitatory RF pulses will increase θ by making more high-energy atoms. When there are equal numbers of high and low energy atoms the net magnetic vector is perpendicular to the z-axis (flip angle 90). When all atoms are in high energy states the net magnetic vector is negative in the z-axis (flip angle 180). The excitatory RF pulse is simply an oscillating magnetic field (B_1). In MRI an electromagnetic coil surrounding the sample supplies these excitatory RF pulses. The frequency of the excitatory RF pulses is specific for the atomic weight of the atomic nuclei being excited. This frequency is called the resonant frequency or Lamour frequency (ω_0) and can be calculated as follows:

$$\omega_0 = \gamma B_0 / 2\pi$$

Where γ is a constant for each atomic nuclei referred to as the gyromagnetic ratio. For example, the gyromagnetic ratio of a hydrogen nucleus is $2.675 \times 10^8 \text{ s}^{-1} \text{ T}^{-1}$. Therefore, in a one tesla B_0 magnetic field hydrogen's Lamour frequency is 42.574 megahertz (Pykett, Newhouse et al. 1982). Most MRI sequences focus on hydrogen atoms as it is abundant in the body and also distinguishes between important structures (e.g. grey and white matter) that have comparable radiodensity and can therefore not be distinguished by CT.

Once the excitatory RF pulses cease the high-energy atoms return to being low-energy atoms. As this occurs the net magnetic field vectors return to the z-axis and the transverse component of the magnetic axis is lost. This process is called 'free

induction decay' (FID). The amplitude and frequency of the emitted signal is dependent upon θ , B_0 , and the density of the atoms (hydrogen atom density in the case of most MRI scans). In MRI a receiver coil is used to detect this electromagnetic field. As stated above, the magnetic vectors of the atoms excited by the RF pulse precess around the z-axis (Figure 3.6.A). Initially the flipped atoms precess in phase giving a large oscillating net component in the x-y plane. In MRI a receiving coil around the tissue measures the transverse component of the tissue magnetic vector (M_{xy}). It can only measure the transverse and longitudinal component of M once the excitatory RF pulse has stopped.

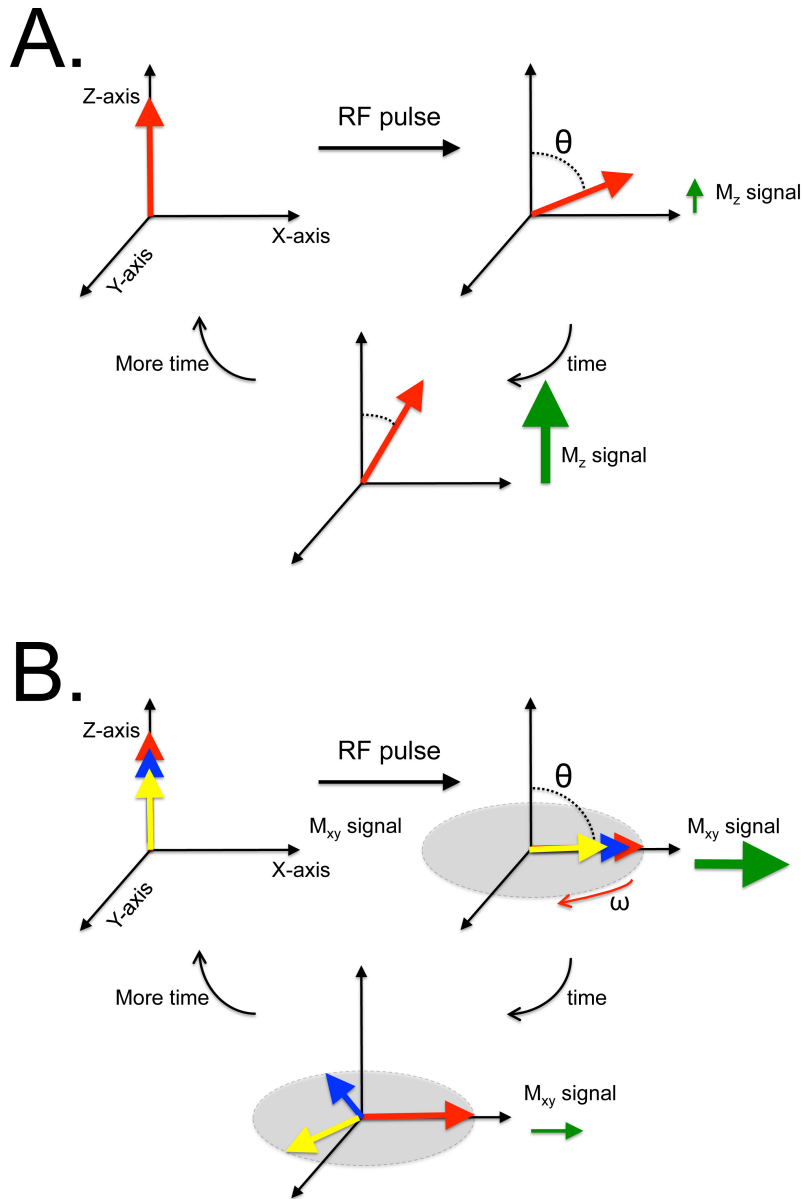


Figure 3.7: T1 and T2 relaxation times

(A) The net magnetic vector (M) is displaced by the excitatory RF pulse to a flip angle (θ) relative to the z-axis, reducing its z-axis component (M_z). As the RF pulse stops and time passes the excited atoms lose energy and revert back to a low-energy state causing M_z to increase until it returns to its pre-excited state. (B) M (the summation of the red, blue and yellow arrows) is displaced to a flip angle of θ . Initially all of the atomic magnetic vectors (represented by the red, blue and yellow arrows) precess in phase giving a large phasic M_{xy} value. As time progresses the atomic magnetic vectors move out of phase with one another and M_{xy} decreases back towards zero. N.B. M_{xy} will return back to zero before M_z has returned to its pre-excited state.

The receiver coil measures two features of the FID relating to how long the magnetisation vector takes to return to the 'normal' pre-excited state, the T1 and T2 relaxation times. The T1 time or longitudinal relaxation time is a measure of the rate at which the net magnetisation vector returns to the z-axis (Figure 3.7A). The T2 time or transverse relaxation is a measure of the rate that the x-y component of the magnetisation vector deteriorates (Figure 3.7B). These two values are not equal. T1 time relates to the rate at which high-energy atoms dissipate their energy and return to low energy states. The transverse component deteriorates not only because high-energy atoms return to low-energy states but also because interference from the magnetic fields of adjacent atoms causes them to rapidly shift out of phase reducing the net magnetic field in any one direction along the x-y plane. Hence, T2 times are significantly shorter than T1 times. A further measure of transverse decay is the T2* time. The T2* takes into account that inhomogeneity in B_0 . In echo-planar imaging (EPI) the magnetic field is manipulated to accelerate the rate of transverse decay and provide a rapid assessment of T2* time. The shorter time frame is particularly useful in fMRI as it provides a more rapid measure of brain processes.

3.4.2. How MRI images are generated

The electromagnetic field generated by the magnetic vectors returning to realign with the main axis of B_0 have properties, which are manipulated to generate MRI images. As stated in the Larmor equation above, the resonance frequency of an atom is proportional to the B_0 field strength applied to it. Gradient coils used in MRI produce a B_0 field with gradually increasing field strength in one spatial direction. The resonance frequency of the atoms along that spatial direction will vary in a predictable manner. Therefore, producing three orthogonal B_0 fields (or a single rotating field) and measuring FID in multiple planes provides spatial information necessary to make a composite image of the proton density, T1, T2, T2*

characteristics at any point in the field(s).

MRI parameters

MRI uses a receiving coil to measure the FID characteristics (i.e. T1, T2 and T2* times) and proton density at different spatial locations within a sample. This allows MRI to differentiate between different tissue types within a sample. Different MRI sequences are optimised for the acquisition of different FID characteristics. The term 'MRI sequence' refers to the waveform of the RF pulse sequence used. The two primary parameters used to describe MRI sequences are *repetition time* (TR), which is the time between two consecutive RF pulses, and *echo time* (TE), which is the delay between the RF pulse and FID signal measurement. For this reason TE is always shorter than TR. By varying TR and TE MRI sequences are able to ascertain the FID characteristics and proton density at different locations within a tissue. The images produced are contrasts of where the FID properties in a tissue differ and the commonest ones used are described briefly below.

3.4.3. T1 weighted-images

These are images that use the T1 (longitudinal relaxation time) to discriminate between tissues. White matter has a much shorter T1 time than grey matter. T1 images therefore give excellent anatomical detail on the contrast between grey and white matter (Figure 3.8). For this reason, T1 weighted images are generally used to provide anatomically detailed brain images. Although the T1 time is longer than both T2 and T2* these MRI sequence used to acquire T1 images requires the shortest TR of all the sequences described and an intermediate TE (full longitudinal relaxation is not required to acquire the T1 time).

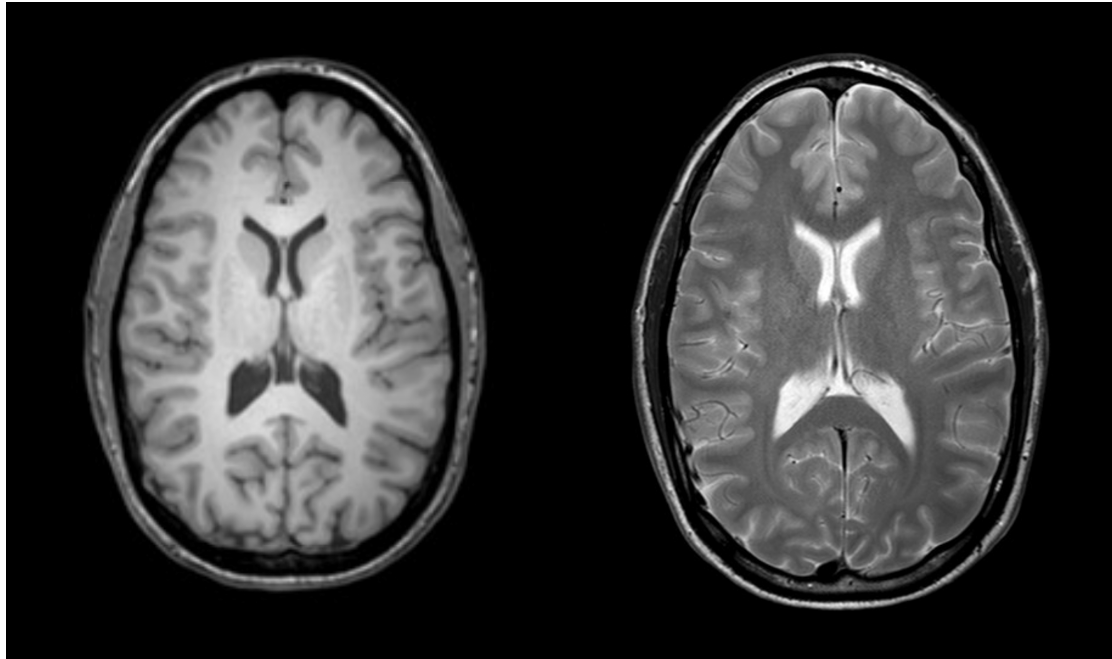


Figure 3.8: MRI axial images of a healthy brain

T1 (left) and T2 weighted (right) axial MRI images of a healthy brain

3.4.4. T2 weighted-images

T2 images rely upon the differences in transverse relaxation times between tissues. There is little difference between the T2 times of grey and white matter and therefore T2 images do not provide the same anatomical detail that T1 images do (Figure 3.8). However, because fat and water have very different T2 relaxation times, T2 weighted images are sensitive to oedema associated with many pathological processes. Just as T1 scans are often considered scans that assess anatomy, T2 scans are often considered as scans that assess pathology. Dedicated T2 scans require a much longer TR time than T1 scans as all tissues need to have achieved complete longitudinal relaxation.

3.4.5. T2* weighted images and Echo-planar imaging

T2* images measure the transverse relaxation time taking into account inhomogeneity within the static magnetic field. The sequences use long TR and medium TE and a magnetic field gradient across the tissue to provide a known field inhomogeneity. By increasing the gradient the T2* time decreases and in this way MRI can create T2* times that are significantly shorter than T2 times.

Echo-planar imaging (EPI) is variation on the T2* process that rapidly changes the magnetic field gradient whilst recoding the tissue signal. EPI allow the sampling of an entire tissue with a single RF pulse. EPI creates low-resolution (usually in the order of 4x4x4 mm voxels) images that can be acquired very quickly. This makes EPI sequences especially useful for monitoring dynamic changes within the brain over time (e.g. functional MRI).

3.4.6. Susceptibility-weighted images

SWI are different to the previously described MRI images. SWI combines amplitude and phase information from a 3D gradient-recall echo sequence to detect local differences in magnetic susceptibility. Given a long enough TE adjacent tissues with different magnetic susceptibilities will become out of phase. This process is enhanced the greater the difference between the susceptibilities. One clinically useful example is the paramagnetic properties of deoxyhaemoglobin in cerebral micro-bleeds compared to the non-magnetic surrounding brain tissue (Chastain, Oyoyo et al. 2009, Beauchamp, Ditchfield et al. 2011). SWI is exquisitely sensitive at detecting such differences.

3.5. Functional Magnetic Resonance imaging

3.5.1. Principles of fMRI

Functional MRI is a MRI technique that provides anatomically detailed information on *in vivo* brain activity. When neuronal populations activate in the brain they cause changes in regional blood flow through a process of neurovascular coupling. Neurons activate and cause increased metabolic demands and concomitant increase in local cerebral blood flow (CBF). This leads to an increase in local oxyhaemoglobin above that which is required for the minimal increase in oxygen consumption. Therefore neuronal activity is associated with a transient net increase in the ratio of oxyhaemoglobin to deoxyhaemoglobin. Deoxyhaemoglobin and oxyhaemoglobin have different magnetic properties. Deoxyhaemoglobin is paramagnetic and oxyhaemoglobin is diamagnetic. The paramagnetic deoxyhaemoglobin causes distortion/inhomogeneity in the local magnetic field of tissues well beyond the walls of the blood vessel it occupies (Ogawa, Lee et al. 1990). These inhomogeneities can be measured using T2* weighted images and can be enhanced using gradient-echo techniques (Ogawa, Lee et al. 1990, Ogawa, Tank et al. 1992). The difference in T2* signal associated with different levels of deoxyhaemoglobin is referred to as the blood-oxygen-level-dependent (BOLD) contrast (Ogawa, Lee et al. 1990).

The BOLD signal was initially used to measure *in vivo* dynamic changes in rat brains exposed to different pharmacological agents (Ogawa, Lee et al. 1990). However, it was soon applied to examining the *in vivo* neuronal response to visual stimuli in humans (Menon, Ogawa et al. 1992, Ogawa, Tank et al. 1992). The change in BOLD signal after neuronal activity was noted to occur in a predictable pattern referred to as the haemodynamic response function (HRF) (Friston, Jezzard et al. 1994). The HRF describes how following neuronal activity the BOLD signal initially dips as local

deoxyhaemoglobin concentration rises. The dip is followed by a peak BOLD signal approximately 5 to 6 seconds after neuronal activity, as the supply of oxyhaemoglobin overshoots the demand. This peak is followed by a slow decay and return to baseline over approximately 10 seconds (Bandettini, Jesmanowicz et al. 1993) (Figure 3.9). Studies have demonstrated that the HRF is largely preserved across individuals and highly reproducible within individuals (Aguirre, Zarahn et al. 1998). The speed at which the T2* signal can be acquired has been increased massively by the introduction of EPI (discussed briefly above). EPI allows T2* signal across the entire brain to be acquired over a single TR (in the order of 2 seconds). EPI therefore provides a measure of BOLD signal with sufficient temporal resolution to measure dynamic changes in brain activity modelled by the HRF

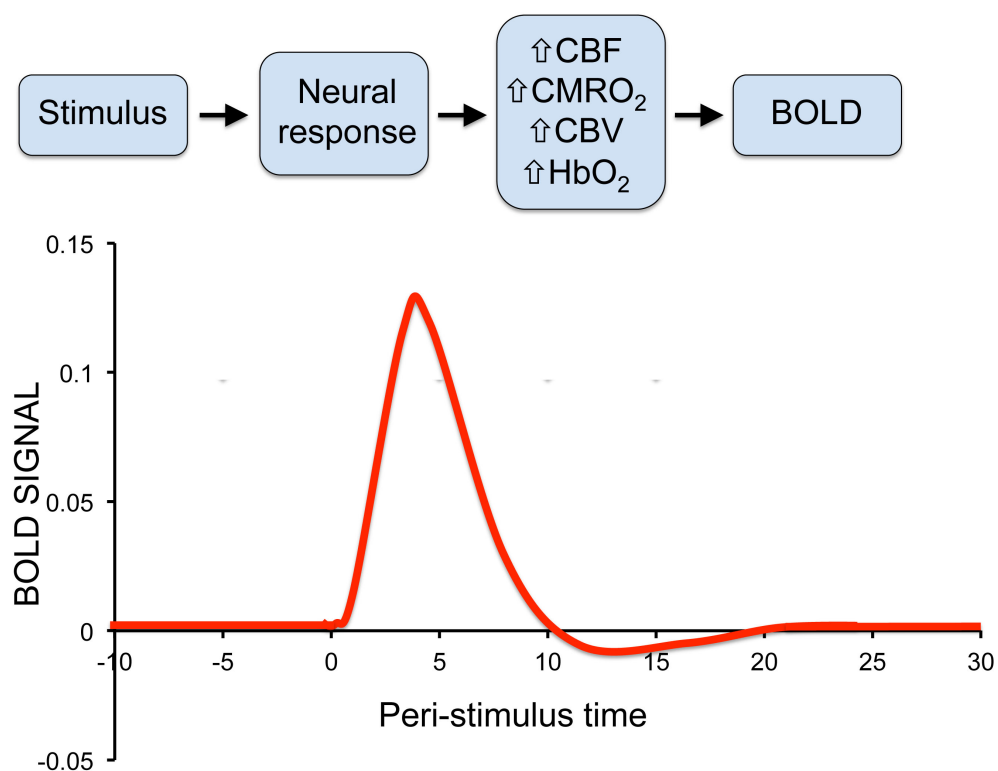


Figure 3.9: The haemodynamic response function

Stimuli that provoke large neuronal populations to activate will result in local increases in cerebral blood flow (CBF), cerebral blood oxygen consumption (CMRO₂), cerebral blood volume (CBV), and oxyhaemoglobin concentration (HbO₂). This causes a predictable transient change in the BOLD signal around the activated neuronal population.

3.5.2. Event-related fMRI

fMRI uses the HRF to model how the BOLD signal should react in brain regions with specific functions when those functions are performed. The function of interest is usually engaged by an experimental manipulation. Data on how the BOLD signal actually changes during the manipulations is acquired using EPI and compared to the HRF based models to see how well they fit. In event-related fMRI the behavioural data acquired during fMRI acquisition is used to generate the predicted model. There are two main ways of approaching this problem either using a block design or a moment-to-moment event-related design. Block designs offer the best signal to noise ratio and are more powerful statistically (Buckner, Bandettini et al. 1996, Kim, Richter et al. 1997, Price, Crinion et al. 2006). However, block designs are inappropriate for use dynamic tasks such as the Simon task and SST. Therefore, I have used event-related designs throughout this thesis. I have used FEAT (fMRI Expert Analysis Tool) version 5.98, which is part of FSL software (FMRIB's Software Library: www.fmrib.ox.ac.uk/fsl) (Smith, Jenkinson et al. 2004), and SPM8 (Wellcome Trust Centre for Neuroimaging: www.fil.ion.ucl.ac.uk/spm) to perform the event-related fMRI analyses in this thesis. Both software packages have benefits relating to the experimental questions they were designed to answer.

3.5.3. Data pre-processing

Prior to any statistical analysis the data needs to be pre-processed. This consists of a number of steps that are largely automated and share considerable overlap between FEAT and SPM.

3.5.3.1. Brain extraction in FEAT

The Brain Extraction Tool (BET) in FSL removes the skull and soft tissues from the (structural) T1 weighted images and (functional) EPI images. BET uses measures of signal intensity from the image to determine the likely volume of the brain and its geometric centre of gravity (COG). BET then creates a sphere with a centre at the COG and a radius that makes the volume roughly half that of the estimated brain (Figure 3.10). The sphere has a surface of tessellated triangles that move away from the centre and re-orientate themselves in an iterative process until the sphere volume and surface approximate that of the brain.



Figure 3.10: BET in FSL

The marker in the left side image indicates the brains centre of gravity as determined by BET. The circle in the centre panel represents an expanding sphere with a surface of tessellated triangles. The right panel shows the final estimated brain shape. Adapted from (Smith 2002).

In FEAT BET is used as the initial stage of linear registration of individual subjects' brains to a standard brain template. There is no equivalent process in SPM.

3.5.3.2. Temporal filtering

Both FEAT and SPM8 employ temporal filtering to remove noise from the EPI data. Most of the noise comes from low frequency trends in the data that may arise from physical sources including "scanner drift" (e.g., slowly-varying changes in ambient temperature and magnetic field strength), from physiological sources (e.g.,

biorhythms, such as the respiratory and cardiac cycles, that are aliased by the slower sampling rate), and from residual movement effects and their interaction with the static magnetic field (Turner, Howseman et al. 1998). FEAT employs a high-pass filter to remove such trends from the EPI data (Figure 3.11). I used the default option of 1/100 Hz cut-off frequency as the minimum frequency allowed through the high-pass filter when using FEAT. SPM8 uses a similar process to remove low-frequency drifts. In SPM8 the data is high-pass filtered using a set of discrete cosine basis functions, and I used the default cut-off value set in SPM8 of 1/128 Hz.

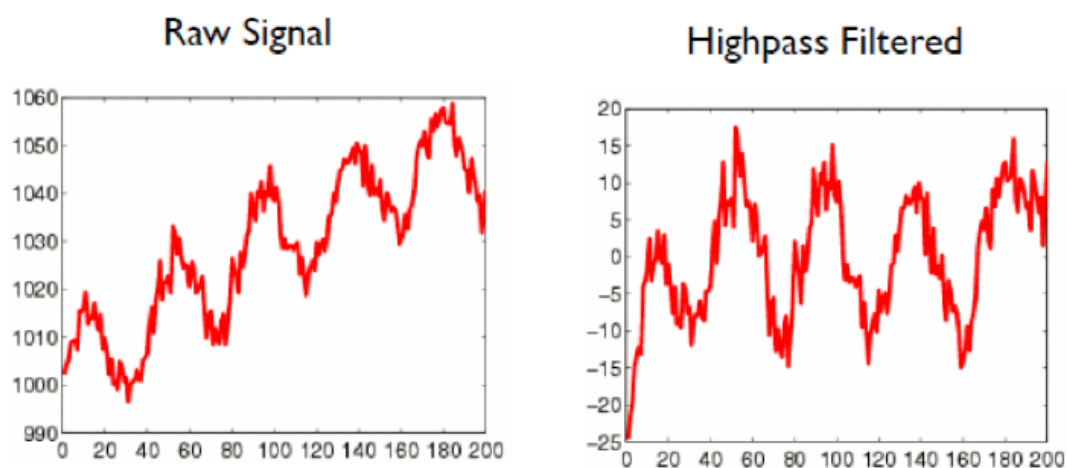


Figure 3.11: Temporal filtering

The panel to the left is data that has not been temporally filtered and there is clearly a slow linear trend affecting the data. The panel to the right is data that has had a high-pass filter applied to it and the trend has been removed.

3.5.3.3. Spatial filtering

In addition to temporal filtering, both FEAT and SPM8 use a process of spatial filtering or smoothing. Spatial smoothing works on the assumption that any noise in the data is distributed randomly across space and independent from voxel to voxel. Therefore averaging across several voxels should trend any noise in the data towards zero. Practically this is achieved by applying a Gaussian kernel to each voxel in each volume of the fMRI data. This effectively blurs the data in each voxel

across several of its neighbours. Smoothing is intended to improve signal to noise ratio but can mask out very small activation areas. I used the default value of 8mm full width half maximum (FWHM) as the diameter of my smoothing kernel in both SPM8 and FEAT.

3.5.3.4. Motion correction

Subjects are instructed to remain as still as possible during MRI acquisition. However, movement artefact is often seen and poses a significant problem if not accounted for. Both SPM8 and FEAT use a rigid body transformation between EPI images to compensate for movement between volumes. This process involves moving each EPI volume in up to 6 planes (i.e. displacement along three orthogonal spatial planes and rotation in the same planes) to better match the other EPI volumes. FSL uses the middle volume in the EPI sequence as the template to which all other EPI volumes should be matched. SPM8 uses a slightly different process and matches each EPI volume to the preceding volume.

3.5.3.5. Registration

In order to compare across subjects all subjects need to be registered to a common brain template. In order to make translation across studies easier this common template is normally an internationally recognised one such as the Montreal Neurological Institute (MNI) 152 template series. Both SPM8 and FEAT do this in slightly different ways but the end result is very similar. The main difference is that SPM8 performs the registration before any statistical analysis, whereas FEAT performs the registration as a final step after statistical analysis has completed.

FEAT uses FLIRT (FMRIB's Linear Image Registration Tool), which is a fully automated robust and accurate tool for linear (affine) intra- and inter-modal brain image registration (Jenkinson and Smith 2001, Jenkinson, Bannister et al. 2002). FLIRT is a two-step registration process that initially registers all low-resolution brain extracted EPI volumes to the structurally detailed brain extracted T1 images of the same subject. It does this using a rigid body transformation with 6 degrees of freedom. A rigid body translation can be used because the T1 and EPI images should be essentially the same shape in slightly different planes (i.e. they are both images of the same brain). This creates EPI images that are registered to high-resolution T1 images called 'func2highres' images. The second stage in FLIRT involves using an affine linear transformation with 12 degrees of freedom to register the highly detailed T1 images onto the MNI 152 standard brain template. The additional 6 degrees of freedom allow FLIRT to warp/distort the T1 image to better fit the MNI template. Once this has been done it creates a T1 image of the subject's brain that should overlap well onto the standard MNI 152 template called a 'highres2standard' image. In doing this FLIRT creates a transformation matrix that can be applied to the func2highres images to register them directly to the standard MNI template. These now registered EPI and T1 subject images are then checked visually to ensure that registration has been performed appropriately and no distorted brains are included in analyses (two TBI patients were excluded from the analysis in Chapter 6 due to poor registration).

3.5.4. Statistical analysis of fMRI

Both SPM8 and FEAT use a multi-level statistical approach to analyse fMRI data. In this thesis, all fMRI studies used multiple subjects and each subject completed multiple 'runs' of the same paradigm. A General Linear Model (GLM) is used to provide summary statistics at the individual run level or first-level analysis (Figure

3.12). These statistics are then grouped together for the individual subject (intermediate-level fixed effects analysis) and finally across subjects at a group level (higher-level random effects analysis) to allow inferences that can be applied to a more general population.

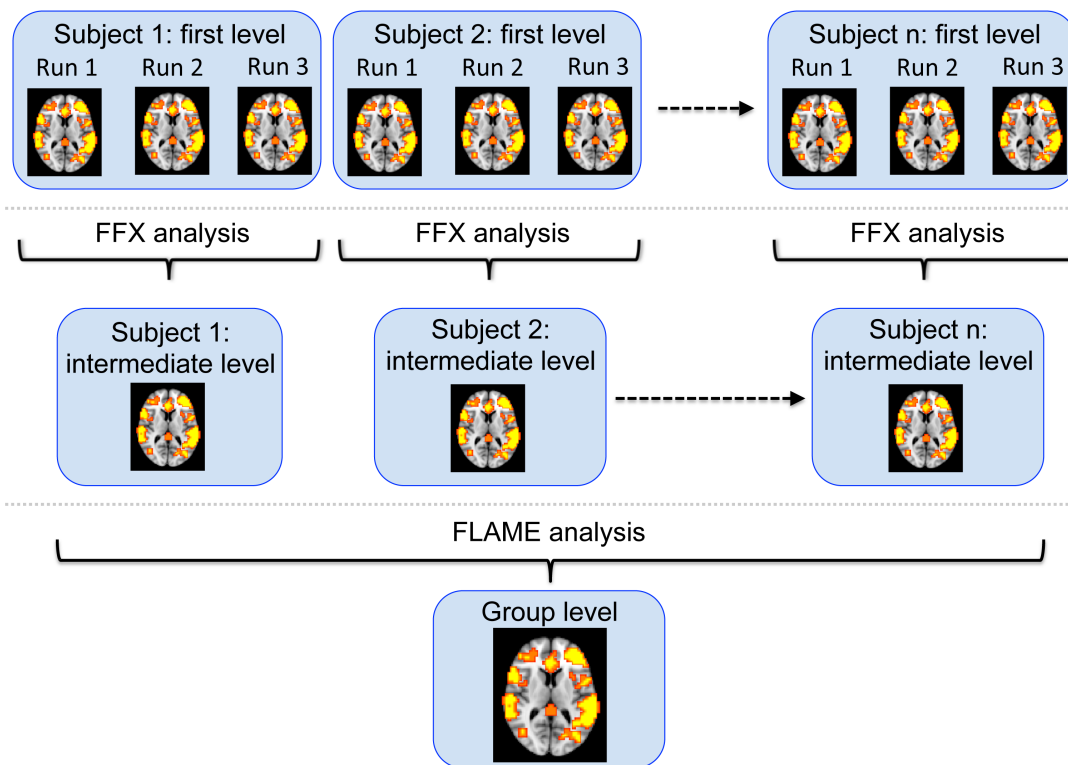


Figure 3.12: Schematic of the three levels of fMRI analysis applied in FEAT.

This demonstrated how a fMRI analysis across ‘n’ subjects who have each performed three runs of the study would be assessed. The top row represents the first-level analysis where every run for every subject is analysed separately. The middle row represents the intermediate-level where first-level results are merged using fixed effects analysis (FFX) to create a single result for every subject. The bottom row represents the final group-level analysis where intermediate-level results for every subject are merged using FLAME mixed effects models to produce a single result representative of the population the subjects were sampled from.

3.5.4.1. First-Level analysis

In an event related fMRI analysis subjects’ behaviour are modelled as a series of delta-stick functions indicating when certain events of interest have occurred (e.g. errors on the Simon task (Figure 3.13)). These stick functions are then convolved

with a synthetic HRF to create HRF models of what we believe the BOLD response would be in areas of the brain that relate to this activity. These HRF models are simply column vectors (e.g. X_1 , X_2 , X_3).

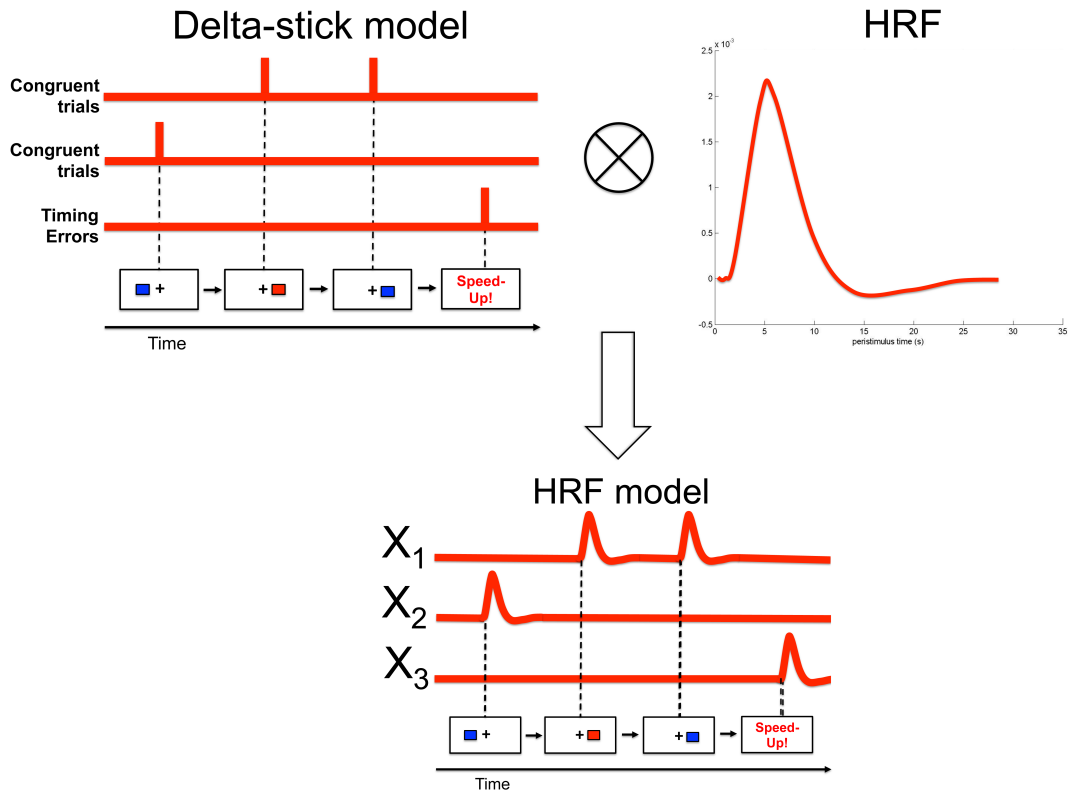


Figure 3.13: Behaviour conversion to HRF model

Behavioural data acquired during the fMRI paradigms are converted to simple delta-stick models that code the timings of events of interest. These delta-stick models are convolved with the HRF to create an HRF model that represents how the BOLD signal should change in brain regions involved with the events of interest.

Using general linear modelling each HRF model is then fitted on a voxel-by-voxel basis to the actual fMRI BOLD signal data (Y). The GLM tries to fit the HRF models as well as it can to the fMRI data using a least sum of the square of the errors approach. In doing this GLM produces beta values representing how well each of the HRF models fits the data in each voxel (e.g. β_1 , β_2 , β_3).

$$Y = \beta_1 X_1 + \beta_2 X_2 + \beta_3 X_3 + \epsilon$$

' ϵ ' in this case is an error function for the data that could not be explained by the models. Each β value has a degree of uncertainty associated with it (i.e. the standard error derived from ϵ). The β values are converted to t-stats (the mean β value divided by the standard error of β), which are in turn normalized to z-scores before any further statistical analysis is made. When comparing between conditions (e.g. errors vs. correct trials) the beta values for the HRF models of those conditions are subtracted from one another on a voxel-by-voxel basis, and a new z-stat image is created (Figure 3.14).

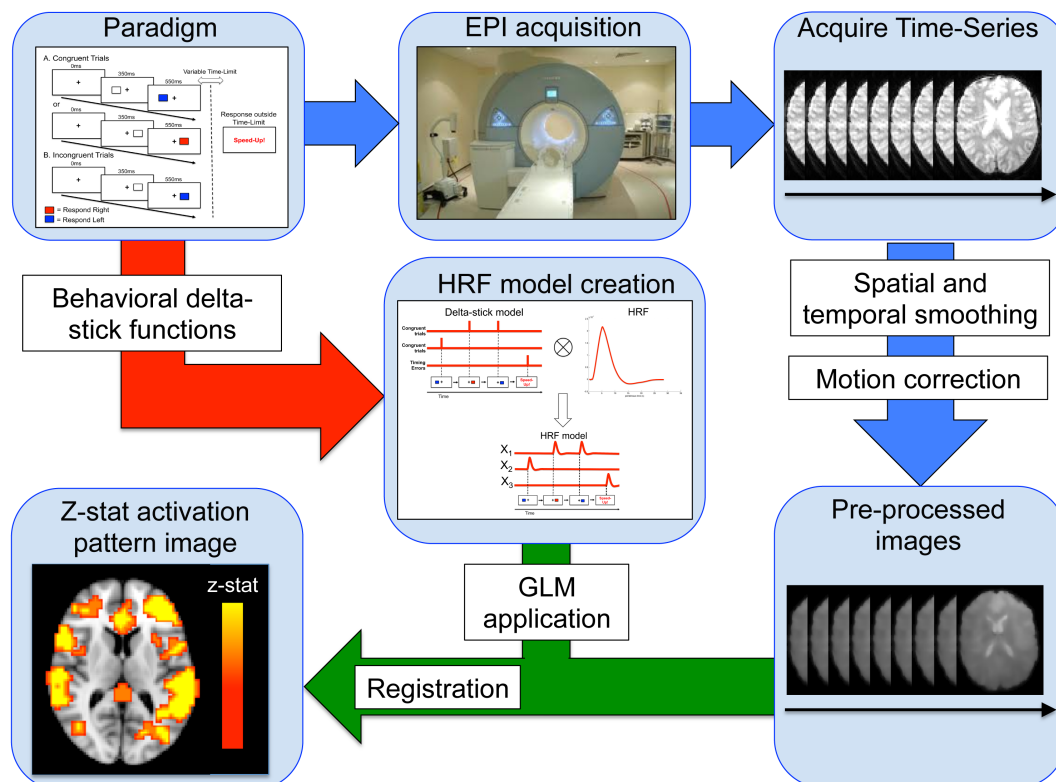


Figure 3.14: Schematic overview of first-level analysis in FEAT

There are two pathways involved: first (red arrow) gathers the behavioural data and makes the HRF model for how brain regions involved in a particular function tested in the paradigm should respond; second (blue arrows) the raw EPI data acquired during the paradigm and pre-processes (spatially and temporally smoothing and correcting for motion). In the final stage (green arrow) a GLM is applied to see how the HRF model fits the pre-processed data. The resulting z-stat image is then registered to a standard brain template.

The first-level analysis is essentially the same in SPM8 and FEAT. The main difference concerns how the two software deal with realignment and registration. In FEAT registration to a standard MNI brain occurs after statistical analysis, whereas in SPM registration is one of the first steps performed. FEAT realigns the fMRI data prior to statistical analysis; SPM8 also does this but in addition uses the 6 rigid body transformation parameters as nuisance regressors in the first-level model. Adding the nuisance regressors in SPM8 is designed to account for any change in BOLD signal due to movement alone.

3.5.4.2. Intermediate-level fMRI analysis

The studies described in this thesis required subjects to perform multiple runs of the same task paradigm. These runs were analysed separately at the first-level and then combined in a fixed effect analysis for each subject (Figure 3.12). Fixed effect analyses assume equal variance in the beta values across sessions for a given subject.

3.5.4.3. Higher-Level fMRI analysis

The GLM process described above provides an estimate of how well the predicted models fit the data observed at each voxel for a single subject, which is of use only on a case-by-case basis. In fMRI we generally want to make inferences on the general population from which the subjects were sampled. To do this the variance within each subject needs to be taken into consideration. This is done using random and mixed effects in SPM8 and FEAT respectively. Mixed effects employed by FEAT uses the hierarchical approach outlined in Figure 3.12, to provide summary statistics about individual runs, individual subjects and finally group that those subjects were sampled from (Smith, Jenkinson et al. 2004). SPM8 adopts a more computationally

demanding ‘all-in-one” random effects approach to group level analysis, where the first-level studies are put back together and reanalysed in the context of the other studies using Bayesian inferences (Friston, Penny et al. 2002). These approaches have been shown to give comparable results (Beckmann, Jenkinson et al. 2003). Using both these approaches allowed me to make inferences about the general population and statistical comparisons between groups (i.e. TBI patients and healthy controls).

3.5.5. Thresholding

By applying the techniques outlined above I created a z-scores for every behavioural model for every voxel in my fMRI data set. There are approximately twenty thousand voxels acquired across the brain in any fMRI analysis. This creates a significant multiple comparison problem that needs to be overcome before the voxel-wise estimates of model fit can be interpreted. Using a p-value for each voxel would create an excessive number of type 1 statistical errors. If the voxels were all thought to be independent then a Bonferroni correction could be applied, but as the voxels are not independent then this would lead to excessive type 2 statistical errors (assuming 20,000 voxels any significant p-value would be $< 2.6 \times 10^{-6}$). Various thresholding measures have been adopted to solve the problem. One solution has been to jointly use intensity and spatial extent thresholds in the same analysis, (i.e. cluster correction (Forman et al., 1995)).

3.5.5.1. Cluster correction in FEAT

Cluster analysis takes into account the evidence of spatially adjacent voxels. The principle being that a voxel is more likely to be genuinely significant if the adjacent voxels are also significant. FEAT uses Gaussian Random Field (GRF) theory to

implement cluster based multiple comparison correction. In brief, the application of GLM described above produces a z-stat value for every voxel for a particular contrast of interest. A threshold is then applied to the z-stat image (>2.3 in all analyses included in this thesis) to define contiguous clusters. All voxels below this threshold are then excluded from further analysis. By applying GRF-theory any suprathreshold voxels without a significant adjacent voxels are also excluded from analysis. The clusters significances are determined by GRF-theory and described in terms of a p-value usually thresholded at <0.05. This creates clusters of contiguous statistically significant voxels, which are then used to mask the original z-stat images and create the images used in the thesis.

3.5.5.2. False Discovery Rate and Family-Wise Error

Cluster correction is a statistically robust way to test for significant activation in fMRI data. However, it may be overly stringent when looking for activation in small regions. Alternatives such as false-discovery rates (FDR) and Family-Wise Error (FWE) rates have been adopted to resolve this issue, as they do not require local spatial correlations. Both FWE and FDR do not rely upon a predetermined p-value to threshold significant voxels. The threshold p-value that corresponds to a particular FDR or FWE threshold is determined by examining the distribution of p-values across all brain voxels (Nichols and Hayasaka 2003). Applied to neuroimaging if ' M ' represented the number of voxels in a data set then the p-values for each voxel would be ordered $\{P_1, P_2, P_3 \dots P_M\}$. The p-value of a single voxel ' k ' can be noted as $P_{(k)}$.

	Null hypothesis true	Null hypothesis false	
Null hypothesis declared significant	V	U	R
Null hypothesis declared false	S	T	M-R
	M_0	$M - M_0$	M

'V' represents the number of voxels where the null hypothesis was true and found to be true on testing (i.e. true negative result); 'S' represents the number of voxels where the null hypothesis was true and found to be false on testing (i.e. a false positive result); 'U' represents the number of voxels where the null hypothesis was false and found to be true on testing (i.e. false negative result); 'T' represents the number of voxels where the null hypothesis is false and found to be false on testing (i.e. a true positive result); M is the total number of voxels under assessment; M_0 is the total number of voxels where the null hypothesis is true.

Using definitions from the table above an FDR level of ' α ' can be determined by examining the p-value distribution across all voxels determining largest value of k that the following equation applies to:

$$P_{(k)} \leq k \cdot \alpha / M$$

The p-value $P_{(k)}$ establishes the p-threshold that can be applied to every voxel to create an FDR corrected images at level ' α '. FDR essentially controls for the probability that the null hypothesis has been incorrectly rejected for a given voxel and provides a less stringent way of performing a multiple comparison correction. FWE is a comparable measure that represents the probability of the null hypothesis being incorrectly accepted for a voxel. The two values are related to one another and they are both calculated by examining the distribution of p-values across all voxels. For FWE the new p-value threshold is calculated with the following formula:

$$P_{(k)} \leq \alpha / (M + 1 - k)$$

SPM8 uses a FWE process to calculate significant areas of activation.

3.5.5.3. Region of interest analysis

The above techniques have all described how to compensate for the multiple-comparison problems when applying the GLM to the entire brain (a whole-brain analysis). An alternative approach is it to constrain analyses to *a priori* regions of interest (ROI). Reducing the data in this manner means that the null hypothesis is only tested for a small number of ROIs, rather than 20,000 voxels. This reduces the multiple comparison problems considerably as the number of ROIs tested is usually significantly smaller than the number of voxels in the data set. ROIs can be defined anatomically (see Chapter 4) or from independent data sets of interest (see Chapter 6). EPI data is sampled from the ROIs and either the mean times series (FEAT) or the single-vector determinant of the time series (SPM8) can then be used in the GLM. This type of analysis is particularly useful in testing a predefined hypothesis looking for small regions of activation. The extracted time series can also be used in other types of fMRI analysis (e.g. PEATE and DCM analyses discussed below). The different methods used to define ROIs in this thesis are described in the relevant chapters.

3.5.6. Functional Connectivity

Event-related fMRI analyses attempt to assign cognitive functions to brain regions activated while performing those functions. However, several newer techniques describe cognitive functions in terms of the interactions between spatially distributed brain regions (e.g. neural network models discussed in Chapter 2). The main measurements used to describe the interactions are functional connectivity (FC) and effective connectivity (EC). FC is a measure of the statistical dependencies between

different brain regions. In practice this is calculated from the temporal correlations between spatially distinct brain regions. Alternatively, EC is a measure of the influence that one neural system has on another (Friston 1994). Calculating effective connectivity is considerably more complex and is discussed below and in Chapter 5 in the context of dynamic causal modelling (DCM). In addition to providing additional information on network function, FC techniques have some additional advantages over event-related fMRI analyses. FC analyses can be used to measure network function in the absence of task (i.e. resting-state fMRI data). This allows the assessment of patients that may not be able to perform tasks, avoids any ambiguity in the cognitive functions that the tasks are testing, and the need to match behaviour across groups.

FC can be assessed in several ways but I shall discuss in detail the two techniques that I used in this thesis: independent component analysis (ICA) (McKeown, Jung et al. 1998, Beckmann, DeLuca et al. 2005) used in Chapter 6 to produce an independent data driven template of the FPCN; and dual regression (Zuo, Kelly et al. 2010, Leech, Braga et al. 2012) to assess how FC within the FPCN differed between TBI patients and healthy controls.

3.5.7. Intrinsic Connectivity Analysis

Principles

ICA is a statistical technique originally designed as an extension of principle component analysis (PCA) for reducing the dimensionality of data (Bell and Sejnowski 1995). The fMRI signal across in every voxel can be viewed as a linear composite of several distinct signals. ICA can be applied to the fMRI signal during task (McKeown, Jung et al. 1998) and rest (Beckmann, DeLuca et al. 2005) to

decompose the fMRI signal into those distinct signal components and derive spatial maps associated with them. In this context, if the data acquired during an fMRI study consists of ‘ n ’ voxels over ‘ t ’ time points then the data can be considered as a two-dimensional matrix ‘ X_{nt} ’. ICA uses an algorithm to derive the following equation:

$$X_{pt} = A_{tq} S_{qn} + \eta$$

Where ‘ A ’ is a $t \times q$ two-dimensional ‘mixing-matrix’ made of ‘ q ’ separate independent component time series (the enforced limit on q is that it must be less than t). ‘ S ’ is a $n \times q$ two-dimensional matrix of spatial maps that correspond to the independent components in A (Figure 3.15). ‘ η ’ represents a Gaussian noise function not explained by the components.

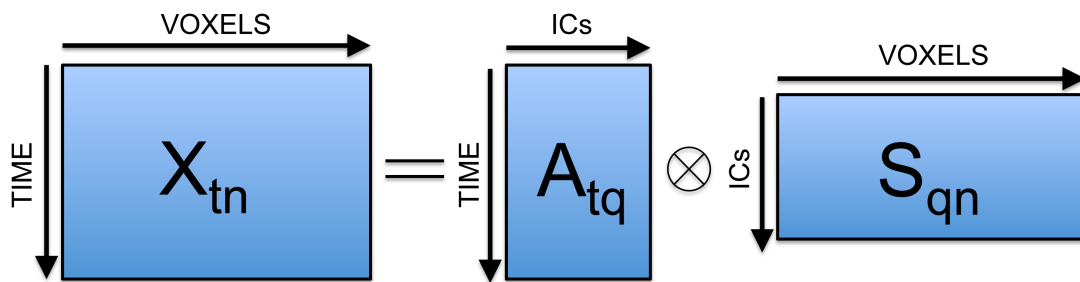


Figure 3.15: Schematic of ICA process applied to fMRI

The fMRI data is represented as a matrix (X) with ‘ n ’ number of voxels and ‘ t ’ number of time points; the mixing matrix (A) with ‘ q ’ number of independent time components and ‘ t ’ number of time points; and spatial matrix (S) with ‘ q ’ number of spatial components and ‘ n ’ number of voxels.

3.5.7.1. Application of ICA

In Chapter 6 I use MELODIC (Multivariate Exploratory Linear Optimised Decomposition into Independent Components) (Beckmann and Smith 2004) to derive spatial maps that correspond to intrinsic connectivity networks. MELODIC is an easy to implement tool that applies ICA principles to fMRI data. MELODIC is used primarily in one of two ways, either a multi-session tensor ICA or temporal

concatenation ICA. Multi-session tensor ICA assumes that the stimuli subjects were exposed to during fMRI were temporally aligned. Since I used resting-state data I could not make this assumption and therefore used the simpler temporal concatenation ICA. Temporal concatenation ICA involves the same principle outlined above for a single data set, only the data from several subjects is now concatenated along the time dimension of the X matrix (Figure 3.16). In doing this, the mixing matrix now contains independent components that explain variance across the time-series of all subjects. The 'S' matrix contains spatial maps that correspond with each independent component in the mixing matrix. These maps are the Independent component networks used in further analyses; they represent the brain regions whose activations correspond to the ICA derived components in the mixing matrix. Networks produced in this way are very consistent across studies and relate well to the previously defined networks seen in traditional event-related fMRI analysis (Smith, Fox et al. 2009).

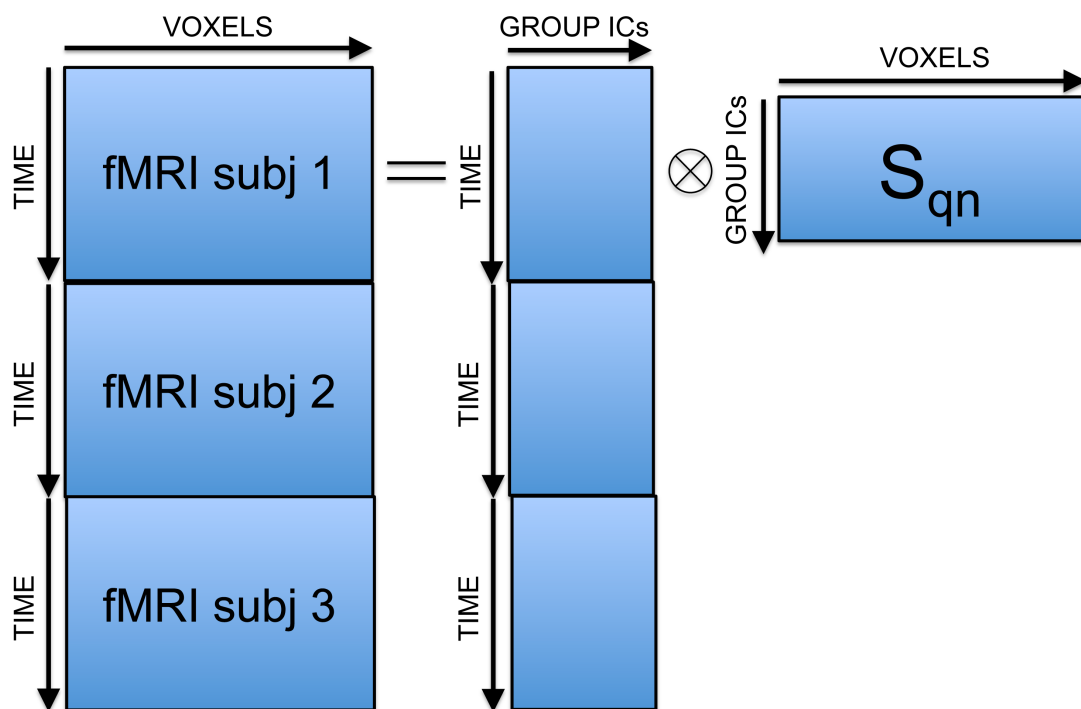


Figure 3.16: Schematic of MELODIC ICA applied to fMRI data

MELODIC requires the same data pre-processing stages that FEAT does (described previously). It also uses additional voxel-wise variance normalising ('whitening') and de-means the data.

3.5.7.2. Dual regression

In Chapter 6 I employed dual regression to study the FC in resting-state fMRI within ICA derived neural networks (Zuo, Kelly et al. 2010, Leech, Braga et al. 2012). One of the major limitations of ICA is that the same components cannot be derived consistently. There is a random element to MELODIC and performing two consecutive ICAs on the same data set will result in the extraction of slightly different components. Therefore the ICA process alone cannot be used to compare ICA networks across different groups (Zuo, Kelly et al. 2010). To compare the functional connectivity within a single ICA component a dual regression approach has been proposed.

The dual regression approach involves two steps. Firstly, each IC spatial map is linearly regressed against the data for a new subject (spatial regression). This creates a subject-specific time series for each IC spatial map. Second, the time series are variance normalized and linearly regressed with the subject's whole fMRI data (temporal regression), converting each time series back into a subject specific spatial map. This provides a subject-specific voxel-wise measure of the FC of each IC spatial map. These subject specific measures can be combined using random-effects framework to provide group level statistics, just as with FEAT.

3.6. Dynamic Causal Modelling

Recent advances in fMRI analysis have allowed us to measure the directed effective connectivity (and condition-dependent changes in coupling) between brain regions. Effective connectivity (EC) is a measure of how the activity of one neural population influences another neuronal population (Friston 1994). It differs fundamentally from FC in that it infers causal relationships between these populations. Directed (functional or effective) connectivity can be studied with dynamic causal modeling (DCM) (Friston, Harrison et al. 2003) or Granger causality (Roebroeck, Formisano et al. 2005). The relatively poor temporal resolution of fMRI has led to a criticism of Granger causality as it is a lag-based method of determining causal relationships, (i.e. it makes inferences based upon the time delay between regions (Smith, Miller et al. 2011)).

I used DCM in Chapter 5 of this thesis as it represents a departure from the previously described fMRI techniques in that it describes the causal relationships between neuronal populations. For example, a traditional univariate fMRI experiment may show that experimental condition (U) is associated with activation of brain regions X, Y and Z. The next question may be: “How do X, Y and Z relate to one another? What provides the input to that system? How does the experimental variable affect the relationships between these regions?” Univariate analysis has no way of answering these questions. DCM potentially can answer these questions and therefore provides a richer explanation of the neuronal activity observed in fMRI experiments.

3.6.1. Principles of DCM

The basic premise of DCM is similar in many respects to the traditional univariate event-related fMRI analysis. DCM involves making a model of a neuronal system, the 'neuronal model'. This model is then convolved with a type of HRF to create the 'haemodynamic model'. The haemodynamic model is then matched with the observed fMRI data as closely as possible. DCM views the brain as a deterministic nonlinear system and predicts that inputs into that system will lead to predictable outputs. The first step in DCM is to design a fairly realistic model of neuronal activity based on how experimental manipulation (U) affects the activity in network nodes (X , Y and Z). The inputs into the system are the experimental manipulations ' U '. U can effect change in the neural activity of nodes X , Y and Z in one of two ways: either directly as a 'driving input' into a particular region, or indirectly via 'modulating' the EC between nodes. The neuronal model in DCM models indirect and direct effects of U in the B-matrix and C-matrix respectively. The nodes may also relate to each other in a manner independent of the experimental condition, this is modeled in the A-matrix. The neuronal model can be written as:

$$\dot{z}_t = \left[A + \sum_{j=1}^M u_t(j) B^j \right] z_t + C u_t$$

Figure 3.17: Example of the neuronal state equation used in DCM

This is a simplified equation where 't' indicates continuous time and the dot notation indicates a time derivative. 'z' is a matrix of 'i' vectors, where the 'ith' entry represents the activity in the ith brain region. 'u_{t(j)}' represents the jth experimental input out of 'M' total inputs. The 'A-matrix' represents all intrinsic connections; the 'B-matrix' represents all of the inter-regional connections that are modulated by experimental condition 'u', 'B^j' represents connections modulated by the jth experimental input; and, the 'C-matrix' represents the inputs into the regions modulated by 'u'.

The parameters in each model are weighted in an iterative process to provide the best fit for the actual data using a least sum of the square of the errors approach,

rather like a GLM. In addition to the model specific estimates of the parameters, each estimation procedure also uses the free-energy criterion to derive a measure of how well the model fits the data as a whole (model evidence) (Friston, Mattout et al. 2007, Penny 2012). The free-energy criterion indicates the accuracy of the model (as log-likelihood of the data) corrected for the complexity of the model. The complexity term depends on both the number of parameters and the dependencies between parameters. Unlike previous measures, such as Akaike's information criterion and Bayes' information criterion (Penny, Stephan et al. 2004, Penny 2012), the free-energy estimate adjusts the penalty for model complexity according to both a priori and a posteriori independence of the model parameters. DCM10 therefore uses the negative free energy estimates to compare models within and between subjects.

DCM provides a measure of how well a model fits the data (the negative free energy). The models are described in terms of A, B and C matrices. DCM also provides an estimate of how each parameter in these matrices effects model fit. The best way to use these measures is still the subject of debate. Traditionally a Bayesian model selection (BMS) process was used to establish the best fitting model. BMS works on the principle of relative evidence and the Bayes ratio. BMS becomes rather 'brittle' when used in this way (Penny, Stephan et al. 2010). This may be in part because when large numbers of models are compared they often share many overlapping features (Penny, Stephan et al. 2010). To accommodate for this I have adopted a two-step hierarchical approach to DCM model comparison. The first step is called Bayesian 'Family level inference', and the second step is Bayesian model averaging (BMA) within families (Penny, Stephan et al. 2010).

3.6.2. Bayesian family level inference

In DCM multiple models are estimated. Depending upon the question being asked these models can be separated into different non-overlapping ‘families’. For example, In Chapter 5 I wanted to determine the most likely input into a network (described in the C-matrix of all models). I separated the models into different families based on their C-matrix and compared the evidence for each family using random effects BMS. This provides an exceedance probability for each family, which corresponds to the belief that that family is more likely than any of the others it was compared to. Family level inference addresses the issue of ‘dilution’ in model selection (Hoeting, Madigan et al. 1999, Penny, Stephan et al. 2010). If models share many features, then excessive prior probability is allocated to similar models. One way of avoiding this problem is to use priors that dilute the probability within subsets of similar models (Hoeting, Madigan et al. 1999). Grouping models into families, and setting model priors according to the number of models in the family achieves this (Penny, Stephan et al. 2010).

3.6.3. Bayesian model averaging

Bayesian model averaging (BMA) moves away from the brittle ‘winning model’ idea. BMA focuses on the parameter estimated in the A, B and C-matrix within a family. BMA provides a weighted average of the parameters estimates across all models within a family (Penny, Stephan et al. 2010). The parameter estimates are weighted depending upon the overall model evidence of the model they come from. Models with high evidence contribute more towards the parameter estimates than those with relatively low evidence. BMA within a winning model family has been proposed as the most robust way of determining neuronal model organization using DCM.

3.7. Limitations of fMRI in TBI

There are several methodological problems that need to be addressed when comparing fMRI results across groups. Below I have highlighted some of the major concerns and how they were addressed in my studies.

3.7.1. Performance matching

When using fMRI measures of brain activation to compare between groups performing a task, the groups should be performing the task to roughly the same level (Price, Crinion et al. 2006). If subjects from one group had impaired performance on task and that was associated with altered brain activation it would be unclear whether the difference in activation was due to neural dysfunction or an inability to perform the task normally (Price, Crinion et al. 2006). Therefore to compare BOLD activation across groups I chose simple tasks that could be manipulated to allow comparable performance across groups. The paradigms described all use adaption of task difficulty and negative feedback to try to equalise performance across groups.

The Simon task is a relatively simple test of cognitive control my research group originally intended for use with patients. However, a small pilot study of the Simon task demonstrated that the task was clearly too difficult for TBI patients to perform with the same degree of accuracy as controls (data not presented). Therefore this paradigm was not applied to TBI patients. The SCT and SST are much simpler tasks and manipulating the SSD, SCD and negative feedback allowed all subjects to perform the task with similar accuracy levels. However, even with the manipulations 6 subjects were excluded from the analysis as they could not perform the task within the normal range.

3.7.2. Focal lesions

Focal lesions create two potential problems in my analyses of TBI patients. Firstly, good registration can be difficult to achieve if lesions have caused the shape of the cortex to change significantly from a standard brain. Secondly, any group differences in neural activation observed may have been due to the reduced grey matter density associated with contusions in the TBI group. These potential problems were dealt with in two ways.

Firstly, I attempted to select patients for the study that had minimal lesion load on their clinical neuroimaging. The admission criteria excluded patients that had required neurosurgical intervention (aside from invasive intra-cranial pressure monitoring in one participant). This reduced the likelihood of patients having very large lesions. In addition I made a case-by-case judgment as to whether or not subjects should be included in the analysis based upon their clinical neuroimaging. Of the remaining subjects, the registration was optimised by manually creating individual lesion masks for subjects. Cortical and white matter lesions were defined manually on high-resolution T1 images using FSLview. These lesions were then used in the registration process to de-weight contusions thus reducing distortion of the remaining intact brain (Brett, Leff et al. 2001). Two of the TBI subjects were excluded from the analyses as their registrations were felt to be too poor despite these measures.

The second issue of grey matter density conferring group differences in neuronal activity was dealt with by using individual grey matter density maps (derived from the `feat_gm_prepare` toolbox in FSL). These maps were included as in the GLM as a nuisance regressor (Oakes, Fox et al. 2007). The lesion analysis demonstrated very little overlap between lesions in the groups (see Chapter 6). It seems unlikely that

any group differences in activation would be due to lesions at a particular site. However, the use of a grey matter density regressor also took into account group differences in grey matter density associated with the general atrophy observed after TBI, which may also have provided a potential confound to the findings.

3.7.3. Altered HRF in TBI

The HRF is a key feature of fMRI analysis and provides the bridge between behavioral models and neuronal activity. The HRF is dependent upon haemodynamic characteristics of the brain such as cerebral blood flow (CBF), cerebral metabolic use (CBM), cerebral blood volume (CBV) and local deoxyhaemoglobin concentration. These characteristics can change with aging and after neurological insults such as stroke causing an altered HRF in these groups (D'Esposito, Deouell et al. 2003, Murata, Sakatani et al. 2006, Nakamura, Sakatani et al. 2010). Variation in the HRF has also been observed across healthy controls (Aguirre, Zarahn et al. 1998).

This is a fundamental limitation of using fMRI to compare healthy to pathological group as I do in Chapter 6. One way of addressing this issue is to compare group differences in the BOLD signal response on a simple control task that you do not expect to be modulated by the disease (Iannetti and Wise 2007). If no group differences are observed in the BOLD signal response to this task then it seems unlikely that there are significant fundamental differences in vascular reactivity between the groups. I performed such an analysis and describe the results in Chapter 6. In addition, I attempted to minimize the influence of group differences in HRF by carefully age and gender matching the control groups. I also excluded patients with a history of stroke and none of the patients had a history of cardiovascular disease. Although, some TBI patients were on vasoactive medication,

(e.g. beta blockers), and some had risk factors for cardiovascular disease (e.g. diabetes and hypertension). The clinical details of the individual patients are described in Chapter 6.

3.8. Advanced structural assessment of TBI

The previous sections have outlined the various functional imaging techniques that I have applied to fMRI data as part of this thesis. I shall now describe the structural imaging techniques I have used in addition to fMRI and standard clinical imaging.

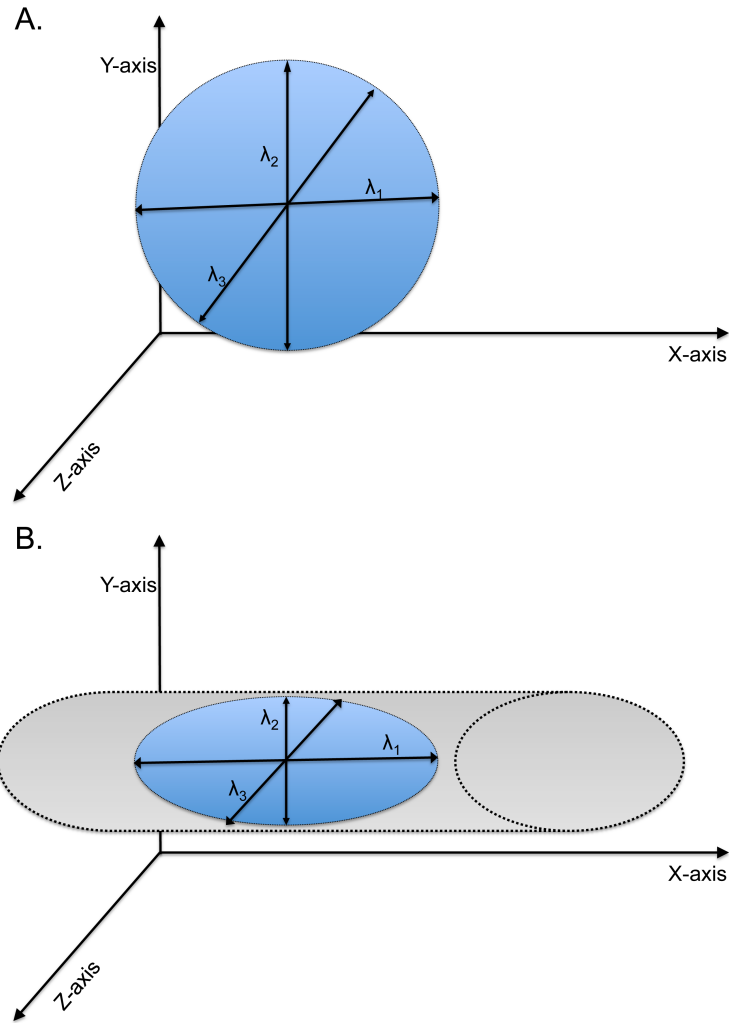
3.8.1. Diffusion tensor imaging

As discussed in Chapter 2, DTI is an MRI sequence that offers a uniquely flexible way of quantifying white matter integrity compared to the previously described structural MRI sequences. Water diffusion within a structure can be measured using MRI (Basser and Pierpaoli 1996, Beaulieu 2002). DTI relies on the principle that the diffusion of water molecules is to a variable extent limited by the cellular components in a particular tissue. This is particularly useful for the study of white matter tracts as the structure of axons constrain diffusion so it preferentially occurs in parallel to the predominant direction of the tract (Basser and Pierpaoli 1996, Beaulieu 2002). This asymmetrical or 'anisotropic' diffusion can be measured using DTI. Hence, DTI provides a non-invasive way of investigating white matter structure at particular anatomical locations.

3.8.2. DTI metrics

Diffusion data are often analyzed by fitting a tensor model to the acquired data (Assaf and Pasternak 2008) (Figure 3.18). This allows the asymmetrical pattern of

diffusion in the white matter to be described quantitatively as fractional anisotropy. Fractional anisotropy is expressed as a numerical value between 0 (equal diffusion in all directions) and 1 (diffusion along one direction only) (Figure 3.18, Eq.4). The direction of maximal diffusion is referred to as axial diffusivity (λ_1). The two remaining mutually perpendicular eigenvalues are called λ_2 and λ_3 and they combine to give the radial diffusivity. (Eq.2) Fractional anisotropy is then calculated as a ratio of the differences between λ_1 to λ_2 and λ_3 (Eq.3). In addition, the apparent diffusion coefficient (ADC) or mean diffusivity are both measures of average diffusivity (Eq.3).



(Eq.1) Axial diffusivity = λ_1

(Eq.2) Radial diffusivity = $(\lambda_2 + \lambda_3)/2$

(Eq.3) Apparent Diffusion Coefficient = $(\lambda_1 + \lambda_2 + \lambda_3)/3$

(Eq.4) Fractional Anisotropy = $\sqrt{\frac{(\lambda_1 - \lambda_2)^2 + (\lambda_1 - \lambda_3)^2 + (\lambda_2 - \lambda_3)^2}{(\lambda_1 + \lambda_2 + \lambda_3)^2}}$

A) Spherical tensor with diffusion is equal in all directions i.e. $\lambda_1 = \lambda_2 = \lambda_3$

Axial diffusivity = $\lambda_1 = \lambda_2 = \lambda_3$

Radial diffusivity = $\lambda_1 = \lambda_2 = \lambda_3$

Apparent Diffusion Coefficient = $\lambda_1 = \lambda_2 = \lambda_3$

Fractional Anisotropy = 0

B) As the tensor tends towards a more anisotropic shape

Axial diffusivity = λ_1

Radial diffusivity $\rightarrow 0$

Apparent Diffusion Coefficient $\rightarrow \lambda_1/3$

Fractional Anisotropy $\rightarrow 1$

Figure 3.18: Principles of Diffusion tensor imaging.

The figures represent the diffusion characteristics of unconstrained (isotropic) water that diffuses equally in all directions (A), and constrained anisotropic water (B) within an axon (represented by the grey tube). As the diffusion becomes more directional, i.e. more anisotropic, λ_2 , λ_3 , and radial diffusivity tend towards zero and fractional anisotropy tends towards 1.

The following section will outline the MRI principles behind DTI acquisition and how I have applied it in my studies.

3.8.3. Measuring water diffusivity with MRI

DTI data is acquired by adding 'diffusion encoding gradients' to standard MRI pulse sequences. As described previously hydrogen atoms in a static magnetic field they precess in phase. In DTI a magnetic gradient pulse is used to push the hydrogen atoms out of phase (a 'dephasing pulse'). How far out of phase the atoms become is dependent upon the location of the hydrogen atom along the axis of the gradient pulse. After a short period of 20-50 milliseconds a second 'rephasing' pulse of equal magnitude but opposite direction is applied. The second pulse should cancel out the dephasing caused by the original. However, because the effect on phase is dependent upon field strength and both pulse are on gradients, then if the atoms have moved between the two scans then there is incomplete rephasing. The difference can be detected as a loss of signal along the axis of the gradient pulses. Diffusion can be measured in this manner along any one direction. In DTI, multiple axes are used allowing water diffusion in several directions to be calculated. The more axes used the better information regarding directionality.

3.8.4. DTI analysis

Data pre-processing

As with fMRI, the raw DTI data needs to go through several stages of pre-processing before it can be interpreted. I used FMRIB's Diffusion Toolbox (FDT v2.0) (Beckmann and Smith 2004) as part of the FSL software package to analyse the DTI

data described in Chapter 6. Each subject's images were registered to their b=0 image using FLIRT and corrected for distortion due to eddy currents created by the large diffusion gradients and head motion. BET (Smith 2002) was used to extract the brain from the skull. Diffusion tensors were then calculated on voxel-by-voxel basis using a simple least squares fit of the tensor model to the diffusion data. In this way individual FA maps for every subject were calculated.

3.8.5. Probabilistic tractography

Probabilistic tractography is an automated process that uses certain assumptions to predict the most likely location of a white matter tract connecting two anatomical regions. Using the diffusivity data a single voxel the probabilistic tractography algorithm produces a probability density function (PDF) for the most likely direction of diffusion in that voxel. It is a density function rather than a single direction as there is a degree of uncertainty inherent to the diffusivity data caused by noise, this uncertainty is modelled by fitting the data to a Gaussian tensor model with incomplete directional data (e.g. in Chapter 6 I use 64 direction DTI data) (Behrens, Woolrich et al. 2003). Probabilistic tractography uses the PDF across all relevant voxels to estimate the global connectivity. This can be used to produce a spatial map where the value of each voxel corresponds to the likelihood that that voxel lies on a white matter tract connecting two predefined regions. By selecting two regions of interest and thresholding the probability level one can extrapolate the white matter regions ('tracts') that are likely to connect two regions. When comparing groups, these tracts can be used to sample DTI measures in the same manner as any other region of interest analysis. Using this process avoids the some of the multiple comparison issues outlined above for fMRI.

Chapter 4: Distinct frontal networks are involved in monitoring and adapting to internally and externally signalled errors.

The aim of this study was to establish the cortical regions involved in the response to different error types. I used two versions of the Simon task described in Chapter 3 to produce a large number of both commission and timing errors to test the following hypothesis.

Hypothesis: The dorsal anterior cingulate cortex within the fronto-parietal control network acts as a generic performance monitor and responds to many different error types that can be measured by fMRI during performance of the Simon task.

4.1. Introduction

As discussed in the general introduction, the ability to adapt behaviour to new demands is a central feature of cognitive control. Errors frequently result in behavioural changes that allow individuals to adapt to new situations. For example, slowing responses after an error is a common strategy that generally makes future performance more accurate in speeded reaction time tasks (Rabbitt 1966). The neural basis of performance monitoring and error processing is unclear. Previous work has focused on the contribution of the dACC to behavioural adaptation. This region is activated soon after errors of many types and appears to be a key part of the neural network mediating error responses (Dehaene, Posner et al. 1994,

Ridderinkhof, Ullsperger et al. 2004, Debener, Ullsperger et al. 2005, Sharp, Scott et al. 2006). The dACC forms a key cortical node in the Salience network (SN) (Dosenbach, Visscher et al. 2006, Seeley, Menon et al. 2007, Menon 2011). The SN is thought to act as an interface between limbic and cognitive aspects of behavioural control (Critchley, Wiens et al. 2004, Seeley, Menon et al. 2007), filtering incoming sensory information for salience and recruiting other cortical regions as required to respond (Menon 2011).

As discussed in Chapter 2, electrophysiological work has revealed an error-related negativity (ERN) that has been suggested as the first neural response to errors (Gehring, Goss et al. 1993). Combined fMRI and EEG studies suggest may be generated by the dACC (Debener, Ullsperger et al. 2005). However, the error processing system is likely to be multi-faceted and the precise contribution of the dACC to error processing remains controversial (Jessup, Busemeyer et al. 2010). Recent work suggests the primary generator for the ERN may lie in the posterior cingulate cortex (Agam, Hamalainen et al. 2011). In addition several regions within the FPCN also show robust activation to errors (Eichele, Debener et al. 2008).

Reinforcement learning theory provides an important framework within which to understand error processing. One influential model proposes that the dACC indexes prediction error signals generated by midbrain dopaminergic cells in response to a mismatch between expected and actual outcomes (Holroyd and Coles 2002, Holroyd, Nieuwenhuis et al. 2004, Holroyd and Coles 2008). In the initial formulation of this model, the dACC was thought to act as a generic error monitor, responding to all types of errors and signalling the need for a change in behaviour. In favour of this general role, activation of the dACC had been observed in response to errors

generated either internally, as a result of a mismatch between expected and actual outcomes, or externally, as the result of explicit feedback (Holroyd, Nieuwenhuis et al. 2004). However, more recent electrophysiological work suggests that the dACC is sensitive to external feedback only when it is perceived as being 'learnable' or directly related to the subject's own behaviour (Holroyd, Krigolson et al. 2009).

As mentioned in Chapter 2, several neuropsychological studies have provided evidence that the dACC is required for certain types of error processing (Swick and Turken 2002, di Pellegrino, Ciaramelli et al. 2007). However, some types of behavioural adaptation have been shown to occur after damage to the dACC, suggesting that involvement of the region is not always required to initiate cognitive control (Fellows and Farah 2005, Kennerley, Walton et al. 2006, Modirrousta and Fellows 2008). Cortical regions in the right lateral temporo-parietal lobes and inferior frontal cortex sometimes referred to as the VAN (Corbetta, Kincade et al. 2002) have also been shown to respond to behaviourally salient events, particularly unexpected ones. This network provides an alternative route by which external information might engage cognitive control potentially independent of the dACC.

I used fMRI to investigate two distinct types of behaviourally salient errors (i.e. timing errors and commission errors). To do this I used a version of the Simon task designed to generate a large number of errors of different types. Commission errors involved responding with an inaccurate key-press, whereas timing errors involved responding after an externally imposed time limit (see Chapter 3 for further details). During training subjects were instructed that both incorrect and late responses were to be considered errors on the task, and this was re-iterated during performance of the task in the scanner. Commission errors were internally recognized, and involved

no explicit feedback. In contrast, timing errors were difficult to monitor internally and were explicitly signalled on slow trials. Comparison of the neural response to these errors measured using fMRI allowed an analysis of the error-processing network associated with these distinct error types.

In this study I specifically tested the hypothesis that the dACC generically monitors and signals the need for behavioural adaptation after errors, by comparing neural responses to internally generated commission errors and to externally signalled timing errors on the same task. This work builds on previous studies of error monitoring, but importantly employs a task in which reward is not present. I reasoned that if the dACC operates as a generic error monitor, one would expect similar activation across distinct error types. However, if dACC activation reflects a subset of error processing, (e.g. only responding to errors perceived as emotionally salient or where it is possible to generate a prediction error signal), differential activation may be present in the dACC despite adaptive behavioural change being triggered.

4.2. Materials and Methods

4.2.1. Participants

Thirty-five subjects performed the main Simon Task paradigm (17 male, mean age 30.6 ± 8.6 years). A further fifteen subjects performed a control variant of the Simon Task designed to further investigate the effect of explicit feedback (4 male, mean age 29.4 ± 6.9 years). Subjects gave written consent. The experiment was approved by the Hammersmith and Queen Charlotte's, and Chelsea Research ethics committee.

4.2.2. Simon Task procedure

I used the two versions of the Simon task to investigate the neural basis of cognitive control and error processing. The Simon task is a stimulus/response compatibility task that uses incongruency between the salient and non-salient features of a stimulus to generate response conflict (Simon 1969, Simon and Small 1969). Both versions of the Simon task I used were designed to produce large numbers of both timing and commission errors. The details of both tasks were discussed in detail in Chapter 3. In brief, during the main Simon task explicit feedback about commission errors was not provided. Hence, any neural response to these errors was internally generated. Errors of timing were generated by explicit feedback given when a subject responded outside the time limit. In the Secondary Simon task additional feedback was supplied after commission errors.

4.2.3. Scanning protocol

Description of scanning session for the Simon task and Secondary Simon task

Subjects had a practice run of the task consisting of 120 trials outside of the scanner (the behavioural results of the practice session were not included in the analyses reported). T1 structural and fMRI images were acquired over a single session. During this session all subjects performed six runs of the task presented in a pseudo-randomised order. Subjects were instructed to respond to the task as quickly and accurately as possible and these instructions were repeated between runs.

Scanner parameters

MRI data were obtained using a Philips (Best, The Netherlands) Intera 3.0 Tesla MRI scanner using Nova Dual gradients, a phased array head coil, and sensitivity encoding (SENSE) with an under-sampling factor of 2.

Structural T1

T1-weighted whole-brain structural images were also obtained in all subjects (78 contiguous slices; slice thickness 2.3 mm; repetition time (TR) = 30 milliseconds; echo time (TE) = 16 milliseconds; field of view (FOV) 220 x 220 x 180 mm, matrix = 192 x 190; flip angle = 12 °; resolution 0.92 x 0.92 x 2.3 mm).

FMRI

Functional MRI images were obtained using a T2*-weighted gradient-echo echo-planar imaging (EPI) sequence with whole-brain coverage (TR/TE = 2000/30; 31 ascending slices with thickness 3.25 mm, gap 0.75 mm, voxel size 2.19×2.19×4 mm, flip angle 90°, field of view 280×220×123 mm, matrix 112×87). Quadratic shim gradients were used to correct for magnetic field inhomogeneities within the brain.

Stimulus presentation

Paradigms were programmed using Matlab® Psychophysics toolbox (Psychtoolbox-3 www.psychtoolbox.org) and stimuli presented through an IFIS-SA system (In Vivo Corporation). Responses were recorded through a fibre optic response box (Nordicneurolab, Norway), interfaced with the stimulus presentation PC running Matlab.

4.2.4. Standard whole-brain fMRI analysis of the Simon task

To investigate the neural basis of timing and commission errors several different trial types were considered. For congruent and incongruent conditions a number of distinct events were modelled: correct trials (appropriate response within the time limit), commission errors (incorrect button press but within the time limit), timing errors (correct button press but outside of the time limit), errors or both timing and commission, and confounded trials (where timing or commission errors occurred

directly after another timing or commission error). The neural activity associated with commission and timing errors were contrasted with correct trials, as well as being directly contrasted with each other. Separate analyses were performed for congruent and incongruent conditions. Concurrent commission and timing errors were too few to be analysed. Group effects analyses were carried out using a GLM framework and FLAME statistical analysis (described in Chapter 3). Final statistical images were thresholded using FDR threshold of $p < 0.05$.

4.2.5. Region of interest analysis

I further investigated the roles of individual anatomical regions within the FPCN using a focused region of interest (ROI) analysis. A number of anatomically defined frontal lobe regions known to be involved in error processing were investigated. These consisted of left and right anterior cingulate cortices (ACC), right anterior insula (RAI), left anterior insula (LAI), as well as left and right pars operculari and pars triangulari within the inferior frontal gyri. Probabilistic masks were defined from the Harvard Cortical Atlas tool in FSL, and were thresholded at 70%. The regions were all available in the atlas apart from the anterior insula. To generate the anterior insula mask the insula atlas map was divided along the anterior-posterior dimension into two halves. For each axial slice the image was divided at the midpoint along the anterior-posterior dimension, producing anterior and posterior insula masks. Using a GLM, the mean percentage signal change associated with contrasts of interest was calculated for all voxels falling within each ROI.

4.2.6. Time-Series Analysis

To investigate whether commission and timing errors were associated with different time-courses Perl Event-related Average Time-course Extraction (PEATE) was used

to further characterize the neural responses within the dACC (www.jonaskaplan.com/peate/peate-tk.html). The mean time series from a 10mm diameter spherical ROI within the dACC was extracted. To test whether the dACC responded to all types of error, I used a ROI centred on the peak activation for the contrast of errors of commission versus correct trials (MNI-co-ordinates: 2, 32, 28). The response was examined for a period 2 seconds preceding to 12 seconds following a subject's response.

4.2.7. Secondary Simon task controlling for external feedback

In the main version of the Simon task timing errors were signalled by explicit 'error' feedback, but commission errors were not. To test whether this difference influenced dACC activation I performed an additional study with a separate group of 14 subjects. Here both types of error were accompanied by explicit feedback. The design of the experiment was the same as that described above except for the presence of audio-visual feedback for errors of commission. This took the form of the word "Wrong!" presented after an error of commission, accompanied by a 500 Hz tone. The timing and duration was the same as for error of timing described above (see Chapter 3 for a discussion of the Secondary Simon task).

4.2.8. Analysis of strategic differences in task performance: comparison of high low timing error groups

The number of timing errors was variable across individuals and runs (see results). This was likely to reflect strategic differences in the perceived salience of timing feedback. During task performance, subjects could either focus on reducing errors of commission, reducing errors of timing, or they could adjust their speed-accuracy trade-off in a more complex way to achieve an optimum reduction in both error types.

Therefore the number of timing errors on a particular run is likely to reflect a subject's strategy on that run. To assess whether this variability affected neural activation within the cognitive control system, I analysed the behavioural data from all subjects and compared runs with high numbers of timing errors to those with low numbers (defined by taking the upper and lower thirds of the distribution). To focus on the effects of variable strategy with respect to timing I only included runs where the commission error rate fell approximately within the ranges the paradigm was designed to produce (i.e. 3%-17% congruent and 12%-30% incongruent errors, see 3 for details). This resulted in the potential inclusion of 169 runs (Figure 4.7A). Three subjects had separate runs that would have been included in the High Timing error and others in Low Timing error groups. In these cases the runs that were in the minority were removed from the analysis, (i.e. if a subject had three runs included in the High and one run in the Low Timing error group then the run in the Low Timing error group would be excluded from the analysis). I did this to avoid mixing between-subject effects and within-subject effects (see Chapter 3). As a result three single runs were removed from the analysis. The Low Timing error group consisted of 53 runs spread across 23 subjects (0.83% - 6.7% timing errors), and the High Timing group of 54 runs across 22 subjects (13.3 - 48.33% timing errors). Comparison of errors of timing against correct trials was made for the two groups using a standard mixed level analysis, and the resulting contrasts were then directly compared.

4.3. Behavioural results

4.3.1. Commission errors associated with high conflict situations

Subjects' behavioural performances were in keeping with previous studies (Christ, Falkenstein et al. 2000). Subjects performing the main version of the Simon Task produced a total of 5992 errors. Relatively large numbers of errors of both

commission (11.7% of all trials) and timing (12.1% of all trials) were committed. This was expected and was probably due to the substantial increase in overall task difficulty the timing feedback adds, coupled with the fact that performances on congruent and incongruent trials are not independent. A significantly larger number of commission errors were produced during the incongruent than congruent conditions ($t=3.65$, $df=34$, $p=0.001$). Furthermore, as a percentage of the number of congruent and incongruent trials, commission errors were substantially more common on incongruent trials ($t= 9.81$, $df=34$, $p<0.0005$) (Figure 4.1A). Consistent with the idea that high conflict situations are more likely to provoke commission errors.

I performed an additional analysis to help clarify reason for the high error rate on congruent trials. I assessed how the congruency of the trial immediately before a trial affected subjects' accuracies. Correct congruent trials were more likely to have been preceded by another congruent trial than incorrect congruent trials (68.5% vs. 56.3%, $df=34$, $t=25.29$, $p<0.0005$). Similarly, correct incongruent trials were more likely to have been preceded by another incongruent trial than incorrect incongruent trials (37.5% vs. 34%, $df=34$, $t=5.76$, $p<0.0005$). The effect size differed between congruent and incongruent trials, indicating that the effect of previous trials was less for incongruent trials.

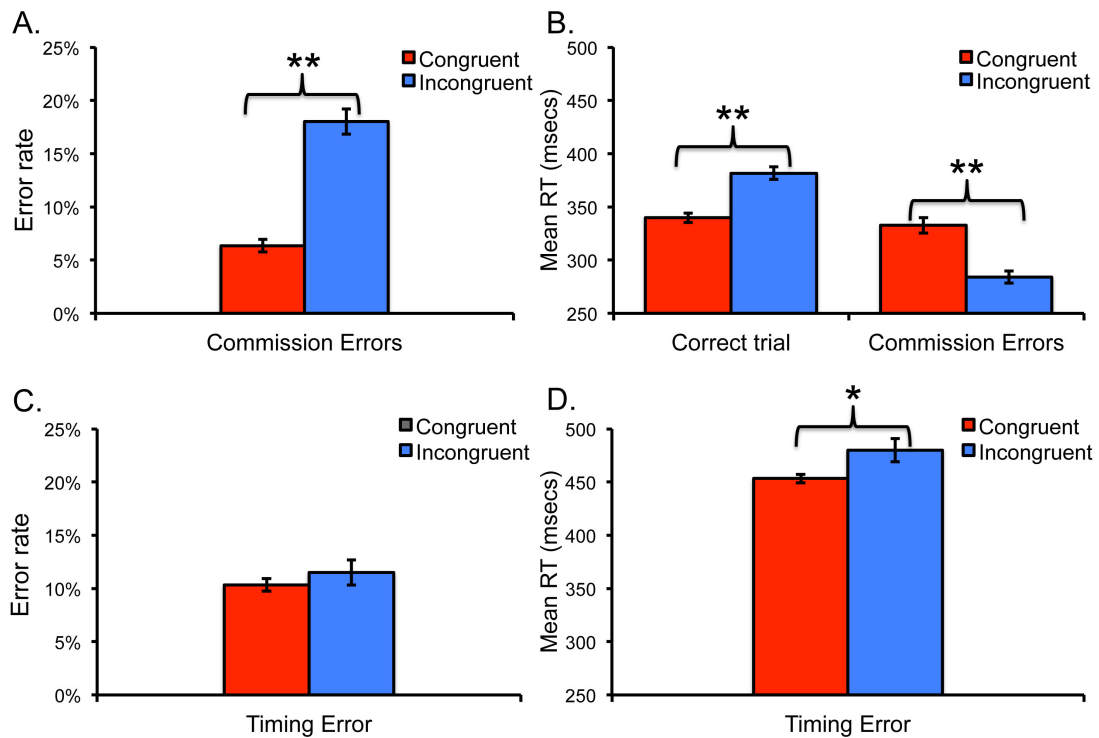


Figure 4.1: Simon task behavioural performance

A) Rate of commission errors shown for congruent and incongruent responses. B) Average reaction times (msecs) for correct trials and commission-errors separated based upon the trial congruency. C) Rate of timing errors for congruent and incongruent trials. D) Average reaction times (msecs) for congruent and incongruent timing errors. '*' signifies $p < 0.05$, and '**' signifies p -value < 0.005 .

4.3.2. Timing errors independent of commission errors and congruency

Most timing errors involved a button press with the correct hand ($87.5 \pm 1.7\%$ of all timing error trials). Significantly more timing errors were produced on congruent than incongruent trials ($t=5.89$, $df=34$, $p < 0.0005$). However, as congruent trials were more frequent, the percentage of timing errors was similar for the two trial types ($t=1.26$, $df=34$, $p=0.216$) (Figure 4.1C). A small number of timing errors were also errors of commission (i.e. a subject responded late and with the wrong hand). The frequency of this type of error was similar for both congruent and incongruent trials ($1.5 \pm 0.28\%$ and $1.2 \pm 0.24\%$ of congruent and incongruent trials respectively). These were not analysed further because of their low number.

4.3.3. Speed accuracy trade off seen on incongruent but not congruent commission error

Response speed had a major effect on the accuracy of incongruent trials (Figure 4.1B). A 2 x 2 ANOVA showed a significant interaction between trial type and accuracy ($F=127.2$, $p<0.0005$). This interaction was due to subjects responding slower on correct incongruent trials than on correct congruent trials ($t=10.6$, $df=34$, $p<0.0001$), and subjects responding faster on incorrect incongruent trials than on incorrect congruent trials ($t=2.89$, $df=34$, $p<0.0001$) (Figure 4.1B). This is consistent with a speed-accuracy trade-off operating for incongruent trials, where fast responses are more likely to be wrong because of a premature response to a spatially contradictory cue. Timing-errors were, by definition, significantly slower than correct trials ($t=10.49$, $df=34$, $p<0.0005$), and incongruent timing errors were slightly slower than congruent timing errors ($t=2.71$, $df=34$, $p=0.01$) (Figure 4.1D).

4.3.4. Commission and timing errors both produce adaptive changes in behaviour

I investigated adaptive behaviour by studying the slowing of responses following errors of commission, and the speeding of responses following feedback after timing errors (Figure 4.2). In the first case the adaptive 'signal' is internally generated, as there is no explicit feedback. In the second, as I only included correct button presses in the analysis, the adaptive 'signal' arises from the external feedback given after a late response.

4.3.4.1. Adaptive behaviour only seen on incongruent trials after internally generated feedback

Both internal and external feedbacks were behaviourally salient. For commission errors the behavioural effect was only present during the incongruent condition (Figure 4.2A). Incongruent commission errors (C) were relatively fast compared to

baseline ($t=15.66$, $df=34$, $p<0.0005$), and post-error slowing was observed on the next trial (C+1) ($t=8.11$, $df=34$, $p<0.0005$). In contrast, commission errors during the congruent condition were not abnormally fast, and were not followed by post-error slowing. Fast responses during the incongruent condition are very likely to result in errors; therefore slowing response speed on the next trial is an effective strategy to improve performance. In contrast, errors on congruent trials are much less influenced by this type of speed-accuracy trade-off, so post-error slowing is far less adaptive in this context.

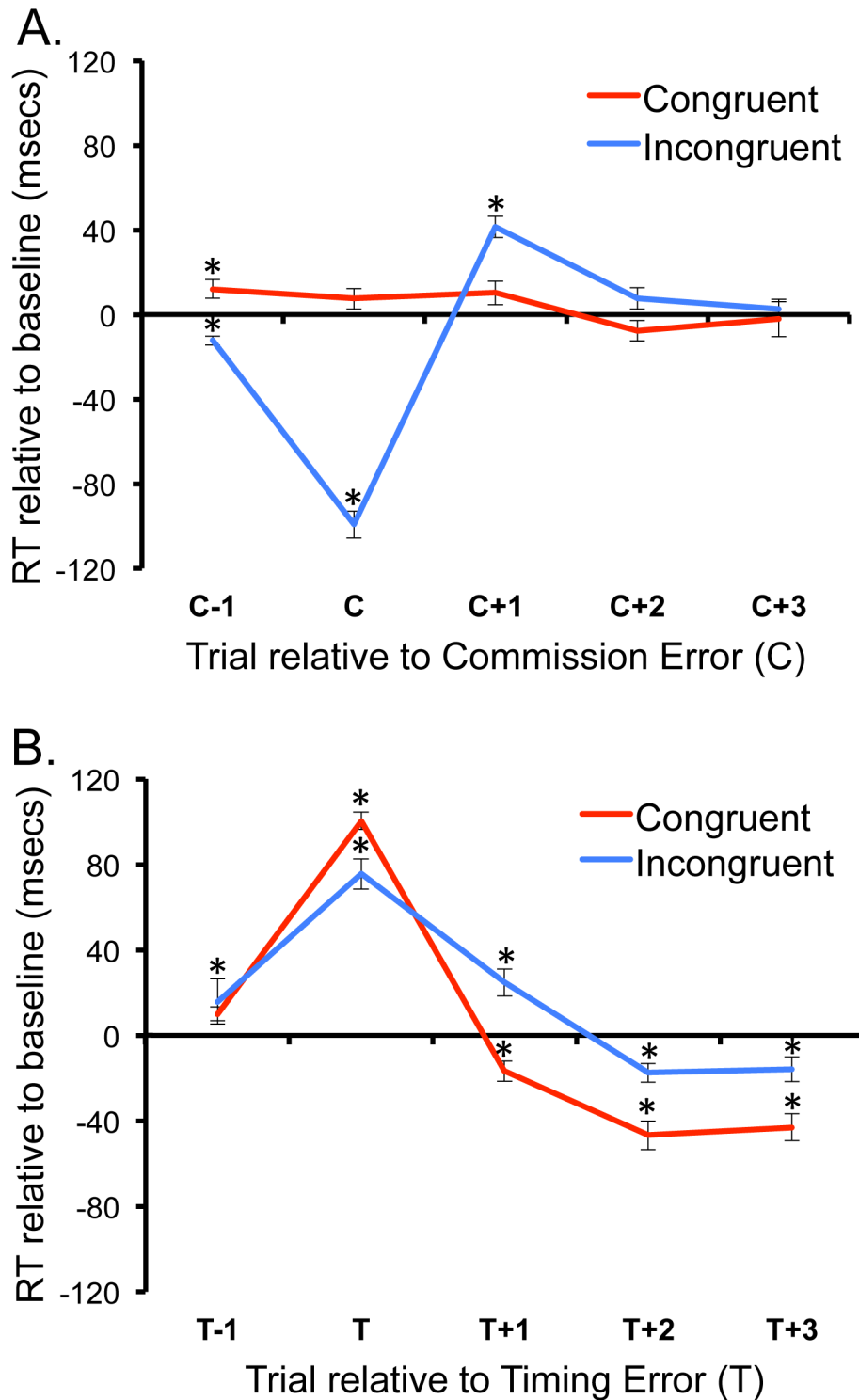


Figure 4.2: Adaptive changes following errors of commission and timing
 A) Post-error slowing on incongruent trials. Reaction time for trials around a commission error 'C' relative to baseline performance. B) Post-feedback speeding following errors of timing. Reaction times for trials around an error of timing 'T' relative to baseline performance. * indicates trials that significantly differed from baseline performance for the preceding ten correct trials of that type.

4.3.4.2. Adaptive behaviour seen on all trials after externally generated feedback

As expected, external feedback after a timing error resulted in speeding of subsequent responses (Figure 4.2B). In contrast to commission errors, both trial types were associated with post-feedback speeding. Errors of timing (T) were by definition slower than average ($t=24.43$, $df=34$, $p<0.0005$) for congruent timing errors; and ($t=10.37$, $df=34$, $p<0.0005$) for incongruent timing errors) (Figure 4.1D and 4.2B). In the case of congruent timing errors, which were far more numerous, all three subsequent trials were faster than baseline ('T+1', $t=-3.47$, $p=0.001$, 'T+2', $t=-6.91$, $p<0.0005$, 'T+3', $t=-4.04$, $p<0.0005$), whereas for incongruent timing errors this was true only for the second and third trials after the timing error ('T+2', $t=-3.79$, $p=0.001$, 'T+3', $t=-2.68$, $p=0.012$).

The post-feedback speeding is not simply a product of responses getting quicker over the course of a run. In fact the opposite trend is observed, with responses generally slowing, which is demonstrated by the first tertile being significantly quicker than the last ($t=9.91$, $df=33$, $p<0.0005$). In addition to being faster, the trial immediately following a timing error (T+1) is also more accurate than a subjects' average accuracy over the run ($t=4.02$, $df=34$, $p<0.0005$), again suggesting that subjects engage greater cognitive control in response to timing feedback.

4.4. Neuroimaging results

4.4.1. Commission errors activate the dACC

The network of brain regions activated by commission errors (Figure 4.4) was consistent with previous work (Garavan, Ross et al. 2002, Ullsperger and von Cramon 2003, Hester, Fassbender et al. 2004, Hester, Foxe et al. 2005). Extensive activation was seen in the dACC during commission errors compared to correct

trials. In addition, peaks of activation were observed in the superior frontal gyrus, bilateral anterior insulae and pars operculari, as well as in the frontal poles and supramarginal and angular gyri (Table 4.1). There was also activation of subcortical structures including the brainstem and bilateral thalami. The extensive activation in the dACC and bilateral anterior insulae fell within what would be termed the SN (Seeley, Menon et al. 2007). Similar patterns of activation were observed for errors of commission on congruent and incongruent trials (see Chapter 5). A direct contrast of commission errors in both congruent and incongruent conditions showed no significant differences in brain activation.

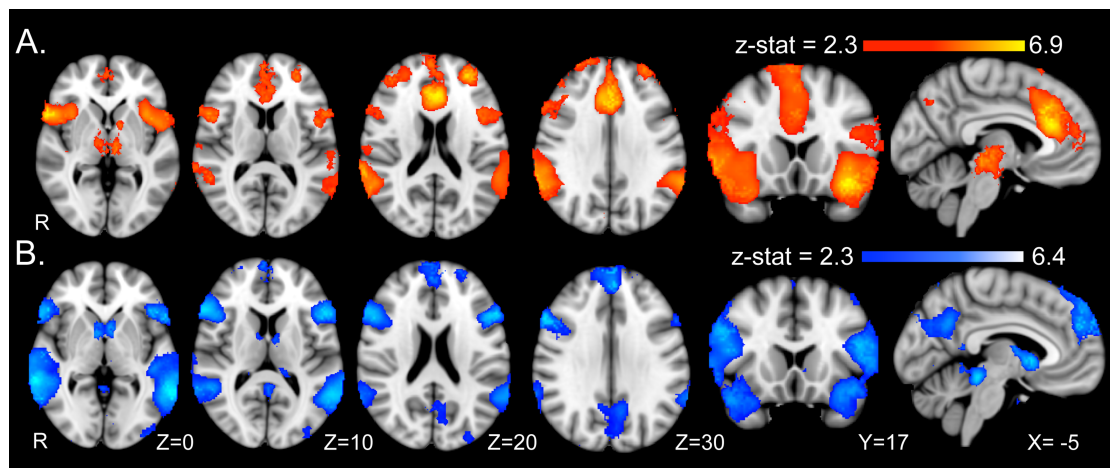


Figure 4.3: Commission and timing errors

A) Areas of significant brain activation associated with commission errors compared to correct trials (red-yellow). B) Areas of significant brain activation associated with timing errors compared to correct trials (light – dark blue). Results are superimposed on the MNI 152 T1 1 mm brain template.

Table 4.1:

Anatomical region	False Discovery Rate (q-value)	MNI co-ordinates		
		X	Y	Z
Commission Errors > Correct Trials				
Anterior Cingulate Gyrus*	<0.05	2	32	28
Left Frontal Pole	<0.05	-30	50	20
Right Frontal Pole	<0.05	28	52	22
Left Insula Cortex	<0.05	-38	16	-14
Right Insula Cortex	<0.05	58	14	-2
Left Supramarginal Gyrus	<0.05	-62	-46	28
Right Supramarginal Gyrus	<0.05	64	-48	28
Left Thalamus	<0.05	-8	-14	3
Right Thalamus	<0.05	7	-16	3
Brain-Stem	<0.05	0	-28	-10
Timing Errors > Correct Trials				
Left Inferior Frontal Gyrus (pars triangularis)	<0.05	-52	23	16
Right Inferior Frontal Gyrus (pars triangularis)	<0.05	60	-44	-6
Frontal Pole (midline)**	<0.05	0	58	28
Precuneus	<0.05	0	-48	12
Left Caudate	<0.05	-8	11	2
Right Caudate	<0.05	8	5	4
Left lateral Occipital Cortex	<0.05	-30	-92	-20
Right lateral Occipital Cortex	<0.05	28	-92	-26
Left Middle Temporal Gyrus	<0.05	-64	-44	-6

Right Middle Temporal Gyrus	<0.05	57	-18	-20
Commission Errors > Timing Errors				
Anterior Cingulate Gyrus	<0.05	4	32	28
Left Insula Cortex	<0.05	-38	12	-8
Right Insula Cortex	<0.05	44	10	-8
Left Frontal Pole	<0.05	-32	48	16
Right Frontal Pole	<0.05	28	54	26
Left Supramarginal Gyrus	<0.05	-52	-40	38
Right Supramarginal Gyrus	<0.05	56	-46	34
Left Thalamus	<0.05	12	-13	1
Right Thalamus	<0.05	-3	-11	-2
Brain-Stem	<0.05	2	-22	-8
Timing Errors > Commission Errors				
Left Inferior Frontal Gyrus (pars triangularis)	<0.05	-56	24	10
Right Inferior Frontal Gyrus (pars triangularis)	<0.05	58	30	14
Left Middle Temporal Gyrus	<0.05	-60	-20	-12
Right Middle Temporal Gyrus	<0.05	64	-15	12
Precuneus	<0.05	3	-53	32
Left Superior Frontal Gyrus	<0.05	-7	56	34
Left Lateral Occipital Lobe	<0.05	-30	-92	-22
Right Lateral Occipital Lobe	<0.05	30	-92	-16
Areas Common to Commission and Timing Errors > Correct Trials				
Left Inferior Frontal Gyrus (pars opercularis)		-47	18	19
Right Inferior Frontal Gyrus (pars opercularis)		50	15	14

Left Supramarginal Gyrus	-63	-48	27
Right Supramarginal Gyrus	62	-44	20
Brain-Stem	2	-29	-10
Left Thalamus	-10	-1	5
Right Thalamus	8	-1	3
Left Temporal Pole	-40	10	-25
Right Temporal Pole	41	10	-25

4.4.2. Timing errors activate lateral prefrontal and superior frontal regions, but not the dACC

Compared to commission errors, timing errors were associated with activation in a distinct and only partially overlapping network. Relative to correct trials, timing errors were associated with activation in the pars opercularis, which extended forward into the pars triangularis bilaterally, and also in the anterior part of the medial superior frontal gyrus (Figure 4.3B). More posteriorly, activation was seen in superior temporal regions extending into the inferior parietal lobe bilaterally. This included activation of the angular and supramarginal gyri bilaterally. Activation was not observed within the dACC and only marginally spread into the anterior insulae from the adjacent inferior frontal gyrus. Significant subcortical activation was seen in the brain stem and bilateral caudate nuclei.

A direct contrast of commission versus timing errors demonstrated that activation was significantly higher in the SN for commission errors. Peaks for this contrast were seen in the dACC, bilateral insulae, as well as in the frontal poles and angular gyri

(Figure 4.4). The reverse contrast showed greater activation bilaterally within the pars triangularis for timing errors, as well as increased activation within the posterior cingulate cortex (Figure 4.4).

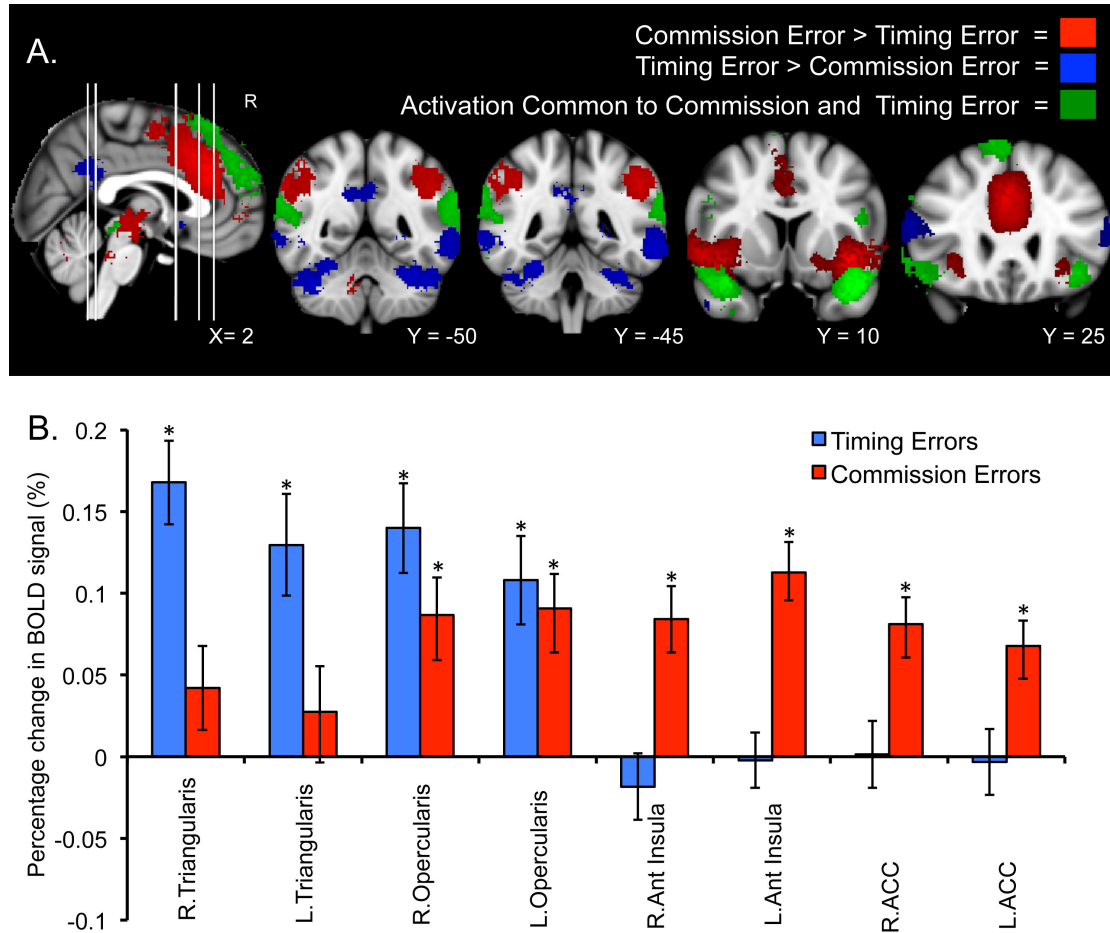


Figure 4.4: Common and distinct activation for errors of commission and timing.

A) A conjunction analysis showing common activation for both types of error (green). The direct contrast of error types shows brain regions more activated by errors of commission (red) or timing (blue). Results are superimposed on the MNI 152 T1 1 mm brain template. B) Region of interest analysis using anatomically derived masks. Significant differences from baseline are shown by *. Right (R), left (L), anterior (ant) and anterior cingulate cortex (ACC).

4.4.3. Common activation for commission and timing errors seen within pars operculari

A conjunction analysis demonstrated brain regions commonly activated by errors of commission and timing (Figure 4.4). Common activation was observed in the pars

operculari bilaterally, as well as within the inferior parietal lobes, and the anterior part of the medial superior frontal gyrus, the anterior thalami and temporal poles bilaterally. A region of interest analysis using anatomically defined frontal masks confirmed the presence of distinct patterns of activation for the two types of error, as well as common activation within the pars operculari (Figure 4.4B). Commission errors resulted in significant activation throughout the SN, (right ACC ($t=4.96$, $df=34$, $p<0.0005$); left ACC ($t=4.37$, $df=34$, $p<0.0005$); RAI ($t=4.04$, $df=34$, $p<0.0005$); and LAI ($t=6.04$, $df=34$, $p<0.0005$)), whereas timing errors were associated with activation of the pars triangulari bilaterally (right $t=6.56$, $df=34$, $p<0.0005$ and left $t=4.17$, $df=34$, $p<0.0005$). There was no significant activation of the ACC or either anterior insulae when comparing timing errors to correct trials. Common activation relative to baseline was seen in the pars opercularis bilaterally for both error types. Timing errors showed significantly greater activation in the left ($t=5.09$, $df=34$, $p<0.0005$) and right pars opercularis ($t=3.99$, $df=34$, $p<0.0005$) compared to baseline; as did commission errors (left pars opercularis ($t=4.31$, $df=34$, $p<0.0005$) and right pars opercularis ($t=3.75$, $df=34$, $p=0.001$)).

4.4.4. Delayed activation of the dACC was not present after timing errors

Although errors of timing occurred slightly later than errors of commission (152 milliseconds average difference), this did not account for the differences I observed in dACC activation. This small difference in timing is highly unlikely to produce difference in activation between the two types of error, and small variations in the hemodynamic response function were modelled using temporal derivatives. In addition, I performed a time course analysis to confirm that delayed dACC activation was not present (Figure 4.5). Dorsal ACC activation was only observed for errors of commission, which peaked around 6 seconds after the response was made. Following a commission error, activation of the dACC was significantly greater than

following either correct trials or timing errors from 3 to 9 seconds after the response. In contrast, timing errors caused no statistically significant signal change compared to correct trials at any time point.

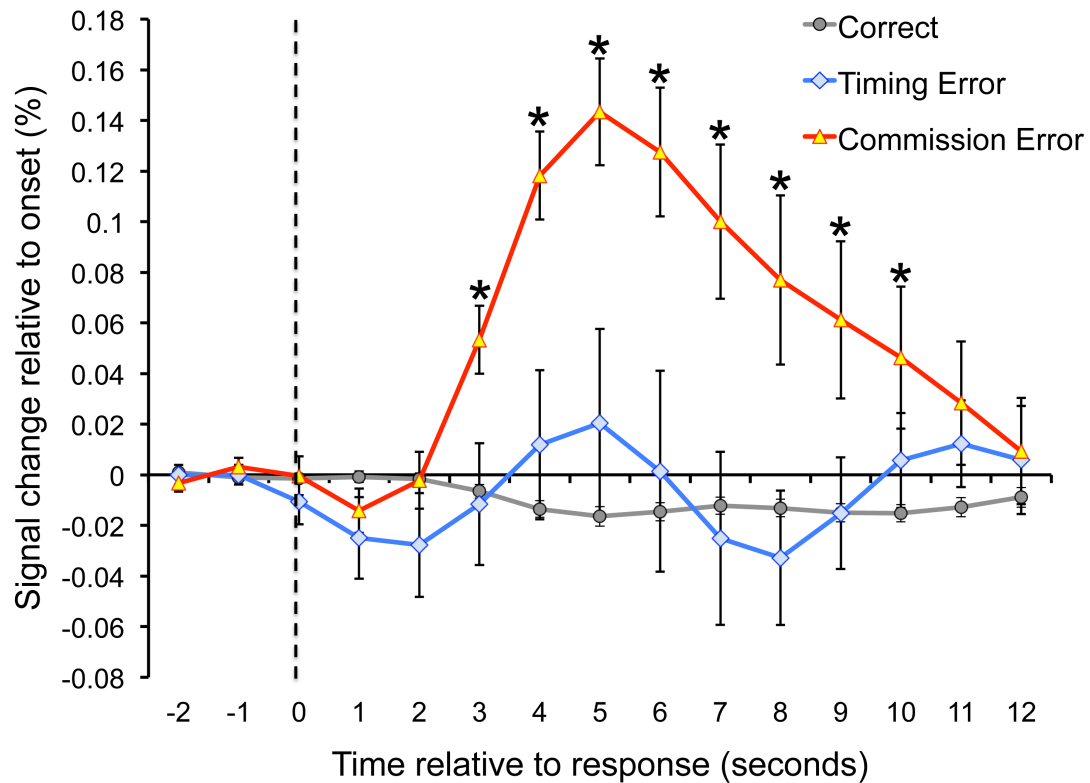


Figure 4.5: Perl Event-related Average Time-course Extraction (PEATE) analysis.

Graph of the averaged BOLD signal change across subjects within the anterior cingulate cortex (ACC) for the 12 seconds following correct trials, commission error trials and timing error trials. ACC activity was sampled from a region around the peak of activation associated with errors of commission versus correct trials. Error bars represent the standard error of the mean, and “*” signifies significant difference from either timing errors or correct trials.

4.4.5. Controlling for the presence of external feedback on timing errors

I also investigated whether the absence of external feedback after commission errors could have influenced the difference in brain activation observed within the dACC. In the Secondary Simon task, errors of commission were also signalled by explicit external feedback in a similar way to timing errors. Overall, the behavioural results for the control experiment were similar to the main experiment. Comparing the two

experiments, there were no significant differences in overall reaction times (351 and 340 milliseconds, $p=0.149$) or number of late responses per run (14.5 and 13.2, $p=0.684$). Similar behavioural adaptation was also observed after errors of commission and timing (Figure 4.6). There were slightly fewer overall errors in the control experiment ($11.7 \pm 0.4\%$ vs. $7.8 \pm 0.9\%$), which was due to both fewer congruent errors ($5.3 \pm 0.4\%$ vs. $3.1 \pm 0.4\%$) and incongruent errors ($6.4 \pm 0.4\%$ vs. $4.7 \pm 0.7\%$). The neuroimaging results were also similar. The contrasts of commission and timing errors with timely correct responses showed similar activation to the main version of the task (Figure 4.6). The direct contrast of commission and timing errors again confirmed increased dACC activation for commission errors using a small volume correction with a 10mm diameter sphere centred on the peak of the activation difference between error types in the main analysis (peak MNI coordinates 2, 32, 26).

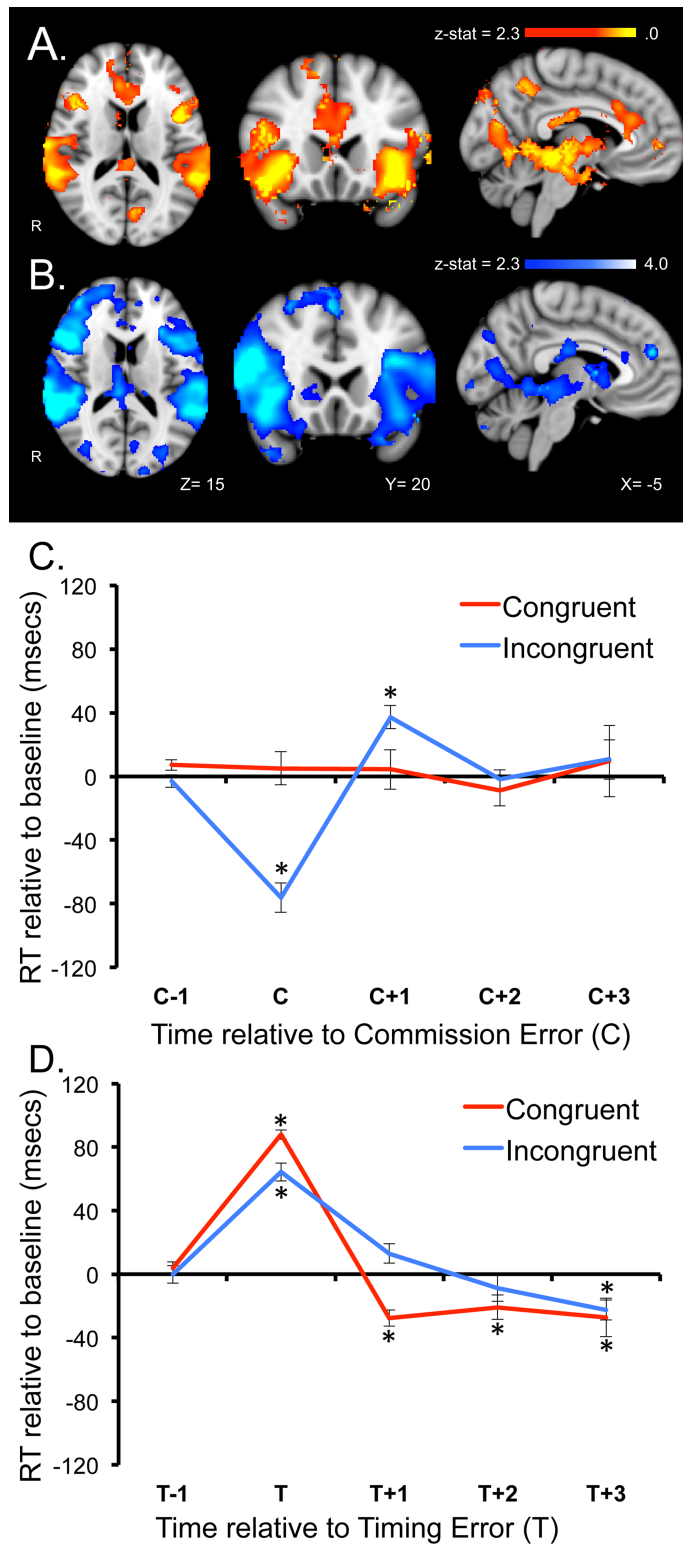


Figure 4.6: Results of Secondary Simon task

Errors of commission and timing in small group of subjects using the Secondary Simon Task paradigm. A) Areas of significant brain activation associated with commission errors compared to correct trials (red-yellow). B) Areas of significant brain activation associated with timing errors compared to correct trials (light – dark blue). Results are superimposed on the MNI 152 T1 1 mm brain template. C) Post-error slowing following commission errors. D) Post error-speeding following timing errors.

4.4.6. Strategic differences in task performance: comparison of High and Low Timing error groups

Runs with low and high numbers of timing errors were compared, as I reasoned that they involve different performance strategies. Low numbers of timing errors suggest that subjects performed the task as requested, maintaining a generally fast response speed. In contrast, high numbers suggest that subjects paid less attention to the timing feedback, which is likely to be the result of a strategic decision to optimize accuracy over timing. Despite this strategic difference, timing feedback still had the effect of changing behaviour in both groups in the immediate period following an error (Figure 4.7B). An ANOVA was performed using group assignment as one factor (High or Low Timing error) and time relative to the timing error trial (T) as a second factor with 5 levels (T-1, T, T+1, T+2 and T+3). There was no interaction between group type and time, demonstrating the similarity of the short-term response to timing feedback. In addition, there was no group difference in the average reaction times for correct trials (338 ± 5 milliseconds for the High-Timing group and 325 ± 5 milliseconds for the Low-Timing group), indicating that non-specific differences in factors such as arousal level were not present.

The contrast of timing error and correct trials in both groups showed a pattern of activation similar to that seen for the overall effect of timing errors (Figure 4.7C and D). Activation was observed in the right superior frontal gyrus, bilateral pars triangulari, operculari and the supramarginal gyri. No regions showed significant differences in activation when directly comparing the two groups. In addition, neither group showed any significant activation of the dACC.

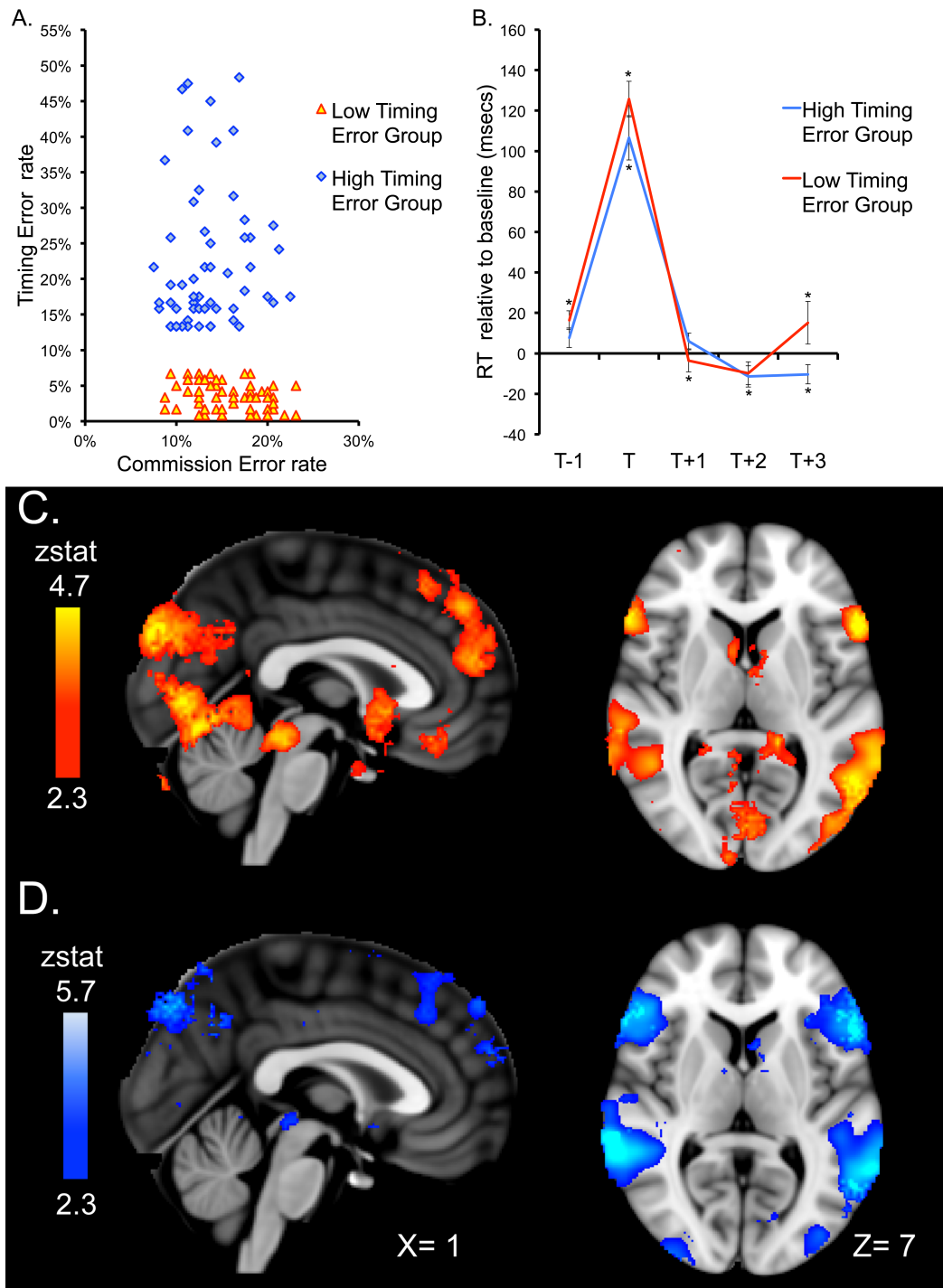


Figure 4.7: Strategy analysis

A) Graph illustrating the timing and error rates of runs used in the analysis. Timing error rates for separate runs plotted against the commission error rate for that run (averaged for congruent and incongruent errors). Runs were used from the upper or lower third of the distribution. B) Graph of reaction times on errors of timing (T) and on trials around this (T-1 and T+1 to 3). Behavioural data is plotted separately for groups with high and low timing errors. C) Brain regions activated by the contrast of timing errors compared to correct trials in the Low Timing error group. D) Brain regions activated by the contrast of timing errors compared to correct trials in the High Timing error group. Results are superimposed on the MNI 152 T1 1 mm brain template.

4.5. Discussion

4.5.1. Results summary

I investigated the neural response to errors using event-related fMRI and provide evidence for a multifaceted error processing system. A modified version of the Simon Task was used to generate large numbers of commission and timing errors. This allowed detailed analysis of the patterns of brain activity associated with these errors. Whilst being quite different in nature (see Chapters 2 for a detailed discussion), both types of error were associated with behavioural adaptation on subsequent trials, suggesting the engagement of cognitive control. As expected, commission errors activated the dACC and other parts of the SN, and led to an adaptive behavioural change in the form of post-error slowing after incongruent trials. In contrast, timing errors were not associated with increased dACC activation, despite being explicitly signalled by feedback and leading to behavioural change. Timing errors were also not associated with activation in the RAI or LAI, both key nodes in the SN. Strategic differences in task performance did not explain this result. The lack of dACC activation associated with timing errors demonstrates that cognitive control processes that affect behaviour can be triggered by errors without an increase in activation of the dACC. In contrast, timing errors were associated with extensive activation elsewhere throughout the ECN, including regions previously described as part of the VAN, with specific activation observed in the pars triangularis. This provides an alternative anatomical route by which behavioural control may be engaged, which is potentially independent of the dACC and SN more generally.

4.5.2. The dACC activation is not necessary to engage cognitive control

Cognitive control links performance monitoring to subsequent task performance, and the dACC has been placed at its heart (Badre and Wagner 2004, Botvinick, Cohen et al. 2004, Kerns, Cohen et al. 2004, Ridderinkhof, Ullsperger et al. 2004, Rushworth, Walton et al. 2004, di Pellegrino, Ciaramelli et al. 2007). My results show that involvement of this region depends on the nature of the error. In keeping with previous work, the region was extensively activated during commission errors (Falkenstein, Hoormann et al. 2000, Ridderinkhof, Ullsperger et al. 2004, Debener, Ullsperger et al. 2005). In contrast timing errors were not associated with increased dACC activity. During performance of the task it was repeatedly emphasized that pressing the wrong button and responding late should both be considered to be an error, and evidence that subjects considered this to be the case is provided by the adaptive changes in behaviour observed. Commission errors during the incongruent condition produced typical post-error slowing, which is often taken to indicate that cognitive control has been engaged. In contrast, timing errors were followed by post-feedback speeding. On this particular task the speeding of responses after an error is distinct from the general trend of responses to slow as each run progresses, and is also associated with a better than average accuracy for the subsequent response. Hence, this adaptive change in response speed is also indicative of increased cognitive control without associated dACC activation.

4.5.3. The dACC may signal a subset of learnable errors

Models of cognitive control frequently propose that the dACC is involved in signalling a need for increased control, which leads to a change in behaviour (Ridderinkhof, Ullsperger et al. 2004). The amount of dACC activation can be related to the magnitude of post-error slowing (Gehring, Goss et al. 1993, Kerns, Cohen et al. 2004), although this is not always observed (Li et al., 2008). In keeping with the

dACC's role in monitoring but not necessarily implementing behavioural change, the results show that high dACC activation is not necessarily associated with behavioural adaptation, as congruent commission errors strongly activated the region but were not followed by post-error slowing (see Figure 5.3A in Chapter 5 and 4.6A). A key question is what does the dACC monitor and over what time scale does it operate? A feedback related negativity (fERN) has been demonstrated with similarities to the ERN (Miltner, Braun et al. 1997). Similarly, certain types of feedback are associated with dACC activation demonstrated with fMRI (Holroyd and Coles 2002, Holroyd, Nieuwenhuis et al. 2004, Ullsperger, Nittono et al. 2007), although differences in reward may influence dACC activity (Bush, Vogt et al. 2002). However, my results are not compatible with the proposal that the dACC signals all behaviourally salient errors (Holroyd and Coles 2002, Holroyd, Nieuwenhuis et al. 2004) nor that the SN acts as a filter for all incoming information (Menon 2011). I observed no increase in dACC activation after timing errors, despite explicit external feedback that changed behaviour. Work in non-human primates shows the preservation of rapid responses to errors, but impaired strategic learning in animals with ACC lesions (Kennerley, Walton et al. 2006), also suggesting that rapid cognitive control can be engaged without dACC involvement.

Subtle changes in timing are often difficult to perceive (Allan 1978, Miltner, Braun et al. 1997, Luu, Flaisch et al. 2000, Grondin 2010), and an important factor in explaining these results is likely to be the unpredictability of the external feedback. A number of factors make it highly unlikely that subjects were able to accurately judge the timing of their responses. Firstly, the cut-off for timing feedback varied from trial-to-trial; secondly, separate timing limits were used for congruent and incongruent trials; and finally, the trial types were randomly inter-mixed making it very difficult to learn the timing rules for the two trial types. The magnitude of the ERN depends on

whether feedback is predictable (Hajcak, Holroyd et al. 2005, Holroyd, Krigolson et al. 2009) providing evidence that the dACC is involved in cognitive control only when action-outcome contingencies can be learned (Holroyd, Krigolson et al. 2009). This has led to a re-formulation of the reinforcement learning theory in which the dACC is involved in cognitive control only when monitoring involves production of an internally generated prediction error. These results are in keeping with this distinction, as unpredictable feedback was not associated with dACC response.

4.5.4. Comparison with previous studies of timing errors

Variation in the predictability of feedback could explain differences between my results and previous limited number of electrophysiological studies of timing errors (Miltner, Braun et al. 1997, Luu, Flaisch et al. 2000). For example, Miltner and colleagues show the presence of a fERN when subjects were provided with feedback 600 milliseconds after an error on a time estimation task. Although the criterion for success was adaptively varied, there remained a relatively predictable relationship between performance and feedback. Hence, the fERN could be interpreted in the context of the generation of a prediction error. In a further study Luu and colleagues studied a cognitively demanding flanker task with a reaction time limit that triggered negative feedback when breached (Luu, Flaisch et al. 2000). This studies design was similar in many ways to ours, but in this case timing errors were associated with the generation of an ERN. However, in contrast to the current study, monetary reward was used to increase motivation, which confounds interpretation of the findings. In addition, the ERN amplitude was shown to increase as responses became later. This is compatible with prediction errors increasing in magnitude as the presence of a timing error became more predictable.

4.5.5. The role of the dACC in conflict detection

A further potential explanation for the absence of dACC activity during timing errors is low levels of response conflict on these trials. The dACC is activated in situations where response conflict is high, which arises when two or more response processes are simultaneously activated (Botvinick, Braver et al. 2001, Botvinick, Cohen et al. 2004) Conflict can occur before a response, for example on incongruent trials when there is conflict between the spatial location and the colour response cue, or after a response, for example as a result of attempts to immediately correct an erroneous response (Yeung, Cohen et al. 2004). Timing errors are likely to have low levels of both pre and post-response conflict, because they are predominantly congruent and cannot be corrected with an alternative response, potentially explaining the absence of increased dACC activity. In contrast, incongruent commission errors are associated with pre-response conflict because of conflicting spatial and colour information, and both congruent and incongruent commission errors are associated with post-response conflict, which may actually be greater for congruent errors, potentially explaining the similar levels of dACC activation on these two trial types (Yeung, Cohen et al. 2004).

4.5.6. Timing errors do not activate the Salience network

The results clearly show distinct patterns of activation within the lateral frontal regions. The anterior insulae show robust activation in response to errors of many types, and may specifically respond to the conscious awareness of errors (Klein, Endrass et al. 2007, Ullsperger, Harsay et al. 2010). These results are compatible with such a role following internally generated errors. However, in a similar way to the dACC, externally signalled timing errors were not associated with anterior insulae activation. These three regions taken as a whole make up the SN. Therefore, these

results suggest more generally that SN activation is not always necessary for behavioural adaptation to occur.

4.5.7. VAN activation after both error types

In contrast, common activation was seen within the pars operculari and the supramarginal gyri. In the right hemisphere these regions form part of what has been termed the VAN (Corbetta and Shulman 2002). This network responds to behaviourally relevant events, particularly when they are unexpected or salient (Corbetta, Kincade et al. 2002, Sharp, Bonnelle et al. 2010), and appears important for reorienting attention. My results are compatible with this role in response to errors, and suggest that both internal and external events trigger similar activity within the network. The VAN is usually considered to be a right lateralised system, which complicates this interpretation as I observed bilateral inferior frontal and inferior parietal activation. However, unexpected behaviourally relevant events such as 'odd ball' stimuli have previously been shown to produce bilateral activation in these regions.(Stevens, Skudlarski et al. 2000, Fichtenholtz, Dean et al. 2004) The bilateral activation I observe may be due to additional cognitive processing required to process the behavioural significance of the errors in this task.

4.5.8. Evidence of a rostro-caudal gradient in the lateral prefrontal cortex

Moving more anteriorly along the inferior frontal gyrus, a striking change in activation pattern was observed. In contrast to the common pars operculari activity, greater activation was observed for timing errors in the pars triangulari. This is an important observation as it provides evidence that timing errors were not simply less internally salient and so associated with less increase in neural activity. The increase in pars triangulari activity may be explained by the rostral-caudal organisation of the lateral

prefrontal cortex initially proposed by Koechlin and colleagues (Koechlin, Ody et al. 2003). In this model cognitive control processes are organised in a cascade, with the sensory control involved in selecting motor actions supported by lateral premotor regions and higher-level control processes supported by more anterior regions. It is proposed that the pars triangularis is involved in the episodic control of behaviour, guiding stimulus-response mapping on the basis of either past-events or future plans. The key difference between timing and commission errors in this respect may be that the former are not perceived as being causally linked to the current behavioural episode, because of their unpredictability, and hence engage control processes that allow behavioural adaptation over an extended time period.

4.5.9. Motivation and the relative salience of different error types

Different types of error can vary in their salience, and the pattern of errors observed in this study suggests that subjects may vary in their motivation for avoiding the two error types. As motivational factors affect the magnitude of the ERN (Gehring, Goss et al. 1993), this might influence the response of the dACC. I investigated this possibility by capitalizing on the large variability in the numbers of errors of timing across different runs and across individuals to investigate this possibility. The number of timing errors was used as a marker of the internal saliency of the feedback, (i.e. how motivated individuals were to consistently provide rapid responses). The analysis showed that runs with high and low numbers of timing errors showed similar patterns of brain activation. In particular the dACC was not activated in either situation, suggesting that variability in internal salience was not the reason for a difference in dACC activation.

4.5.10. Addressing potential experimental confounds

The difference in dACC activation was unlikely to be because of methodological issues. Firstly, the absence of external feedback during errors of commission did not in any way influence the dACC result, as demonstrated by the control experiment using the Secondary Simon task. Secondly, the frequency of error occurrence was not an important factor as errors of timing and commission accounted for similar proportions of the total number of trials. Finally, subtle timing differences between error types were not an important factor. Errors of timing occurred on average around 150 milliseconds after errors of commission. I explicitly modelled this in the event-related design, and added temporal derivatives of the error timings (Smith, Jenkinson et al. 2004), which has the effect of correcting for inter-subject temporal differences in the generation of the BOLD response. In addition, although the physiological response to timing errors might be expected to occur around 200 milliseconds after than the response to commission errors (Miltner et al 2007), my fMRI analysis is highly unlikely to be sensitive to this temporal difference. I observed widespread activation of other brain regions in response to timing errors, which provides evidence that the slight delay in timing error was not enough to explain the lack of dACC activation. Furthermore, the additional time-series analysis of neural activation within the dACC confirmed that there was no late dACC activation following timing errors.

4.5.11. Conclusions

Taken together, these results suggest that the dACC does not respond to all types of behaviourally salient error. In keeping with neuropsychological work (Modirrousta and Fellows 2008), the results suggest that the performance monitoring system is multi-faceted, and cognitive control can be triggered independently of the dACC. Differences in dACC activity associated with timing and commission errors may be

due to different levels of feedback predictability or conflict present in the two situations. An alternative route exists to engage cognitive control, and this involves a bilateral fronto-parietal network that overlaps with what has been described as the VAN. The common activation of the pars opercularis across both types of error is in keeping with this region signalling a general requirement for a shift in cognitive control.

Chapter 5: Cognitive control and the Salience Network: an investigation of error processing and effective connectivity

The aim of this study was to establish the individual roles of the cortical regions that make up the Salience Network (SN). I have chosen to study commission errors as they produce robust activation of the SN previously described in Chapter 4. I used the same fMRI data set as described in the previous chapter to perform this analysis, and tested the following specific hypothesis:

Hypothesis: The dorsal anterior cingulate cortex and right anterior insula have distinct roles in the salience network that can be established using dynamic causal modeling fMRI techniques

5.1. Introduction

As discussed in the previous chapters, the SN is a key in the neural response to behaviourally salient events (Seeley, Menon et al. 2007), and is thought important for the initiation of cognitive control (Menon and Uddin 2010), the maintenance and implementation of task sets (Dosenbach, Visscher et al. 2006, Nelson, Bernat et al. 2008) and the coordination of behavioural (Medford and Critchley 2010) and neuronal response to salient events (Menon 2011). The SN consists of three main cortical areas: the dorsal anterior cingulate cortex (dACC), left anterior insula (LAI) and right anterior insula (RAI) and the adjacent inferior frontal gyri (Seeley, Menon et al. 2007). As demonstrated in the previous chapter, increased SN activity is observed

after commission errors and in many other situations where it may be important to adapt behaviour (Carter, Braver et al. 1998, Holroyd, Nieuwenhuis et al. 2004, Dosenbach, Fair et al. 2007).

An influential theory states that the dACC monitors performance, and signals the need for behavioural adaptation (Holroyd, Nieuwenhuis et al. 2004, Ridderinkhof, Ullsperger et al. 2004). Electrophysiological studies have identified an 'Error Related Negativity' (ERN) a very early response to errors (80-110 milliseconds) (Gehring, Goss et al. 1993) thought to arise from the dACC (Dehaene, Posner et al. 1994, Debener, Ullsperger et al. 2005). It is proposed that activity in the dACC signals the need for increased cognitive control (Ridderinkhof, Ullsperger et al. 2004), and interactions between the dACC and lateral prefrontal structures implement subsequent behavioural changes (Ridderinkhof, Ullsperger et al. 2004, Egnor 2009, Kouneiher, Charron et al. 2009).

An alternative theory proposes that the RAI is a 'cortical outflow hub', co-ordinating changes in activity across multiple brain networks (Sridharan, Levitin et al. 2008, Menon and Uddin 2010, Bonnelle, Ham et al. 2012). It has been recently demonstrated that the structural integrity of the white matter connection between the RAI and the dACC predicts behavioural and physiological abnormalities after TBI (Bonnelle, Ham et al. 2012). In addition, Granger causality analysis has provided some support for the view that the RAI causally influences activity in other brain networks (Sridharan, Levitin et al. 2008), although there are methodological problems with using lag-based methods to infer causality from fMRI data (Smith, Miller et al. 2011).

Chapter 4 demonstrated that SN activation is linked to the neural response to predictable/internally signalled errors. However, the causal interactions of nodes within the SN remain unclear. This is partly because activity in the dACC and anterior insulae tend to show tightly correlated neural activity (Ullsperger, Harsay et al. 2010), which makes discriminating their roles difficult using traditional event-related fMRI analysis (Friston, Price et al. 1996). In this chapter I investigate the causal relationships between the cortical nodes of the SN using dynamic causal modelling (DCM) (Friston, Harrison et al. 2003), a technique that infers effective connectivity from fMRI data (for a more detailed discussion see Chapter 3). I performed this analysis using the fMRI data set from the main Simon task described in Chapter 4, (i.e. a large group (n=35) healthy volunteers who performed six runs of the Simon task). The Simon task has two different conditions (congruent and incongruent) leading to two distinct types of commission error as demonstrated by the differences in their subsequent behavioural adaptations (see Chapter 4). This allowed me to compare patterns of SN connectivity across distinct types of behaviourally salient events. Standard fMRI analysis was used to assess the pattern of relative activation within the SN, and DCM was used to test where input entered the SN and whether errors were associated with modulation of connections within the SN.

5.2. Materials and Methods

The data used for this analysis was the same as that used in Chapter 4's analyses of the main Simon task. I shall briefly reiterate the key details.

5.2.1. Participants

35 healthy subjects performed six runs of the Simon Task (17 male, mean age 30.6 ± 8.6 years).

5.2.2. Simon Task procedure

The Simon task procedure is described in detail in Chapters 3 and 4.

5.2.3. Functional MRI analysis

Structural and functional data were acquired using the standard settings described in Chapter 4.

5.2.4. Whole brain fMRI analysis

Statistical parametric mapping was performed using the SPM8 software (Wellcome Trust Centre for Neuroimaging: www.fil.ion.ucl.ac.uk/spm). Images were motion corrected, registered, spatially smoothed and temporally filtered using the procedures detailed in Chapter 3. A first-level fixed effects statistical analysis was performed for every subject. Two types of event were modelled for congruent and incongruent trials separately: correct trials (appropriate response within the time limit) and errors (incorrect button press within the time limit). Parameter estimates were calculated for these events across all brain voxels using the general linear model, a synthetic hemodynamic response function and its first temporal derivative. Four contrasts were examined: congruent errors > congruent correct; incongruent errors > incongruent correct; congruent errors > incongruent errors; and incongruent errors > congruent errors. Contrast images were performed at the individual level and then the combined analysis at the between-subject level using random effects (Friston, Holmes et al. 1999). Final statistical images were thresholded using Family-Wise Error (FWE) threshold of $p < 0.05$. In addition a conjunction analysis was performed to define regions common to both congruent error > congruent correct, and incongruent error > incongruent correct contrasts (Nichols, Brett et al. 2005).

5.2.5. Dynamic Causal Modelling analysis

I used the DCM10 package in SPM8 to perform the analyses described below. Congruent and incongruent trials had different frequencies (33.3% vs. 66.6% of trials), were conceptually different (spatial incongruency vs. congruency), and were behaviourally distinct in terms of both the error and post-error trials (see Chapter 4). As a result, I analysed each condition (congruent and incongruent) separately. This had the advantage of providing an opportunity to test the reproducibility of results across different conditions. Moreover, to allow me to relate changes in the DCM B-matrix (those connections altered by the experimental variable, i.e. errors) to behaviour, I compared the effects of trial type (correct vs. error) within condition (congruent and incongruent), and thus against the appropriate baseline. The final stage of the analysis involved comparing across the two conditions.

ROIs used to define the SN were identified from each subject's 1st level univariate fMRI analysis. These were then used in the DCM analysis by fitting the data to a variety of different models in order to establish the connectivity of the SN. I did this in three stages: first I identified where the inputs to the SN entered the system using Bayesian Model Selection (BMS) and family level inference; second, using Bayesian Model Averaging (BMA) for both congruent and incongruent conditions, I tested which connections within the SN were significantly modulated by both trial types (correct and error), and which were differentially modulated (correct vs. error). Lastly I directly compared the resultant connection strengths across conditions to see if any connections were significantly modulated in the condition by trial type interaction (incongruent errors vs. congruent errors), and then sought a behavioural correlation for any significantly modulated connection.

5.2.5.1. Defining subjects' regions of Interest

Whole brain cluster analysis was used on the group-level analyses to determine the peak voxels of interest for the given contrasts. The cluster analysis allowed me to establish the peak voxels within the dACC, RAI and LAI at a group level for the contrasts of interest (i.e. congruent errors > congruent correct trials; and, incongruent errors > incongruent correct trials) (Figure 5.3). Spherical regions of interest (radius 4 mm) were extracted for each contrast of interest adjusted for the equivalent F-contrast. ROIs were initially centred on the peak voxels from the group-level contrasts. To accommodate inter-individual variability and provide the optimal signal to noise ratio data in the time-series for each region, the centres of the ROIs were allowed to move no more than 8mm from the peak of the group level contrast depending on the individual pattern of activity. ROIs were extracted in an incremental fashion. The uncorrected p-threshold started at 0.001 and increased in 0.001 increments until more than two supra-threshold voxels were included within a ROI. For each subject and contrast, if any of the three regions required thresholds above $p=0.05$ the subject was excluded from further DCM analyses of that contrast. The exclusion criteria applied to seven subjects for incongruent errors and seven subjects for congruent errors, five of the subjects overlapped and were therefore excluded from both contrasts.

5.2.5.2. Model construction, family construction and model estimation

For each condition (congruent and incongruent), DCM10 was used to create a series of models from the 3 node SN. Each model consists of three matrices, the 'A', 'B' and 'C' matrices, each describing a different feature of model space:

A-matrices

The 'A' matrix represented the context-independent intrinsic connections within the model (correct and incorrect trials treated equally). With a three-node model there were six possible connections described in the A-matrices (i.e. dACC to RAI; RAI to dACC; dACC to LAI; LAI to dACC; LAI to RAI; and, RAI to LAI) (Figure 5.1). In all of the models, the A-matrices used were fully connected to each other to allow for average effects of trial type to be expressed (that is, correct and error trials treated equally). The A-matrices were not varied across models.

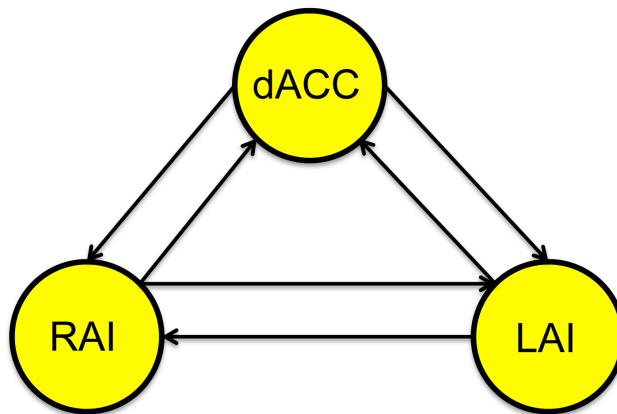


Figure 5.1: The Salience Network model

A schematic representing the three node Salience network and all the potential intrinsic connections within it. Yellow circles represent the three SN nodes discussed in the text and black arrows represent the effective connectivity between nodes.

The B and C-matrices

The 'B' and 'C' matrices describe the two ways that the experimental conditions could affect regional neuronal activity:

In DCM brain responses are evoked by known deterministic inputs (experimentally controlled stimuli) that embody designed changes in sensory stimulation or cognitive

set. These experimental variables can change the predicted BOLD response in one of two ways. First, they can elicit responses through direct influences on specific network nodes as inputs into the network and this expressed in the C matrix. The second class of inputs exert their effects vicariously, through a modulation of the coupling among nodes, in this case, the difference between correct vs. incorrect trials, expressed in the B matrix.

C-matrices

The 'C' matrix represented the potential inputs into the model after an error. These inputs arise elsewhere in the brain, for example from subcortical structures, although the current work focuses only on the cortical contributions to error processing. I wanted to experimentally test where neural activity entered the three node SN. Each node could have two possible states (i.e. an input or not). There were therefore $2^3 = 8$ mathematically possible combinations of C-matrix required to thoroughly explore model space. The input arrangements possible were: dACC alone; RAI alone; LAI alone; dACC and RAI in combination; dACC and LAI in combination; LAI and RAI in combination; all nodes; and, no nodes. Because 'no nodes' was biologically implausible, this option was excluded from further analysis, leaving seven remaining input arrangements

B-matrices

The 'B' matrix represented the same connections as the A-matrix but here coding how effective connectivity between regions was affected by the two conditions (correct vs. incorrect). These changes in the 'hidden' neuronal states were considered the indirect influence of the errors on regional activity. In previous fMRI analyses the B-matrix has described how task demands have increased effective connectivity between regions (Friston, Harrison et al. 2003). Just as with the A-

matrix, there were six possible connections described in the B-matrices (i.e. dACC to RAI; RAI to dACC; dACC to LAI, LAI to dACC; LAI to RAI; and, RAI to LAI). In the B-matrix each connection could exist in two states (i.e. modulated or un-modulated by trial type). There were therefore $2^6 = 64$ mathematically possible combinations of B-matrix required to thoroughly explore model space (Figure 5.2).

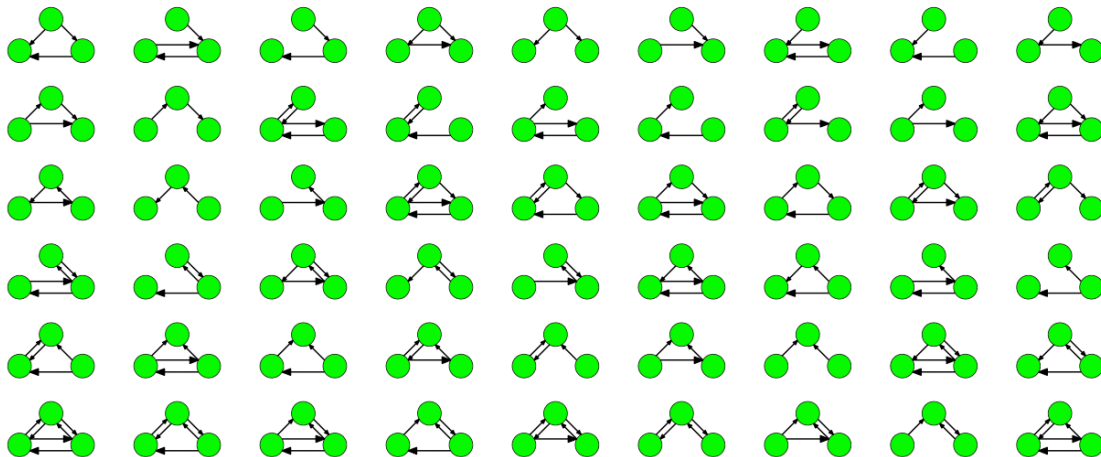


Figure 5.2: B-matrix combinations

A schematic representing the 64 potential variants of the B-matrix tested in each model family. Yellow circles represent the three SN nodes and black arrows represent the effective connectivity between the nodes.

I then combined the three matrices to into $7 \times 64 = 448$ models to allow comprehensive review of model space. I grouped the models together into families. Every family contained 64 models, each model within a family had the same input (C-matrix), and all models had one of the 64 possible B-matrices. The B-matrices were equally distributed across the families, but the C-matrices were distinct to each family. The families therefore represented seven groups with identical distributions of B-matrices/modulated-connections but distinct C-matrices/input characters. Every model had a fully connected A-matrix. In doing this I created all arithmetically possible combinations of models, and grouped them into non-overlapping families that were distinguished only by their inputs and therefore appropriate for family level inference (Penny, Stephan et al. 2010). This process created 448 models in total (the

family with no-inputs was excluded from further analysis) that were then estimated in DCM10 (Friston, Harrison et al. 2003, Penny, Stephan et al. 2010).

DCM Analysis 1: Where do inputs enter the SN?

The 448 models were sorted into the seven input families, each containing 64 models. The families were compared using the random effects option of the family level Bayesian inference, (Penny, Stephan et al. 2010). This computes the frequency with which each family of models is used in the population from which the subjects were drawn. It also computes an exceedance probability (xp), which is the probability that a model family has the highest frequency. The sum of all seven families' exceedance probabilities equals 1. The threshold xp was set at >80%, as has been used in previous studies using this technique (Leff, Schofield et al. 2008, Penny, Stephan et al. 2010). The 'winning' famil(ies) were then taken onto the next analysis while the 'losing' ones (those with little evidence) were rejected at this point.

DCM Analysis 2: What are the intrinsic SN connections and are they modulated by errors?

Two input families were taken forward into this analysis (128 models in total). I then used a BMA analysis to identify the average connection strengths (weighted by subject, by model, on the model evidence) across all models (Penny, Stephan et al. 2010). I did this to calculate both the average effect of trial type (correct and error trials treated equally within both congruent and incongruent conditions treated separately: the 'A' matrix) and the differential effect of trial type (correct vs. error trials, within both congruent and incongruent conditions treated separately: the 'B' matrix). This process moves away from inferences based on the overall connectivity

structure of the best model, towards asking which connections are significantly modulated by trial type (Stephan, Penny et al. 2010). The BMA provides the mean connection strength for each inter-regional connection within the A and B matrices for every subject. The starting point (prior) for the inter-regional connections is zero, a value that can be altered at the model estimation phase. The resulting connection strength values were then entered into a one-sample t-test to see if their values had been significantly moved away from the starting prior with significance set at $p < 0.05$ (Schofield, Penny et al. 2012).

DCM Analysis 3: Are there distinct effects of errors in congruent and incongruent trials, and do these relate to behaviour?

In the final analysis, I investigated between-condition effects on any connections that were significantly modulated by trial type (correct vs. error). I have already shown in Chapter 4 that the Simon task different trial types produce distinct behavioural profiles depending upon the condition. In 'Analysis 2' there is no common baseline across the conditions, because the congruent correct and incongruent correct trials are different behaviourally and cognitively (see Chapter 3 and 4 for details). Therefore, to test for a significant between-condition effect a direct comparison of the within-condition changes in effective connectivity is needed. There was only one connection where this was the case (see results). I performed a single, paired t-test on connectivity values for this connection only. As above, the significance was set at $p < 0.05$, there were no multiple-comparison issues as only one parameter was tested. Lastly I tested if the connectivity values from this connection correlated with behaviour. I did this using a Spearman rank coefficient test to assess any the relationship between subjects' post-error slowing across all errors (both congruent

and incongruent) and the alteration in effective connectivity associated with the errors.

5.3. Behavioural results

5.3.1. Behaviour summary of the Simon task performance

All subjects were included in the behavioural analyses ($n=35$) and the results are described in detail in the previous chapter. I shall mention in brief the salient features of the behavioural analysis as they relate to this new study. On average subjects produced errors on $7.9 \pm 3.5\%$ of congruent trials; and $19.3 \pm 7.0\%$ of incongruent trials. As expected, response speed had a major effect on the accuracy of the incongruent condition but interestingly not for the congruent condition. Congruent and incongruent errors had different effects on subsequent behaviour, which were studied by investigating the slowing of responses following errors. Post-error slowing was only seen after incongruent errors.

5.4. Neuroimaging results

5.4.1. Congruent and incongruent errors produce similar activation within the Salience Network

The network of brain regions activated by errors was consistent with previous work and included significant activation of the SN (Figure 5.3A and 4.3A) (Garavan, Ross et al. 2002, Ullsperger and von Cramon 2003, Hester, Fassbender et al. 2004, Hester, Foxe et al. 2005). Importantly, similar activation was observed in the SN for errors during the congruent and incongruent conditions, despite the distinct effect of these errors on subsequent behavioural adaptation. In addition to activation within the SN, both types of error produced peaks of activation in the bilateral

supramarginal and angular gyri, compared to correct trials (Table 5.1). Congruent errors were associated with additional activation in the left planum polare, right superior parietal lobule and left occipital cortex. Incongruent errors were associated with additional activation within the brain stem, right and left frontal poles. Although these analyses were performed in SPM8 the results were almost identical to the analysis performed in FEAT reported in Chapter 4. When congruent and incongruent errors were directly contrasted small regions within the left superior parietal lobule and left occipital cortex regions showed greater activation for congruent errors that survived correction (Table 5.1). However, no regions survived correction on a contrast of activity in incongruent errors > congruent errors. Activation within the SN was similar for congruent and incongruent errors. The results of the conjunction analysis showed common activity for both types of errors within the dACC, and both insulae, as well as the right Supramarginal gyrus (Table 5.1 and Figure 5.3C).

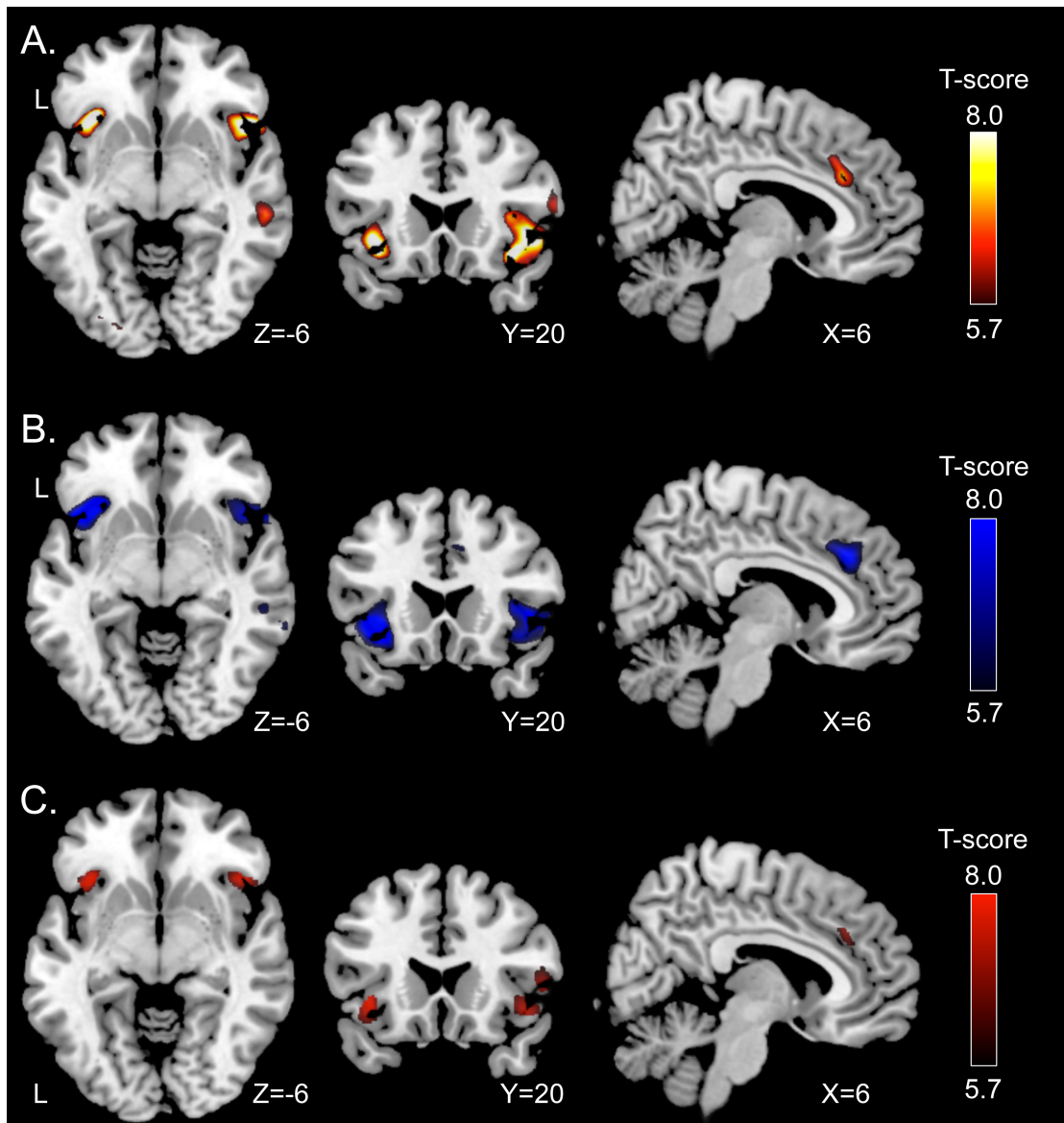


Figure 5.3: Congruent and incongruent errors activate the Salience Network
 A) Areas of significant brain activation associated with congruent errors compared to congruent correct trials (red-yellow). B) Areas of significant brain activation associated with incongruent errors compared to incongruent correct trials (light – dark blue). C) Areas of significant activation on both congruent and incongruent errors (red) as the result of a conjunction analysis. All images are thresholded ($p < 0.05$ (FWE)). Results are superimposed on the MNI 152 T1 1 mm brain template.

Table 5.1: FWE analysis of contrasts

Anatomical region	Peak T-score	MNI co-ordinates		
		X	Y	Z
Congruent Errors > Congruent Correct Trials				
Right anterior insula/inferior frontal gyrus	10.42	46	16	-5
Left anterior insula/inferior frontal gyrus	9.78	-34	20	-11
Right supramarginal gyrus	8.63	60	40	19
Left supramarginal gyrus	7.99	54	-38	27
Anterior cingulate cortex	7.27	6	28	29
Left planum polare	6.90	-42	-4	15
Left occipital cortex	6.07	-30	-84	-9
Incongruent Errors > Incongruent Correct Trials				
Left anterior insula/inferior frontal gyrus	10.90	-34	22	-5
Right anterior insula/inferior frontal gyrus	9.17	44	44	1
Dorsal anterior cingulate cortex	8.51	6	30	33
Left supramarginal gyrus	8.42	-58	-46	31
Left frontal pole	8.05	-30	52	27
Right supramarginal gyrus	7.66	60	-40	29
Brain stem	6.58	2	-10	-25
Right frontal pole	6.19	30	50	25
Congruent Errors > Incongruent Errors				
Left superior parietal lobule	6.74	-24	-44	51
Left occipital cortex	6.56	-38	-68	-17
Incongruent Errors > Congruent Errors				
Nil				
Conjunction analysis: Congruent errors > Congruent Correct AND Incongruent errors > Incongruent correct				

Left anterior Insula/inferior frontal gyrus	8.13	-37	22	-5
Right anterior insula/inferior frontal gyrus	7.71	46	22	-9
Dorsal anterior cingulate cortex	6.87	7	32	34
Right supramarginal gyrus	6.57	58	-37	33

Whole brain cluster analysis of the contrasts of interest. All clusters were thresholded ($p < 0.05$ (FWE)).

5.5. Dynamic causal modelling analyses results

5.5.1. DCM Analysis 1: Input into Salience network is through the right insula

For both conditions (congruent and incongruent) there was the most evidence for families with input into the RAI (78.1% xp for congruent and 62.5% for incongruent). The next most likely family of models had input into the LAI (xp of 11.7% for congruent and 22.7% for incongruent). Combining these two families resulted in an xp greater than 80%. Therefore, subsequent analysis focused on these models, and families with other types of input were rejected (Figure 5.4). Within these families there was no clear single winning model. For the congruent condition the maximum xp of any model was 2.4%, which fell within the RAI input family. The mean xp across all models was $0.2 \pm 0.3\%$, whereas the mean xp for the RAI input family was $1.2 \pm 0.4\%$. For the incongruent condition the maximum xp of any model was 2.8%, again within the RAI input family. The mean xp across all models was $0.2 \pm 0.3\%$, whereas the RAI input family mean xp was $1 \pm 0.4\%$. These seemingly small numbers are not surprising as 448 models were tested (64 models in seven input families) and the xp sums to one over all models. If all models had equal evidence then their xp value would be $\sim 0.2\%$. As no clear winning model was identified I proceeded to the next stage of the analysis.

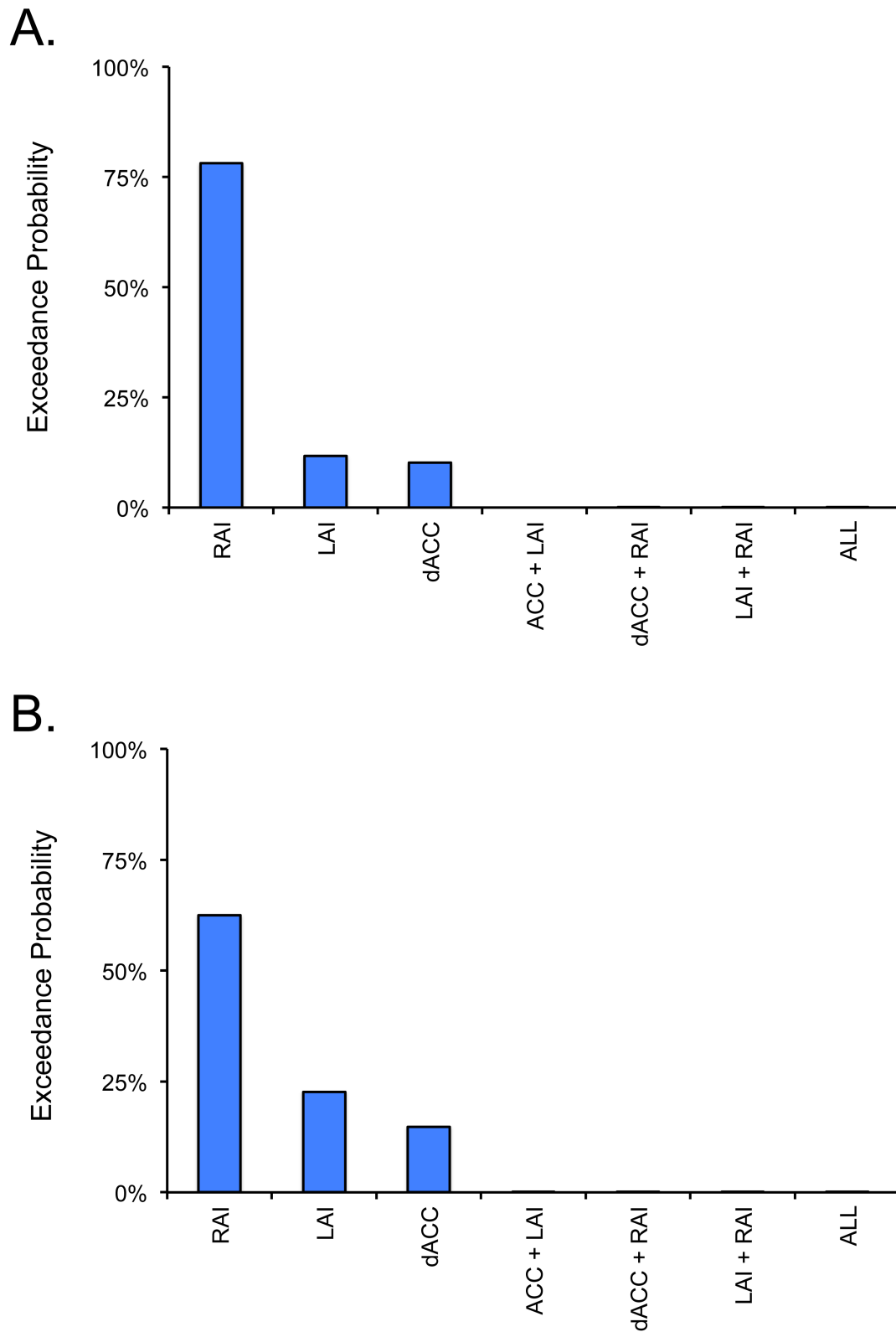


Figure 5.4: Inputs into the Saliency Network.

The likelihood of families of models with input into specific nodes or combinations of nodes are illustrated for (A) congruent and (B) incongruent conditions. The exceedance probabilities for each family are shown after Bayesian Model Averaging.

5.5.2. DCM Analysis 2: What are the intrinsic SN connections and are they modulated by errors?

Analysis of the pattern of intrinsic connectivity within the SN demonstrated that the insulae were functionally connected to the dACC via the RAI. For the congruent condition, average connectivity across correct and error trials (represented in the 'A' matrix) was significant for four connections: a) from the RAI to the dACC ($t=2.76$, $df=26$, $p=0.010$); b) from the LAI to the RAI ($t=2.18$, $df=26$, $p=0.0386$); c) from the RAI to the LAI ($t=2.81$, $df=26$, $p=0.0093$); and d) from the dACC to the RAI ($t=2.09$, $df=36$, $p=0.046$) (black arrows, Figure 5.5A). For the incongruent condition, only two of these connections were significant: a) from the RAI to the dACC ($t=2.95$, $df=26$, $p=0.0066$); and b), from the LAI to the RAI ($t=2.52$, $df=26$, $p=0.0178$) (black arrows, Figure 5.5B). For both conditions there was no direct connection between the dACC and LAI.

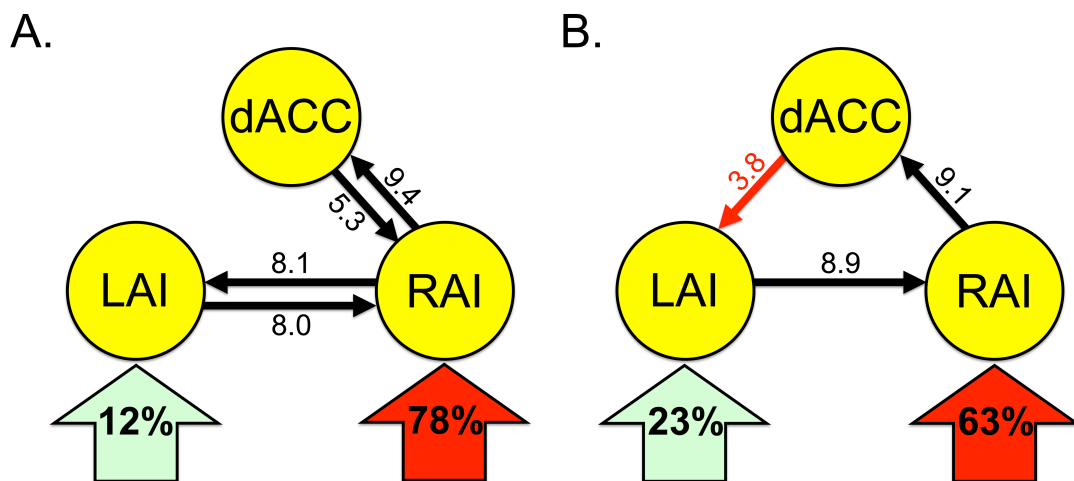


Figure 5.5: Saliency Network structure.

Schematic representations are shown of the winning models for (A) congruent and (B) incongruent conditions. Yellow circles represent nodes within the SN; black arrows represent significant intrinsic connectivity between nodes; and the red arrow represents increased effective connectivity between the dACC and LAI following incongruent errors. Large arrows beneath nodes contain the exceedance probabilities that that node provides the input to the network. The numbers next to the arrows represent the intrinsic connection strength (black) and the change in effective connectivity (red). Effective and intrinsic connectivity is expressed in 10^{-3} Hertz.

We next investigated whether the connection strengths between nodes of the SN were modulated by errors. For the incongruent condition, the connection from the dACC to LAI significantly increased in strength following errors ($t=2.81$, $df=26$, $p=0.008$) (red arrow, Figure 5.5B). For the congruent condition no modulation of any connection strengths were observed.

5.5.3. DCM Analysis 3: Are there distinct effects of errors in the congruent and incongruent conditions, and do these relate to behaviour?

Finally, I directly compared the effect of errors on the connection strengths of the SN in the congruent and incongruent conditions. This confirmed a specific modulation of the dACC to LAI connection during the incongruent condition ($t=2.65$, $df=24$, $p=0.014$ for the comparison of incorrect > correct across the two conditions). As only incongruent trials were associated with post-error slowing, I next tested whether the change in this connections effective connectivity related quantitatively to how much behaviour changed after the error. Averaged across all errors for every subject, the change in effective connectivity strength of the dACC to LAI connection positively correlated with the extent of post-error slowing (Spearman correlation coefficient=0.392, $p=0.035$, two-tailed). This suggests that in situations where behavioural adaptation is required, the dACC shows increased interaction with the LAI, which correlates with the subsequent change in behaviour.

5.6. Discussion

5.6.1. Results summary

Using DCM analyses I have expanded upon the univariate analysis methods I discussed in Chapter 3 and 4 by investigating the causal interactions of the three main cortical nodes within the SN. My results suggest that the RAI plays a central

role in the SN response to errors. Input into the SN was most likely to come through the RAI, and this was the only node showing intrinsic connectivity to the other two parts of the SN. This is in keeping with the proposal that the RAI acts as a 'cortical-outflow hub' regulating activity in other brain regions (Sridharan, Levitin et al. 2008, Menon and Uddin 2010).

5.6.2. The role of the dACC in error processing

A large body of previous work suggests the dACC is a key structure involved in cognitive control (Miltner, Braun et al. 1997, MacDonald, Cohen et al. 2000, Botvinick, Cohen et al. 2004, Holroyd, Nieuwenhuis et al. 2004). Electrophysiological work has demonstrated the ERN, which occurs 80-110 milliseconds after an error (Falkenstein, Hohnsbein et al. 1991). Source localization suggests the ERN originates in the dACC (Dehaene, Posner et al. 1994, Debener, Ullsperger et al. 2005), which has led many to the conclusion that the dACC provides the first cortical signal used for error detection (for a review see (Falkenstein, Hoormann et al. 2000)). The experimental design allowed me to probe the relationship between adjustments in cognitive control, measured by the amount of post-error slowing, and SN activity. Although input to the SN appears to come through the RAI, my results do support an important role for the dACC in the implementation of cognitive control. Changes in effective connectivity between the dACC and LAI correlated with post-error slowing, suggesting that the interactions of the dACC are important for moment-to-moment adjustments in behavioural control.

5.6.3. The role of the RAI in error processing

I adopted a hierarchical approach to analysing the organisation of the SN. This involved a stepwise process that builds towards identifying the most likely network

configuration. In the initial step I compared 'families' of networks with inputs to different nodes. By far the most likely input route was the through the RAI. The importance of this region's influences on the rest of the network was re-enforced by subsequent analysis of intrinsic connectivity. The RAI is known to be structurally and functionally connected to a range of cortical regions involved in various aspects of cognitive control. The RAI is functionally connected to networks responsible for adaptive behaviour including the SN (Seeley, Menon et al. 2007), as well as other parts of the fronto-parietal control network (Vincent, Kahn et al. 2008). Tractography evidence shows the region has direct white matter connections to other key regions within these networks including the dACC (van den Heuvel, Mandl et al. 2009), the temporo-parietal junction (Kucyi, Moayed et al. 2012), and the inferior parietal lobe (Uddin, Supekar et al. 2010). This connectivity make the anterior insula well placed to perform its putative role of reorienting attention (Ullsperger, Harsay et al. 2010), evaluating (Eckert, Menon et al. 2009) and switching between cognitive resources in response to salient events (Uddin and Menon 2009, Menon 2011).

5.6.4. Relationship to previous studies

Tight control of the balance of activity in the SN and the DMN appears important for efficient cognitive function, as rapid deactivation of the DMN is required for focused attention (Weissman, Roberts et al. 2006). It has previously been demonstrated that damage to the connection between the RAI and the dACC after TBI, can impair default mode network (DMN) function (Bonnelle, Ham et al. 2012). Specifically it was shown that damage to the white matter tract connecting the RAI to dACC was associated with a failure to control activity in DMN, and behavioural difficulty in rapidly switching actions. Consistent with this result, Granger causality analysis has provided evidence that the RAI plays a key role in switching between distinct brain states, which included deactivation of the DMN (Sridharan, Levitin et al. 2008). The

validity of this type of “lag-based” approach to the analysis of causal interaction in fMRI data have recently been called into question due to poor temporal resolution of the data (Smith, Miller et al. 2011). As the DCM procedure I used does not rely on a lag-based measure, these results provide more robust evidence for the causal interactions of nodes within the SN.

5.6.5. Increased sensitivity of effective connectivity measures over traditional univariate analysis

Previously, the amplitude of dACC and lateral prefrontal activation has been related to the extent behavioural adaptation (Gehring and Knight 2000, Gehring and Fencsik 2001, Klein, Endrass et al. 2007, Li, Huang et al. 2008). My work extends these findings by showing a relationship between the change in dACC effective connectivity and the magnitude of behavioural adaptation. On average, congruent errors produced no change in effective connectivity and resulted in no change in behaviour. In contrast, increased effective connectivity following incongruent errors was associated with significant post-error slowing. Therefore, despite similar levels of SN activation in each condition, changes in effective connectivity within the network encode information about whether behaviour needs to be adapted to improve subsequent performance. The observed increase in effective connectivity between the dACC and LAI for incongruent but not congruent errors suggests that the dACC exerts greater influence over the LAI when increased cognitive control is required.

5.6.6. Future research directions

As demonstrated in Chapter 4, there are different types of behaviourally salient errors, and not all activate the SN (Holroyd, Krigolson et al. 2009). In the current study I investigated errors that can be viewed as internally signalled, because explicit

external feedback is not provided. In Chapter 4 I investigated the externally signalled timing errors, which did not activate the SN, even though they produced clear behavioural change on subsequent trials. However, common activation was observed for both errors types in the pars operculari, a region adjacent to the anterior insulae. This result suggested that the SN is not required for all types of cognitive control adjustment, and that future work should examine causal interactions between the pars opercularis and the rest of the SN in a variety of situations where increased cognitive control is required.

5.6.7. Study limitations

One potential limitation of this study is that I focused the analysis on the main cortical nodes within the SN (Dosenbach, Fair et al. 2007, Seeley, Menon et al. 2007). Other brain regions are activated by errors, but these were not included in the analyses. I feel that this focus is justified because the SN forms such an important component of the error processing system, and increasing the number of nodes in DCM analyses has significant computational consequences that make comprehensively analysing the total model space problematic. This approach is supported by the conjunction analysis of responses to congruent and incongruent errors, which shows common activation to different types of errors is present in only one region outside the SN (the right supramarginal gyrus). It is nevertheless clear that brain regions outside the SN make important contributions to error processing, including brainstem dopaminergic and thalamic nuclei (Hollerman and Schultz 1998). Future studies should investigate the interaction of the SN with other brain regions including the contribution of subcortical inputs, although this work will need to carefully control potential artefacts that can confound analysis of brainstem fMRI signals (Limbrick-Oldfield, Brooks et al. 2012). A further important limitation is that fMRI is insensitive to rapid interactions between network nodes. DCM on fMRI data assesses the longer-lasting time-varying

properties of the systems, (i.e. the 'hidden states' produced by changes in effective connectivity), to provide insight into network hierarchy (Stephan, Penny et al. 2010). Future studies could apply DCM to modalities with higher temporal resolutions to study higher frequency interactions (e.g. MEG and EEG).

5.6.8. Conclusions

This DCM analysis provided evidence that the RAI plays a central role in the response of the SN to errors. Input was most likely to come through this node after internally signalled errors, and this node was unique in showing strong interactions with all other nodes in the network. It also provided evidence that changes in the effective connectivity of the dACC is important for moment-to-moment adjustments in cognitive control and behavioural response to salient stimuli.

Chapter 6: The neural basis of impaired self-awareness after traumatic brain injury

The aim of this study was to establish the neural basis of the self-awareness deficits commonly seen after TBI. I used 'on-line' performance monitoring as a surrogate marker of awareness, and assessed the structural and functional integrity of the fronto-parietal control network both rest and during error processing. In this study I tested the following three hypotheses:

Hypothesis 1: Dysfunction of the fronto-parietal control network leads to self-awareness deficits following traumatic brain injury. This dysfunction can be observed from the functional connectivity of the network at rest.

Hypothesis 2: Fronto-parietal control network dysfunction following traumatic brain injury can be observed from the activation of the network in response to errors during a cognitively demanding task.

Hypothesis 3: Fronto-parietal control network dysfunction after traumatic brain injury is due to structural disconnection between key nodes of the network, which can be measure using diffusion tensor imaging.

6.1. Introduction

As discussed in the general introduction to this thesis, TBI frequently produces impairments of awareness (Prigatano and Altman 1990, Vanderploeg, Belanger et al. 2007). This presents a major clinical problem as it limits the effectiveness of rehabilitation (Sherer, Hart et al. 2005), and is associated with poor functional outcomes (Sherer, Hart et al. 2003, O'Keeffe, Dockree et al. 2007). An objective, measure of self-awareness can be obtained by studying patients' abilities to monitor and respond to their own errors (Hart, Giovannetti et al. 1998, O'Keeffe, Dockree et al. 2004, Modirrousta and Fellows 2008, Ornstein, Levin et al. 2009). Healthy adults normally rapidly identify and correct their own errors (Rabbitt 1966, Rabbitt 1968), whereas impaired response to errors is common after TBI (Larson, Perlstein et al. 2006, Larson, Kaufman et al. 2007, Ornstein, Levin et al. 2009).

The work I described in Chapter 4, along with other recent neuroimaging studies has helped clarify the brain regions involved in performance monitoring (Ullsperger and von Cramon 2003, Ullsperger and von Cramon 2004, Sharp, Scott et al. 2006, Modirrousta and Fellows 2008). Structures within the medial prefrontal cortex, particularly the dACC, respond to many, but not all, types of error (Dehaene, Posner et al. 1994, Ridderinkhof, Ullsperger et al. 2004) and appear to be necessary for certain aspects rapid on-line error processing (Modirrousta and Fellows 2008). The dACC and anterior insulae of the SN contain an unusual class of cells, von Economo neurons, which are found in humans and other great apes (Allman, Tetreault et al. 2010, Allman, Tetreault et al. 2011). One prominent theory proposes that by integrating motivation, social and cognitive processing, the RAI and its connections to the dACC play a particularly important role in supporting awareness (Craig 2009). The SN is considered a sub-network of the larger fronto-parietal control network (FPCN), which includes bilateral inferior frontal gyri and inferior parietal lobes

(Vincent, Kahn et al. 2008, Spreng 2012). The SN's role in cognition is debated but the influential 'triple-network' theory suggests that the SN filters and ascribes significance to new sensory information and recruits the ECN and DMN as required to respond to this information (Menon 2011).

Here, I investigate for the first time whether impairments of self-awareness are associated with network dysfunction after TBI. Two groups of patients with high and low levels of performance monitoring (High-PM/Low-PM) were carefully defined on the basis of their ability to correct errors made on a simple cognitive task. This measure has previously been shown to provide a robust 'on-line' measure of performance monitoring (O'Keeffe, Dockree et al. 2007, Modirrousta and Fellows 2008). I particularly focused the neuroimaging analysis on the FPCN. I did not focus entirely upon the SN as the results of my previous study of the Simon task had suggested that regions within the FPCN but outside of the SN are also involved in performance monitoring and error processing (e.g. the IFG and SMG). I tested the hypothesis that impaired performance monitoring is associated with abnormal functional connectivity within FPCN. Advanced multi-modal neuroimaging allowed a detailed investigation of the structure and function of this network in the absence of a specific task ('rest'), and during error processing. Functional MRI was used to measure the interactions between nodes in these networks and their response to errors. DTI and structural MR imaging were used to assess the integrity of brain regions and structural connections within the networks.

6.2. Materials and methods

6.2.1. Patients: demographic and clinical details

Seventy-three patients with a history of TBI were recruited from a neurology clinic where they had been referred for persistent neurological symptoms following their TBI. Patients with a range of injury severities were recruited to provide variability of cognitive disabilities. Ten patients were excluded: two had distorted MR images that could not be registered accurately; six could not perform the cognitive tasks adequately; and two were found after recruitment to have premorbid psychiatric illness. The 63 patients included in the main analysis (46 males, mean age 38.0 ± 12 , range 18-66 years) were all in the post-acute/chronic phase post injury (mean 29 ± 74 months, range 2-578 months) (table 6.1 provides the patients' individual clinical details).

TBI severity was assessed according to the Mayo Classification system (Malec, Brown et al. 2007). This integrates the duration of loss of consciousness; length of post-traumatic amnesia (PTA); lowest recorded Glasgow coma scale (GCS) in the first 24 hours; and neuroimaging results. Using this system 89% (56 patients) were classified moderate/severe, 8% (5 patients) mild, and 3% (2 patients) symptomatic. Exclusion criteria were: neurosurgery, except for invasive intracranial pressure monitoring (1 patient); psychiatric or neurological illness prior to their head injury; significant previous TBI; current or previous drug or alcohol abuse; or contraindication to MRI. Subjects had no neurological, major medical, or psychiatric disorders prior to TBI. All participants gave written consent. The study was approved by Hammersmith and Queen Charlotte's and Chelsea Research ethics committee.

Table 6.1: Demographics and clinical data of High and Low-PM traumatic brain injury patients

PM	Age	Sex	Severity ¹	Cause	GCS	PTA	Medication at time of scanning	Structural MRI findings
Low	25	M	Mod/Sev	Assault	13	NK	Nil	NAD
Low	37	M	Mod/Sev	Fall	4	52d	Nil	MB
Low	50	M	Mod/Sev	RTA	4	42d	Ramipril 10mg OD, and Amlodipine 10mg OD	R fronto-temporal contusions and SS
Low	49	M	Mod/Sev	Assault	NK	NK	Nil	Bifrontal and R temporal SS
Low	48	M	Mod/Sev	Assault	NK	5d	Anti-TNF alpha	Bifrontal contusions and L temporal contusion and SS
Low	47	F	Mod/Sev	RTA	5	42d	Nil	MB
Low	36	M	Mod/Sev	RTA	NK	10d	Nil	MB
Low	66	F	Mod/Sev	RTA	NK	77d	Amitriptyline OD and tramadol QDS	L frontal contusion and bilateral parietal SS
Low	34	M	Mod/Sev	RTA	14	8h	Theophylline 300mg OD, and Seretide inhaler BD	L frontal, L parietal and L temporal contusions; and MB
Low	42	F	Mod/Sev	RTA	12	56d	Co-codamol QDS	NAD
Low	50	M	Mod/Sev	Assault	NK	5d	Nil	MB

Low	22	F	Mod/Sev	RTA	15	8h	Propranolol 40mg BD	L temporal SS
Low	34	F	Mod/Sev	RTA	15	5m	Thyroxine OD	R temporal contusion
Low	39	M	Mod/Sev	RTA	NK	Nil	Citalopram 40mg OD and Omeprazole 20mg OD	Bifrontal contusions and SS
Low	26	F	Mod/Sev	RTA	14	6h	Nil	R frontal contusion
Low	34	M	Mod/Sev	Assault	14	12h	Nil	L fronto-temporal contusions and SS
Low	67	M	Mod/Sev	Assault	NK	NK	Citalopram 20mg OD, Simvastatin 10mg OD, Aspirin 75mg OD and glucosamine 1g OD	Bifrontal contusions
Low	50	F	Mod/Sev	Fall	9	21d	Amitriptyline OD, Salbutamol and Becotide BD, Thiamine OD and Vit-B-Co-strong OD	R frontal contusion with SS, L frontal SS, R occipital contusion and SS, and MB
Low	36	M	Mod/Sev	Fall	NK	28d	Glargine 30u BD, and Humalog 16u TDS	Bifrontal contusions, R temporal contusion and R parietal SS
Low	20	F	Mod/Sev	RTA	NK	28d	OCP OD	MB
Low	32	F	Mod/Sev	Fall	14	16h	Salbutamol BD	R sylvian fissure SS
Low	21	F	Mod/Sev	Fall	NK	3d	Nil	R temporal contusion and R frontal SS

Low	41	M	Mod/Sev	RTA	NK	7d	Diclofenac 75mg BD and co-dydramol 500mg BD	L frontal contusion
High	18	M	Mod/Sev	Fall	15	<1m	Nil	NAD
High	23	M	Mod/Sev	Assault	15	12d	Nil	Bifrontal contusions, and L hemisphere SS
High	54	M	Mod/Sev	Fall	NK	Nil	Alpha blockers	R fronto-temporal contusions and SS
High	56	M	Mod/Sev	Fall	3	NK	Telmisartan 80mg OD	MB and left frontal SS
High	41	M	Mod/Sev	RTA	6	30d	Nil	MB
High	39	F	Mod/Sev	RTA	6	30d	Nil	MB, pontine and L temporo-occipital SS
High	33	F	Mod/Sev	Fall	NK	NK	Nil	Bifrontal SS
High	33	M	Mod/Sev	RTA	3	42d	Nil	Bifrontal contusions
High	23	M	Probable	Sport injury	NK	30m	Nil	MB
High	53	M	Symp	Fall	15	Nil	Nil	NAD
High	29	F	Mod/Sev	NK	NK	NK	NK	MB, R occipital and temporal contusions, R parietal SS
High	52	M	Mod/Sev	NK	3	NK	Nil	R fronto-temporal contusions, SS and MB

High	34	M	Mod/Sev	Assault	14	42d	Nil	MB, bifrontal contusions, L fronto-temporal contusions, L SDH and SS
High	53	F	Symp	Sport injury	15	Nil	Nil	NAD
High	24	M	Mod/Sev	Assault	NK	2d	Nil	Bifrontal contusions
High	45	M	Mod/Sev	Assault	8	30d	Thiamine 100mg OD	NAD
High	26	M	Mod/Sev	Fall	15	5m	Nil	Bifrontal contusions
High	33	M	Mod/Sev	Assault	NK	12h	Ciprofloxacin 250mg Od	L temporal and R frontal contusions
High	49	M	Mod/Sev	Assault	NK	1d	Nil	Bifronto-temporal contusions and bifrontal SS
High	44	M	Mod/Sev	Fall	9	1d	Nil	MB and L temporal SS
High	25	M	Mod/Sev	Assault	NK	NK	Tramadol QDS, Codeine QDS, and Paracetamol QDS	Bifrontal and R temporal contusions with SS
High	48	M	Probable	RTA	NK	1h	Nil	NAD
High	50	M	Mod/Sev	Fall	NK	2d	Amlodipine 10mg	NAD
High	29	M	Mod/Sev	RTA	NK	2d	Nil	L frontal and bitemporal contusions
High	53	F	Mod/Sev	Sport injury	NK	1.5d	Methotrexate 25md once weekly, Folic acid, Etanercept	MB, bifrontal contusion and pontine SS

High	55	M	Mod/Sev	RTA	3	1d	50 mg once weekly, and Levothyroxine 25mcg OD	MB and R fronto-temporal contusions
High	21	M	Mod/Sev	Sport injury	15	3d	Amitriptyline 20 mg OD, Tramadol QDS, Diclofenac (TDS), and Paracetamol QDS	NAD
High	32	M	Mod/Sev	Fall	NK	7d	Carbamazepine MR 400mg BD	MB and bifrontal contusions
High	37	M	Mod/Sev	Assault	NK	8h	Phenytoin 200/300mg BD, and Levetiracetam 250/500mg BD	MB, bifrontal and bitemporal contusions, and L parietal SS
High	33	M	Probable	RTA	NK	1.5h	Nil	NAD
High	21	M	Mod/Sev	Sport injury	NK	1h	Nil	NAD
High	46	F	Probable	RTA	NK	5m	Gabapentin TDS	NAD
High	35	F	Mod/Sev	RTA	NK	1d	Thyroxine 100mcg OD, and Levothyroxine 50mcg OD	NAD
High	33	M	Mod/Sev	Assault	7	1d	Nil	Bifrontal and R temporal contusion, R temporal and occipital SS
High	22	M	Mod/Sev	Fall	6	16d	Salbutamol BD	R fronto-temporal contusion with SS

High	21	M	Mod/Sev	Assault	3	35d	Nil	MB, L temporal contusion and SS, left frontal SS, and pontine SS
High	49	M	Mod/Sev	RTA	15	7d	Nil	Left temporal contusion
High	47	M	Probable	RTA	NK	1h	Amitriptyline 50mg TDS	L midbrain and pontine SS
High	36	M	Mod/Sev	RTA	3	30d	Citalopram 20mg OD	MB, and R frontal contusion with SS
High	35	M	Mod/Sev	Assault	NK	2d	Nil	MB, R frontal and temporal SS

Severity classification based on MAYO criteria (Malec, Brown et al. 2007). Moderate-Severe (Mod/Sev), Mild/Probable (Mild), Symptomatic/Possible (Symp). Not Know (NK). Road Traffic Accident (RTA), Glasgow Coma Scale (GCS), Post-traumatic amnesia (PTA), days (d), hours (h), minutes (m), Oral Contraceptive pill (OCP), once daily (OD), twice daily (BD), three times daily (TDS), four times daily (QDS). Structural findings on MR imaging: microbleeds on gradient echo imaging (MB), superficial siderosis (SS), no anomalies detected (NAD), right (R), left (L). Performance monitoring (PM) was defined as either Low or High indicating inclusion in the Low and High-PM groups respectively.

6.2.2. Standard clinical imaging

Each patient was assessed using standard T1, T2 and T2-FLAIR MRI, as well as gradient echo imaging to provide improve sensitivity in detecting micro-bleeds, a surrogate marker of DAI (Scheid, Preul et al. 2003). MRI scans were reviewed by a senior neuroradiologist. Abnormalities on initial CT imaging or follow-up MRI were seen in 89% of the patients. Of the fifty-one initial CT reports available: 56% had at least one contusion; 53% had a skull fracture; 33% had a subarachnoid hemorrhage; 25% had a sub-dural hematoma; 24% had an extra-dural hematoma; and, 6% had evidence of cerebral oedema. As expected, many of the patients had multiple clinical findings on the standard clinical MR imaging performed for the study (see Table 6.1 for individual details).

6.2.3. Control groups

Five separate control groups were needed for the different branches of the study (Figure 6.1). One group of controls was used to define the FPCN and Visual network (VN) in an unbiased way (19 subjects, 12 male, mean age 24.5 ± 2.75 years) (see below, Figure 6.1C). A further four groups were used to assess: a) neuropsychological function (25, 11 male, mean age 35.75 ± 11 years); b) SCT behaviour (11 subjects, 4 males, mean age 30.4 ± 7.7 years) (Figure 6.1A); c) Resting-state functional connectivity and DTI analyses (24 subjects, 16 males, mean age 36.2 ± 10.2 years) (Figure 6.1B and 6.1D); and d) SST fMRI (25 subjects, 17 males, mean age 34.8 ± 9.6 years) (Figure 6.1E). Controls subjects had no history of neurological or psychiatric disorders.

6.3. Neuropsychological Assessment

A battery of neuropsychological tests was used to test the type of cognitive dysfunction commonly experience after TBI. This included assessment of premorbid intelligence, current verbal and spatial reasoning, processing speed and verbal fluency (see Chapter 3 for details of the battery). A subset of patients (n=39) also completed the Hospital Anxiety and Depression Scale (HADS) questionnaire assessments. Both patients and their relatives completed the Frontal Systems Behaviour (FrSBe) questionnaire (Grace, Stout et al. 1999). The FrSBe provides a measure of pre-TBI and post-TBI dysexecutive symptoms assessed by the patient and their relative. The disparity between observers' and patients' scores provides a 'meta-cognitive' measure of self-awareness (Reid-Arndt, Nehl et al. 2007), which I compared to the 'on-line' measure derived from the stop-change task (see below).

6.3.1. Methods overview

A high-level description of the methods is provided in Figure 6 1.

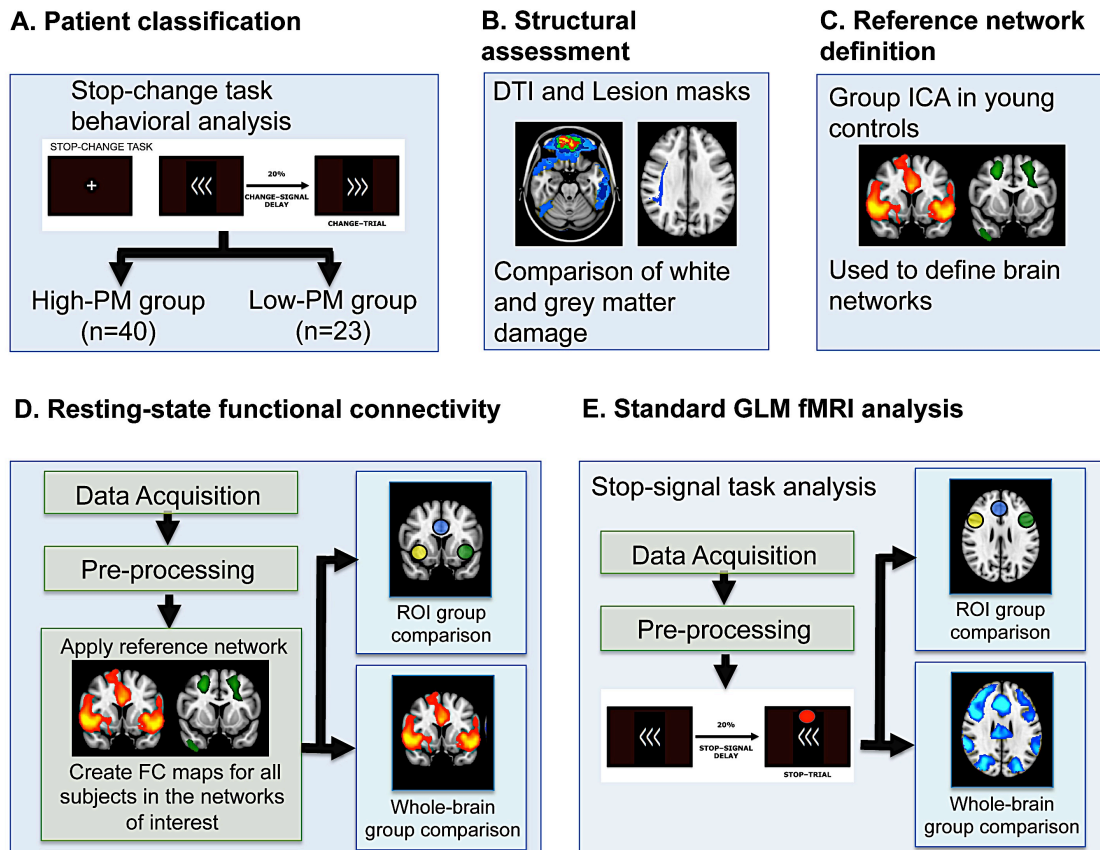


Figure 6.1: Methods overview

A high-level description of the processing steps for behavioural, structural, rest and task functional MRI data analysis. (A) Behaviour on the stop-change task was used to identify patients with High and Low levels of performance monitoring. (B) Traumatic brain injury was assessed structurally by mapping the location of focal injuries using high-resolution T1 MRI, and the location of traumatic axonal injury using diffusion tensor imaging. (C) Reference Fronto-parietal control and Visual networks were defined from a young control group. (D) These networks were used to investigate functional connectivity in 'resting' state fMRI data. (E) Brain activation in response to errors was assessed using fMRI data acquired during performance of the stop-signal task. DTI = Diffusion Tensor Imaging; ICA = independent component analysis; FC = functional connectivity; and, ROI= region of interest.

6.3.2. Behavioural assessment: Stop-change task

Performance monitoring was investigated behaviourally using the stop-change task (SCT), which was performed outside the scanner to define with High-PM and Low-

PM groups (Figure 6.1A). The SCT is a timed choice-reaction task where subjects are presented with an arrow cue that they respond to with either a right or left button press (Bekker, Overtom et al. 2005, Verbruggen and Logan 2008, Verbruggen and Logan 2009). On an unpredictable subset of trials subjects are signalled to withhold their initial response and respond with the alternate button press by a switch in the direction of the arrow (change-trials) (Figure 6.2A). The delay between the initial presentation of the arrow and the change of its direction is adaptively varied using a staircase procedure to produce an error rate of approximately 50% in each subject. If subjects fail to inhibit their initial response they are instructed to correct themselves by subsequently pressing the correct button. For a more detailed discussion of the task see Chapter 3. This correction response provides a rapid on-line performance monitoring measure, as it will only be made if subjects are aware of having made an error. Patients were split into Low-PM and High-PM groups based on the number of errors they corrected on the SCT compared to healthy controls (see results).

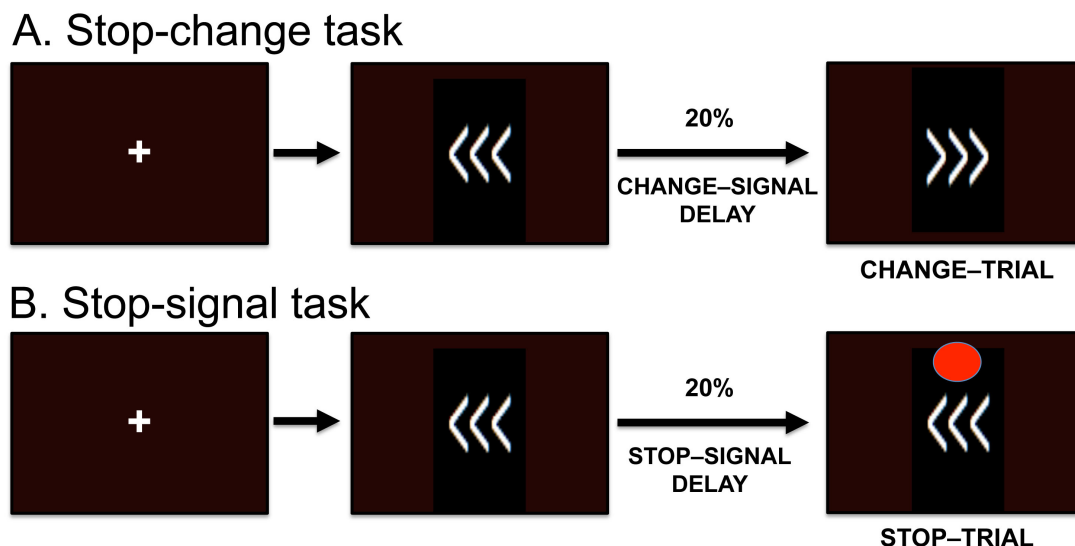


Figure 6.2: SCT and SST paradigms

Schematic representation of the (A) Stop-change task and the (B) Stop-signal task. Both tasks involved the presentation of a fixation cross, followed by arrows pointing to the right or left. Subjects respond to the direction of the arrow with an appropriate finger press. 20% of the SCT trials were “change-trials” where the arrows changed direction after a short delay. Subjects had to respond to the final direction of the arrows. 20% of the SST trials were “stop-trials” where a red dot appeared after a short delay indicating that subjects were to inhibit all responses. The timing of the

Stop and Change cues both varied adaptively to generate an error rate of approximately 50%.

6.3.3. Structural and functional magnetic resonance imaging acquisition

Description of the scanning sessions for TBI patients and controls

TBI patients had two MRI sessions each, a 'structural' and a 'functional' session. The structural session consisted of ten minutes of resting-state fMRI, prior to which subjects were instructed to close their eyes and relax. The resting-state fMRI was followed by T1, T2, T2-FLAIR, T2 FFE and SWI structural imaging, which lasted approximately 20 minutes. The traditional structural imaging was followed by four 16-direction DTI scans, each lasting approximately 5 minutes. The 'functional' session consisted entirely of task fMRI. Prior to scanning all subjects had a practice run of the tasks they would perform in the scanner. During this session subject performed two runs of a simple choice reaction task (data not used in this thesis), followed by two runs of the SST, and two runs of a modified version of the SST (data not used in this thesis). The SST runs were presented in a pseudo-randomized order. One age and sex matched control groups had the same 'functional' session as patient, with the addition of a T1 structural image for registration purposes. A second control group had a variation on the 'structural' session consisting of ten minutes of resting state followed by DTI and T1 imaging.

6.3.4. Clinical imaging

A senior radiologist reviewed all structural MRI scans. Evidence of focal brain injury was assessed on T1 and T2 weighted images. T2-FLAIR and SWI sequences were used to facilitate the detection of micro-bleeds.

Scanner parameters

MRI data were obtained using a Philips (Best, The Netherlands) Intera 3.0 Tesla MRI scanner using Nova Dual gradients, a phased array head coil, and sensitivity encoding (SENSE) with an under-sampling factor of 2.

Structural T1

T1-weighted whole-brain structural images were also obtained in all subjects (78 contiguous slices; slice thickness 2.3 mm; repetition time (TR) = 30 milliseconds; echo time (TE) = 16 milliseconds; field of view (FOV) 220 x 220 x 180 mm, matrix = 192 x 190; flip angle = 12 °; resolution 0.92 x 0.92 x 2.3 mm).

DTI

Diffusion-weighted volumes with gradients applied in 16 non-collinear directions were collected in each of the four DTI runs, resulting in a total of 64 directions. The following parameters were used: 73 contiguous slices, slice thickness = 2 mm, field of view (FOV) 224 mm, matrix 128 x 128 (voxel size = 1.75 x 1.75 x 2 mm³), *b* value = 1000, and four imaging runs with no diffusion weighting (*b* = 0 s/mm²).

FMRI

Functional MRI images were obtained using a T2*-weighted gradient-echo EPI sequence with whole-brain coverage (TR/TE = 2000/30; 31 ascending slices with thickness 3.25 mm, gap 0.75 mm, voxel size 2.19×2.19×4 mm, flip angle 90°, field of view 280×220×123 mm, matrix 112×87). Quadratic shim gradients were used to correct for magnetic field inhomogeneities within the brain.

Stimulus presentation

Paradigms were programmed using Matlab® Psychophysics toolbox (Psychtoolbox-3 www.psychtoolbox.org) and stimuli presented through an IFIS-SA system (In Vivo Corporation). Responses were recorded through a fibre optic response box (Nordicneurolab, Norway), interfaced with the stimulus presentation PC running Matlab.

6.3.5. Functional connectivity analysis of ‘resting’ brain networks

I employed a dual regression, ICA to study functional connectivity in resting-state fMRI (Zuo, Kelly et al. 2010, Leech, Braga et al. 2012) (Figure 6.1C and 6.1D). This provided a voxel-wise measure of functional connectivity that reflects the correlation between the activity of each voxel and the rest of the network being tested. The first analysis step involved the generation of reference brain networks from the based on the resting-state data 19 healthy control subjects who were not included in subsequent analyses. Temporal concatenation ICA was performed on these healthy controls’ resting-state data. The number of components produced by the ICA was constrained to facilitate comparison with previous work (Damoiseaux, Rombouts et al. 2006). This resulted in twenty-five independent group components including 11 well recognized brain networks, as well as physiological noise and movement artefacts (Figure 6.3)(Beckmann, DeLuca et al. 2005, Smith, Fox et al. 2009).

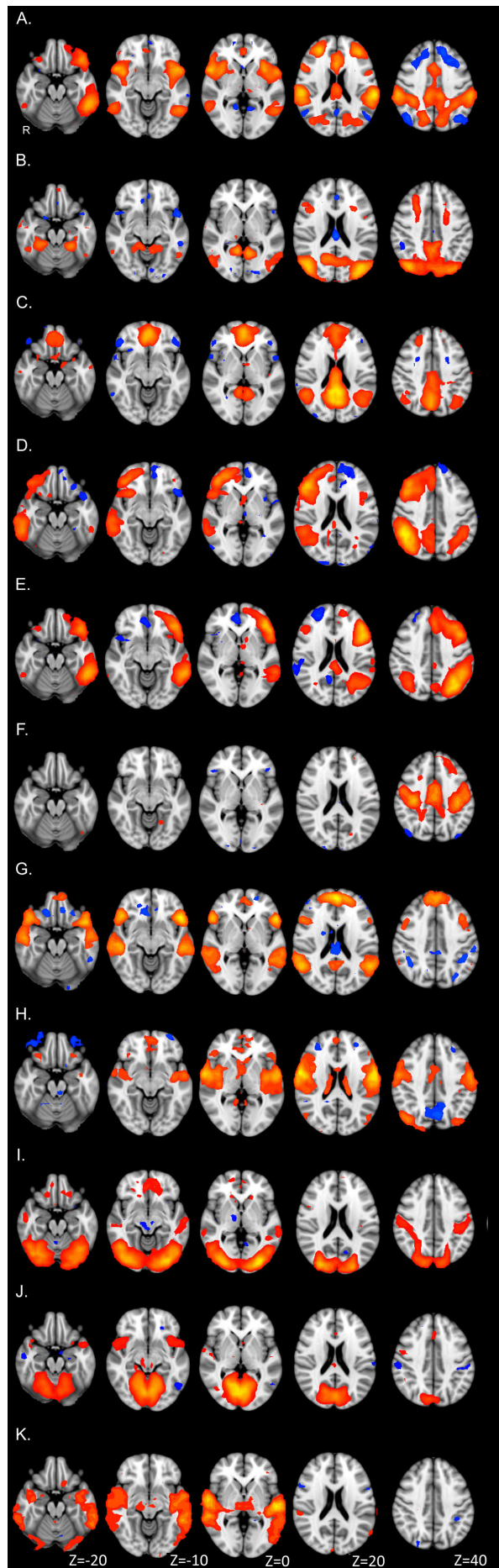


Figure 6.3: ICA results. The eleven established neural networks produced by the ICA analysis of 19 independent healthy volunteers. (A) The Fronto-parietal control network: including the dorsal anterior cingulate, bilateral insulae and adjacent inferior frontal gyri, angular gyri, supramarginal gyri and lateral prefrontal cortices (Vincent, Kahn et al. 2008). (B) The Visual network: this component included dorsal and ventral visual pathways as well as lateral and medial aspects of the occipital lobes. Three visual networks were produced during the analysis but this network explained the highest percentage variance in the fMRI data. (C) The Default mode network: this component included regions in the posterior cingulate cortex, the adjacent precuneus, lateral parietal lobes and ventromedial prefrontal cortex (Raichle, MacLeod et al. 2001). (D) The Ventral attentional network: a right lateralized network including regions in the right insula, the right middle and inferior frontal gyri, right supramarginal and angular gyri (Corbetta and Shulman 2002). (E) The Language network: a left lateralized network including regions in the left insula, the left middle and inferior frontal gyri, right supramarginal and angular gyri (Corbetta and Shulman 2002). (F) The Primary motor network: this component included bilateral motor strips and extending anteriorly into the adjacent supplementary motor area. (G) The Executive control network: this component included the medial superior frontal gyri, bilateral insulae and adjacent inferior frontal gyri, angular gyri, supramarginal gyri and lateral prefrontal cortices (Menon 2011). This network is similar to the fronto-parietal control network but importantly excludes the anterior cingulate. (H) A second motor network: this component included bilateral motor strips and extending anteriorly into the adjacent supplementary motor area. (I) The Medial visual network: this component included the primary visual cortex and a small region of medial ventral prefrontal cortex. (J) A second Medial visual network: this component again included the primary visual cortex along with bilateral insulae and a small region of the dorsal anterior cingulate cortex. (K) The Auditory network: this component included the primary auditory cortex, bilateral insulae and superior temporal gyri. All images are cluster corrected (z -stat >2.3).

Because of its potential involvement in performance monitoring I focused the analysis on the FPCN component, which contained the dACC, RAI, LAI as well as other frontal and parietal regions (Vincent, Kahn et al. 2008, Spreng, Stevens et al. 2010) (Figure 6.4A and table 6.2). In addition, I investigated a Visual Network (VN), where I did not expect to see major functional abnormalities, to demonstrate that any effects were specific to the FPCN. The VN included occipital regions as well as regions within the dorsal and ventral visual pathways in the superior parietal and inferior temporal lobes (Figure 6.4B).

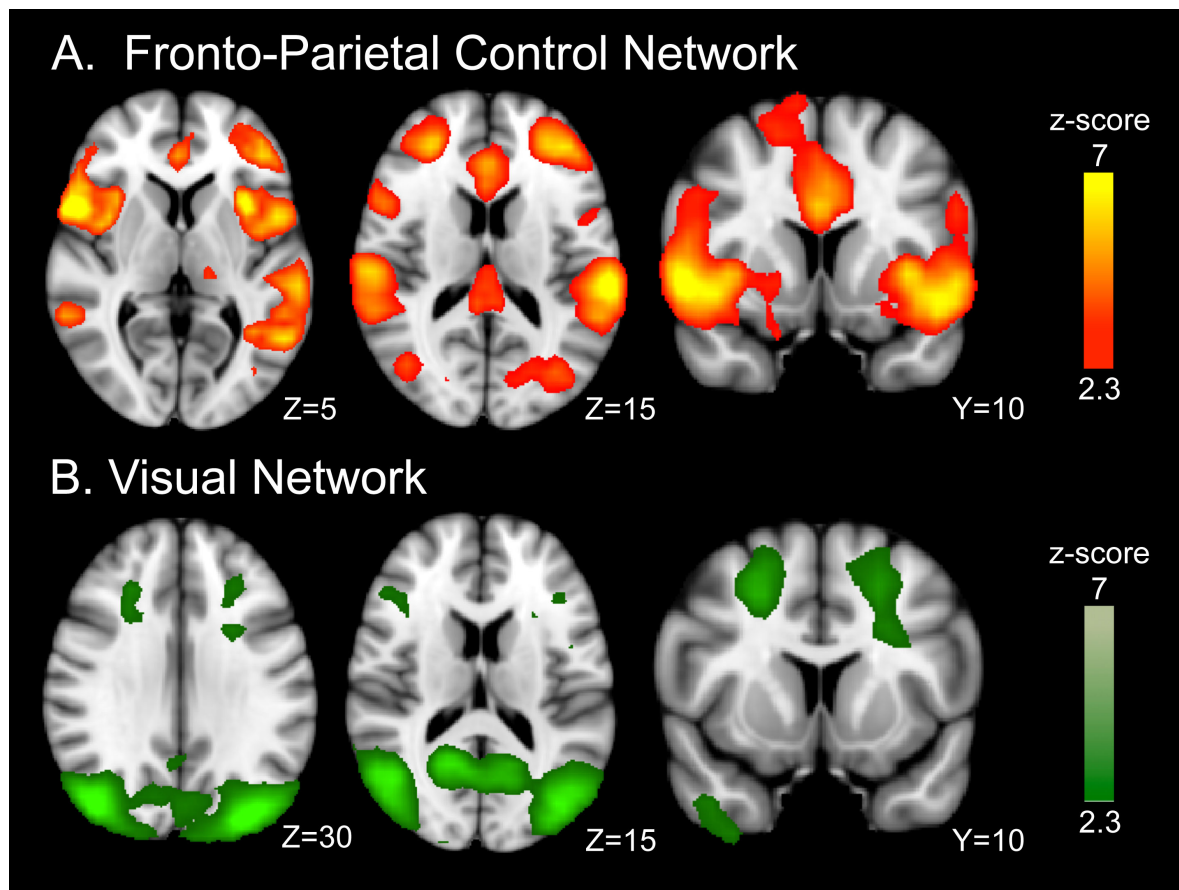


Figure 6.4: ICA networks

References intrinsic connectivity networks extracted from the independent component analysis of young controls: (A) Fronto-Parietal Control Network; and (B) Visual network. Images are thresholded at z-stat (>2.3).

Table 6.2: Peaks of ICA analysis

Intrinsic Connectivity Network	MNI co-ordinates		
	X	Y	Z
Fronto-Parietal Control Network			
Dorsal anterior cingulate cortex	6	34	36
Right Insula	42	10	-4
Left Insula	-42	10	-6
Visual Network			
Right occipital lobe	42	-78	32
Left Occipital lobe	-34	-82	32
Right Precuneus	14	-54	8
Left Precuneus	-10	-58	-8

The co-ordinates represent the peaks of activation from the independently derived ICNs under investigation. The co-ordinates defined the centre of 10mm diameter spheres used in all regions of interest analyses in this study.

Functional connectivity was compared in the two patient groups and a control group as follows: (i) the networks chosen from the ICA were used as weighted seed regions to derive individual time courses for those regions for each subject; and (ii) these subject and network-specific time courses were then re-regressed onto each subject's data resulting in a subject-specific spatial map of functional connectivity (Filippini, MacIntosh et al. 2009). Spatial maps were tested for voxel-wise between-group differences using non-parametric permutation testing (Smith et al., 2004). Voxel-wise estimates of the probability of grey matter membership intensity were included as a covariate to control for the effects of atrophy and cortical damage associated with TBI. To correct for multiple comparisons, results were cluster corrected using threshold free cluster enhancement (TFCE) and a FWE rate of <0.05.

In addition to the voxel-wise analyses, a number of regions of interest were used to probe the relationship between performance monitoring and functional connectivity in theoretically motivated nodes of the FPCN (Figure 6.1D). To avoid bias, I used peaks of the ICA derived networks defined from the young controls. Peaks from the FPCN and VN were used to define the centre of 10mm diameter spherical region of interests (table 6.2). A 10mm diameter ROI was chosen as it was of comparable size to the smoothing kernel used to process the fMRI data. The FPCN was used to define the: dACC; RAI; and, LAI. The VN was used to define regions in bilateral occipital lobe and precuneus.

6.3.6. Stop-signal task

I investigated error processing in patients with high and low performance monitoring abilities in a sub-group of 48 patients using fMRI analysis of the stop-signal task (SST) (thirty-seven males, mean age 35.7 ± 10.9 , range 18-54 years) (Figure 6.1E). The SST allowed me to investigate phasic responses to behaviorally salient events. For methodological reasons I did not use the SCT in the scanner (see Chapter 3). When subjects are aware of an error on the SCT and correct it, they make two motor responses. In contrast, when subjects are unaware of an error they make only one response. The effect of different numbers of motor responses on the FPCN and other networks cannot be easily separated in fMRI studies. Therefore, in the scanner I used a simpler variant of the SCT, the SST (Logan, Cowan et al. 1984, Aron, Fletcher et al. 2003, Sharp, Bonnelle et al. 2010, Bonnelle, Leech et al. 2011) (Figure 6.2B). Like the SCT, an arrow signals the direction of response on go-trials. On an unpredictable sub-set of trials, a stop-signal appears and subjects have to withhold but not change their response (stop-trials) (Figure 6.2B, and Chapter 3 Figure 3.4). Like the SCT the delay between the appearance of the arrow and the stop-signal is

adaptively varied to produce errors on around 50% of the trials. Unlike the SCT, the SST only requires response inhibition, rather than response inhibition and correction.

6.3.7. FMRI analysis of the SST

Standard fMRI analysis was performed using FSL (see Chapter 3 for details). Lesion maps were used to improve brain registration to standard space (Brett, Leff et al. 2001). The following contrast images were generated: incorrect stop-trial vs. go-trials and correct stop-trials vs. go-trials. The two SST runs were first analysed separately and then combined by using fixed effects analysis. Group effects were analysed using FLAME in FSL. Mean changes in activation patterns were then compared between groups. The final statistical images were thresholded by using Gaussian random field-based cluster inference with a height threshold of $Z > 2.3$ and a cluster significance threshold of $p < 0.05$. Individual grey matter density maps were included in the FEAT GLM as a confound regressor (see Chapter 3) (Oakes, Fox et al. 2007).

6.3.8. Structural lesion analysis

We next investigated whether the pattern of focal injury or traumatic axonal injury related to impairment of self-awareness (Figure 6.1B).

6.3.8.1. Focal lesions

Cortical lesions were defined manually on high-resolution T1 images using FSLview. White matter and cortical lesions were registered to a standard MNI 152 T1 1mm template using FLIRT in FSL (Jenkinson and Smith 2001, Jenkinson, Bannister et al. 2002). Lesion overlap images were then created and compared using `fslmaths`.

6.3.8.2. Structural connectivity: DTI

The primary goal of the DTI analysis was to test whether self-awareness problems after TBI were associated with white matter damage within the FPCN. Sixty-four direction DTI data were acquired and standard DTI pre-processing methods were employed using the FMRIB software library (Smith, Jenkinson et al. 2004). I then used probabilistic tractography to create masks of the white matter connecting peak regions within the reference networks. Tracts created within the FPCN connected dACC to RAI and LAI and tracts within the VN connected the right and left precuneus to the respective lateral occipital cortices. By using the white matter skeleton produced by Tract Based Spatial Statistics (Smith, Jenkinson et al. 2006) I constrained the analysis to the central parts of these tracts. It has been shown that this technique more accurately estimates white matter integrity after TBI than alternative approaches (Squarcina, Bertoldo et al. 2012). Using these masks, translated into each subject's brain space, fractional anisotropy (FA) values for each tract of interest and the average FA for whole-brain white matter were determined.

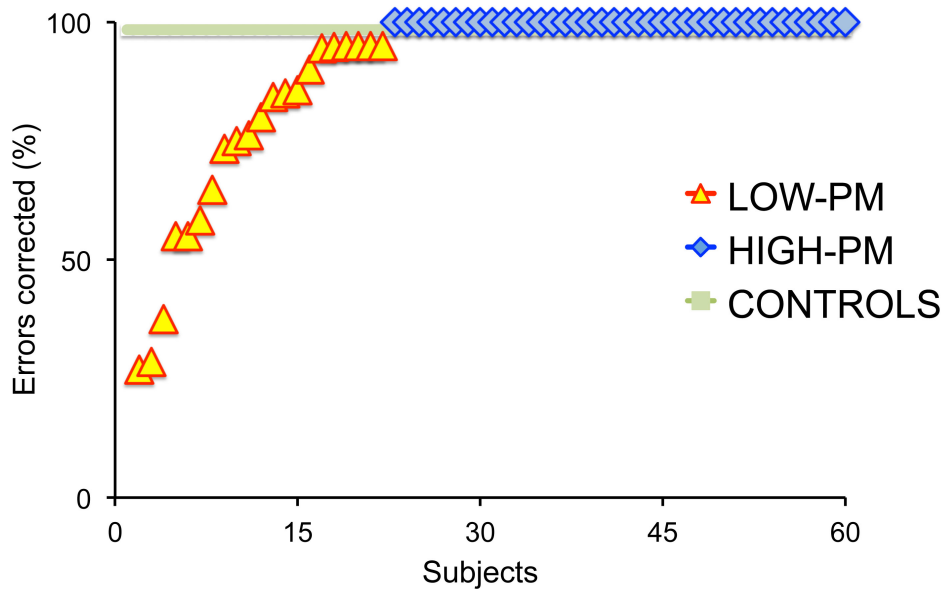
6.4. Behavioural results

6.4.1. Using the SCT to define self-awareness

During the SCT subjects were instructed to correct any perceived errors, providing an explicit measure of 'on-line' performance monitoring. The control group consistently corrected their errors during the SCT ($98.4 \pm 0.96\%$), demonstrating that errors on this task are usually easily identified and corrected. In contrast, TBI patients were highly variable in the proportion of errors they corrected. Most patients ($n=40$) had a similar range to controls for error correction (<2 standard deviations from the mean of the control group). These patients formed the High-PM group. In contrast, a significant minority of patients ($n=23$) performed outside this range,

correcting significantly fewer errors than controls ($68.8 \pm 5.6\%$). These patients formed the Low-PM group (Figure 6.5A).

A. Error correction during the stop-change task



B. Frontal systems behavior scale (FrSBe) scores

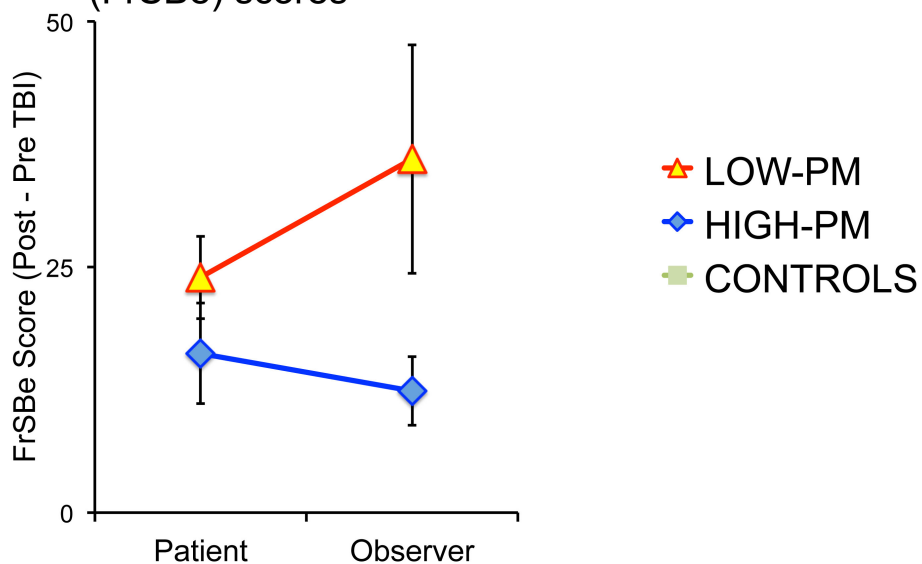


Figure 6.5: Behavioural performance on the SCT and FrSBe questionnaire
Impairments of self-awareness demonstrated by abnormal performance monitoring and meta-cognitive self-assessment. (A) The percentage of stop-change task errors corrected by individuals in the Control (green), High-PM (blue) and Low-PM (yellow) groups. (B) Changes in Frontal Systems Behavioural (FrSBe) Score after traumatic brain injury in High and Low-PMs, as assessed by the subjects themselves and an observer who knew the patient well. Error bars indicate standard error of the mean.

Low-PMs showed abnormal performance on other aspects of the SCT in addition to the number of errors they corrected. The time taken for the Low-PMs to correct an error was significantly slower than High-PMs (420 vs. 278 milliseconds, ($t=5.73$, $df=61$, $p<0.001$)) and controls (420 vs. 250 milliseconds, $t=4.30$, $df=32$, $p<0.001$); as was the reaction time on go-trials compared to High-PMs (533 vs. 387 milliseconds, ($t=6.34$, $df=61$, $p<0.001$)) and controls (533 vs. 400 milliseconds, $t=3.47$, $df=31$, $p=0.002$). Intra-individual variability of reaction times on go-trials was also significantly greater in Low-PMs than High-PMs (0.227 vs. 0.174, ($t=4.33$, $df=61$, $p<0.001$)) and controls (0.227 vs. 0.155, $t=3.78$, $df=32$, $p=0.001$). In contrast, the High-PM group did not differ significantly from healthy controls in any of these measures. These results are consistent with impaired performance monitoring being part of a more general attentional deficit in the Low-PM group.

Table 6.3:

Group performance on the stop-change task			
	Controls	High-PM	Low-PM
Mean go-trial reaction time	400 msecs	387 msecs	533msecs */**
IIV of go-trial reaction time	0.155	0.174	0.227 */**
Mean error correction time	250 msecs	278 msecs	420 msecs */**
Post-error slowing	50 msecs	39 msecs	87 msecs *

‘’ signifies significant difference from Controls and ‘**’ signifies significant differences from the High-PM patient group.*

In many other ways, the High and Low-PM groups were similar. The groups performed equally well on tests of memory, verbal and non-verbal reasoning In

addition, both patient groups had similar scores on the HADS questionnaire assessment of anxiety and depression. There was also no significant difference between the two groups in: a) age, (Low-PM 39.4 ± 12.8 years (range 20-67 years) vs. High-PM 37.3 ± 11.6 years (range 18-56 years)); b) time since injury (Low-PM 46.9 ± 115.3 months (range 2-563 months) vs. High-PM 19.7 ± 30.1 months (range 2-168 months)); or c) injury severity (Low-PM 100% severe vs. High-PM 82.5% severe). There were significantly more men in the High-PM group than the Low-PM group (59% vs. 82%, $\chi^2 = 5.0$, $df=1$, $p = 0.025$) (table 6.1). The subgroup of patients ($n=48$) who had fMRI consisted of Low-PM ($n=18$) and High-PM patients ($n=30$). These groups were also matched for age, gender, time since injury, and injury severity.

6.4.2. Post-error slowing on the SCT

Importantly, compared to the High-PM group, the Low-PM group did not show post-error slowing on the trial after errors they failed to immediately correct. This supports the inference that patients in the Low-PM group were unaware of their uncorrected errors. Conversely, compared to the High-PM group they showed greater post error slowing after the errors they did correct (87 vs. 39 milliseconds, ($t=2.94$, $df=59$, $p=0.005$)), and compared to controls there was also a trend towards greater post-error slowing after corrected errors (87 vs. 50 milliseconds, ($t=1.79$, $df=29.7$, $p=0.084$)). The increase in post-error slowing after corrected errors indicates that the group was engaged in the task, and that they were able to appropriately adapt to errors if they were initially recognized.

On more general neuropsychometric testing, the Low-PM group also performed more poorly than the High-PM group and controls on several tasks of processing speed and executive function (table 6.4).

Table 6.4. Neuropsychometric testing

	Healthy Controls (mean ± SD)	Low-PM group (mean ± SD)	High-PM group (mean ± SD)
Executive function			
Stroop inhibition	21.63 ± 4.66	65.68 ± 24.37 */**	51.65 ± 16.2 **
Stroop inhibition switching	47.25 ± 11.51	75.41 ± 26.55 */**	62.78 ± 20.39
Trail Making B – Trail Making A (s)	25.25 ± 15.36	45.60 ± 31.75	31.26 ± 26.25
Processing Speed			
Stroop Colour naming & word reading	24.25 ± 3.22	31.57 ± 6.14 */**	27.93 ± 6.39
Trail Making A (s)	19.88 ± 3.27	29.17 ± 10.66 **	25.54 ± 9.69
Trail Making B (s)	45.13 ± 15.37	74.77 ± 37.31 */**	56.79 ± 31.81
Verbal fluency, letter fluency	49.00 ± 13.11	36.23 ± 13.67	42.62 ± 12.63
Verbal and Non-verbal reasoning			
WTAR scaled	113.88 ± 9.09	95.55 ± 39.67	95.14 ± 38.99
WASI - Similarities	36.13 ± 6.06	37.27 ± 3.76	37.86 ± 5.06

WASI - Matrix reasoning	26.38 ± 3.11	26.68 ± 3.43	26.30 ± 8.62
Memory			
Digit span total	17.25 ± 3.33	17.64 ± 4.01	17.84 ± 4.18
People test from DAP – Immediate	27.00 ± 4.17	24.14 ± 5.53	24.81 ± 6.31
People test from DAP – Delayed	8.13 ± 3.14	8.95 ± 2.90	9.16 ± 3.09
Logical memory I – first recall total	27.38 ± 8.78	26.64 ± 5.98	26.32 ± 8.11
Logical memory I – recall total	45.50 ± 12.74	43.86 ± 8.21	42.78 ± 11.73
Logical memory II – recall total	26.38 ± 7.69	28.14 ± 6.88	29.11 ± 7.65
Psychiatric symptoms			
HADS – anxiety score		8.45 ± 3.78	7.36 ± 4.62
HADS – depression score		5.41 ± 4.69	4.76 ± 4.85

***' signifies significant difference from another patient group (p<0.05); and, '**' signifies significant difference from healthy controls (p<0.05). Healthy controls did not complete the Hospital Anxiety and Depression Scales (HADS). Subjects completed neuropsychometric tests of a range of domains of cognition including: Wechsler's Test of adult reading (WTAR); Wechsler's Abbreviated Test of Intelligence (WASI); and, Doors and People (DAP) test of memory. Details of the other assessments are outlined in the methods section.*

6.4.3. Impaired error processing is a marker of more general self-awareness problems

The FrSBe provided additional evidence that the Low-PM group had a general impairment of self-awareness (Figure 6.5B). Both patient groups reported similar levels of disability on the FrSBe. However, the carers of the Low-PM group made more severe assessments of severity than the carers of High-PM patients ($p=0.01$), providing evidence for a general impairment of self-awareness in the Low-PM group.

6.5. Neuroimaging results: Resting state analyses

6.5.1. Impaired performance monitoring is associated with abnormal function within the FPCN

At rest Low-PM patients showed reduced functional connectivity within the FPCN, compared to both the High-PM patients and controls. Whole-brain analysis comparing patient groups showed the dACC, right IFG, and right MFG were significantly less functionally connected to the rest of the FPCN in the Low-PM group (Figure 6.6A and table 6.5). A targeted region of interest analysis also assessed the main nodes of the FPCN and VN. This revealed that Low-PM patients also showed reduced dACC functional connectivity compared to controls ($t=-2.3$, $df=45$, $p<0.028$), although this result was not significant on whole-brain analysis (Figure 6.6B). In contrast, no other nodes within the FPCN showed reduced functional connectivity in Low-PM patients, and there were no abnormalities in the functional connectivity of the VN either on whole-brain or region of interest analysis (Figure 6.6C).

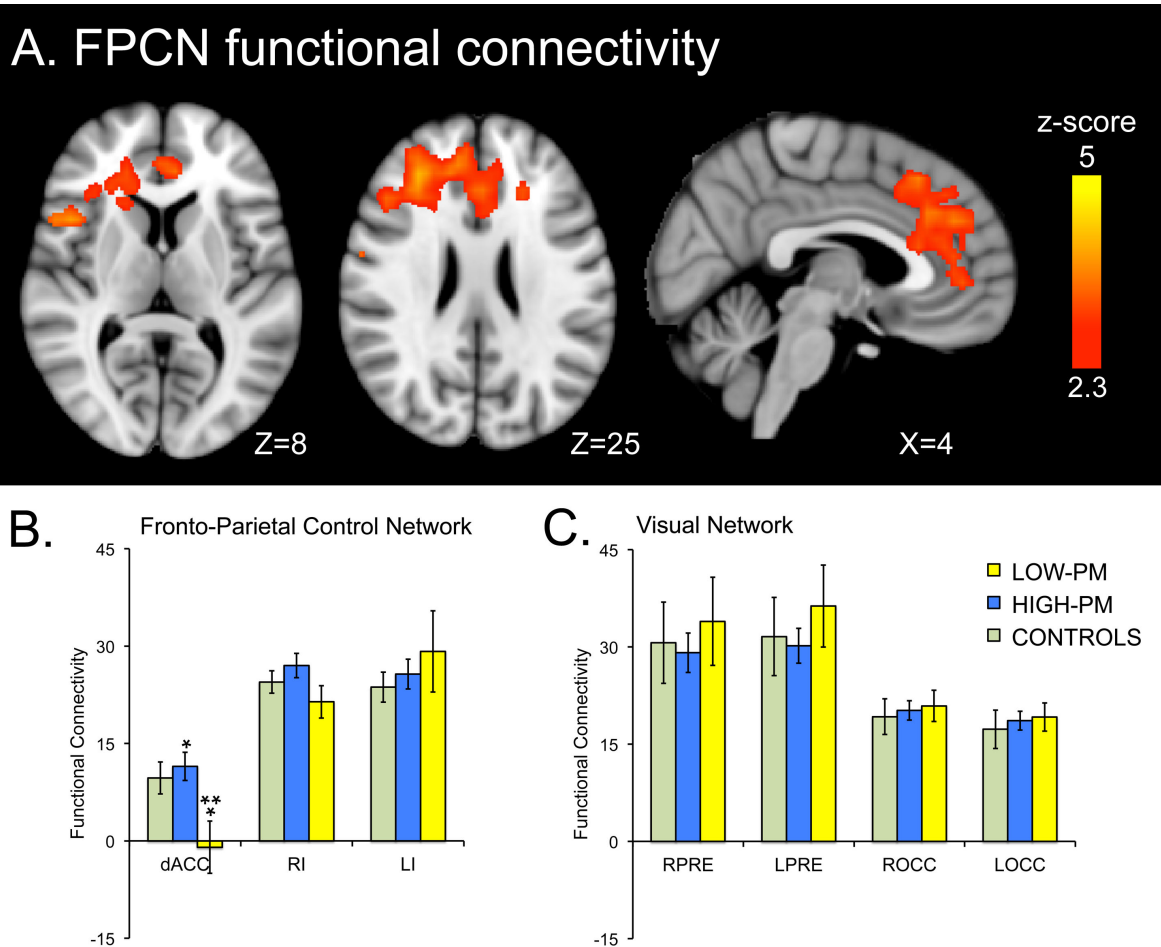


Figure 6.6: Functional connectivity in the fronto-parietal control network
 Impaired performance monitoring is associated with reduced functional connectivity of the dorsal anterior cingulate cortex at rest. (A) Comparison of the functional connectivity within the FPCN of the High-PM and Low-PM groups. The image was thresholded using threshold free cluster enhancement (TFCE) (FWE correction <0.05). (B-C) Region interest analyses comparing the functional connectivity of key regions within the FPCN (B), and control Visual network (C) across the three subject groups. “*” signifies a significant difference between the High and Low-PM groups ($p < 0.05$). “***” signifies a significant difference between Low-PM and healthy controls ($p < 0.05$). Error bars indicate standard error of the mean. Region of interest were the dorsal anterior cingulate cortex (dACC), right insula (RI), left insula (LI), left precuneus (LPRE), right precuneus (RPRES), left occipital lobe (LOCC) and right occipital lobe (ROCC).

Table 6.5:

	Peak z-score	MNI co-ordinates		
		X	Y	Z
Fronto-Parietal Control Network resting state functional connectivity:				
<i>High-SA > Low-SA groups</i>				
Dorsal anterior cingulate cortex	3.81	1	38	32
Right inferior frontal gyrus	3.90	46	14	8
Right middle frontal gyrus	4.04	30	33	27

6.6. Neuroimaging results: SST event-related fMRI analysis

6.6.1. SST behavioural results

Overall, the groups performed the tasks well. Low and High-PMs were equally accurate on stop (49.8% vs. 52.0%) and go-trials (97.8% vs. 96.7%), and these accuracies were not significantly different to controls. Similar to their performances on the SCT, the Low-PM group was slower (624 vs. 460 milliseconds, ($t=4.37$, $df=46$, $p<0.001$)), and showed greater intra-individual variability on go-trials compared to the High-PM group (0.210 vs. 0.174, ($t=2.58$, $df=46$, $p=0.013$)) and controls (0.210 vs. 0.170, ($t=3.51$, $df=40$, $p=0.001$)). Interestingly, Low-PMs showed greater post-error slowing following errors on the SST than both High-PMs (79 vs. 23 milliseconds, ($t=4.13$, $df=46$, $p<0.001$)) and controls (79 vs. 29 milliseconds, ($t=3.47$, $df=40$, $p=0.001$)). This was similar to the enhanced post-error slowing observed after corrected errors in the SCT, and suggests that Low-PMs were aware of at least a proportion of these errors.

6.6.2. All groups activated a similar distribution of cortical regions within the FPCN in response to errors

The direct contrast between neural activity on incorrect stop-trials and go-trials allows an investigation of the neural correlates of error processing. As expected, errors were associated with activation in a network of regions including the dACC, bilateral insulae, the frontal poles, lateral pre-frontal cortex, and SMG in all groups (Figure 6.7).

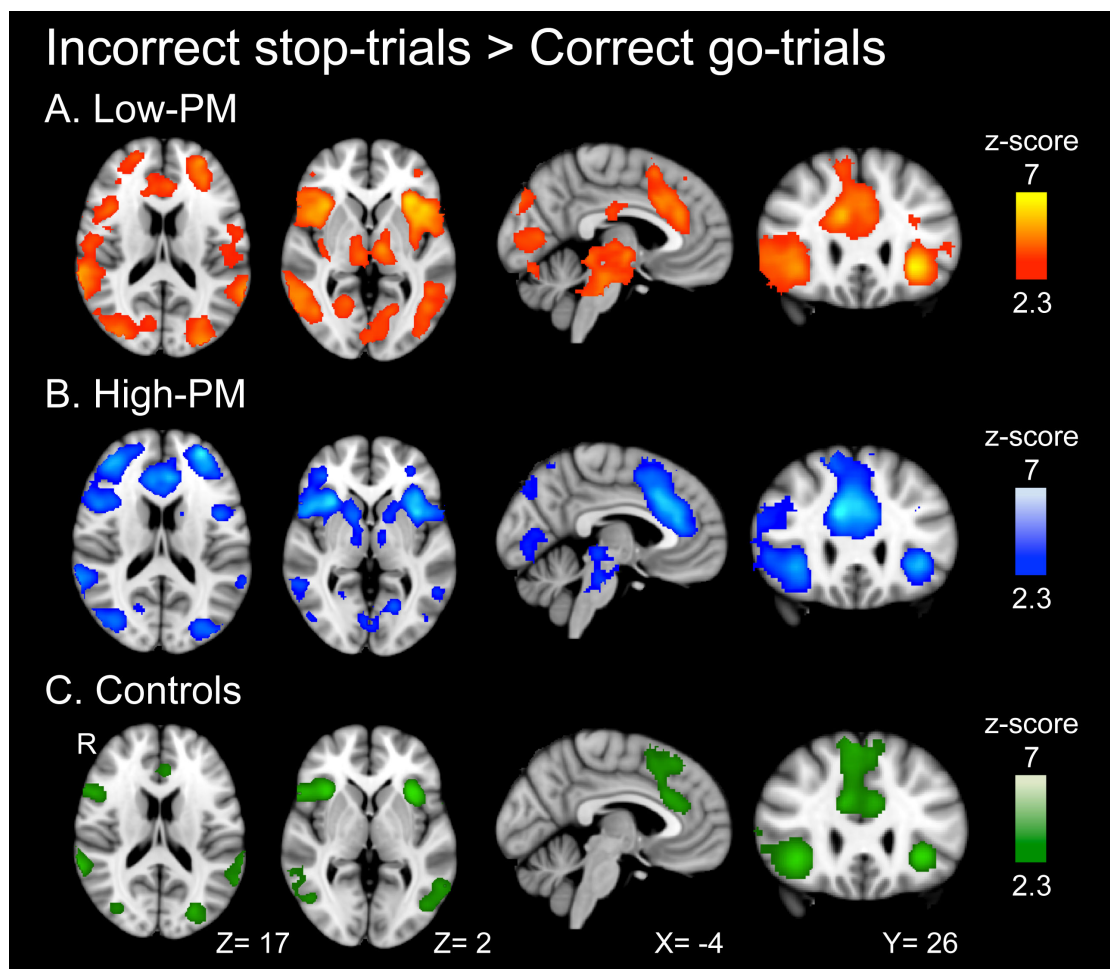


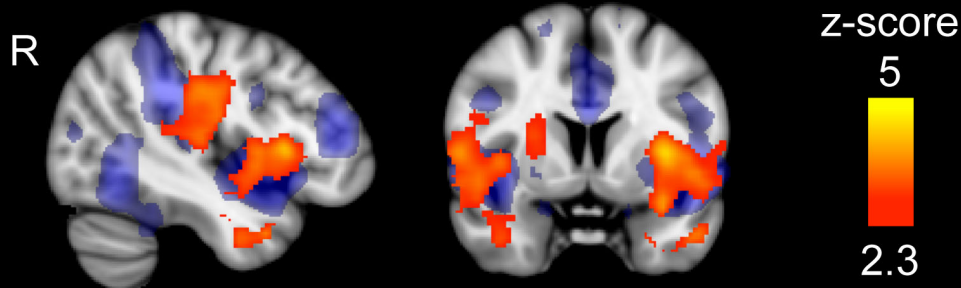
Figure 6.7: Group activation after inhibition errors
Brain activation after errors on the SST (incorrect stop-trials vs. correct Go-trials) in the Low-SA group (A) (red-yellow); High-SA group (B) (blue-light blue); and controls (C) (green-light green). Images are cluster corrected ($z\text{-stat} > 2.3$).

6.6.3. Impaired performance monitoring is associated with increased activation in the insulae following errors

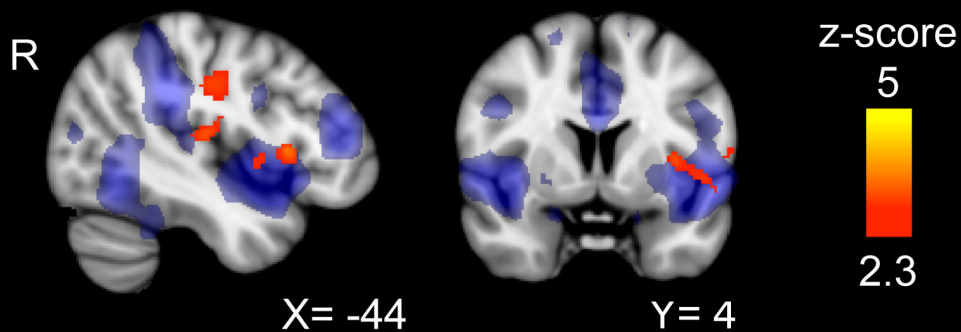
Whole-brain analysis revealed that the Low-PM group showed greater activation of the bilateral insulae and parietal operculum in response to errors than controls (Figure 6.8A and table 6.6). A similar effect was seen when comparing Low and High-PM groups, although the increases in insula and parietal operculum activation were lateralized to the left hemisphere (Figure 6.8B and table 6.6). These abnormal activity patterns overlapped with the FPCN defined from analysis of 'resting' fMRI (blue background in Figure 6.8). Dorsal ACC activation after errors was similar across the groups. No brain regions showed increased activity in the High-PM or control groups compared to Low-PM group following errors. In contrast, the High-PM group showed greater activation than controls in the right MFG and bilateral putamen and the left caudate nucleus after errors, which again partly overlapped with the FPCN (Figure 6.8C and table 6.6)

Incorrect stop-trial > Correct go-trials

A. Low-PM > Controls



B. Low-PM > High-PM



C. High-PM > Controls

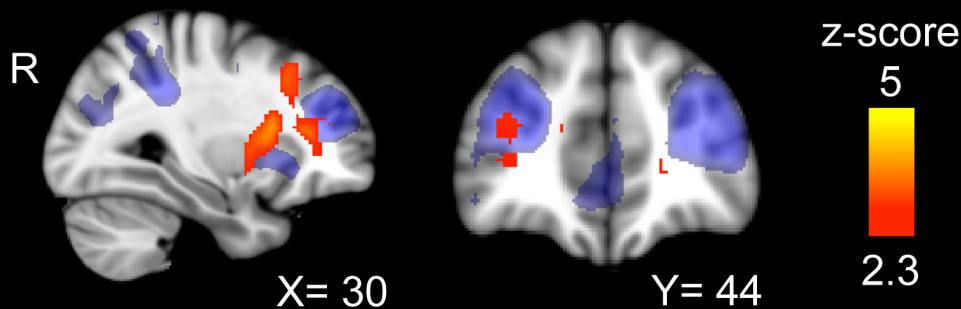


Figure 6.8: Group differences in activation after inhibition errors: Abnormal error-related activity in the FPCN in TBI patients. Group contrasts of brain activation after inhibition errors on the SST (incorrect stop-trials vs. correct go-trials). The figures are comparisons between: (A) Low-PM patients greater than controls; (B) Low-PM greater than High-PM patients. and (C) High-PM patients greater than controls. Areas with greater activation are shown red-yellow. All contrasts are superimposed on an image of the FPCN (blue) for reference. Images are cluster corrected ($z\text{-stat} > 2.3$).

Table 6.6: Group contrasts of activation in response to errors on the SST

Contrast	Peak z-score	MNI co-ordinates		
		X	Y	Z
SST activation: Incorrect Stops-trials > Correct Go-trials				
<i>Low-SA > Control group</i>				
Right post-central gyrus	4.00	62	-6	26
Right parietal operculum	4.81	60	-4	6
Right insula	3.33	46	6	-2
Left insula	4.74	-34	2	6
Left Inferior frontal gyrus	4.30	-46	16	6
Left post-central gyrus	3.85	-60	-10	32
<i>Low-SA > High-SA group</i>				
Left post-central gyrus	4.00	-36	-18	40
Left insula	3.54	-44	16	6
Left parietal operculum	3.33	-46	-16	14
<i>High-SA > Control group</i>				
Left caudate nucleus	4.28	-14	6	14
Left putamen	3.20	-28	0	10
Right putamen	3.85	26	8	10
Right middle frontal gyrus	3.35	28	24	42

6.6.4. Successful response inhibition is associated with similar brain activity, regardless of the level of performance monitoring

The neural correlates of successful response inhibition, rather than error processing, were studied by comparing correct stop-trials with go-trials. High and Low-PM groups both showed increased activity in the PCC/precuneus when compared to controls. However, there was no significant difference in activity between patient groups. Similarly, a whole-brain analysis comparing go-trials to rest-trials revealed a predictable pattern of brain activation within bilateral sensory, motor, and superior parietal regions, as well as in the supplementary motor area, occipital regions, and the putamen. Task related activation was similar for both patient groups and controls, no differences were seen on whole-brain statistical comparison between the groups, suggesting an absence of general, non-specific changes in brain physiology following TBI.

6.7 Structural imaging results

6.7.1. Lesion location and extent does not relate to performance monitoring deficits

There was no obvious relationship between the location or extent of focal injuries and performance monitoring ability. There were very few locations where more than two patients in either group had common focal lesions (Figure 6.9). This meant a formal statistical analysis of the relationship between lesion location and the likelihood of impaired performance monitoring was not possible. In the High-PM group the greatest overlap was an area of less than 1cm^3 (964mm^3), centered in the orbitofrontal cortex (peak -2,-54,-26), where 12.5% (5/40) of the subjects shared a lesion. In the Low-PM group the greatest overlap was an area approximately 3cm^3 (3005mm^3), centered in the right inferior temporal gyrus (peak 52,-59,-4), where

8.7% (2/23) of the subjects shared a lesion. There was no difference in lesion volume between the groups (Low-PM 12,960mm³ vs. High-PM 19,634mm³ (p=0.67)). I also used DTI measures of white matter integrity to investigate whether the FA of tracts connecting key regions of the FPCN and VN were different across the two groups (i.e. dACC to left and right insula, and bilateral precuneus to occipital cortex). In both patient groups, all tracts showed significantly greater white matter damage than controls. However, no tracts showed significantly different FA values between High and Low-PM groups.

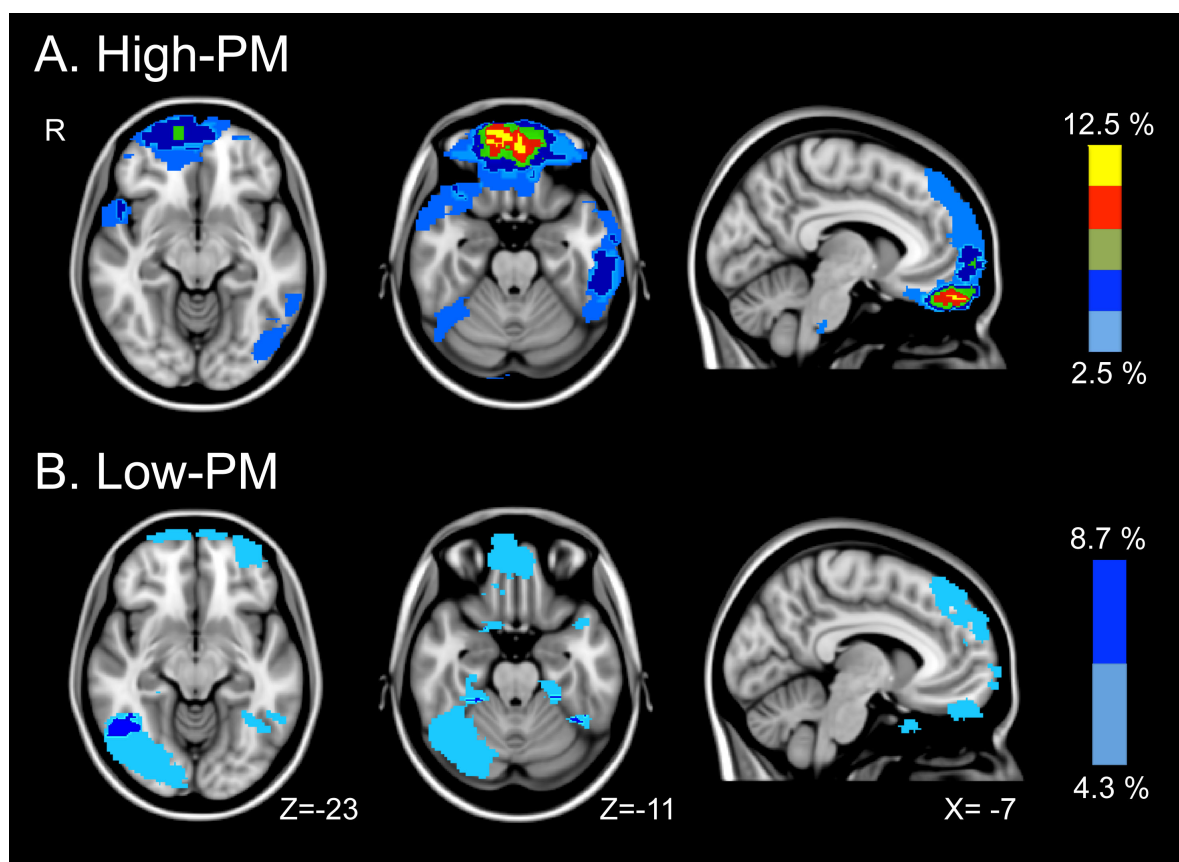


Figure 6.9: Lesion analysis of TBI groups

Manually defined lesion overlap maps for High-PM subjects (A), and Low-PM subjects (B).

7.7. Discussion

6.7.1. Results summary

The neural basis for awareness has been unclear. Impairments of awareness are common after TBI, and here I show evidence that low self-awareness is associated with dysfunction within the FPCN. Awareness is likely to be an emergent property of interactions within large-scale distributed brain networks. In keeping with this hypothesis, I found that patients with impaired self-awareness showed reduced functional connectivity from the dACC and other frontal regions to the rest of the FPCN. This change was accompanied by an abnormal response to errors within the insulae, which are normally tightly linked to the dACC. These results are in keeping with the proposal that the insulae and dACC are key structures in supporting the internal monitoring important for self-awareness.

6.7.2. Role of the salience network in self-awareness

The functional abnormalities observed within the insulae and dACC suggest that self-awareness may be particularly dependent on a sub-network within the FPCN, the SN. My first two studies and a large body of literature supports an important role for the SN in performance monitoring (Oliveira, McDonald et al. 2007), error detection (Falkenstein, Hoormann et al. 2000, Holroyd, Nieuwenhuis et al. 2004, Ullsperger, Harsay et al. 2010), self-reflection (Johnson, Baxter et al. 2002), and feedback evaluation (Walton, Croxson et al. 2007). Interestingly, the insulae and dACC contain an unusual class of cells, von Economo neurons, found in humans and other great apes (Allman, Tetreault et al. 2010). These are large projection neurons, which may be specialized for rapid signalling of internal states required for efficient performance monitoring (Allman, Tetreault et al. 2011). Behaviourally salient events usually enter conscious awareness, and it has been proposed that the activity of the anterior

insulae and its connections to the dACC provide a neural substrate for awareness (Craig 2009). My results are broadly in keeping with this suggestion. The 'baseline' reduction in functional connectivity indicates that nodes of FPCN are less tightly coupled in Low-PM patients. In particular the dACC is less coupled to other parts of the network including the insulae. This is accompanied by a phasic abnormality in the way the insulae respond to errors, suggesting that baseline changes in the functional organization of the FPCN affects the insulae response to the behaviourally salient events that would normally enter consciousness.

6.7.3. Abnormal activation pattern in the salience network may reflect network inefficiency

Behaviourally important events normally trigger a tightly coupled functional response within the SN, and the right anterior insulae appears to provide the networks driving input (results described in Chapter 5, (Sridharan, Levitin et al. 2008, Menon and Uddin 2010)). Actions always occur in the context of background brain activity, and in other contexts these background fluctuations have been shown to influence behavioural responses and associated brain activity (Fox, Snyder et al. 2006, Sharp, Beckmann et al. 2011), as well as to bias perceptual processing (Boly, Balteau et al. 2007, Hesselmann, Kell et al. 2008). Therefore, it is not unexpected that abnormalities in the 'baseline' functional connectivity of one node of the FPCN or SN might be associated with phasic abnormalities within another part of those networks. In other contexts increased event-related fMRI responses have been related to impaired or inefficient neural processing (Baltes 1993, Cabeza, Anderson et al. 2002, Ward, Newton et al. 2006). In the case of the insulae's enhanced response to errors, disruption to the normal tight functional coupling within the SN may reflect this neural inefficiency.

6.7.4. Benefits and limitations of using the SST instead of SCT in event-related fMRI analysis

An important caveat in interpreting the event-related analysis of error processing is that it is unclear whether subjects were aware of their errors on the SST. The SCT was used to behaviourally define the patient groups because error correction on this task provides an explicit indication of awareness. However, for methodological reasons I used the SST, which is a simpler version of the SCT, in the neuroimaging part of the study. The SST does not involve an explicit correction of errors, but has the advantage that it provides a measure of performance monitoring not complicated by the initiation and execution of a second motor response. An indication that Low-PM patients were aware of at least a proportion of the errors on the SST is provided by the post-error slowing data. When errors on the SCT were not rapidly corrected there was no significant post-error slowing, supporting the inference that the subjects were not aware of these errors. In contrast, when SCT errors were rapidly corrected, there was abnormally large post-error slowing. This demonstrates that subjects were capable of making adjustments to their behaviour, and that subjects were generally engaged by the task. During the SST post-error slowing was increased overall. This suggests that subjects were aware of at least a proportion of the errors they made. Therefore, it is likely that increased insulae activity in response to errors in the Low-PM group is related to inefficient processing of errors that, at least in some cases, reach conscious awareness.

6.7.5. Compensatory activation of the right MFG seen in High-PM patients

In patients with preserved performance monitoring (High-PMs) I also observed abnormally high activity in the right MFG following errors. A recent study has proposed that the right MFG represents an amodal centre for co-ordinating 'top-down' attention (Braga, Wilson et al. 2013). This enhanced activation may represent

a 'top-down' attentional compensation that the Low-PM patients might be unable to engage. In the context of spatial neglect patients, the deficit can be overcome, at least temporarily, by both externally (Robertson, Mattingley et al. 1998) and internally signalled changes in attention (Soto, Funes et al. 2009). The increased activity observed in the FPCN may be the neurological correlate of this top-down attentional drive in the High-PM group. In the Low-PM group, prolonged reaction times and increased behavioural variability indicate broad attentional problems in addition to impaired performance monitoring. These general problems with engaging or maintaining attention may interact with more specific problems with performance monitoring to produce the behavioural deficits observed.

6.7.6. Low-PM patients showed altered self-awareness on metacognitive testing

Patient groups were defined on their ability to rapidly correct errors. Although this measures one facet of self-awareness, importantly Low-PM patients also showed 'meta-cognitive' measures of impaired awareness. As discussed in Chapter 2, self-awareness can be quantified in a number of ways (Fleming, Strong et al. 1996, O'Keeffe, Dockree et al. 2007) and I used two methods in this study, questionnaires (FrSBe) and the on-line performance monitoring metric from the SCT. Questionnaires have been widely used to identify discrepancies between assessments of disability made by the patient and others, providing a 'meta-cognitive' measure of self-awareness (O'Keeffe, Dockree et al. 2007). Whilst useful, this type of assessment is limited by its subjective nature and the inconsistency of observer evaluations (Fleming, Strong et al. 1996). I used an 'on-line' measure of performance monitoring as the primary objective measure self-awareness (Hart, Giovannetti et al. 1998, O'Keeffe, Dockree et al. 2004). On-line measures of this type have previously been shown to variably relate to other measures of self-awareness

(Hart, Giovannetti et al. 1998, O'Keeffe, Dockree et al. 2004, O'Keeffe, Dockree et al. 2007). In this study, Low-PM patients also showed evidence of 'metacognitive' impairments of awareness, which impacted on their behaviour. This provided further validation for the use of performance monitoring as a surrogate marker of self-awareness.

6.7.7. Self-awareness deficits not predicted by lesion load, location or DTI metrics

The large functional differences between patient groups were not the result of differences in the amount of structural brain injury. I did not find a clear relationship between impaired performance monitoring and either patterns of focal brain damage or more diffuse white matter injury. Damage to the white matter tracts was assessed using DTI. As expected, the TBI patients showed evidence of diffuse axonal injury, but contrary to my predictions this did not explain the performance monitoring impairment. In particular, there was no relationship between the functional connectivity between FPCN nodes and structural damage to the white matter tracts connecting these nodes. It has previously been shown that damage to the tract connecting the RAI to the dACC/pre-SMA is associated with attentional impairment (Bonnelle, Ham et al. 2012) but in the case of performance monitoring I did not observe any significant relationships. This could be because the techniques I used are not sensitive enough to identify subtle damage to these tracts, or perhaps because impairments of self-awareness emerge in a complex way from the interactions of multiple brain networks and reflect the integrity of a large number of white matter tracts (Thompson and Varela 2001). Multivariate approaches to analysing traumatic axonal injury may be well suited to identifying these complex relationships (Hellyer, Leech et al. 2012). Future work could employ such techniques

to investigate the possibly subtle patterns of structural damage that may underlie the functional network abnormalities I have observed.

6.7.8. Limitations

There are some potential limitations to this study. Firstly, some of the TBI patients had focal cortical lesions that might have affected the registration process required to compare across individuals. However, this is unlikely to have produced major errors in the analysis. In general, patients did not have large lesions and the results of registration were checked carefully, resulting in the exclusion of two subjects. In addition, masks of the lesion location were used to improve registration (Brett, Leff et al. 2001). Lesion masks and measures of grey matter density were used as covariates in the fMRI analyses. A second potential limitation is that I focused the 'resting-state' and DTI analyses on the connections of the FPCN, using the VN as a control. This choice was motivated by large amounts of literature, suggesting that the dACC and anterior insulae are critical for performance monitoring (Carter, Braver et al. 1998, Botvinick, Cohen et al. 2004, Kerns, Cohen et al. 2004, di Pellegrino, Ciaramelli et al. 2007). In keeping with a key role for these regions in performance monitoring, the event-related analysis of error response, which was not constrained to the FPCN, also showed abnormalities within the anterior insulae. It is possible that impaired performance monitoring after TBI is associated with abnormalities in other brain networks or tract connections, and future studies will need to address this issue. The VAN may be of particular interest in future analysis given the results of Chapter 4.

6.7.9. Conclusion

In summary, I used detailed behavioural assessment and multi-modal neuroimaging to investigate the neural basis of impaired self-awareness after TBI. Functional abnormality with the FPCN was associated with impaired performance monitoring. This finding is consistent with the principle that awareness is an emergent property of multiple brain regions, and that intact connectivity of the dACC and anterior insulae are necessary for rapid error processing.

Chapter 7: Discussion

7.1. Results summary

TBI is a growing health problem in the UK (NICE 2007, Gustavsson, Svensson et al. 2011) with both short and long-term health implications (Whitnall, McMillan et al. 2006, McMillan, Teasdale et al. 2011). The cognitive sequelae of TBI are particularly disabling and currently there is little in the way of effective intervention. The underlying cause of the cognitive problems remains elusive with lesion load and location, and clinical severity correlating poorly with the degree of long-term disability. The first step to developing effective treatments of these problems is to better understand the neural mechanisms that mediate them. There is a growing body of evidence suggesting that dysfunction of distributed neural networks is a major factor in the cognitive problems that follow TBI. TBI may be particularly disruptive to neural network function due to DAI damaging the white matter connecting key regions within these networks. In this thesis I used fMRI and DTI techniques to provide insight into the altered network structure and function that cause the self-awareness deficits seen after TBI.

In Chapter 4 I provided evidence that cognitive control could be engaged without activation of the dorsal anterior cingulate cortex (dACC), which suggests that the dACC could therefore not act as a generic error monitor as had been suggested previously (Holroyd and Coles 2002). This result may also explain why certain responses to error are preserved in animals and humans with damage to the dACC (Fellows and Farah 2005, Kennerley, Walton et al. 2006, Modirrousta and Fellows 2008). I also provided evidence for two distinct frontal lobe networks involved in performance monitoring: the Salience network (SN), which responded to internally

signalled/predictable errors; and, the ventral attentional network (VAN), which responded to externally signalled/unpredictable errors.

In Chapter 5 I used DCM to clarify the roles of the cortical nodes within the SN. I provided evidence that the SN receives input through the right anterior insula (RAI) and subsequent behavioural adaptation is associated with increased effective connectivity from the dACC to left anterior insula (LAI). As information enters the SN via the RAI, this result is more consistent with the dACC having a role in either evaluation or responding to salient stimuli following detection of the stimuli by the RAI. This provided further evidence against theories that assign the role of performance monitoring to the dACC (Holroyd and Coles 2002, Swick and Turken 2002, di Pellegrino, Ciaramelli et al. 2007).

In Chapter 6 I investigated the FPCN in a large group of TBI patients into those with impaired and those with normal performance monitoring abilities (Low-PMs and High PMs respectively). The FPCN contains within it the SN as well as other regions Chapter 4 implicated in performance monitoring (Vincent, Kahn et al. 2008). The Low-PM group displayed abnormal FPCN activity both at rest and in response to errors. The abnormalities were largely localised to regions within the FPCN that alone would constitute the SN. The dACC showed reduced functional connectivity to the remainder of the FPCN at rest, and the insulae showed increased activation in response to errors. These results highlight the dACC and insulae as key neural elements involved in self-awareness, possibly as an extension of their role in more general performance monitoring.

This work has helped identify the key neural structures involved in performance monitoring, and demonstrated that abnormal function of these structures and their interactions play a role in the development of self-awareness deficits after TBI.

7.2. Relationship of the main findings to existing work

7.2.1. Neural networks involved in performance monitoring

Influential models such as the 'triple- network' model state that the SN monitors all incoming information and act as a gateway into the selective recruitment of other brain networks (Menon 2011). The results of my first experiment demonstrated that while the SN is clearly involved in monitoring a subset of errors there is at least one alternative neural mechanism that can be used to monitor events and engage cognitive control (i.e. the VAN). If the SN consists of just the anterior insulae and dACC then this result is inconsistent with models like the 'triple network' model. My results showed that cognitive control and recruitment of a wide variety of cortical regions could be engaged in response to externally signalled or unpredictable errors without the need for either dACC or insulae activation.

When interpreting this result it should be mentioned that previous studies of the SN have considered the anterior insulae and adjacent IFG together as a fronto-insular unit containing the pars operculari (Seeley, Menon et al. 2007, Sridharan, Levitin et al. 2008, White, Joseph et al. 2010, Zielinski, Gennatas et al. 2010). As the pars operculari did show activation across both predictable and unpredictable errors, it could be argued that at least part of the SN was activated in both error types. However, as key portions of the SN were not activated (i.e. the anterior insulae and dACC), I believe my findings are still inconsistent with models where the SN generically orchestrates the neuronal response to salient events (e.g. the triple

network model). Future studies should investigate the causal relationships between the pars opercularis and anterior insulae during error processing and other behaviourally salient events (discussed below).

7.2.2. Right anterior insula provides the input into salience network

Other models have proposed that the RAI, rather than the whole SN, monitors on going events and recruits different cortical regions to respond to those events (Sridharan, Levitin et al. 2008, Menon and Uddin 2010). My studies have produced evidence both for and against these models. The DCM analysis in Chapter 5 provided evidence for these models by demonstrating that the driving input into the SN enters via the RAI. However, the event related analysis in Chapter 4 provided evidence against these models by showing that significant behavioural adaptation and VAN activation could be generated in response to unpredictable errors *without* RAI activation. Therefore, while the RAI may provide the driving input to the SN, it does not appear to provide the input into the VAN. (Badre 2008, Kounieher, Charron et al. 2009, Taren, Venkatraman et al. 2011). Taken together these results suggest that current models where the RAI alone regulates functions across networks outside of the SN are incomplete. Further work needs to be done to establish the driving input into the VAN. It may be that this the input to the VAN originates from the right IFG, in which case the RAI and right IFG may share similar functions but respond to different salient events and recruit different cortical networks (i.e. the RAI providing the input to the SN after predictable errors, and the IFG providing the input to the VAN after unpredictable errors). This idea is discussed in detail below.

7.2.3. Effective connectivity measures provide additional information to traditional univariate fMRI analyses

The DCM study in Chapter 5 adds to the growing body of evidence that suggests effective connectivity measures can provide a richer interpretation of fMRI data than univariate analysis (Rowe, Hughes et al. 2010). The univariate analysis in Chapters 4 and 5 demonstrated SN activation in response to errors but could not establish the roles of the regions within the SN. Similarly, univariate analysis did not differentiate between activation during congruent and incongruent commission errors despite considerable differences in the factors that cause them and the behavioural adaptations they provoke (discussed in detail in Chapters 4 and 5). In this study effective connectivity measures not only discriminated between conditions and anatomical regions but the change in effective connectivity magnitude correlated with the ensuing behavioural adaptation. The replication of the SN structure across two different experimental conditions lends further weight to the use of DCM as a reliable tool that can add considerable information to the interpretation of fMRI data.

7.2.4. FPCN breakdown and models of impaired self-awareness after TBI

These results of my TBI patient study described in Chapter 6 are highly suggestive that FPCN dysfunction plays a role in impaired awareness after TBI. One influential model proposed by Northoff suggests that awareness and evaluation of on-going events are regulated by midline cortical structures including the ACC but excluding any regions outside of the midline (Northoff and Bermpohl 2004). My results are inconsistent with the Northoff model primarily because they heavily implicate regions outside of the midline structures (i.e. the insulae). The reduced connectivity between the dACC and remainder of the FPCN found in Low-PM subjects is consistent with Craig's model of awareness (Craig 2009). In Craig's model the anterior insulae receives information from the dACC and other frontal regions to update its re-

representations of 'self'. These re-representations are integrated with the representation of 'self' encoded in the posterior insula, producing a dynamic evolving representation of the 'self' and self-awareness. I would predict from Craig's model that any process that functionally disconnects the dACC from the insulae would result in the type of altered awareness of on-going events observed in the Low-PM patients. One caveat on this conclusion is that I examined one facet of awareness that relates to on-line performance monitoring and adaptation to dynamic events (although the Low-PM patients did display broader deficits of self-awareness on meta-cognitive measures). Future studies should investigate the neural basis of these broader deficits directly (discussed below).

7.3. Development of existing models of performance monitoring and awareness

My results are not entirely consistent with any existing theory of performance monitoring or awareness. I have outlined below some modifications to the existing frameworks that may help to explain the data I have produced.

7.3.1. Modified model of performance monitoring

Taken together these studies provide considerable evidence about how the brain detects, evaluates, and responds to various types of salient event. Critically, Chapter 4 demonstrated that the RAI/SN and IFG/VAN respond differently to salient events depending upon their predictability, possibly as a reflection of whether the events are causally related to subjects' actions or can generate a prediction error (grey arrows, Figure 7.1A). This indicates that current theories where either the RAI or SN as a whole function as generic filters of all incoming information are incorrect. I propose a new model with two parallel streams: predictable salient events are detected by the RAI, which provides the driving input into the SN; whereas, unpredictable salient events are detected by the right IFG, which provides the driving input into the VAN (Figure 7.1A).

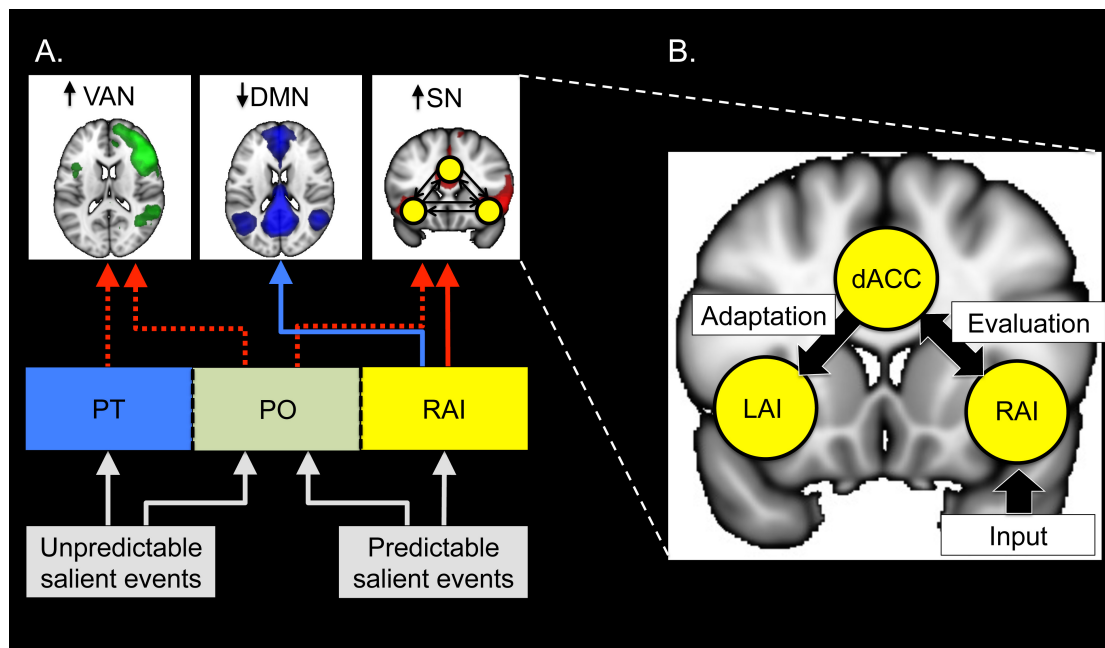


Figure 7.1: The role of the fronto-insula complex in response to salient events and awareness.

A.) Unpredictable salient events cause activation of the pars triangularis (PT) and pars opercularis (PO), whereas predictable salient events cause activation in the anterior insula (RAI) and PO (grey arrows). The RAI with or without the PO drive SN activation (solid red arrow) and DMN deactivation (solid blue arrow) in response to predictable salient events. The PO and/or the PT provide a hypothesised driving input into the VAN (dashed red arrow) in response to unpredictable salient events. B.) Information enters the SN via the RAI. The interaction between the RAI and dACC facilitates evaluation of moment-to-moment salient events that require immediate behavioural adaptation. The dACC produces behavioural adaptation after salient events by influencing other cortical regions (e.g. the LAI).

7.3.1.1. Neural response to predictable salient events

Chapter 4 showed convincingly that the SN detects predictable salient events, and Chapter 5 demonstrated that this information comes into the system through the RAI (solid red arrow Figure 7.1A). These results are consistent with previous models of RAI function where the RAI recruits other cortical regions within the SN to respond to the behaviorally salient events (e.g. the dACC) (Sridharan, Levitin et al. 2008, Uddin and Menon 2009, Menon and Uddin 2010). My results emphasise the importance of the RAI in the organisation of the SNs response to a subset of salient events, and

several previous studies have demonstrated the importance of the RAI in determining activity across other networks including the ECN and DMN. For example, the integrity of the white matter connecting RAI to the dACC has been correlated with subject's ability to deactivate the DMN during attentionally demanding tasks both after TBI (Bonnelle, Ham et al. 2012) and in healthy aging (in submission) (solid blue arrows Figure 7.1A); and, a Granger causality analysis has shown activation within the RAI and adjacent IFG regulates activation in the central executive network and deactivation in the DMN (Sridharan, Levitin et al. 2008). The SN is clearly important in organising the response to salient events but its response appears dependent upon the type of event and therefore cannot be a generic system, as proposed by previous models.

7.3.1.2. Neural response to unpredictable salient events

Both the pars opercularis and triangularis in the IFG responded to unpredictable salient events when the RAI did not. Unpredictable events were also associated with extensive activation within the VAN (Figure 4.3 and 4.4). As the RAI was not activated during this condition it does not seem plausible the RAI drives the neural response in the VAN. Therefore another region must provide the cortical input into this network. This conclusion is inconsistent with current models of RAI function that would have predicted that the RAI provides the input into the VAN (Menon and Uddin 2010, Menon 2011). I propose that the right IFG provides the input to the VAN (dashed red arrows Figure 7.1A). There is existing evidence that the IFG plays a key role within the VAN. Previous studies have implicated the right IFG in the detection of salient events (Hampshire, Chamberlain et al. 2010) generating response inhibition (Aron, Fletcher et al. 2003, Aron, Robbins et al. 2004, Verbruggen and Logan 2008); moment-to-moment activity in the right IFG can predict subsequent attentional levels (Weissman, Roberts et al. 2006); and, lesions to the right IFG have been shown to

selectively impair functions subsequently attributed to the VAN (Wilkins, Shallice et al. 1987, Corbetta and Shulman 2002). Direct evidence for the causal role of the right IFG in the VAN could be established by performing a DCM analysis comparable to that described in Chapter 5, but this is beyond the scope of my thesis. I predict that if such an analysis were performed it would determine that the input to the VAN originates in the right IFG (dashed red arrows Figure 7.1A).

7.3.1.3. Role of the pars opercularis and a fronto-insular complex

In Chapter 4 the pars opercularis responded to both predictable and unpredictable errors, and may represent a generic salience detection system that could potentially provide the driving input into both the SN and VAN (dashed red arrows Figure 7.1A). The DCM analysis in Chapter 5 did not include the pars opercularis and therefore a comparison between models with input into the pars opercularis or the RAI could not be performed to either confirm or refute this theory. Alternatively, the combination of the RAI, pars opercularis and pars triangularis may represent a hierarchical fronto-insula complex with a rostro-caudal gradient. In this fronto-insula complex the most caudal elements (i.e. the RAI) respond to predictable salient events, the most rostral elements (i.e. the pars triangularis) respond to unpredictable salient events, and the regions between (i.e. the pars opercularis) may respond to both. Previous studies have considered the insula and IFG as a single functional unit (Seeley, Menon et al. 2007, Sridharan, Levitin et al. 2008, White, Joseph et al. 2010, Zielinski, Gennatas et al. 2010) and the hierarchical organisation I propose is similar to those described in other prefrontal structures (e.g. the lateral (Badre and D'Esposito 2007, Badre 2008) and medial prefrontal cortex (Badre 2008, Kouneiher, Charron et al. 2009, Taren, Venkatraman et al. 2011)). However, further analysis examining the causal relationships between these regions, the VAN and SN needs to be done to establish this theory definitively.

7.3.2. Craig's model of self-awareness

My results suggest that regions of the SN, within the FPCN, play key role in the awareness of and adaptation to on-going events. Although the RAI supplies the information to the SN, insula activation alone does not appear to be sufficient for error detection or error-awareness. The Low-PMs group had greater bilateral insulae activation after errors but reduced behavioral adaptation and broader deficits of self-awareness indicating that they were unaware despite greater insulae activation. The role of the dACC is unclear from these studies but the dACC's influence (i.e. the effective connectivity) over other regions in the SN indicates a role in evaluation and behavioral modification in response to salient events (Figure 7.1.B). The results of my study fit well with Craig's model of awareness. This model suggests that the interaction between the dACC and the insulae may be key to producing awareness of on-going events (Craig 2009). Specifically, it proposes that the dACC continually 'updates' a representation of oneself encoded in the insulae with ongoing contextual information to provide a dynamic representation of self and one's relationship to this new information. Based on this model disruption to the interaction between the insulae and dACC would produce impaired awareness of events such as dynamic errors. Chapter 6 provided strong evidence for Craig's model by demonstrating that the Low-PM group did indeed have reduced functional connectivity between the dACC and the remainder of the FPCN, including the insulae, and that this disconnection was associated with deficits in both performance monitoring and broader meta-cognitive measures of awareness.

However, a conflict exists in interpreting my data in the context of Craig's model. Craig's model states that information about ongoing events is transferred from the ACC to the anterior insulae. The results from Chapter 5 suggest that information enters the SN from the RAI, which then exerts its influence over the dACC. It may be

that Craig's model is an oversimplification and that a reciprocal relationship between these structures is necessary for the type of dynamic awareness tested in this study. Further analysis examining the effective connectivity between these regions and the LAI may help to establish the organization of this system in the context of errors that occur with and without awareness.

7.4. Future developments

The work described has helped elucidate several of the structures and mechanisms involved in performance monitoring and self-awareness. However, these are broad subjects and there are several aspects that future studies need to investigate to expand upon and clarify my results.

7.4.1. Experimentally vary the predictability of timing errors

Dorsal ACC activation was not seen following timing errors in Chapter 4. I argue that this is because timing errors in the paradigm were inherently difficult to predict and therefore could not be associated with a prediction error. To test this theory, future experiments should design paradigms that allow subjects to make a range of quantitatively different timing errors. Timing errors that occur very close to a time limit are difficult to predict because the difference between the response time and the time limit is small. Increasingly late response times will breach the time limit to a greater extent and be easier to recognise and predict (Miltner, Braun et al. 1997). A single previous EEG study has designed a study that allows subjects to make timing errors of different magnitudes (Miltner, Braun et al. 1997). They showed that very late responses, (i.e. more predictable timing errors), were associated with a larger feedback related negativity, presumed to arise in the dACC of the SN. In addition, a fixed time limit may also help make timing errors easier to predict. Further evidence

from studies with the spatial resolution of fMRI could help clarify whether the dACC and SN respond to timing errors when they are predictable. From the results of my experiment in Chapter 4, I would predict more predictable timing errors would illicit activation in the SN in a similar distribution to that seen after commission errors.

7.4.2. Expansion of DCM analysis

7.4.2.1. Applying DCM to the patient group

In Chapter 5, I used DCM to help elucidate the organisation of the SN in healthy brains. Future work should examine the organisation of the SN after TBI and relate measures of white matter integrity to the DCM estimates of effective connectivity. My study highlighted the insulae and dACC as key regions with abnormal function in TBI patients with awareness deficits but no causal relationship between the regions could be established because of the nature of the analyses I performed. Assessment of effective connectivity may help clarify how the relationship between the dACC and insulae changes in TBI patients and gives rise to their self-awareness deficits. From Craig's model I would predict that subjects with impaired awareness would show reduced effective connectivity from the dACC to the insulae.

7.4.2.2. Assess network-to-network interaction using DCM

In this thesis I studied the roles of networks in particular cognitive functions, and the role of nodes within networks. However, the networks described do not work in isolation and it is likely that interaction between networks is key for efficient cognitive processes. A recent study from my research group demonstrated that deactivation of the DMN is important for successful inhibition control during a cognitively demanding task (Bonnelle, Ham et al. 2012). Importantly, they demonstrated for the first time that DMN deactivation depended upon the structural integrity of white matter tracts

within the SN, specifically the tract connecting the RAI to the dACC/Pre-SMA (Bonnelle, Ham et al. 2012). This result highlights the importance of network interactions in control of even the most rudimentary of tasks. Further research should use effective connectivity measures to examine how networks interact with one another in health and disease. Networks of particular interest would be the SN, DMN and the VAN. Studying the interaction between the VAN and SN could help clarify their roles in cognition.

7.4.2.3. Stochastic DCM

DCM is context dependent. In Chapter 5 I used random effects procedure to make inferences about the general population that my sample of healthy volunteers came from (Stephan, Penny et al. 2009). However, I could only make generalisations of the network structure in the context of the task assessed, or more generally in terms of internally signalled errors. The model of the SN I produced may change outside of the context of errors performed during a cognitively demanding choice reaction task. This is a limitation of DCM design. Until recently DCM had been based upon a deterministic model. Deterministic DCM requires an experimental perturbation to make a contrast so that inferences about network organisation can be made (see Chapter 3). All deterministic DCM models therefore require task based data and one can only make inferences in the context of that task. Stochastic (s)DCM is a recent development that unlike deterministic DCM does not require an explicitly modelled experimental perturbation and therefore does not require a task. SDCM uses stochastic variables to make inferences about effective connectivity between brain regions in the absence of task (Daunizeau, Friston et al. 2009, Li, Daunizeau et al. 2011, Daunizeau, Stephan et al. 2012). Applying sDCM to resting-state fMRI data has been used to establish the organisation of the DMN (Di and Biswal 2013) and could determine the SN organisation in the absence of a task or particular

behavioural context. Resting-state sDCM could establish whether the SN model produced by my study represents the generic SN organisation or if it is specific to the task assessed. Furthermore one of the potential limitations of working with patients is that some will not be able or willing to perform the experimental tasks, (e.g. 6 subjects from my final study were excluded because they were unable to perform the tasks to a sufficient level of accuracy). As sDCM does not require a task resting-state sDCM analysis would allow detailed assessment of brain network organisation in patients groups unable to perform experimental tasks. I believe sDCM technique offers an exciting opportunity to expand current fMRI patient research that should be acted upon.

7.4.3. Examining other facets of self-awareness

Consistent with previous literature, I used on-line performance monitoring as a surrogate marker of self-awareness. This was validated to an extent by the association of abnormal disability assessments in the Low-PM group (see Chapter 6). This represents one important facet of self-awareness, which has been associated with ability to perform practical daily activities (Hart, Giovannetti et al. 1998). Another key aspect of awareness is the integration and long-term representation of self. By focusing on on-line awareness I did not assess how the subjects' perception of their abilities changed over time. These functions are related but neuroimaging models of self-awareness have given them distinct anatomical bases. In Craig's model, the representation of self is encoded in the posterior insula (Craig 2009), whereas in the Northoff's model the integration of self-referential information takes place in the PCC /Precuneus and the representation is encoded in the orbitofrontal cortex (Northoff and Bermppohl 2004). My study is broadly supportive of Craig's model in that it suggests that the insulae and dACC are involved updating subjects moment-to-moment with incoming information. However, I did not gather

information on how performance on a task changed subjects' beliefs about their ability to perform the task (i.e. how reflection on performance effected their longer term representation of self). This could have been established simply by asking subjects to gauge their performance before and after performing the tests (Hart, Giovannetti et al. 1998). However, the SST study design was not ideally suited to this type of assessment as performance was normalised across individuals (i.e. all subjects made roughly the same number of errors). Interpreting the results of such a survey would therefore be complicated by the fact that subjects with similar performance may have played tasks with different levels of difficulty. Further studies should address the issue of how long-term representations of the self are updated in patients with self-awareness problems.

7.4.4. Brain stem imaging

In the three studies presented I chose to focus on the patterns of cortical activation rather than subcortical or brainstem activation. There were several reasons for doing this: firstly, to resolve existing controversy over the roles of the dACC and RAI in error processing and awareness; secondly, adding a single subcortical node to the DCM models described in Chapter 5 would increase the number of models from 448 to 61,440, massively increasing the computational load of the study; and, thirdly, recent studies have shown that accurately establishing brainstem activation requires dedicated MRI sequences (Limbrick-Oldfield, Brooks et al. 2012), which would have been inappropriate given that it was not the primary research question and data was acquired as part of a larger study of TBI patients. Future work should address the roles of brainstem structures, as there is a large body of literature considering how the brainstem contributes to error processing. It is likely that by applying DCM one could establish how structures such as the dopaminergic midbrain influence the cortical nodes of the SN. This question is of particular relevance to TBI as the

dopaminergic system has been implicated in the cognitive deficits that follow TBI and dopaminergic therapy has been used with varying levels of success as a cognitive enhancer after TBI (Bales, Wagner et al. 2009).

7.5. Potential treatment of self-awareness deficits after TBI

7.5.1. Dopamine and the salience network

There is a large body of research that has suggested the dopamine transmission innervates key regions of the SN. Studies of rats, humans and other primates have demonstrated the ACC is heavily innervated by dopaminergic structures in the midbrain including the ventral tegmental area and substantia nigra (Berger, Gaspar et al. 1991, Raghanti, Stimpson et al. 2008). Furthermore, histological studies in humans have shown that dopaminergic innervation of the cortex is densest in the ACC, bilateral insulae along with the primary and secondary motor areas, (Gaspar, Berger et al. 1989, Berger, Gaspar et al. 1991, Ciliax, Drash et al. 1999). The functional relevance of this innervation is unclear but an influential theory suggests that it the connection between the dopaminergic midbrain and cortical structures, particularly the dACC, is a key part of reinforcement learning (Holroyd and Coles 2002, Holroyd, Nieuwenhuis et al. 2004, Holroyd and Coles 2008).

7.5.2. Dopamine and cognition

One influential model of reinforcement learning proposes that the dACC indexes prediction error signals generated by midbrain dopaminergic cells in response to a mismatch between expected and actual outcomes (Holroyd and Coles 2002, Holroyd, Nieuwenhuis et al. 2004, Holroyd and Coles 2008). Animal studies have demonstrated repeatedly that during tasks positive and negative reinforcement are associated with bursts and dips of dopaminergic activity in the midbrain respectively

(Frank, Seeberger et al. 2004). Studies in humans have demonstrated convincingly that augmenting and depleting dopaminergic activity leads to changes in the adaptive behaviour seen after positive and negative feedback. It is suggested that this change is due to alteration of the midbrain signal of reward and punishment, (i.e. positive and negative reinforcement). Enhancing dopaminergic transmission augments the effects of reward but reduces the effect of negative stimuli on subsequent behaviour (Frank, Seeberger et al. 2004). In terms of using dopamine agonists as cognitive enhancers this is obviously something of a double-edged sword. Interestingly, although the dopamine and the dACC are thought to be central to the reinforcement learning model, studies in rats have shown that error related behaviour remains consistent after chemically removing the effect of dopamine on the ACC (Walton, Croxson et al. 2005). This raises the possibility that the dACC may not be the key site of dopaminergic innervation to the prefrontal cortex and the insulae offers an alternative route for dopaminergic activity to affect the limbic system and produce its behavioural effects.

7.5.3. Previous trials of dopamine potentiating agents in TBI

Dopamine transmission has been proposed as a potential therapy for the cognitive deficits after TBI for over a decade. Dopaminergic pathways from the midbrain to the cortex are vulnerable to damage after TBI and dopamine has a well-established role in many of the cognitive functions typically impaired by TBI (Bales, Wagner et al. 2009). Therefore replacing dopamine may be an effective treatment in patients who are dopamine deficient. Methylphenidate (MPH) is a dopaminergic and noradrenergic re-uptake inhibitor, and is a promising candidate for a pharmacological cognitive enhancer in TBI (Bales, Wagner et al. 2009). Several trials have shown that MPH provides a modest benefit for cognitive functions, such as attention and information processing speed (Whyte, Hart et al. 2004, Lee, Kim et al. 2005), mood (Lee, Kim et

al. 2005) and post-concussive symptoms (Lee, Kim et al. 2005) following TBI. However, these findings are not universal. Some studies have shown no benefit from MPH after TBI (Speech, Rao et al. 1993, Plenger, Dixon et al. 1996, Williams, Ris et al. 1998) and another small trial has shown cognitive benefits acutely but no long term benefit at three months (Plenger, Dixon et al. 1996). The negative trials are relatively small compared to those that showed treatment effects, with either 12 (Speech, Rao et al. 1993) or 10 (Williams, Ris et al. 1998) subjects with chronic TBI. The discrepancy in MPH's effects may be due to several reasons: firstly, dopamine has been shown to have both beneficial effects and deleterious effects on different cognitive tasks (Mehta, Swainson et al. 2001) and aspects of behaviour (Frank, Seeberger et al. 2004); and secondly, the aforementioned studies all treated the TBI as a homogeneous group, with no attempt made to select patients most likely to benefit from the intervention. Part of the challenge in modern medicine is to target treatments individual patients. My work described in Chapter 6, and previous studies on self-awareness after TBI, have demonstrated that lesion analysis is insufficient to predict disability. However, the results of Chapter 6 suggest functional imaging measures may provide a more sensitive way to classify and stratify patients for treatment.

7.5.4. Methods of targeting patients

TBI patients are heterogeneous and as a result, treatments for cognitive impairment will probably need to be targeted to subgroups to be really effective. Outside of TBI, functional connectivity measures in the SN have been shown to be capable of discriminating other patient groups including Alzheimer's disease and behavioural variant fronto-temporal dementia (Zhou, Greicius et al. 2010). Effective connectivity measures have been used to demonstrate different network structures in patients with Parkinson's disease compared to healthy controls. Interestingly, Parkinson's

disease patients reverted to the same network structure as healthy controls after treatment with dopaminergic therapy (Rowe, Hughes et al. 2010). This suggests that effective connectivity measures can be used to assess the mechanism of action of certain drugs. Recently fMRI has been applied to investigate the neural correlates of behavioural response to MPH treatment of attention deficits after TBI (Kim, Whyte et al. 2012). During performance of a sustained attention task activation of the left parietal lobe was specifically modulated by MPH, and the magnitude of this modulation correlated with improvements in behaviour after drug administration. Taken together these studies indicate that effective and functional connectivity measures can be used to both differentiate patients and monitor the mechanisms of action of cognitive enhancing drugs.

The results I have presented suggest that self-awareness deficits are due to FPCN and particularly the SN sub-network, dysfunction. There is a sound physiological rationale behind using dopaminergic therapy to alter activation in the SN (outlined above). However, dopaminergic therapy has thus far proven relatively ineffective in treating cognitive symptoms after TBI. I believe that treating patients with either specific cognitive profile thought to result from damage to the SN (e.g. impaired self-awareness) or with fMRI measures of dysfunction within the SN (e.g. reduced functional connectivity) may help target the use of dopaminergic therapy as a cognitive enhancer after TBI.

7.6. Conclusion

Current investigations of TBI do not accurately predict cognitive deficits or long-term outcome. This is partly because they fail to identify the effects of TBI on network function. I have utilised advanced functional imaging techniques to establish the neural basis of two key elements of successful adaptive behaviour (performance

monitoring and cognitive control). I have also provided evidence to resolve the roles of the anterior insulae and dACC within the SN. By applying a network based approach I have demonstrated that TBI patients with self-awareness deficits show dysfunction within the FPCN both during task and at rest. This dysfunction is largely localised to the SN subcomponent of the FPCN (i.e. the dACC and insulae). This result supports the importance of dACC and insula interaction highlighted in Craig's model of awareness. This work also implicates the SN and FPCN as a potential target for treatment of self-awareness deficits after TBI. One possible treatment option is the use of dopaminergic therapy, which is known to alter SN activation but further studies will be needed to validate this theory.

8. References

Adams, J. H. (1982). "Diffuse axonal injury in non-missile head injury." *Injury* 13(5): 444-445.

Adams, J. H., D. I. Graham, T. A. Gennarelli and W. L. Maxwell (1991). "Diffuse axonal injury in non-missile head injury." *J Neurol Neurosurg Ps* 54(6): 481-483.

Adams, R. A., K. E. Stephan, H. R. Brown, C. D. Frith and K. J. Friston (2013). "The computational anatomy of psychosis." *Front Psychiatry* 4: 47.

Agam, Y., M. S. Hamalainen, A. K. Lee, K. A. Dyckman, J. S. Friedman, M. Isom, N. Makris and D. S. Manoach (2011). "Multimodal neuroimaging dissociates hemodynamic and electrophysiological correlates of error processing." *P Natl Acad Sci USA* 108(42): 17556-17561.

Aguirre, G. K., E. Zarahn and M. D'Esposito (1998). "The variability of human, BOLD hemodynamic responses." *Neuroimage* 8(4): 360-369.

Allan, L. G. (1978). "Comments on current ratio-setting models for time perception." *Percept Psychophys* 24(5): 444-450.

Allman, J. M., N. A. Tetreault, A. Y. Hakeem, K. F. Manaye, K. Semendeferi, J. M. Erwin, S. Park, V. Goubert and P. R. Hof (2010). "The von Economo neurons in frontoinsular and anterior cingulate cortex in great apes and humans." *Brain Struct Funct* 214(5-6): 495-517.

Allman, J. M., N. A. Tetreault, A. Y. Hakeem, K. F. Manaye, K. Semendeferi, J. M. Erwin, S. Park, V. Goubert and P. R. Hof (2011). "The von Economo neurons in the frontoinsular and anterior cingulate cortex." *Ann NY Acad Sci* 1225: 59-71.

Anderson, S. W. and D. Tranel (1989). "Awareness of disease states following cerebral infarction, dementia, and head trauma: Standardized assessment." *Clin Neuropsychol* 3(4): 327-339.

Andlin-Sobocki, P., B. Jonsson, H. Å. Wittchen and J. Olesen (2005). "Cost of disorders of the brain in Europe." *Eur J Neurol* 12(s1): 1-27.

Arciniegas, D. B., K. Held and P. Wagner (2002). "Cognitive Impairment Following Traumatic Brain Injury." *Curr Treat Options Neurol* 4(1): 43-57.

Arfanakis, K., V. M. Haughton, J. D. Carew, B. P. Rogers, R. J. Dempsey and M. E. Meyerand (2002). "Diffusion tensor MR imaging in diffuse axonal injury." *Ame J Neuroradiol* 23(5): 794-802.

Aron, A. R., P. C. Fletcher, E. T. Bullmore, B. J. Sahakian and T. W. Robbins (2003). "Stop-signal inhibition disrupted by damage to right inferior frontal gyrus in humans." *Nat Neurosci* 6(2): 115-116.

Aron, A. R., T. W. Robbins and R. A. Poldrack (2004). "Inhibition and the right inferior frontal cortex." *Trends Cogn Sci* 8(4): 170-177.

Assaf, Y. and O. Pasternak (2008). "Diffusion tensor imaging (DTI)-based white matter mapping in brain research: a review." *J Mol Neurosci* 34(1): 51-61.

Bach, L. J. and A. S. David (2006). "Self-awareness after acquired and traumatic brain injury." *Neuropsych Rehabil* 16(4): 397-414.

Baddeley, A. D., H. Emslie and I. Nimmo-Smith (1994). *Doors and People Test: A Test of Visual and Verbal Recall and Recognition*. Bury-St-Edmunds, Thames Valley Test Company.

Badre, D. (2008). "Cognitive control, hierarchy, and the rostro-Å-caudal organization of the frontal lobes." *Trends Cogn Sci* 12(5): 193-200.

Badre, D. and M. D'Esposito (2007). "Functional magnetic resonance imaging evidence for a hierarchical organization of the prefrontal cortex." *J Cogn Neurosci* 19(12): 2082-2099.

Badre, D. and A. D. Wagner (2004). "Selection, integration, and conflict monitoring; assessing the nature and generality of prefrontal cognitive control mechanisms." *Neuron* 41(3): 473-487.

Bagurdes, L. A., M. M. Mesulam, D. R. Gitelman, S. Weintraub and D. M. Small (2008). "Modulation of the spatial attention network by incentives in healthy aging and mild cognitive impairment." *Neuropsychologia* 46(12): 2943-2948.

Bales, J. W., A. K. Wagner, A. E. Kline and C. E. Dixon (2009). "Persistent cognitive dysfunction after traumatic brain injury: A dopamine hypothesis." *Neurosci Biobehav R* 33(7): 981-1003.

Baltes, P. B. (1993). "The aging mind: potential and limits." *Gerontologist* 33(5): 580-594.

Bandettini, P. A., A. Jesmanowicz, E. C. Wong and J. S. Hyde (1993). "Processing strategies for time-course data sets in functional MRI of the human brain." *Magnetic Reson Med* 30(2): 161-173.

Bartels, A. and S. Zeki (2004). "The neural correlates of maternal and romantic love." *Neuroimage* 21(3): 1155-1166.

Basser, P. J. and C. Pierpaoli (1996). "Microstructural and physiological features of tissues elucidated by quantitative-diffusion-tensor MRI." *J Magn Reson S B* 111(3): 209-219.

Bazarian, J. J., J. McClung, M. N. Shah, Y. T. Cheng, W. Flesher and J. Kraus (2005). "Mild traumatic brain injury in the United States, 1998--2000." *Brain injury* 19(2): 85-91.

Bazarian, J. J., J. Zhong, B. Blyth, T. Zhu, V. Kavcic and D. Peterson (2007). "Diffusion tensor imaging detects clinically important axonal damage after mild traumatic brain injury: a pilot study." *J Neurotraum* 24(9): 1447-1459.

Beauchamp, M. H., M. Ditchfield, F. E. Babl, M. Kean, C. Catroppa, K. O. Yeates and V. Anderson (2011). "Detecting Traumatic Brain Lesions in Children: CT versus MRI versus susceptibility weighted imaging (SWI)." *J Neurotraum*.

Beaulieu, C. (2002). "The basis of anisotropic water diffusion in the nervous system - a technical review." *NMR Biomed* 15(7-8): 435-455.

Beaulieu, C., M. D. Does, R. E. Snyder and P. S. Allen (1996). "Changes in water diffusion due to Wallerian degeneration in peripheral nerve." *Magnetic Reson Med* 36(4): 627-631.

Beckmann, C. F., M. DeLuca, J. T. Devlin and S. M. Smith (2005). "Investigations into resting-state connectivity using independent component analysis." *Philos T Roy Soc B* 360(1457): 1001-1013.

Beckmann, C. F., M. Jenkinson and S. M. Smith (2003). "General multilevel linear modeling for group analysis in FMRI." *Neuroimage* 20(2): 1052-1063.

Beckmann, C. F. and S. M. Smith (2004). "Probabilistic independent component analysis for functional magnetic resonance imaging." *IEEE transactions on medical imaging* 23(2): 137-152.

Behrens, T. E., M. W. Woolrich, M. Jenkinson, H. Johansen-Berg, R. G. Nunes, S. Clare, P. M. Matthews, J. M. Brady and S. M. Smith (2003). "Characterization and propagation of uncertainty in diffusion-weighted MR imaging." *Magnetic Reson Med* 50(5): 1077-1088.

Bekker, E. M., C. C. Overtom, J. L. Kenemans, J. J. Kooij, I. De Noord, J. K. Buitelaar and M. N. Verbaten (2005). "Stopping and changing in adults with ADHD." *Psychol Med* 35(6): 807-816.

Belanger, H. G., G. Curtiss, J. A. Demery, B. K. Lebowitz and R. D. Vanderploeg (2005). "Factors moderating neuropsychological outcomes following mild traumatic brain injury: a meta-analysis." *J Int Neuropsych Soc* 11(3): 215-227.

Bell, A. J. and T. J. Sejnowski (1995). "An information-maximization approach to blind separation and blind deconvolution." *Neural Comput* 7(6): 1129-1159.

Berger, B., P. Gaspar and C. Verney (1991). "Dopaminergic innervation of the cerebral cortex: unexpected differences between rodents and primates." *Trends Neurosci* 14(1): 21-27.

Bernstein, D. M. (2002). "Information processing difficulty long after self-reported concussion." *J Int Neuropsych Soc* 8(5): 673-682.

Bigler, E. D. (2001). "Distinguished Neuropsychologist Award Lecture 1999. The lesion(s) in traumatic brain injury: implications for clinical neuropsychology." *Arch Clin Neuropsych* 16(2): 95-131.

Bigler, E. D. (2004). "Neuropsychological results and neuropathological findings at autopsy in a case of mild traumatic brain injury." *J Int Neuropsych Soc* 10(5): 794-806.

Biswal, B., F. Z. Yetkin, V. M. Haughton and J. S. Hyde (1995). "Functional connectivity in the motor cortex of resting human brain using echo-planar MRI." *Magn Reson Med* 34(4): 537-541.

Bleiberg, J., W. S. Garmoe, E. L. Halpern, D. L. Reeves and J. D. Nadler (1997). "Consistency of within-day and across-day performance after mild brain injury." *Neuropsychiatry Neuropsychol Behav Neurol* 10(4): 247-253.

Blumbergs, P. C., G. Scott, J. Manavis, H. Wainwright, D. A. Simpson and A. J. McLean (1994). "Staining of amyloid precursor protein to study axonal damage in mild head injury." *Lancet* 344(8929): 1055-1056.

Boake, C., S. R. Millis, W. M. High Jr, R. L. Delmonico, J. S. Kreutzer, M. Rosenthal, M. Sherer and C. B. Ivanhoe (2001). "Using early neuropsychologic testing to predict long-term productivity outcome from traumatic brain injury." *Arch Phys Med Rehab* 82(6): 761-768.

Boly, M., E. Balteau, C. Schnakers, C. Degueldre, G. Moonen, A. Luxen, C. Phillips, P. Peigneux, P. Maquet and S. Laureys (2007). "Baseline brain activity fluctuations predict somatosensory perception in humans." *P Natl Acad Sci USA* 104(29): 12187-12192.

Boly, M., L. Tshibanda, A. Vanhaudenhuyse, Q. Noirhomme, C. Schnakers, D. Ledoux, P. Boveroux, C. Garweg, B. Lambermont, C. Phillips, A. Luxen, G. Moonen, C. Bassetti, P. Maquet and S. Laureys (2009). "Functional connectivity in the default

network during resting state is preserved in a vegetative but not in a brain dead patient." *Hum Brain Mapp* 30(8): 2393-2400.

Bonnelle, V., T. E. Ham, R. Leech, K. M. Kinnunen, M. A. Mehta, R. J. Greenwood and D. J. Sharp (2012). "Salience network integrity predicts default mode network function after traumatic brain injury." *P Natl Acad of Sci USA* 109(12): 4690-4695.

Bonnelle, V., R. Leech, K. M. Kinnunen, T. E. Ham, C. F. Beckmann, X. De Boissezon, R. J. Greenwood and D. J. Sharp (2011). "Default mode network connectivity predicts sustained attention deficits after traumatic brain injury." *J Neurosci* 31(38): 13442-13451.

Botvinick, M. M., T. S. Braver, D. M. Barch, C. S. Carter and J. D. Cohen (2001). "Conflict monitoring and cognitive control." *Psychol Rev* 108(3): 624-652.

Botvinick, M. M., J. D. Cohen and C. S. Carter (2004). "Conflict monitoring and anterior cingulate cortex: an update." *Trends Cogn Sci* 8(12): 539-546.

Braga, R. M., L. R. Wilson, D. J. Sharp, R. J. Wise and R. Leech (2013). "Separable networks for top-down attention to auditory non-spatial and visuospatial modalities." *NeuroImage*.

Brett, M., A. P. Leff, C. Rorden and J. Ashburner (2001). "Spatial normalization of brain images with focal lesions using cost function masking." *Neuroimage* 14(2): 486-500.

Buckner, R. L., J. R. Andrews-Hanna and D. L. Schacter (2008). "The brain's default network: anatomy, function, and relevance to disease." *Ann N Y Acad Sci* 1124: 1-38.

Buckner, R. L., P. A. Bandettini, K. M. O'Craven, R. L. Savoy, S. E. Petersen, M. E. Raichle and B. R. Rosen (1996). "Detection of cortical activation during averaged single trials of a cognitive task using functional magnetic resonance imaging." *P Natl Acad Sci USA* 93(25): 14878-14883.

Bush, G., B. A. Vogt, J. Holmes, A. M. Dale, D. Greve, M. A. Jenike and B. R. Rosen (2002). "Dorsal anterior cingulate cortex: a role in reward-based decision making." *P Natl Acad Sci USA* 99(1): 523-528.

Cabeza, R., N. D. Anderson, J. K. Locantore and A. R. McIntosh (2002). "Aging gracefully: compensatory brain activity in high-performing older adults." *Neuroimage* 17(3): 1394-1402.

Caeyenberghs, K., N. Wenderoth, B. C. Smits-Engelsman, S. Sunaert and S. P. Swinnen (2009). "Neural correlates of motor dysfunction in children with traumatic brain injury: exploration of compensatory recruitment patterns." *Brain* 132(Pt 3): 684-694.

Carroll, L. J., J. D. Cassidy, P. M. Peloso, J. Borg, H. von Holst, L. Holm, C. Paniak and M. Pepin (2004). "Prognosis for mild traumatic brain injury: results of the WHO Collaborating Centre Task Force on Mild Traumatic Brain Injury." *J Rehabil* (43 Suppl): 84-105.

Carter, C. S., T. S. Braver, D. M. Barch, M. M. Botvinick, D. Noll and J. D. Cohen (1998). "Anterior cingulate cortex, error detection, and the online monitoring of performance." *Science* 280(5364): 747-749.

Castellanos, N. P., N. Paul, V. E. Ordonez, O. Demuynck, R. Bajo, P. Campo, A. Bilbao, T. Ortiz, F. del-Pozo and F. Maestu (2010). "Reorganization of functional connectivity as a correlate of cognitive recovery in acquired brain injury." *Brain* 133(8): 2365-2381.

Catani, M. and D. H. ffytche (2005). "The rises and falls of disconnection syndromes." *Brain* 128(10): 2224-2239.

Cauda, F., B. M. Micon, K. Sacco, S. Duca, F. D'Agata, G. Geminiani and S. Canavero (2009). "Disrupted intrinsic functional connectivity in the vegetative state." *J Neurol Neurosurg Ps* 80(4): 429-431.

Charlton, R. A., T. R. Barrick, D. J. McIntyre, Y. Shen, M. O'Sullivan, F. A. Howe, C. A. Clark, R. G. Morris and H. S. Markus (2006). "White matter damage on diffusion

tensor imaging correlates with age-related cognitive decline." *Neurology* 66(2): 217-222.

Chastain, C. A., U. E. Oyoyo, M. Zipperman, E. Joo, S. Ashwal, L. A. Shutter and K. A. Tong (2009). "Predicting outcomes of traumatic brain injury by imaging modality and injury distribution." *J Neurotraum* 26(8): 1183-1196.

Christ, S., M. Falkenstein, H. Heuer and J. Hohnsbein (2000). "Different error types and error processing in spatial stimulus-response-compatibility tasks: behavioural and electrophysiological data." *Biol Psychol* 51(2-3): 129-150.

Christensen, M. S., T. Z. Ramsay, T. E. Lund, K. H. Madsen and J. B. Rowe (2006). "An fMRI study of the neural correlates of graded visual perception." *Neuroimage* 31(4): 1711-1725.

Christodoulou, C., J. DeLuca, J. H. Ricker, N. K. Madigan, B. M. Bly, G. Lange, A. J. Kalnin, W. C. Liu, J. Steffener, B. J. Diamond and A. C. Ni (2001). "Functional magnetic resonance imaging of working memory impairment after traumatic brain injury." *J Neurol Neurosurg Ps* 71(2): 161-168.

Chu, Z., E. A. Wilde, J. V. Hunter, S. R. McCauley, E. D. Bigler, M. Troyanskaya, R. Yallampalli, J. M. Chia and H. S. Levin (2010). "Voxel-based analysis of diffusion tensor imaging in mild traumatic brain injury in adolescents." *Am J Neuroradiol* 31(2): 340-346.

Cifu, D. X., L. Keyser-Marcus, E. Lopez, P. Wehman, J. S. Kreutzer, J. Englander and W. High (1997). "Acute predictors of successful return to work 1 year after traumatic brain injury: a multicenter analysis." *Arch Phys Med Rehab* 78(2): 125-131.

Ciliax, B. J., G. W. Drash, J. K. Staley, S. Haber, C. J. Mobley, G. W. Miller, E. J. Mufson, D. C. Mash and A. I. Levey (1999). "Immunocytochemical localization of the dopamine transporter in human brain." *J Comp Neurol* 409(1): 38-56.

Corbetta, M., J. M. Kincade and G. L. Shulman (2002). "Neural systems for visual orienting and their relationships to spatial working memory." *J Cogn Neurosci* 14(3): 508-523.

Corbetta, M. and G. L. Shulman (2002). "Control of goal-directed and stimulus-driven attention in the brain." *Nat Rev Neurosci* 3(3): 201-215.

Corbetta, M. and G. L. Shulman (2011). "Spatial neglect and attention networks." *Annu Rev Neurosci* 34: 569-599.

Corso, P., E. Finkelstein, T. Miller, I. Fiebelkorn and E. Zaloshnja (2006). "Incidence and lifetime costs of injuries in the United States." *Inj Prev* 12(4): 212-218.

Craig, A. (2005). "Forebrain emotional asymmetry: a neuroanatomical basis?" *Trends Cogn Sci* 9(12): 566-571.

Craig, A. D. (2009). "How do you feel--now? The anterior insula and human awareness." *Nat Rev Neurosci* 10(1): 59-70.

Craig, A. D., K. Chen, D. Bandy and E. M. Reiman (2000). "Thermosensory activation of insular cortex." *Nature Neurosci* 3(2): 184-190.

Critchley, H. D., S. Wiens, P. Rotshtein, A. Ohman and R. J. Dolan (2004). "Neural systems supporting interoceptive awareness." *Nat Neurosci* 7(2): 189-195.

Cubon, V. A., M. Putukian, C. Boyer and A. Dettwiler (2011). "A diffusion tensor imaging study on the white matter skeleton in individuals with sports-related concussion." *J Neurotraum* 28(2): 189-201.

D'Esposito, M., L. Y. Deouell and A. Gazzaley (2003). "Alterations in the BOLD fMRI signal with ageing and disease: a challenge for neuroimaging." *Nat Rev Neurosci* 4(11): 863-872.

Damoiseaux, J. S. and M. D. Greicius (2009). "Greater than the sum of its parts: a review of studies combining structural connectivity and resting-state functional connectivity." *Brain Struct Funct* 213(6): 525-533.

Damoiseaux, J. S., S. A. Rombouts, F. Barkhof, P. Scheltens, C. J. Stam, S. M. Smith and C. F. Beckmann (2006). "Consistent resting-state networks across healthy subjects." *P Natl Acad Sci USA* 103(37): 13848-13853.

Daunizeau, J., K. Friston and S. Kiebel (2009). "Variational Bayesian identification and prediction of stochastic nonlinear dynamic causal models." *Physica D: nonlinear phenomena* 238(21): 2089-2118.

Daunizeau, J., K. E. Stephan and K. J. Friston (2012). "Stochastic dynamic causal modelling of fMRI data: Should we care about neural noise?" *Neuroimage* 62(1): 464-481.

Debener, S., M. Ullsperger, M. Siegel, K. Fiehler, D. Y. von Cramon and A. K. Engel (2005). "Trial-by-trial coupling of concurrent electroencephalogram and functional magnetic resonance imaging identifies the dynamics of performance monitoring." *J Neurosci* 25(50): 11730-11737.

Dehaene, S., M. I. Posner and D. M. Tucker (1994). "Localization of a neural system for error detection and compensation. ." *Psychol Sci* 5(303–305).

Delis, D. C., E. Kaplan and J. H. Kramer (2001). *Delis-Kaplan Executive Function System*. San Antonio, San Antonio, TX: Psychological Corporation.

Di Martino, A., K. Ross, L. Q. Uddin, A. B. Sklar, F. X. Castellanos and M. P. Milham (2009). "Functional brain correlates of social and nonsocial processes in autism spectrum disorders: an activation likelihood estimation meta-analysis." *Biol Psychiat* 65(1): 63-74.

di Pellegrino, G., E. Ciaramelli and E. Ladavas (2007). "The regulation of cognitive control following rostral anterior cingulate cortex lesion in humans." *J Cogn Neurosci* 19(2): 275-286.

Di, X. and B. B. Biswal (2013). "Identifying the default mode network structure using dynamic causal modeling on resting-state functional magnetic resonance imaging." *Neuroimage*.

Dikmen, S. S., N. R. Temkin, J. E. Machamer, A. L. Holubkov, R. T. Fraser and H. R. Winn (1994). "Employment following traumatic head injuries." *Arch Neurol* 51(2): 177.

Dosenbach, N. U., D. A. Fair, F. M. Miezin, A. L. Cohen, K. K. Wenger, R. A. Dosenbach, M. D. Fox, A. Z. Snyder, J. L. Vincent, M. E. Raichle, B. L. Schlaggar and S. E. Petersen (2007). "Distinct brain networks for adaptive and stable task control in humans." *P Natl Acad Sci USA* 104(26): 11073-11078.

Dosenbach, N. U., K. M. Visscher, E. D. Palmer, F. M. Miezin, K. K. Wenger, H. C. Kang, E. D. Burgund, A. L. Grimes, B. L. Schlaggar and S. E. Petersen (2006). "A core system for the implementation of task sets." *Neuron* 50(5): 799-812.

Draper, K. and J. Ponsford (2008). "Cognitive functioning ten years following traumatic brain injury and rehabilitation." *Neuropsychol* 22(5): 618.

Eckert, M. A., V. Menon, A. Walczak, J. Ahlstrom, S. Denslow, A. Horwitz and J. R. Dubno (2009). "At the heart of the ventral attention system: the right anterior insula." *Hum Brain Mapp* 30(8): 2530-2541.

Egner, T. (2009). "Prefrontal cortex and cognitive control: motivating functional hierarchies." *Nat Neurosci* 12(7): 821-822.

Eichele, T., S. Debener, V. D. Calhoun, K. Specht, A. K. Engel, K. Hugdahl, D. Y. von Cramon and M. Ullsperger (2008). "Prediction of human errors by maladaptive changes in event-related brain networks." *P Natl Acad Sci USA* 105(16): 6173-6178.

Enriquez-Geppert, S., T. Eichele, K. Specht, H. Kugel, C. Pantev and R. J. Huster (2012). "Functional parcellation of the inferior frontal and midcingulate cortices in a flanker-stop-change paradigm." *Hum Brain Mapp*.

Falkenstein, M., J. Hohnsbein, J. Hoormann and L. Blanke (1991). "Effects of crossmodal divided attention on late ERP components. II. Error processing in choice reaction tasks." *Electroen Clin Neuro* 78(6): 447-455.

Falkenstein, M., J. Hoormann, S. Christ and J. Hohnsbein (2000). "ERP components on reaction errors and their functional significance: a tutorial." *Biol Psychol* 51(2-3): 87-107.

Featherstone, R. E., S. Kapur and P. J. Fletcher (2007). "The amphetamine-induced sensitized state as a model of schizophrenia." *Progress Neuro-Psychoph* 31(8): 1556-1571.

Feinstein, J. S., M. B. Stein and M. P. Paulus (2006). "Anterior insula reactivity during certain decisions is associated with neuroticism." *Soc Cogn Affect Neurosci* 1(2): 136-142.

Fellows, L. K. and M. J. Farah (2005). "Is anterior cingulate cortex necessary for cognitive control?" *Brain* 128(4): 788-796.

Fichtenholtz, H. M., H. L. Dean, D. G. Dillon, H. Yamasaki, G. McCarthy and K. S. LaBar (2004). "Emotion-attention network interactions during a visual oddball task." *Brain research. Cognitive Brain Res* 20(1): 67-80.

Filippini, N., B. J. MacIntosh, M. G. Hough, G. M. Goodwin, G. B. Frisoni, S. M. Smith, P. M. Matthews, C. F. Beckmann and C. E. Mackay (2009). "Distinct patterns of brain activity in young carriers of the APOE-epsilon4 allele." *P Natl Acad Sci USA* 106(17): 7209-7214.

Fleming, J. M., J. Strong and R. Ashton (1996). "Self-awareness of deficits in adults with traumatic brain injury: how best to measure?" *Brain Inj* 10(1): 1-15.

Fletcher, P. C. and C. D. Frith (2009). "Perceiving is believing: a Bayesian approach to explaining the positive symptoms of schizophrenia." *Nat Rev Neurosci* 10(1): 48-58.

Fossati, P., S. J. Hevenor, S. J. Graham, C. Grady, M. L. Keightley, F. Craik and H. Mayberg (2003). "In search of the emotional self: an fMRI study using positive and negative emotional words." *Am J Psychiat* 160(11): 1938-1945.

Fox, M. D., M. Corbetta, A. Z. Snyder, J. L. Vincent and M. E. Raichle (2006). "Spontaneous neuronal activity distinguishes human dorsal and ventral attention systems." *P Natl Acad Sci USA* 103(26): 10046-10051.

Fox, M. D., A. Z. Snyder, J. M. Zacks and M. E. Raichle (2006). "Coherent spontaneous activity accounts for trial-to-trial variability in human evoked brain responses." *Nat Neurosci* 9(1): 23-25.

Frank, M. J., L. C. Seeberger and C. O'Reilly R (2004). "By carrot or by stick: cognitive reinforcement learning in parkinsonism." *Science* 306(5703): 1940-1943.

Fraser, R., S. Dikmen, A. McLean and B. Miller (1988). "Employability of head injury survivors: First year post-injury." *Rehab Couns Bull*.

Friedman, N. P. and A. Miyake (2004). "The relations among inhibition and interference control functions: a latent-variable analysis." *J Exp Psycho-Gen* 133(1): 101.

Friston, K. (2002). "Beyond phrenology: what can neuroimaging tell us about distributed circuitry?" *Annu Rev Neurosci* 25: 221-250.

Friston, K., P. Jezzard and R. Turner (1994). "Analysis of functional MRI time-series." *Hum Brain Mapp* 1(2): 153-171.

Friston, K., J. Mattout, N. Trujillo-Barreto, J. Ashburner and W. Penny (2007). "Variational free energy and the Laplace approximation." *Neuroimage* 34(1): 220-234.

Friston, K., C. Price, P. Fletcher, C. Moore, R. Frackowiak and R. Dolan (1996). "The trouble with cognitive subtraction." *Neuroimage* 4(2): 97-104.

Friston, K. J. (1994). "Functional and effective connectivity in neuroimaging: a synthesis." *Hum Brain Mapp* 2(1,2): 56-78.

Friston, K. J., L. Harrison and W. Penny (2003). "Dynamic causal modelling." *Neuroimage* 19(4): 1273-1302.

Friston, K. J., A. P. Holmes, C. J. Price, C. Buchel and K. J. Worsley (1999). "Multisubject fMRI studies and conjunction analyses." *Neuroimage* 10(4): 385-396.

Friston, K. J., W. Penny, C. Phillips, S. Kiebel, G. Hinton and J. Ashburner (2002). "Classical and Bayesian inference in neuroimaging: theory." *Neuroimage* 16(2): 465-483.

Frith, C. D. and U. Frith (1999). "Interacting minds--a biological basis." *Science* 286(5445): 1692-1695.

Garavan, H., T. J. Ross, K. Murphy, R. A. Roche and E. A. Stein (2002). "Dissociable executive functions in the dynamic control of behavior: inhibition, error detection, and correction." *Neuroimage* 17(4): 1820-1829.

Gaspar, P., B. Berger, A. Febvret, A. Vigny and J. P. Henry (1989). "Catecholamine innervation of the human cerebral cortex as revealed by comparative immunohistochemistry of tyrosine hydroxylase and dopamine, β -hydroxylase." *J Comp Neurol* 279(2): 249-271.

Gehring, W., B. Goss and M. Coles (1993). "A neural system for error detection and compensation." *Psychol Sci* 4: 385-390.

Gehring, W. J. and D. E. Fencsik (2001). "Functions of the medial frontal cortex in the processing of conflict and errors." *J Neurosci* 21(23): 9430-9437.

Gehring, W. J. and R. T. Knight (2000). "Prefrontal-cingulate interactions in action monitoring." *Nature Neurosci* 3(5): 516-520.

Gentry, L. R., J. C. Godersky and B. Thompson (1988). "MR imaging of head trauma: review of the distribution and radiopathologic features of traumatic lesions." *Am J Roentgenol* 150(3): 663-672.

Gentry, L. R., J. C. Godersky, B. Thompson and V. D. Dunn (1988). "Prospective comparative study of intermediate-field MR and CT in the evaluation of closed head trauma." *Am J Roentgenol* 150(3): 673-682.

Geschwind, N. (1965). "Disconnexion syndromes in animals and man. I." *Brain* 88(2): 237-294.

Geschwind, N. (1965). "Disconnexion syndromes in animals and man. II." *Brain* 88(3): 585-644.

Goran, D. A., R. J. Fabiano and N. Crewe (1997). "Employment following severe traumatic brain injury: the utility of the Individual Ability Profile system (IAP)." *Arch Clin Neuropsych* 12(7): 691-698.

Grace, J., J. C. Stout and P. F. Malloy (1999). "Assessing frontal lobe behavioral syndromes with the frontal lobe personality scale." *Assessment* 6(3): 269-284.

Greicius, M. (2008). "Resting-state functional connectivity in neuropsychiatric disorders." *Curr Opin Neurol* 21(4): 424-430.

Greicius, M. D., V. Kiviniemi, O. Tervonen, V. Vainionpaa, S. Alahuhta, A. L. Reiss and V. Menon (2008). "Persistent default-mode network connectivity during light sedation." *Hum Brain Mapp* 29(7): 839-847.

Greicius, M. D., K. Supekar, V. Menon and R. F. Dougherty (2009). "Resting-state functional connectivity reflects structural connectivity in the default mode network." *Cereb Cortex* 19(1): 72-78.

Grondin, S. (2010). "Timing and time perception: a review of recent behavioral and neuroscience findings and theoretical directions." *Atten Percept Psychophys* 72(3): 561-582.

Gronwall, D. and P. Wrightson (1981). "Memory and information processing capacity after closed head injury." *J Neurol Neurosurg Ps* 44(10): 889-895.

Gusnard, D. A., E. Akbudak, G. L. Shulman and M. E. Raichle (2001). "Medial prefrontal cortex and self-referential mental activity: relation to a default mode of brain function." *P Natl Acad Sci USA* 98(7): 4259-4264.

Gustavsson, A., M. Svensson, F. Jacobi, C. Allgulander, J. Alonso, E. Beghi, R. Dodel, M. Ekman, C. Faravelli, L. Fratiglioni, B. Gannon, D. H. Jones, P. Jennum, A. Jordanova, L. Jonsson, K. Karampampa, M. Knapp, G. Kobelt, T. Kurth, R. Lieb, M. Linde, C. Ljungcrantz, A. Maercker, B. Melin, M. Moscarelli, A. Musayev, F. Norwood, M. Preisig, M. Pugliatti, J. Rehm, L. Salvador-Carulla, B. Schlehofer, R.

Simon, H. C. Steinhausen, L. J. Stovner, J. M. Vallat, P. Van den Bergh, J. van Os, P. Vos, W. Xu, H. U. Wittchen, B. Jonsson and J. Olesen (2011). "Cost of disorders of the brain in Europe 2010." *Eur Neuropsychopharm* 21(10): 718-779.

Haacke, E. M., S. Mittal, Z. Wu, J. Neelavalli and Y. C. Cheng (2009). "Susceptibility-weighted imaging: technical aspects and clinical applications, part 1." *Am J Neuroradiol* 30(1): 19-30.

Hajcak, G., C. B. Holroyd, J. S. Moser and R. F. Simons (2005). "Brain potentials associated with expected and unexpected good and bad outcomes." *Psychophysiology* 42(2): 161-170.

Hajcak, G., N. McDonald and R. F. Simons (2003). "To err is autonomic: Error-related brain potentials, ANS activity, and post-error compensatory behavior." *Psychophysiology* 40(6): 895-903.

Hampshire, A., S. R. Chamberlain, M. M. Monti, J. Duncan and A. M. Owen (2010). "The role of the right inferior frontal gyrus: inhibition and attentional control." *Neuroimage* 50(3): 1313-1319.

Hart, T., T. Giovannetti, M. W. Montgomery and M. F. Schwartz (1998). "Awareness of errors in naturalistic action after traumatic brain injury." *J Head Trauma Rehab* 13(5): 16-28.

He, B. J., A. Z. Snyder, J. L. Vincent, A. Epstein, G. L. Shulman and M. Corbetta (2007). "Breakdown of functional connectivity in frontoparietal networks underlies behavioral deficits in spatial neglect." *Neuron* 53(6): 905-918.

Hellyer, P. J., R. Leech, T. E. Ham, V. Bonnelle and D. J. Sharp (2012). "Individual prediction of white matter injury following traumatic brain injury." *Ann Neurol*.

Henry, L. C., J. Tremblay, S. Tremblay, N. Lepore, H. Theoret, D. Elleberg and M. Lassonde (2011). "Acute and Chronic Changes in Diffusivity Measures after Sports Concussion." *J Neurotraum*.

Hesselmann, G., C. A. Kell, E. Eger and A. Kleinschmidt (2008). "Spontaneous local variations in ongoing neural activity bias perceptual decisions." *P Natl Acad Sci USA* 105(31): 10984-10989.

Hester, R., C. Fassbender and H. Garavan (2004). "Individual differences in error processing: a review and reanalysis of three event-related fMRI studies using the GO/NOGO task." *Cereb Cortex* 14(9): 986-994.

Hester, R., J. J. Foxe, S. Molholm, M. Shpaner and H. Garavan (2005). "Neural mechanisms involved in error processing: a comparison of errors made with and without awareness." *Neuroimage* 27(3): 602-608.

Hillary, F. G., J. Slocumb, E. C. Hills, N. M. Fitzpatrick, J. D. Medaglia, J. Wang, D. C. Good and G. R. Wylie (2011). "Changes in resting connectivity during recovery from severe traumatic brain injury." *Int J Psychophysiol* 82(1): 115-123.

Himanen, L., R. Portin, H. Isoniemi, H. Helenius, T. Kurki and O. Tenovuo (2006). "Longitudinal cognitive changes in traumatic brain injury: a 30-year follow-up study." *Neurology* 66(2): 187-192.

Hoeting, J. A., D. Madigan, A. E. Raftery and C. T. Volinsky (1999). "Bayesian model averaging: A tutorial." *Statist Sci*: 382-401.

Hofbauer, R. K., P. Rainville, G. H. Duncan and M. C. Bushnell (2001). "Cortical representation of the sensory dimension of pain." *J Neurophysiol* 86(1): 402-411.

Hollerman, J. R. and W. Schultz (1998). "Dopamine neurons report an error in the temporal prediction of reward during learning." *Nature Neurosci* 1(4): 304-309.

Holroyd, C. B. and M. G. Coles (2002). "The neural basis of human error processing: reinforcement learning, dopamine, and the error-related negativity." *Psychol Rev* 109(4): 679-709.

Holroyd, C. B. and M. G. Coles (2008). "Dorsal anterior cingulate cortex integrates reinforcement history to guide voluntary behavior." *Cortex* 44(5): 548-559.

Holroyd, C. B., O. E. Krigolson, R. Baker, S. Lee and J. Gibson (2009). "When is an error not a prediction error? An electrophysiological investigation." *Cogn Affect Behav Neurosci* 9(1): 59-70.

Holroyd, C. B., S. Nieuwenhuis, N. Yeung, L. Nystrom, R. B. Mars, M. G. Coles and J. D. Cohen (2004). "Dorsal anterior cingulate cortex shows fMRI response to internal and external error signals." *Nat Neurosci* 7(5): 497-498.

Huang, M. X., S. Nichols, A. Robb, A. Angeles, A. Drake, M. Holland, S. Asmussen, J. D'Andrea, W. Chun, M. Levy, L. Cui, T. Song, D. G. Baker, P. Hammer, R. McLay, R. J. Theilmann, R. Coimbra, M. Diwakar, C. Boyd, J. Neff, T. T. Liu, J. Webb-Murphy, R. Farinpour, C. Cheung, D. L. Harrington, D. Heister and R. R. Lee (2012). "An automatic MEG low-frequency source imaging approach for detecting injuries in mild and moderate TBI patients with blast and non-blast causes." *Neuroimage* 61(4): 1067-1082.

Huang, M. X., R. J. Theilmann, A. Robb, A. Angeles, S. Nichols, A. Drake, J. D'Andrea, M. Levy, M. Holland, T. Song, S. Ge, E. Hwang, K. Yoo, L. Cui, D. G. Baker, D. Trauner, R. Coimbra and R. R. Lee (2009). "Integrated imaging approach with MEG and DTI to detect mild traumatic brain injury in military and civilian patients." *J Neurotraum* 26(8): 1213-1226.

Huisman, T. A., L. H. Schwamm, P. W. Schaefer, W. J. Koroshetz, N. Shetty-Alva, Y. Ozsunar, O. Wu and A. G. Sorensen (2004). "Diffusion tensor imaging as potential biomarker of white matter injury in diffuse axonal injury." *Am J Neuroradiol* 25(3): 370-376.

Husain, M. and C. Rorden (2003). "Non-spatially lateralized mechanisms in hemispatial neglect." *Nat Rev Neurosci* 4(1): 26-36.

Husain, M., K. Shapiro, J. Martin and C. Kennard (1997). "Abnormal temporal dynamics of visual attention in spatial neglect patients." *Nature* 385(6612): 154-156.

Iannetti, G. D. and R. G. Wise (2007). "BOLD functional MRI in disease and pharmacological studies: room for improvement?" *Magn Reson imaging* 25(6): 978-988.

Inglese, M., S. Makani, G. Johnson, B. A. Cohen, J. A. Silver, O. Gonen and R. I. Grossman (2005). "Diffuse axonal injury in mild traumatic brain injury: a diffusion tensor imaging study." *J Neurosurg* 103(2): 298-303.

Jabbi, M., M. Swart and C. Keysers (2007). "Empathy for positive and negative emotions in the gustatory cortex." *Neuroimage* 34(4): 1744-1753.

James, W. (1890). *The Principles of Psychology*. New York, Dover.

Jenkinson, M., P. Bannister, M. Brady and S. Smith (2002). "Improved optimization for the robust and accurate linear registration and motion correction of brain images." *Neuroimage* 17(2): 825-841.

Jenkinson, M. and S. Smith (2001). "A global optimisation method for robust affine registration of brain images." *Med Image Anal* 5(2): 143-156.

Jessup, R. K., J. R. Busemeyer and J. W. Brown (2010). "Error effects in anterior cingulate cortex reverse when error likelihood is high." *J Neurosci* 30(9): 3467-3472.

Johnson, S. C., L. C. Baxter, L. S. Wilder, J. G. Pipe, J. E. Heiserman and G. P. Prigatano (2002). "Neural correlates of self-reflection." *Brain* 125(8): 1808-1814.

Johnstone, T., C. M. van Reekum, T. R. Oakes and R. J. Davidson (2006). "The voice of emotion: an fMRI study of neural responses to angry and happy vocal expressions." *Soc Cogn Affect Neurosci* 1(3): 242-249.

Jorge, R. and R. G. Robinson (2003). "Mood disorders following traumatic brain injury." *Int Rev Psychiatry* 15(4): 317-327.

Kane, N. M., T. H. Moss, S. H. Curry and S. R. Butler (1998). "Quantitative electroencephalographic evaluation of non-fatal and fatal traumatic coma." *Electroen Clin Neuro* 106(3): 244-250.

Kapur, S. (2004). "How antipsychotics become anti-"psychotic"--from dopamine to salience to psychosis." *Trends Pharmacol Sci* 25(8): 402-406.

Kapur, S. and D. Mamo (2003). "Half a century of antipsychotics and still a central role for dopamine D2 receptors." *Prog Neuro-Psychoph* 27(7): 1081-1090.

Kapur, S., R. Mizrahi and M. Li (2005). "From dopamine to salience to psychosis--linking biology, pharmacology and phenomenology of psychosis." *Schizophr Res* 79(1): 59-68.

Kasahara, M., D. K. Menon, C. H. Salmond, J. G. Outtrim, J. V. Tavares, T. A. Carpenter, J. D. Pickard, B. J. Sahakian and E. A. Stamatakis (2011). "Traumatic brain injury alters the functional brain network mediating working memory." *Brain Inj* 25(12): 1170-1187.

Kasahara, M., D. K. Menon, C. H. Salmond, J. G. Outtrim, J. V. Taylor Tavares, T. A. Carpenter, J. D. Pickard, B. J. Sahakian and E. A. Stamatakis (2010). "Altered functional connectivity in the motor network after traumatic brain injury." *Neurology* 75(2): 168-176.

Kennerley, S. W., M. E. Walton, T. E. Behrens, M. J. Buckley and M. F. Rushworth (2006). "Optimal decision making and the anterior cingulate cortex." *Nat Neurosci* 9(7): 940-947.

Kerns, J. G., J. D. Cohen, A. W. MacDonald, 3rd, R. Y. Cho, V. A. Stenger and C. S. Carter (2004). "Anterior cingulate conflict monitoring and adjustments in control." *Science* 303(5660): 1023-1026.

Kim, J., J. Whyte, S. Patel, E. Europa, J. Wang, H. B. Coslett and J. A. Detre (2012). "Methylphenidate modulates sustained attention and cortical activation in survivors of traumatic brain injury: a perfusion fMRI study." *Psychopharmacology* 222(1): 47-57.

Kim, S. G., W. Richter and K. Ugurbil (1997). "Limitations of temporal resolution in functional MRI." *Magnet Reson Med* 37(4): 631-636.

Kim, Y. H., W. K. Yoo, M. H. Ko, C. H. Park, S. T. Kim and D. L. Na (2009). "Plasticity of the attentional network after brain injury and cognitive rehabilitation." *Neurorehabilitation and neural repair* 23(5): 468-477.

Kinnunen, K. M., R. Greenwood, J. H. Powell, R. Leech, P. C. Hawkins, V. Bonnelle, M. C. Patel, S. J. Counsell and D. J. Sharp (2011). "White matter damage and cognitive impairment after traumatic brain injury." *Brain* 134(2): 449-463.

Klein, T. A., T. Endrass, N. Kathmann, J. Neumann, D. Y. von Cramon and M. Ullsperger (2007). "Neural correlates of error awareness." *Neuroimage* 34(4): 1774-1781.

Kochanek, P. M. (1993). "Ischemic and traumatic brain injury: pathobiology and cellular mechanisms." *Crit Care Med* 21(9): S333-S334.

Koechlin, E., C. Ody and F. Kouneiher (2003). "The architecture of cognitive control in the human prefrontal cortex." *Science* 302(5648): 1181-1185.

Koechlin, E. and C. Summerfield (2007). "An information theoretical approach to prefrontal executive function." *Trends Cogn Sci* 11(6): 229-235.

Kong, J., N. S. White, K. K. Kwong, M. G. Vangel, I. S. Rosman, R. H. Gracely and R. L. Gollub (2006). "Using fMRI to dissociate sensory encoding from cognitive evaluation of heat pain intensity." *Hum Brain Mapp* 27(9): 715-721.

Koponen, S., T. Taiminen, R. Portin, L. Himanen, H. Isoniemi, H. Heinonen, S. Hinkka and O. Tenovuo (2002). "Axis I and II psychiatric disorders after traumatic brain injury: a 30-year follow-up study." *Am J Psychiat* 159(8): 1315-1321.

Kouneiher, F., S. Charron and E. Koechlin (2009). "Motivation and cognitive control in the human prefrontal cortex." *Nat Neurosci* 12(7): 939-945.

Kraus, J. F., D. L. McArthur and T. A. Silberman (1994). "Epidemiology of mild brain injury." *Semin Neurol* 14(1): 1-7.

Kraus, J. F. and P. Nourjah (1988). "The epidemiology of mild, uncomplicated brain injury." *J Trauma* 28(12): 1637-1643.

Kucyi, A., M. Moayedi, I. Weissman-Fogel, M. Hodaie and K. D. Davis (2012). "Hemispheric asymmetry in white matter connectivity of the temporoparietal junction with the insula and prefrontal cortex." *PLoS One* 7(4): e35589.

Kumar, R., R. K. Gupta, M. Husain, C. Chaudhry, A. Srivastava, S. Saksena and R. K. Rathore (2009). "Comparative evaluation of corpus callosum DTI metrics in acute mild and moderate traumatic brain injury: its correlation with neuropsychometric tests." *Brain Inj* 23(7): 675-685.

Larson, M. J., J. E. Fair, T. J. Farrer and W. M. Perlstein (2011). "Predictors of performance monitoring abilities following traumatic brain injury: the influence of negative affect and cognitive sequelae." *Int J Psychophysiol* 82(1): 61-68.

Larson, M. J., T. J. Farrer and P. E. Clayson (2011). "Cognitive control in mild traumatic brain injury: Conflict monitoring and conflict adaptation." *Int J Psychophysiol*.

Larson, M. J., D. A. Kaufman, I. M. Schmalfluss and W. M. Perlstein (2007). "Performance monitoring, error processing, and evaluative control following severe TBI." *J Int Neuropsychol Soc* 13(6): 961-971.

Larson, M. J., W. M. Perlstein, J. A. Demery and D. A. Stigge-Kaufman (2006). "Cognitive control impairments in traumatic brain injury." *J Clin Exp Neuropsychol* 28(6): 968-986.

Lavie, N. (2011). "'Load theory' of attention. Nilli Lavie." *Curr Biol* 21(17): R645-647

Lavie, N., A. Hirst, J. W. de Fockert and E. Viding (2004). "Load theory of selective attention and cognitive control." *J Exp Psychol. Gen* 133(3): 339-354.

Lawrence, N. S., T. J. Ross, R. Hoffmann, H. Garavan and E. A. Stein (2003). "Multiple neuronal networks mediate sustained attention." *J Cogn Neurosci* 15(7): 1028-1038.

Lee, H., S. Ä. Kim, J. Ä. Kim, I. Ä. Shin, S. Ä. Yang and J. Ä. Yoon (2005). "Comparing effects of methylphenidate, sertraline and placebo on neuropsychiatric sequelae in patients with traumatic brain injury." *Hum Psychopharm Clin* 20(2): 97-104.

Lee, H., M. Wintermark, A. D. Gean, J. Ghajar, G. T. Manley and P. Mukherjee (2008). "Focal lesions in acute mild traumatic brain injury and neurocognitive outcome: CT versus 3T MRI." *J Neurotraum* 25(9): 1049-1056.

Leech, R., R. Braga and D. J. Sharp (2012). "Echoes of the brain within the posterior cingulate cortex." *J Neurosci* 32(1): 215-222.

Leech, R., S. Kamourieh, C. F. Beckmann and D. J. Sharp (2011). "Fractionating the default mode network: distinct contributions of the ventral and dorsal posterior cingulate cortex to cognitive control." *J Neurosci* 31(9): 3217-3224.

Leff, A. P., T. M. Schofield, K. E. Stephan, J. T. Crinion, K. J. Friston and C. J. Price (2008). "The cortical dynamics of intelligible speech." *J Neurosci* 28(49): 13209-13215.

Lemogne, C., G. le Bastard, H. Mayberg, E. Volle, L. Bergouignan, S. Lehericy, J. F. Allilaire and P. Fossati (2009). "In search of the depressive self: extended medial prefrontal network during self-referential processing in major depression." *Soc Cogn Affect Neurosci* 4(3): 305-312.

Levin, H. S. (1995). "Prediction of recovery from traumatic brain injury." *J Neurotraum* 12(5): 913-922.

Levin, H. S., H. E. Gary, Jr., H. M. Eisenberg, R. M. Ruff, J. T. Barth, J. Kreutzer, W. M. High, Jr., S. Portman, M. A. Foulkes, J. A. Jane and et al. (1990). "Neurobehavioral outcome 1 year after severe head injury. Experience of the Traumatic Coma Data Bank." *J Neurosurg* 73(5): 699-709.

Levin, H. S., E. Wilde, M. Troyanskaya, N. J. Petersen, R. Scheibel, M. Newsome, M. Radaideh, T. Wu, R. Yallampalli, Z. Chu and X. Li (2010). "Diffusion tensor imaging of mild to moderate blast-related traumatic brain injury and its sequelae." *J Neurotraum* 27(4): 683-694.

Levine, B., S. E. Black, G. Cheung, A. Campbell, C. O'Toole and M. L. Schwartz (2005). "Gambling task performance in traumatic brain injury: relationships to injury severity, atrophy, lesion location, and cognitive and psychosocial outcome." *Cogn Behav Neurol* 18(1): 45-54.

Levine, B., R. Cabeza, A. R. McIntosh, S. E. Black, C. L. Grady and D. T. Stuss (2002). "Functional reorganisation of memory after traumatic brain injury: a study with H(2)(15)O positron emission tomography." *J Neurol Neurosurg Ps* 73(2): 173-181.

Li, B., J. Daunizeau, K. E. Stephan, W. Penny, D. Hu and K. Friston (2011). "Generalised filtering and stochastic DCM for fMRI." *Neuroimage* 58(2): 442-457.

Li, C. S., H. H. Chao and T. W. Lee (2009). "Neural correlates of speeded as compared with delayed responses in a stop signal task: an indirect analog of risk taking and association with an anxiety trait." *Cereb Cortex* 19(4): 839-848.

Li, C. S., C. Huang, P. Yan, P. Paliwal, R. T. Constable and R. Sinha (2008). "Neural correlates of post-error slowing during a stop signal task: a functional magnetic resonance imaging study." *J Cogn Neurosci* 20(6): 1021-1029.

Li, C. S., P. Yan, K. L. Bergquist and R. Sinha (2007). "Greater activation of the "default" brain regions predicts stop signal errors." *Neuroimage* 38(3): 640-648.

Li, J., X. Y. Li, D. F. Feng and L. Gu (2011). "Quantitative evaluation of microscopic injury with diffusion tensor imaging in a rat model of diffuse axonal injury." *The Eur J Neurosci* 33(5): 933-945.

Limbrick-Oldfield, E. H., J. C. Brooks, R. J. Wise, F. Padormo, J. V. Hajnal, C. F. Beckmann and M. A. Ungless (2012). "Identification and characterisation of midbrain nuclei using optimised functional magnetic resonance imaging." *Neuroimage* 59(2): 1230-1238.

Logan, G. D., W. B. Cowan and K. A. Davis (1984). "On the ability to inhibit simple and choice reaction time responses: a model and a method." *J Exp Psychol Human* 10(2): 276-291.

Logan, G. D., R. J. Schachar and R. Tannock (1997). "Impulsivity and inhibitory control." *Psychol Sci* 8(1): 60-64.

Lowenstein, D. H. (2009). "Traumatic brain injury: a glimpse of order among the chaos?" *Ann Neurol* 66(4): A7-8.

Luu, P., T. Flaisch and D. M. Tucker (2000). "Medial frontal cortex in action monitoring." *J Neurosci* 20(1): 464-469.

Maas, A. I., N. Stocchetti and R. Bullock (2008). "Moderate and severe traumatic brain injury in adults." *Lancet Neurol* 7(8): 728-741.

Mac Donald, C. L., K. Dikranian, P. Bayly, D. Holtzman and D. Brody (2007). "Diffusion tensor imaging reliably detects experimental traumatic axonal injury and indicates approximate time of injury." *J Neurosci* 27(44): 11869-11876.

Mac Donald, C. L., K. Dikranian, S. K. Song, P. V. Bayly, D. M. Holtzman and D. L. Brody (2007). "Detection of traumatic axonal injury with diffusion tensor imaging in a mouse model of traumatic brain injury." *Exp Neurol* 205(1): 116-131.

MacDonald, A. W., 3rd, J. D. Cohen, V. A. Stenger and C. S. Carter (2000). "Dissociating the role of the dorsolateral prefrontal and anterior cingulate cortex in cognitive control." *Science* 288(5472): 1835-1838.

Magno, E., J. J. Foxe, S. Molholm, I. H. Robertson and H. Garavan (2006). "The anterior cingulate and error avoidance." *J Neurosci* 26(18): 4769-4773.

Mainero, C., P. Pantano, F. Caramia and C. Pozzilli (2006). "Brain reorganization during attention and memory tasks in multiple sclerosis: insights from functional MRI studies." *J Neurol Sci* 245(1-2): 93-98.

Malec, J. F., A. W. Brown, C. L. Leibson, J. T. Flaada, J. N. Mandrekar, N. N. Diehl and P. K. Perkins (2007). "The mayo classification system for traumatic brain injury severity." *J Neurotraum* 24(9): 1417-1424.

Manly, T., A. M. Owen, L. McAvinue, A. Datta, G. H. Lewis, S. K. Scott, C. Rorden, J. Pickard and I. H. Robertson (2003). "Enhancing the sensitivity of a sustained attention task to frontal damage: convergent clinical and functional imaging evidence." *Neurocase* 9(4): 340-349.

Margulies, D. S., J. L. Vincent, C. Kelly, G. Lohmann, L. Q. Uddin, B. B. Biswal, A. Villringer, F. X. Castellanos, M. P. Milham and M. Petrides (2009). "Precuneus

shares intrinsic functional architecture in humans and monkeys." *P Natl Acad Sci USA* 106(47): 20069-20074.

Marquez de la Plata, C., A. Ardelean, D. Koovakkattu, P. Srinivasan, A. Miller, V. Phuong, C. Harper, C. Moore, A. Whittemore, C. Madden, R. Diaz-Arrastia and M. Devous, Sr. (2007). "Magnetic resonance imaging of diffuse axonal injury: quantitative assessment of white matter lesion volume." *J Neurotraum* 24(4): 591-598.

Marshall, L. F., S. B. Marshall, M. R. Klauber, M. Van Berkum Clark, H. Eisenberg, J. A. Jane, T. G. Luerksen, A. Marmarou and M. A. Foulkes (1992). "The diagnosis of head injury requires a classification based on computed axial tomography." *J Neurotraum* 9 Suppl 1: S287-292.

Martins, E. T., M. N. Linhares, D. S. Sousa, H. K. Schroeder, J. Meinerz, L. A. Rigo, M. M. Bertotti, J. Gullo, A. Hohl, F. Dal-Pizzol and R. Walz (2009). "Mortality in severe traumatic brain injury: a multivariate analysis of 748 Brazilian patients from Florianopolis City." *J Trauma* 67(1): 85-90.

Matthews, B. R. (2009). "Cognitive Neurology: a clinical textbook." Oxford University Press

Mayer, A. R., J. Ling, M. V. Mannell, C. Gasparovic, J. P. Phillips, D. Doezema, R. Reichard and R. A. Yeo (2010). "A prospective diffusion tensor imaging study in mild traumatic brain injury." *Neurology* 74(8): 643-650.

Mayer, A. R., M. V. Mannell, J. Ling, C. Gasparovic and R. A. Yeo (2011). "Functional connectivity in mild traumatic brain injury." *Hum Brain Mapp* 32(11): 1825-1835.

Mcallister, T. W., L. A. Flashman, M. B. Sparling and A. J. Saykin (2004). "Working memory deficits after traumatic brain injury: catecholaminergic mechanisms and prospects for treatment-a review." *Brain Inj* 18(4): 331-350.

McAllister, T. W., A. J. Saykin, L. A. Flashman, M. B. Sparling, S. C. Johnson, S. J. Guerin, A. C. Mamourian, J. B. Weaver and N. Yanofsky (1999). "Brain activation

during working memory 1 month after mild traumatic brain injury: a functional MRI study." *Neurology* 53(6): 1300-1308.

McCrea, M., L. Prichep, M. R. Powell, R. Chabot and W. B. Barr (2010). "Acute effects and recovery after sport-related concussion: a neurocognitive and quantitative brain electrical activity study." *J Head Trauma Rehab* 25(4): 283-292.

McDowell, S., J. Whyte and M. D'Esposito (1997). "Working memory impairments in traumatic brain injury: evidence from a dual-task paradigm." *Neuropsychologia* 35(10): 1341-1353.

McKeown, M. J., T. P. Jung, S. Makeig, G. Brown, S. S. Kindermann, T. W. Lee and T. J. Sejnowski (1998). "Spatially independent activity patterns in functional MRI data during the stroop color-naming task." *P Natl Acad Sci USA* 95(3): 803-810.

McMillan, T. and G. Teasdale (2007). "Death rate is increased for at least 7 years after head injury: a prospective study." *Brain* 130(10): 2520-2527.

McMillan, T. M., G. M. Teasdale and E. Stewart (2012). "Disability in young people and adults after head injury: 12-14 year follow-up of a prospective cohort." *J Neurol Neurosurg Ps* 83(11): 1086-1091.

McMillan, T. M., G. M. Teasdale, C. J. Weir and E. Stewart (2011). "Death after head injury: the 13 year outcome of a case control study." *J Neurol Neurosurg Ps* 82(8): 931-935.

Meaney, D. F. and D. H. Smith (2011). "Biomechanics of concussion." *Clin Sport Med* 30(1): 19-31, vii.

Meaney, D. F., D. H. Smith, D. I. Shreiber, A. C. Bain, R. T. Miller, D. T. Ross and T. A. Gennarelli (1995). "Biomechanical analysis of experimental diffuse axonal injury." *J Neurotraum* 12(4): 689-694.

Medana, I. M. and M. M. Esiri (2003). "Axonal damage: a key predictor of outcome in human CNS diseases." *Brain* 126(3): 515-530.

Medford, N. and H. D. Critchley (2010). "Conjoint activity of anterior insular and anterior cingulate cortex: awareness and response." *Brain Struct Funct* 214(5-6): 535-549.

Mehta, M. A., R. Swainson, A. D. Ogilvie, B. Sahakian and T. W. Robbins (2001). "Improved short-term spatial memory but impaired reversal learning following the dopamine D2 agonist bromocriptine in human volunteers." *Psychopharmacology* 159(1): 10-20.

Menon, D. K., K. Schwab, D. W. Wright and A. I. Maas (2010). "Position statement: definition of traumatic brain injury." *Arch Phys Med Rehab* 91(11): 1637-1640.

Menon, R. S., S. Ogawa, S. G. Kim, J. M. Ellermann, H. Merkle, D. W. Tank and K. Ugurbil (1992). "Functional brain mapping using magnetic resonance imaging. Signal changes accompanying visual stimulation." *Invest Radiol* 27 Suppl 2: S47-53.

Menon, V. (2011). "Large-scale brain networks and psychopathology: a unifying triple network model." *Trends Cogn Sci* 15(10): 483-506.

Menon, V. and L. Q. Uddin (2010). "Saliency, switching, attention and control: a network model of insula function." *Brain Struct Funct* 214(5-6): 655-667.

Messe, A., S. Caplain, G. Paradot, D. Garrigue, J. F. Mineo, G. Soto Ares, D. Ducreux, F. Vignaud, G. Rozec, H. Desal, M. Pelegrini-Issac, M. Montreuil, H. Benali and S. Lehericy (2011). "Diffusion tensor imaging and white matter lesions at the subacute stage in mild traumatic brain injury with persistent neurobehavioral impairment." *Hum Brain Mapp* 32(6): 999-1011.

Mesulam, M. M. (1981). "A cortical network for directed attention and unilateral neglect." *Ann Neurol* 10(4): 309-325.

Mesulam, M. M. (1990). "Large-scale neurocognitive networks and distributed processing for attention, language, and memory." *Ann Neurol* 28(5): 597-613.

Miles, L., R. I. Grossman, G. Johnson, J. S. Babb, L. Diller and M. Inglese (2008). "Short-term DTI predictors of cognitive dysfunction in mild traumatic brain injury." *Brain Inj* 22(2): 115-122.

Miller, E. K. (2000). "The prefrontal cortex and cognitive control." *Nat Rev Neurosci* 1(1): 59-65.

Milner, B. (1963). "Effects of different brain lesions on card sorting: The role of the frontal lobes." *Arch Neurol* 9(1): 90-00.

Miltner, W. H. R., C. H. Braun and M. G. H. Coles (1997). "Event-related brain potentials following incorrect feedback in a time-estimation task: Evidence for a "generic" neural system for error detection." *J Cogn Neurosci* 9(6): 788-798.

Mittal, S., Z. Wu, J. Neelavalli and E. M. Haacke (2009). "Susceptibility-weighted imaging: technical aspects and clinical applications, part 2." *Am J Neurorad* 30(2): 232-252.

Mittl, R. L., R. I. Grossman, J. F. Hiehle, R. W. Hurst, D. R. Kauder, T. A. Gennarelli and G. W. Alburger (1994). "Prevalence of MR evidence of diffuse axonal injury in patients with mild head injury and normal head CT findings." *Am J Neurorad* 15(8): 1583-1589.

Modinos, G., J. Ormel and A. Aleman (2009). "Activation of Anterior Insula during Self-Reflection." *PLoS One* 4(2): e4618.

Modirrousta, M. and L. K. Fellows (2008). "Dorsal medial prefrontal cortex plays a necessary role in rapid error prediction in humans." *J Neurosci* 28(51): 14000-14005.

Moriguchi, Y., T. Ohnishi, R. D. Lane, M. Maeda, T. Mori, K. Nemoto, H. Matsuda and G. Komaki (2006). "Impaired self-awareness and theory of mind: an fMRI study of mentalizing in alexithymia." *Neuroimage* 32(3): 1472-1482.

Muller, N. G. and R. T. Knight (2006). "The functional neuroanatomy of working memory: contributions of human brain lesion studies." *Neuroscience* 139(1): 51-58.

Murata, Y., K. Sakatani, T. Hoshino, N. Fujiwara, T. Kano, S. Nakamura and Y. Katayama (2006). "Effects of cerebral ischemia on evoked cerebral blood oxygenation responses and BOLD contrast functional MRI in stroke patients." *Stroke* 37(10): 2514-2520.

Murphy, C. F., F. M. Gunning-Dixon, M. J. Hoptman, K. O. Lim, B. Ardekani, J. K. Shields, J. Hrabe, D. Kanellopoulos, B. R. Shanmugham and G. S. Alexopoulos (2007). "White-matter integrity predicts stroop performance in patients with geriatric depression." *Biol Psychiat* 61(8): 1007-1010.

Nakamura, S., K. Sakatani, T. Kano, T. Hoshino, N. Fujiwara, Y. Murata and Y. Katayama (2010). "Effects of revascularisation on evoked cerebral blood oxygenation responses in stroke patients." *Adv Exp Med Biol* 662: 525-530.

Natesan, S. and S. Kapur (2012). "Antipsychotic therapy over half a century: a tale of discovery from chlorpromazine to aripiprazole." *Nat Med J Ind* 25(4): 193-195.

Naunheim, R. S., M. Treaster, J. English, T. Casner and R. Chabot (2010). "Use of brain electrical activity to quantify traumatic brain injury in the emergency department." *Brain Inj* 24(11): 1324-1329.

Nelson, L. D., E. M. Bernat, C. B. Holroyd, W. J. Gehring and C. J. Patrick (2008). "Loss and error information impact feedback-locked brain potentials in a gambling task." *Int J Psychophysiol* 69(3): 208-208.

Newcombe, V. F., J. G. Outtrim, D. A. Chatfield, A. Manktelow, P. J. Hutchinson, J. P. Coles, G. B. Williams, B. J. Sahakian and D. K. Menon (2011). "Parcellating the neuroanatomical basis of impaired decision-making in traumatic brain injury." *Brain* 134(3): 759-768.

Newsome, M. R., J. L. Steinberg, R. S. Scheibel, M. Troyanskaya, Z. Chu, G. Hanten, H. Lu, S. Lane, X. Lin, J. V. Hunter, C. Vasquez, J. Zientz, X. Li, E. A. Wilde and H. S. Levin (2008). "Effects of traumatic brain injury on working memory-related brain activation in adolescents." *Neuropsychology* 22(4): 419-425.

NICE (2007). *Triage, assessment, investigation and early management of head injury in infants, children and adults.*

Nichols, T., M. Brett, J. Andersson, T. Wager and J. B. Poline (2005). "Valid conjunction inference with the minimum statistic." *Neuroimage* 25(3): 653-660.

Nichols, T. and S. Hayasaka (2003). "Controlling the familywise error rate in functional neuroimaging: a comparative review." *Stat Method Med Res* 12(5): 419-446.

Niogi, S. N., P. Mukherjee, J. Ghajar, C. Johnson, R. A. Kolster, R. Sarkar, H. Lee, M. Meeker, R. D. Zimmerman, G. T. Manley and B. D. McCandliss (2008). "Extent of microstructural white matter injury in postconcussive syndrome correlates with impaired cognitive reaction time: a 3T diffusion tensor imaging study of mild traumatic brain injury." *Am J Neuroradiol* 29(5): 967-973.

Nordstrom, A., B. B. Edin, S. Lindstrom and P. Nordstrom (2013). "Cognitive function and other risk factors for mild traumatic brain injury in young men: nationwide cohort study." *Brit Med J* 346: f723.

Northoff, G. and F. Bermpohl (2004). "Cortical midline structures and the self." *Trends Cogn Sci* 8(3): 102-107.

Norton, L., R. M. Hutchison, G. B. Young, D. H. Lee, M. D. Sharpe and S. M. Mirsattari (2012). "Disruptions of functional connectivity in the default mode network of comatose patients." *Neurology* 78(3): 175-181.

O'Keefe, F., P. Dockree, P. Moloney, S. Carton and I. H. Robertson (2007). "Awareness of deficits in traumatic brain injury: a multidimensional approach to assessing metacognitive knowledge and online-awareness." *J Int Neuropsych Soc* 13(1): 38-49.

O'Keefe, F. M., P. M. Dockree and I. H. Robertson (2004). "Poor insight in traumatic brain injury mediated by impaired error processing? Evidence from electrodermal activity." *Brain Res Cogn Brain Res* 22(1): 101-112.

O'Sullivan, M., D. K. Jones, P. E. Summers, R. G. Morris, S. C. Williams and H. S. Markus (2001). "Evidence for cortical "disconnection" as a mechanism of age-related cognitive decline." *Neurology* 57(4): 632-638.

Oakes, T. R., A. S. Fox, T. Johnstone, M. K. Chung, N. Kalin and R. J. Davidson (2007). "Integrating VBM into the General Linear Model with voxelwise anatomical covariates." *Neuroimage* 34(2): 500-508.

Obenaus, A., M. Robbins, G. Blanco, N. R. Galloway, E. Snissarenko, E. Gillard, S. Lee and M. Curras-Collazo (2007). "Multi-modal magnetic resonance imaging alterations in two rat models of mild neurotrauma." *J Neurotraum* 24(7): 1147-1160.

Ochsner, K. N., J. S. Beer, E. R. Robertson, J. C. Cooper, J. D. Gabrieli, J. F. Kihlstrom and M. D'Esposito (2005). "The neural correlates of direct and reflected self-knowledge." *Neuroimage* 28(4): 797-814.

Ogawa, S., T. M. Lee, A. R. Kay and D. W. Tank (1990). "Brain magnetic resonance imaging with contrast dependent on blood oxygenation." *P Natl Acad Sci USA* 87(24): 9868-9872.

Ogawa, S., D. W. Tank, R. Menon, J. M. Ellermann, S. G. Kim, H. Merkle and K. Ugurbil (1992). "Intrinsic signal changes accompanying sensory stimulation: functional brain mapping with magnetic resonance imaging." *P Natl Acad Sci USA* 89(13): 5951-5955.

Oliveira, F. T., J. J. McDonald and D. Goodman (2007). "Performance monitoring in the anterior cingulate is not all error related: expectancy deviation and the representation of action-outcome associations." *J Cogn Neurosci* 19(12): 1994-2004.

Ornstein, T. J., H. S. Levin, S. Chen, G. Hanten, L. Ewing-Cobbs, M. Dennis, M. Barnes, J. E. Max, G. D. Logan and R. Schachar (2009). "Performance monitoring in children following traumatic brain injury." *J Child Psychol Psyc* 50(4): 506-513.

Palaniyappan, L., P. Mallikarjun, V. Joseph, T. P. White and P. F. Liddle (2011). "Reality distortion is related to the structure of the salience network in schizophrenia." *Psychol Med* 41(8): 1701-1708.

Park, J. H., S. W. Park, S. H. Kang, T. K. Nam, B. K. Min and S. N. Hwang (2009). "Detection of traumatic cerebral microbleeds by susceptibility-weighted image of MRI." *J Korean Neurosurg Soc* 46(4): 365-369.

Park, N. W. and J. L. Ingles (2001). "Effectiveness of attention rehabilitation after an acquired brain injury: a meta-analysis." *Neuropsychology* 15(2): 199-210.

Paulus, M. P. and M. B. Stein (2006). "An insular view of anxiety." *Biol Psychiat* 60(4): 383-387.

Penny, W. D. (2012). "Comparing dynamic causal models using AIC, BIC and free energy." *Neuroimage* 59(1): 319-330.

Penny, W. D., K. E. Stephan, J. Daunizeau, M. J. Rosa, K. J. Friston, T. M. Schofield and A. P. Leff (2010). "Comparing families of dynamic causal models." *PLoS Comp Biol* 6(3): e1000709.

Penny, W. D., K. E. Stephan, A. Mechelli and K. J. Friston (2004). "Comparing dynamic causal models." *Neuroimage* 22(3): 1157-1172.

Perin, B., O. Godefroy, S. Fall and G. de Marco (2010). "Alertness in young healthy subjects: an fMRI study of brain region interactivity enhanced by a warning signal." *Brain Cogn* 72(2): 271-281.

Perlstein, W. M., M. A. Cole, J. A. Demery, P. J. Seignourel, N. K. Dixit, M. J. Larson and R. W. Briggs (2004). "Parametric manipulation of working memory load in traumatic brain injury: behavioral and neural correlates." *J Int Neuropsych Soc* 10(5): 724-741.

Perlstein, W. M., M. J. Larson, V. M. Dotson and K. G. Kelly (2006). "Temporal dissociation of components of cognitive control dysfunction in severe TBI: ERPs and the cued-Stroop task." *Neuropsychologia* 44(2): 260-274.

Plenger, P. M., C. E. Dixon, R. M. Castillo, R. F. Frankowski, S. A. Yablon and H. S. Levin (1996). "Subacute methylphenidate treatment for moderate to moderately severe traumatic brain injury: a preliminary double-blind placebo-controlled study." *Arch Phys Med Rehab* 77(6): 536-540.

Polo, M. D., P. Newton, D. Rogers, C. Escera and S. Butler (2002). "ERPs and behavioural indices of long-term preattentive and attentive deficits after closed head injury." *Neuropsychologia* 40(13): 2350-2359.

Ponsford, J., K. Draper, M. SchONberger, A. Baddeley, H. Emslie, I. Nimmo-Smith, A. Benton, K. Hamsher, G. Rey and A. Sivan (2008). "Functional outcome 10 years

after traumatic brain injury: Its relationship with demographic, injury severity, and cognitive and emotional status." *J Int Neuropsych Soc* 14(2): 233.

Posner, M. I. and S. E. Petersen (1990). "The attention system of the human brain." *Annu Rev Neurosci* 13: 25-42.

Povlishock, J. T. (1993). "Pathobiology of traumatically induced axonal injury in animals and man." *Ann Emerg Med* 22(6): 980-986.

Povlishock, J. T., D. P. Becker, C. L. Cheng and G. W. Vaughan (1983). "Axonal change in minor head injury." *J Neuropath Exp Neurol* 42(3): 225-242.

Price, C. J., J. Crinion and K. J. Friston (2006). "Design and analysis of fMRI studies with neurologically impaired patients." *J Magn Reson Im* 23(6): 816-826.

Prichep, L. S., M. McCrea, W. Barr, M. Powell and R. J. Chabot (2012). "Time Course of Clinical and Electrophysiological Recovery After Sport-Related Concussion." *J Head Trauma Rehab*.

Prigatano, G. P. and I. M. Altman (1990). "Impaired awareness of behavioral limitations after traumatic brain injury." *Arch Phys Med Rehab* 71(13): 1058-1064.

Prigatano, G. P., I. M. Altman and K. P. O'brien (1990). "Behavioral limitations that traumatic-brain-injured patients tend to underestimate." *Clin Neuropsychol* 4(2): 163-176.

Prigatano, G. P. and D. L. Schacter (1991). *Awareness of deficit after brain injury: Clinical and theoretical issues*, Oxford University Press.

Pykett, I. L., J. H. Newhouse, F. S. Buonanno, T. J. Brady, M. R. Goldman, J. P. Kistler and G. M. Pohost (1982). "Principles of nuclear magnetic resonance imaging." *Radiology* 143(1): 157-168.

Rabbitt, P. M. (1966). "Error correction time without external error signals." *Nature* 212(5060): 438.

Rabbitt, P. M. (1966). "Errors and error correction in choice-response tasks." *J Exp Psychol* 71(2): 264-272.

Rabbitt, P. M. (1968). "Three kinds of error-signalling responses in a serial choice task." *Q J Exp Psychol* 20(2): 179-188.

Raghanti, M. A., C. D. Stimpson, J. L. Marcinkiewicz, J. M. Erwin, P. R. Hof and C. C. Sherwood (2008). "Cortical dopaminergic innervation among humans, chimpanzees, and macaque monkeys: a comparative study." *Neuroscience* 155(1): 203-220.

Raghupathi, R., D. I. Graham and T. K. McIntosh (2000). "Apoptosis after traumatic brain injury." *J Neurotraum* 17(10): 927-938.

Raichle, M. E., A. M. MacLeod, A. Z. Snyder, W. J. Powers, D. A. Gusnard and G. L. Shulman (2001). "A default mode of brain function." *P Natl Acad Sci USA* 98(2): 676-682.

Raichle, M. E., A. M. MacLeod, A. Z. Snyder, W. J. Powers, D. A. Gusnard and G. L. Shulman (2001). "A default mode of brain function." *P Natl Acad Sci USA* 98(2): 676-682.

Rainville, P., G. H. Duncan, D. D. Price, B. t. Carrier and M. C. Bushnell (1997). "Pain affect encoded in human anterior cingulate but not somatosensory cortex." *Science* 277(5328): 968-971.

Raja Beharelle, A., D. Tisserand, D. T. Stuss, A. R. McIntosh and B. Levine (2011). "Brain activity patterns uniquely supporting visual feature integration after traumatic brain injury." *Front Hum Neurosci* 5: 164.

Rasmussen, I. A., J. Xu, I. K. Antonsen, J. Brunner, T. Skandsen, D. E. Axelson, E. M. Berntsen, S. Lydersen and A. Haberg (2008). "Simple dual tasking recruits prefrontal cortices in chronic severe traumatic brain injury patients, but not in controls." *J Neurotraum* 25(9): 1057-1070.

Reid-Arndt, S. A., C. Nehl and J. Hinkebein (2007). "The Frontal Systems Behaviour Scale (FrSBe) as a predictor of community integration following a traumatic brain injury." *Brain Inj* 21(13-14): 1361-1369.

Reitan, R. (1958). "The validity of the Trail Making test as an indicator of organic brain damage." *Percept Motor Skill* 8: 271-276

Ridderinkhof, K. R., M. Ullsperger, E. A. Crone and S. Nieuwenhuis (2004). "The role of the medial frontal cortex in cognitive control." *Science* 306(5695): 443-447.

Rios, M., J. A. Perianez and J. M. Munoz-Cespedes (2004). "Attentional control and slowness of information processing after severe traumatic brain injury." *Brain Inj* 18(3): 257-272.

Robertson, I. H., T. Manly, J. Andrade, B. T. Baddeley and J. Yiend (1997). "'Oops!': performance correlates of everyday attentional failures in traumatic brain injured and normal subjects." *Neuropsychologia* 35(6): 747-758.

Robertson, I. H., J. B. Mattingley, C. Rorden and J. Driver (1998). "Phasic alerting of neglect patients overcomes their spatial deficit in visual awareness." *Nature* 395(6698): 169-172.

Roebroeck, A., E. Formisano and R. Goebel (2005). "Mapping directed influence over the brain using Granger causality and fMRI." *Neuroimage* 25(1): 230-242.

Rowe, J. B., L. E. Hughes, R. A. Barker and A. M. Owen (2010). "Dynamic causal modelling of effective connectivity from fMRI: Are results reproducible and sensitive to Parkinson's disease and its treatment?" *Neuroimage* 52(3): 1015-1026.

Rueckert, L. and J. Grafman (1996). "Sustained attention deficits in patients with right frontal lesions." *Neuropsychologia* 34(10): 953-963.

Rushworth, M. F., M. E. Walton, S. W. Kennerley and D. M. Bannerman (2004). "Action sets and decisions in the medial frontal cortex." *Trends Cogn Sci* 8(9): 410-417.

Salmond, C. H., D. K. Menon, D. A. Chatfield, G. B. Williams, A. Pena, B. J. Sahakian and J. D. Pickard (2006). "Diffusion tensor imaging in chronic head injury survivors: correlations with learning and memory indices." *Neuroimage* 29(1): 117-124.

Scheibel, R. S., M. R. Newsome, J. L. Steinberg, D. A. Pearson, R. A. Rauch, H. Mao, M. Troyanskaya, R. G. Sharma and H. S. Levin (2007). "Altered brain activation during cognitive control in patients with moderate to severe traumatic brain injury." *Neurorehabilitation and neural repair* 21(1): 36-45.

Scheibel, R. S., D. A. Pearson, L. P. Faria, K. J. Kotrla, E. Aylward, J. Bachevalier and H. S. Levin (2003). "An fMRI study of executive functioning after severe diffuse TBI." *Brain Inj* 17(11): 919-930.

Scheid, R., C. Preul, O. Gruber, C. Wiggins and D. Y. von Cramon (2003). "Diffuse axonal injury associated with chronic traumatic brain injury: evidence from T2*-weighted gradient-echo imaging at 3 T." *Am J Neuroradiol* 24(6): 1049-1056.

Scheid, R., K. Walther, T. Guthke, C. Preul and D. Y. von Cramon (2006). "Cognitive sequelae of diffuse axonal injury." *Arch Neurol* 63(3): 418-424.

Schmitz, T. W., H. A. Rowley, T. N. Kawahara and S. C. Johnson (2006). "Neural correlates of self-evaluative accuracy after traumatic brain injury." *Neuropsychologia* 44(5): 762-773.

Schofield, T. M., W. D. Penny, K. E. Stephan, J. T. Crinion, A. J. Thompson, C. J. Price and A. P. Leff (2012). "Changes in auditory feedback connections determine the severity of speech processing deficits after stroke." *J Neurosci* 32(12): 4260-4270.

Seeley, W. W., R. K. Crawford, J. Zhou, B. L. Miller and M. D. Greicius (2009). "Neurodegenerative diseases target large-scale human brain networks." *Neuron* 62(1): 42-52.

Seeley, W. W., V. Menon, A. F. Schatzberg, J. Keller, G. H. Glover, H. Kenna, A. L. Reiss and M. D. Greicius (2007). "Dissociable intrinsic connectivity networks for salience processing and executive control." *J Neurosci* 27(9): 2349-2356.

Seignourel, P. J., D. L. Robins, M. J. Larson, J. A. Demery, M. Cole and W. M. Perlstein (2005). "Cognitive control in closed head injury: context maintenance dysfunction or prepotent response inhibition deficit?" *Neuropsychology* 19(5): 578-590.

Seung, H. S. (2009). "Reading the book of memory: sparse sampling versus dense mapping of connectomes." *Neuron* 62(1): 17-29.

Sharp, D. J., C. F. Beckmann, R. Greenwood, K. M. Kinnunen, V. Bonnelle, X. De Boissezon, J. H. Powell, S. J. Counsell, M. C. Patel and R. Leech (2011). "Default mode network functional and structural connectivity after traumatic brain injury." *Brain* 134(8): 2233-2247.

Sharp, D. J., V. Bonnelle, X. De Boissezon, C. F. Beckmann, S. G. James, M. C. Patel and M. A. Mehta (2010). "Distinct frontal systems for response inhibition, attentional capture, and error processing." *P Natl Acad Sci USA* 107(13): 6106-6111.

Sharp, D. J., S. K. Scott, M. A. Mehta and R. J. Wise (2006). "The Neural Correlates of Declining Performance with Age: Evidence for Age-Related Changes in Cognitive Control." *Cereb Cortex* 16: 1739-1749.

Sherer, M., T. Hart, T. G. Nick, J. Whyte, R. N. Thompson and S. A. Yablon (2003). "Early impaired self-awareness after traumatic brain injury." *Arch Phys Med Rehab* 84(2): 168-176.

Sherer, M., T. Hart, J. Whyte, T. G. Nick and S. A. Yablon (2005). "Neuroanatomic basis of impaired self-awareness after traumatic brain injury: findings from early computed tomography." *J Head Trauma Rehab* 20(4): 287-300.

Sherer, M., A. M. Sander, T. G. Nick, W. M. High, Jr., J. F. Malec and M. Rosenthal (2002). "Early cognitive status and productivity outcome after traumatic brain injury: findings from the TBI model systems." *Arch Phys Med Rehab* 83(2): 183-192.

Sherer, M., J. Stouter, T. Hart, R. Nakase-Richardson, J. Olivier, E. Manning and S. A. Yablon (2006). "Computed tomography findings and early cognitive outcome after traumatic brain injury." *Brain Inj* 20(10): 997-1005.

Shulman, G. L., J. A. Fiez, M. Corbetta, R. L. Buckner, F. M. Miezin, M. E. Raichle and S. E. Petersen (1997). "Common Blood Flow Changes across Visual Tasks: II. Decreases in Cerebral Cortex." *J Cogn Neurosci* 9: 648-663.

Shumskaya, E., T. M. Andriessen, D. G. Norris and P. E. Vos (2012). "Abnormal whole-brain functional networks in homogeneous acute mild traumatic brain injury." *Neurology* 79(2): 175-182.

Sidaros, A., A. W. Engberg, K. Sidaros, M. G. Liptrot, M. Herning, P. Petersen, O. B. Paulson, T. L. Jernigan and E. Rostrup (2008). "Diffusion tensor imaging during recovery from severe traumatic brain injury and relation to clinical outcome: a longitudinal study." *Brain* 131(2): 559-572.

Signorini, D. F., P. J. Andrews, P. A. Jones, J. M. Wardlaw and J. D. Miller (1999). "Predicting survival using simple clinical variables: a case study in traumatic brain injury." *J Neurol Neurosurg Ps* 66(1): 20-25.

Simon, J. R. (1969). "Reactions toward the source of stimulation." *J Exp Psychol* 81(1): 174-176.

Simon, J. R. and A. M. Small, Jr. (1969). "Processing auditory information: interference from an irrelevant cue." *J Appl Psychol* 53(5): 433-435.

Singh-Curry, V. and M. Husain (2009). "The functional role of the inferior parietal lobe in the dorsal and ventral stream dichotomy." *Neuropsychologia* 47(6): 1434-1448.

Singh, K. D. and I. P. Fawcett (2008). "Transient and linearly graded deactivation of the human default-mode network by a visual detection task." *Neuroimage* 41(1): 100-112.

Smith, D. H., D. F. Meaney and W. H. Shull (2003). "Diffuse axonal injury in head trauma." *J Head Trauma Rehab* 18(4): 307-316.

Smith, S. M. (2002). "Fast robust automated brain extraction." *Hum Brain Mapp* 17(3): 143-155.

Smith, S. M., P. T. Fox, K. L. Miller, D. C. Glahn, P. M. Fox, C. E. Mackay, N. Filippini, K. E. Watkins, R. Toro, A. R. Laird and C. F. Beckmann (2009). "Correspondence of the brain's functional architecture during activation and rest." *P Natl Acad Sci USA* 106(31): 13040-13045.

Smith, S. M., M. Jenkinson, H. Johansen-Berg, D. Rueckert, T. E. Nichols, C. E. Mackay, K. E. Watkins, O. Ciccarelli, M. Z. Cader, P. M. Matthews and T. E. Behrens (2006). "Tract-based spatial statistics: voxelwise analysis of multi-subject diffusion data." *Neuroimage* 31(4): 1487-1505.

Smith, S. M., M. Jenkinson, M. W. Woolrich, C. F. Beckmann, T. E. Behrens, H. Johansen-Berg, P. R. Bannister, M. De Luca, I. Drobnjak, D. E. Flitney, R. K. Niazy, J. Saunders, J. Vickers, Y. Zhang, N. De Stefano, J. M. Brady and P. M. Matthews (2004). "Advances in functional and structural MR image analysis and implementation as FSL." *Neuroimage* 23 Suppl 1: S208-219.

Smith, S. M., K. L. Miller, G. Salimi-Khorshidi, M. Webster, C. F. Beckmann, T. E. Nichols, J. D. Ramsey and M. W. Woolrich (2011). "Network modelling methods for FMRI." *Neuroimage* 54(2): 875-891.

Smits, M., G. C. Houston, D. W. Dippel, P. A. Wielopolski, M. W. Vernooij, P. J. Koudstaal, M. G. Hunink and A. van der Lugt (2010). "Microstructural brain injury in post-concussion syndrome after minor head injury." *Neuroradiology*.

Smits, M., M. G. Hunink, D. A. van Rijssel, H. M. Dekker, P. E. Vos, D. R. Kool, P. J. Nederkoorn, P. A. Hofman, A. Twijnstra, H. L. Tanghe and D. W. Dippel (2008). "Outcome after complicated minor head injury." *Am J Neuroradiol* 29(3): 506-513.

Soeda, A., T. Nakashima, A. Okumura, K. Kuwata, J. Shinoda and T. Iwama (2005). "Cognitive impairment after traumatic brain injury: a functional magnetic resonance imaging study using the Stroop task." *Neuroradiology* 47(7): 501-506.

Sommer, I. E., K. M. Diederer, J. D. Blom, A. Willems, L. Kushan, K. Slotema, M. P. Boks, K. Daalman, H. W. Hoek, S. F. Neggers and R. S. Kahn (2008). "Auditory verbal hallucinations predominantly activate the right inferior frontal area." *Brain* 131(12): 3169-3177.

Song, S. K., S. W. Sun, M. J. Ramsbottom, C. Chang, J. Russell and A. H. Cross (2002). "Dysmyelination revealed through MRI as increased radial (but unchanged axial) diffusion of water." *Neuroimage* 17(3): 1429-1436.

Sonuga-Barke, E. J. and F. X. Castellanos (2007). "Spontaneous attentional fluctuations in impaired states and pathological conditions: a neurobiological hypothesis." *Neurosci Biobehav R* 31(7): 977-986.

Soto, D., M. J. Funes, A. Guzman-Garcia, T. Warbrick, P. Rotshtein and G. W. Humphreys (2009). "Pleasant music overcomes the loss of awareness in patients with visual neglect." *P Natl Acad Sci USA* 106(14): 6011-6016.

Speech, T. J., S. M. Rao, D. C. Osmon and L. T. Sperry (1993). "A double-blind controlled study of methylphenidate treatment in closed head injury." *Brain Inj* 7(4): 333-338.

Spreng, R. N. (2012). "The fallacy of a "task-negative" network." *Front Psych* 3: 145.

Spreng, R. N., W. D. Stevens, J. P. Chamberlain, A. W. Gilmore and D. L. Schacter (2010). "Default network activity, coupled with the frontoparietal control network, supports goal-directed cognition." *Neuroimage* 53(1): 303-317.

Squarcina, L., A. Bertoldo, T. E. Ham, R. Heckemann and D. J. Sharp (2012). "A robust method for investigating thalamic white matter tracts after traumatic brain injury." *Neuroimage*.

Sridharan, D., D. J. Levitin and V. Menon (2008). "A critical role for the right fronto-insular cortex in switching between central-executive and default-mode networks." *P Natl Acad Sci USA* 105(34): 12569-12574.

Stein, M. B., A. N. Simmons, J. S. Feinstein and M. P. Paulus (2007). "Increased amygdala and insula activation during emotion processing in anxiety-prone subjects." *Am J Psychiat* 164(2): 318-327.

Stephan, K. E., W. D. Penny, J. Daunizeau, R. J. Moran and K. J. Friston (2009). "Bayesian model selection for group studies." *Neuroimage* 46(4): 1004-1017.

Stephan, K. E., W. D. Penny, R. J. Moran, H. E. den Ouden, J. Daunizeau and K. J. Friston (2010). "Ten simple rules for dynamic causal modeling." *Neuroimage* 49(4): 3099-3109.

Stevens, A. A., P. Skudlarski, J. C. Gatenby and J. C. Gore (2000). "Event-related fMRI of auditory and visual oddball tasks." *Magn Reson Imaging* 18(5): 495-502.

Stevens, M. C., D. Lovejoy, J. Kim, H. Oakes, I. Kureshi and S. T. Witt (2012). "Multiple resting state network functional connectivity abnormalities in mild traumatic brain injury." *Brain Imag Behav* 6(2): 293-318.

Strich, S. J. (1956). "Diffuse degeneration of the cerebral white matter in severe dementia following head injury." *J Neurol Neurosurg Ps* 19(3): 163-185.

Stroop, J. R. (1935). "Studies of interference in serial verbal reactions." *J Exp Psych* 18(6): 643.

Sturm, W., A. de Simone, B. J. Krause, K. Specht, V. Hesselmann, I. Radermacher, H. Herzog, L. Tellmann, H. W. Muller-Gartner and K. Willmes (1999). "Functional anatomy of intrinsic alertness: evidence for a fronto-parietal-thalamic-brainstem network in the right hemisphere." *Neuropsychologia* 37(7): 797-805.

Stuss, D. T., M. P. Alexander, T. Shallice, T. W. Picton, M. A. Binns, R. Macdonald, A. Borowiec and D. I. Katz (2005). "Multiple frontal systems controlling response speed." *Neuropsychologia* 43(3): 396-417.

Stuss, D. T., L. L. Stethem, H. Hugenholtz, T. Picton, J. Pivik and M. T. Richard (1989). "Reaction time after head injury: fatigue, divided and focused attention, and consistency of performance." *J Neurol Neurosurg Ps* 52(6): 742-748.

Sugiyama, K., T. Kondo, Y. Oouchida, Y. Suzukamo, S. Higano, M. Endo, H. Watanabe, K. Shindo and S. Izumi (2009). "Clinical utility of diffusion tensor imaging for evaluating patients with diffuse axonal injury and cognitive disorders in the chronic stage." *J Neurotraum* 26(11): 1879-1890.

Sun, S. W., H. F. Liang, A. H. Cross and S. K. Song (2008). "Evolving Wallerian degeneration after transient retinal ischemia in mice characterized by diffusion tensor imaging." *Neuroimage* 40(1): 1-10.

Swick, D. and A. U. Turken (2002). "Dissociation between conflict detection and error monitoring in the human anterior cingulate cortex." *P Natl Acad Sci USA* 99(25): 16354-16359.

Tagliaferri, F., C. Compagnone, M. Korsic, F. Servadei and J. Kraus (2006). "A systematic review of brain injury epidemiology in Europe." *Acta Neurochirurgica* 148(3): 255-268; discussion 268.

Taren, A. A., V. Venkatraman and S. A. Huettel (2011). "A parallel functional topography between medial and lateral prefrontal cortex: evidence and implications for cognitive control." *J Neurosci* 31(13): 5026-5031.

Taylor, J. G. (1997). "Neural networks for consciousness." *Neural Networks* 10(7): 1207-1225.

Tennant, A. (2005). "Admission to hospital following head injury in England: incidence and socio-economic associations." *BMC Pub Health* 5: 21.

Thompson, E. and F. J. Varela (2001). "Radical embodiment: neural dynamics and consciousness." *Trends Cogn Sci* 5(10): 418-425.

Thornhill, S., G. M. Teasdale, G. D. Murray, J. McEwen, C. W. Roy and K. I. Penny (2000). "Disability in young people and adults one year after head injury: prospective cohort study." *Brit Med J* 320(7250): 1631-1635.

Thurman, D. J., C. Alverson, K. A. Dunn, J. Guerrero and J. E. Sniezek (1999). "Traumatic brain injury in the United States: A public health perspective." *J Head Trauma Rehab* 14(6): 602-615.

Turner, G. R. and B. Levine (2008). "Augmented neural activity during executive control processing following diffuse axonal injury." *Neurology* 71(11): 812-818.

Turner, G. R., A. R. McIntosh and B. Levine (2011). "Prefrontal Compensatory Engagement in TBI is due to Altered Functional Engagement Of Existing Networks and not Functional Reorganization." *Front Syst Neurosci* 5: 9.

Turner, R., A. Howseman, G. E. Rees, O. Josephs and K. Friston (1998). "Functional magnetic resonance imaging of the human brain: data acquisition and analysis." *Experimental brain research. Experimentelle Hirnforschung. Experimentation cerebrale* 123(1-2): 5-12.

Uddin, L. Q. and V. Menon (2009). "The anterior insula in autism: under-connected and under-examined." *Neurosci Biobehav R* 33(8): 1198-1203.

Uddin, L. Q., K. Supekar, H. Amin, E. Rykhlevskaia, D. A. Nguyen, M. D. Greicius and V. Menon (2010). "Dissociable connectivity within human angular gyrus and intraparietal sulcus: evidence from functional and structural connectivity." *Cereb Cortex* 20(11): 2636-2646.

Ullsperger, M., H. A. Harsay, J. R. Wessel and K. R. Ridderinkhof (2010). "Conscious perception of errors and its relation to the anterior insula." *Brain Struct Funct* 214(5-6): 629-643.

Ullsperger, M., H. Nittono and D. Y. von Cramon (2007). "When goals are missed: dealing with self-generated and externally induced failure." *Neuroimage* 35(3): 1356-1364.

Ullsperger, M. and D. Y. von Cramon (2003). "Error monitoring using external feedback: specific roles of the habenular complex, the reward system, and the cingulate motor area revealed by functional magnetic resonance imaging." *J Neurosci* 23(10): 4308-4314.

Ullsperger, M. and D. Y. von Cramon (2004). "Neuroimaging of performance monitoring: error detection and beyond." *Cortex* 40(4-5): 593-604.

van den Heuvel, M. P., R. C. Mandl, R. S. Kahn and H. E. Hulshoff Pol (2009). "Functionally linked resting-state networks reflect the underlying structural connectivity architecture of the human brain." *Hum brain Mapp* 30(10): 3127-3141.

van der Meer, L., S. Costafreda, A. Aleman and A. S. David (2010). "Self-reflection and the brain: A theoretical review and meta-analysis of neuroimaging studies with implications for schizophrenia." *Neurosci Biobehav R* 34(6): 935-946

Vanderploeg, R. D., H. G. Belanger, J. D. Duchnick and G. Curtiss (2007). "Awareness problems following moderate to severe traumatic brain injury: Prevalence, assessment methods, and injury correlates." *J Rehabil Res Dev* 44(7): 937-950.

Vanderploeg, R. D., G. Curtiss and H. G. Belanger (2005). "Long-term neuropsychological outcomes following mild traumatic brain injury." *J Int Neuropsychol Soc* 11(3): 228-236.

Vanhaudenhuyse, A., Q. Noirhomme, L. J. Tshibanda, M. A. Bruno, P. Boveroux, C. Schnakers, A. Soddu, V. Perlberg, D. Ledoux, J. F. Brichtant, G. Moonen, P. Maquet, M. D. Greicius, S. Laureys and M. Boly (2010). "Default network connectivity reflects the level of consciousness in non-communicative brain-damaged patients." *Brain* 133(1): 161-171.

Verbruggen, F. and G. D. Logan (2008). "After-effects of goal shifting and response inhibition: a comparison of the stop-change and dual-task paradigms." *Q J Exp Psychol* 61(8): 1151-1159.

Verbruggen, F. and G. D. Logan (2008). "Response inhibition in the stop-signal paradigm." *Trends Cogn Sci* 12(11): 418-424.

Verbruggen, F. and G. D. Logan (2009). "Models of response inhibition in the stop-signal and stop-change paradigms." *Neurosci Biobehav R* 33(5): 647-661.

Vincent, J. L., I. Kahn, A. Z. Snyder, M. E. Raichle and R. L. Buckner (2008). "Evidence for a frontoparietal control system revealed by intrinsic functional connectivity." *J Neurophysiol* 100(6): 3328-3342.

Walton, M. E., P. L. Croxson, T. E. Behrens, S. W. Kennerley and M. F. Rushworth (2007). "Adaptive decision making and value in the anterior cingulate cortex." *Neuroimage* 36 Suppl 2: T142-154.

Walton, M. E., P. L. Croxson, M. F. Rushworth and D. M. Bannerman (2005). "The mesocortical dopamine projection to anterior cingulate cortex plays no role in guiding effort-related decisions." *Behav Neurosci* 119(1): 323-328.

Ward, N. S., J. M. Newton, O. B. Swayne, L. Lee, A. J. Thompson, R. J. Greenwood, J. C. Rothwell and R. S. Frackowiak (2006). "Motor system activation after subcortical stroke depends on corticospinal system integrity." *Brain* 129(3): 809-819.

Wardlaw, J. M., V. J. Easton and P. Statham (2002). "Which CT features help predict outcome after head injury?" *J Neurol Neurosurg Ps* 72(2): 188-192; discussion 151.

Wechsler, D. (1997). *Wechsler Memory Scale- Third Edition: Administration and Scoring Manual*. San Antonio, TX: Psychological Corporation.

Wechsler, D. (1999). *WASI: Wechsler Abbreviated Scale of Intelligence*. San Antonio, TX: The Psychological Corporation.

Wechsler, D. (2001). *Wechsler Test of Adult Reading*. San Antonio, TX: The Psychological Corporation.

Weissman, D. H., K. C. Roberts, K. M. Visscher and M. G. Woldorff (2006). "The neural bases of momentary lapses in attention." *Nat Neurosci* 9(7): 971-978.

Werner, C. and K. Engelhard (2007). "Pathophysiology of traumatic brain injury." *Brit J Anaesth* 99(1): 4-9.

White, T. P., V. Joseph, S. T. Francis and P. F. Liddle (2010). "Aberrant salience network (bilateral insula and anterior cingulate cortex) connectivity during information processing in schizophrenia." *Schizophr Res* 123(2): 105-115.

Whitnall, L., T. M. McMillan, G. D. Murray and G. M. Teasdale (2006). "Disability in young people and adults after head injury: 5-7 year follow up of a prospective cohort study." *J Neurol Neurosurg Ps* 77(5): 640-645.

Whyte, J., T. Hart, M. Vaccaro, P. Grieb-Neff, A. Risser, M. Polansky and H. B. Coslett (2004). "Effects of methylphenidate on attention deficits after traumatic brain

injury: a multidimensional, randomized, controlled trial." *American journal of physical medicine & rehabilitation / Association of Academic Physiatrists* 83(6): 401-420.

Wiech, K., M. Ploner and I. Tracey (2008). "Neurocognitive aspects of pain perception." *Trends Cogn Sci* 12(8): 306-313.

Wilde, E. A., S. R. McCauley, J. V. Hunter, E. D. Bigler, Z. Chu, Z. J. Wang, G. R. Hanten, M. Troyanskaya, R. Yallampalli, X. Li, J. Chia and H. S. Levin (2008). "Diffusion tensor imaging of acute mild traumatic brain injury in adolescents." *Neurology* 70(12): 948-955.

Wilkins, A., T. Shallice and R. McCarthy (1987). "Frontal lesions and sustained attention." *Neuropsychologia* 25(2): 359-365.

Williams, S. E., M. D. Ris, R. Ayyangar, B. K. Scheffi and D. Berch (1998). "Recovery in pediatric brain injury: is psychostimulant medication beneficial?" *J Head Trauma Rehab* 13(3): 73-81.

Witt, S. T., D. W. Lovejoy, G. D. Pearlson and M. C. Stevens (2010). "Decreased prefrontal cortex activity in mild traumatic brain injury during performance of an auditory oddball task." *Brain Imag Behav* 4(3-4): 232-247.

Wood, R. L. and N. A. Rutterford (2006). "Demographic and cognitive predictors of long-term psychosocial outcome following traumatic brain injury." *J Int Neuropsych Soc* 12(3): 350-358.

Wu, T. C., E. A. Wilde, E. D. Bigler, R. Yallampalli, S. R. McCauley, M. Troyanskaya, Z. Chu, X. Li, G. Hanten, J. V. Hunter and H. S. Levin (2010). "Evaluating the relationship between memory functioning and cingulum bundles in acute mild traumatic brain injury using diffusion tensor imaging." *J Neurotraum* 27(2): 303-307.

Yates, P. J., W. H. Williams, A. Harris, A. Round and R. Jenkins (2006). "An epidemiological study of head injuries in a UK population attending an emergency department." *J Neurol Neurosurg Ps* 77(5): 699-701.

Yeung, N., J. D. Cohen and M. M. Botvinick (2004). "The neural basis of error detection: conflict monitoring and the error-related negativity." *Psychol Rev* 111(4): 931-959.

Zhang, D. and M. E. Raichle (2010). "Disease and the brain's dark energy." *Nature reviews. Neurology* 6(1): 15-28.

Zhang, K., B. Johnson, D. Pennell, W. Ray, W. Sebastianelli and S. Slobounov (2010). "Are functional deficits in concussed individuals consistent with white matter structural alterations: combined fMRI & DTI study." *Experimental brain research. Experimentelle Hirnforschung. Experimentation cerebrale* 204(1): 57-70.

Zhou, J., M. D. Greicius, E. D. Gennatas, M. E. Growdon, J. Y. Jang, G. D. Rabinovici, J. H. Kramer, M. Weiner, B. L. Miller and W. W. Seeley (2010). "Divergent network connectivity changes in behavioural variant frontotemporal dementia and Alzheimer's disease." *Brain* 133(5): 1352-1367.

Zielinski, B. A., E. D. Gennatas, J. Zhou and W. W. Seeley (2010). "Network-level structural covariance in the developing brain." *P Natl Acad Sci USA* 107(42): 18191-18196.

Zigmond, A. S. and R. P. Snaith (1983). "The hospital anxiety and depression scale." *Acta Psychiatr Scand* 67(6): 361-370.

Zuo, X. N., C. Kelly, J. S. Adelstein, D. F. Klein, F. X. Castellanos and M. P. Milham (2010). "Reliable intrinsic connectivity networks: test-retest evaluation using ICA and dual regression approach." *Neuroimage* 49(3): 2163-2177.

Zysset, S., O. Huber, E. Ferstl and D. Y. von Cramon (2002). "The anterior frontomedian cortex and evaluative judgment: an fMRI study." *Neuroimage* 15(4): 983-991.